



SYNTHESIS OF FLUORINATED ANALOGS OF KRN7000

David Collado Fernández

ADVERTIMENT. L'accés als continguts d'aquesta tesi doctoral i la seva utilització ha de respectar els drets de la persona autora. Pot ser utilitzada per a consulta o estudi personal, així com en activitats o materials d'investigació i docència en els termes establerts a l'art. 32 del Text Refós de la Llei de Propietat Intel·lectual (RDL 1/1996). Per altres utilitzacions es requereix l'autorització prèvia i expressa de la persona autora. En qualsevol cas, en la utilització dels seus continguts caldrà indicar de forma clara el nom i cognoms de la persona autora i el títol de la tesi doctoral. No s'autoritza la seva reproducció o altres formes d'explotació efectuades amb finalitats de lucre ni la seva comunicació pública des d'un lloc aliè al servei TDX. Tampoc s'autoritza la presentació del seu contingut en una finestra o marc aliè a TDX (framing). Aquesta reserva de drets afecta tant als continguts de la tesi com als seus resums i índexs.

ADVERTENCIA. El acceso a los contenidos de esta tesis doctoral y su utilización debe respetar los derechos de la persona autora. Puede ser utilizada para consulta o estudio personal, así como en actividades o materiales de investigación y docencia en los términos establecidos en el art. 32 del Texto Refundido de la Ley de Propiedad Intelectual (RDL 1/1996). Para otros usos se requiere la autorización previa y expresa de la persona autora. En cualquier caso, en la utilización de sus contenidos se deberá indicar de forma clara el nombre y apellidos de la persona autora y el título de la tesis doctoral. No se autoriza su reproducción u otras formas de explotación efectuadas con fines lucrativos ni su comunicación pública desde un sitio ajeno al servicio TDR. Tampoco se autoriza la presentación de su contenido en una ventana o marco ajeno a TDR (framing). Esta reserva de derechos afecta tanto al contenido de la tesis como a sus resúmenes e índices.

WARNING. Access to the contents of this doctoral thesis and its use must respect the rights of the author. It can be used for reference or private study, as well as research and learning activities or materials in the terms established by the 32nd article of the Spanish Consolidated Copyright Act (RDL 1/1996). Express and previous authorization of the author is required for any other uses. In any case, when using its content, full name of the author and title of the thesis must be clearly indicated. Reproduction or other forms of for profit use or public communication from outside TDX service is not allowed. Presentation of its content in a window or frame external to TDX (framing) is not authorized either. These rights affect both the content of the thesis and its abstracts and indexes.



UNIVERSITAT ROVIRA i VIRGILI

David Collado Fernández

Synthesis of fluorinated analogs of KRN7000

PhD Thesis

Supervised by Prof. M. Isabel Matheu Malpartida and Dr. Omar
Boutureira Martín

Department of Analytical Chemistry and Organic Chemistry



**UNIVERSITAT
ROVIRA i VIRGILI**

Tarragona 2017



**UNIVERSITAT
ROVIRA i VIRGILI**

Departament de Química Analítica i Química Orgànica
C/ Marcel·lí Domingo, 1
Campus Sescelades
43007, Tarragona

Prof. M. Isabel Matheu Malpartida and Dr. Omar Boutureira Martín from
Department of Analytical Chemistry and Organic Chemistry, University
Rovira i Virgili,

We STATE that the present study, entitled “Synthesis of fluorinated
analogs of KRN7000”, presented by David Collado Fernández for the
award of the degree of Doctor, has been carried out under our
supervision at the Department of Analytical Chemistry and Organic
Chemistry of this university.

Tarragona, 18 September, 2017.

Prof. M. Isabel Matheu Malpartida

Dr. Omar Boutureira Martín

The work performed in the present Doctoral Thesis has been possible thanks to the Martí-Franquès grants program (reference: 2012BPURV-16), funded by the URV.

This Thesis has been carried out thanks to the funding of the research project:

CTQ 2014-58664-R, funded by the Ministerio de Economía y Competitividad.



UNIVERSITAT ROVIRA I VIRGILI



Agraïments/Agradecimientos/Acknowledgements

En primer lloc, vull agrair a la Professora Maribel Matheu per dirigir aquesta tesi doctoral. Gràcies per tenir sempre la porta del despatx oberta i dedicar-me temps per resoldre espectres, donar-me un informe corregit o donar-me ànims, sobretot en els moments més durs. Soc conscient que durant el pas per aquesta etapa, he progressat molt, tant com a científic com a nivell personal i crec que et mereixes gran part del mèrit. També vull agrair al meu co-director, el Dr. Omar Boutureira. Les nostres converses i les teves ganes de anar sempre mes enllà m'han motivat i ajudat molt, sobretot en l'última etapa de la tesi.

Per suposat, també vull donar les gràcies al Professor Sergio Castellón per donar-me l'oportunitat de treballar en aquest grup d'investigació i per les experiències que se n'han derivat. També he d'agrair a la Professora Yolanda Díaz per els consells en les reunions de grup i per estar sempre disponible per qualsevol necessitat.

I would like to thank Prof. Gennaro De Libero for acceding to establish a fruitful collaboration and for its implication in the biological part of this thesis.

De la mateixa manera també vull agrair la col·laboració i els grans esforços invertits per el Dr. Miquel Mulero del departament de Bioquímica i Biotecnologia i al Dr. Francisco Corzana de l' universitat de La Rioja en la realització de la part biològica d'aquesta tesi.

Als nostres veïns de polímers, Alev, Zeynep, Marc, Monty, Carmen, Lorena, Adrian i Cristina per els moments gaudits (converses pels passadissos, esmorzars..).

Finalment, toca parlar dels companys de laboratori. Començaré pels "grans" que van ser els meus mentors dins del laboratori i que tants consells m'han donat (que no sempre els he sabut aprofitat). Isidro, tu vas guiar els meus primers passos en el laboratori. Recordo més d'una nit al laboratori per culpa de la meva mala organització... Gràcies per tot. També vull agrair al Xavi, l' Ismael, l' Emma, el Seb i les Miriams per acollir-me com un més en els meus primers dies pel laboratori. A tu també, Joan, no m'he oblidat de tu. Sempre recordaré els teus "ja t'ho havia dit" i els "Miteeeeer Dangeer", que solien arribar cap a les 7 de la tarda. Van ser grans moments, difícils d'oblidar.

Evidentment, no em puc oblidar dels "actuals" companys de laboratori amb els que he passat tantes i tantes hores, que he compartit tants bons moments i tantes històries que no oblidaré. Segurament em quedaré curt a l'hora de agrair-vos els moments que hem viscut junts. És ben cert que els sentiments són difícils d'explicar amb paraules. Per ordre d'arribada, començo pel Jordi. Recordo els inicis durant el treball experimental i després el Màster. Mare meva quines en fèiem. Les maleïdes benzilacions, mescles de diferents crús de reacció en la mateixa columna (o placa filtrant)...Més tard, vam començar a agafar confiança i vam començar a viure moments mes...."divertits", per dir-ho d'alguna manera. Des de converses d'un nivell intel·lectual innegable, fins a unes sessions musicals només aptes per als paladars més fins. Precisament seran aquests moments els que més enyori al deixar el laboratori. I parlant de moments... el següent en arribar, ets tu Adrià. El crack dels cracks, sens dubte. Intento escriure algo "a l'alçada de l'ocasió" però em resulta impossible, penso que em quedaré curt. Suposo que a part d'agair-te els grans moments compartits, de divertits, i no tant divertits, només em queda desitjar no perdre mai el contacte i recordar, de tant en tant i tot rient, aquests moments. He de fer una

menció especial per a vatos dos, i ho sabeu... Heu sigut uns grans companys de viatge (també coneguts com els tres "jinetes"), i això no hagués sigut el mateix sense vosaltres. Ah, per cert, lo de la caravana segueix en peu eh, ja sigui ara o sent ja uns jubilats!

Y seguimos con Macarena. Ayy Macarena, Macarena...Has sido una gran compañera de laboratorio y mejor persona. Lo que más he valorado de ti es que siempre me ha resultado fácil hablar de cualquier cosa contigo, y, aunque digas lo contrario, es imposible llevar-se mal contigo. Ánimos para la recta final, ya sabes que al final todo sale bien, te lo mereces. Vamos a ver, la siguiente de la lista es...Ah si, Irene, "morenikah 8292" Te suena...?? (tómalo como una confesión). Bueno a parte de ser la chica mas ordenada que he conocido y probablemente conoceré, aportaste mucho "cuquismo" al laboratorio. Un lunes es menos lunes con un "Holi"... Espero que disfrutes tu estancia en USA (a ver si consigues que sean seis meses) y muchos ánimos para la tesis, aunque ya la tengas casi toda escrita...(madre mia que pedante...pero que envidia...lo bien que me iria ahora tener unos informes tan bien escritos). Margarita, también quiero agradecerle tu paciencia en el laboratorio de los chicos y tus sabios consejos. Espero que hayas disfrutado de mi compañía tanto como lo he hecho yo. Mucha suerte en el futuro! Y finalmente, el último flamante fichaje del laboratorio, Arnau, otro crack para el equipo. Muchos ánimos, tienes por delante un largo viaje, que aunque duro, estoy seguro que tu lo convertirás en algo muy interesante. Espero tu invitación para tu tesis. Te voy a dar el mismo consejo que se me dió a mi en su momento: "Piensa y luego actúa". Aunque muchas veces difícil de seguir, es la mejor fórmula del éxito.

També vull recordar a tots aquells que han passat per el laboratori: Otty, mucha suerte para el futuro, eres una chica muy trabajadora, y a la

que le aguardeu grandes coses! Xochitl, Jenny, Alex, Kevin (que grande eres), Miguel, Joan Saltó i Ester, us desitjo tot el millor.

Per últim, però no menys important, també vull mencionar a tots aquells que m'han recolzat fora de laboratori. Primer de tot, he d'agrair profundament als meus pares el gran esforç que han dedicat per instruir-me en la cultura del treball i de l'esforç. Sempre heu sigut el millor exemple a seguir i per això us mereixeu gran part del mèrit d'aquesta tesi. Vull agrair, com no podia ser d'altre manera, a tota la família, pares, Víctor, als valencianets i a "l'abuela". Els problemes es tornen relatius amb vosaltres al costat.

També vull agrair als amics reusencs de l'infància, que tot i que ultimament, com vosaltres dieu: "sòc car de veure" sempre m'he sentit molt recolzat amb vosaltres i m'heu donat ànims per continuar endavant. Gràcies!

No puc deixar de mencionar-vos a vosaltres Arnau i Lourdes. Poc a poc, hem anat guanyant (o recuperant) l'amistat fins que un dia em sorpreneu venint a la tesi. Moltes gràcies.

Finalment, gràcies a tu, Patri, per estar sempre en els moments bons i en els no tant bons. No és cap secret que aquesta ha sigut una etapa molt dura per a mi, i per tant, també per a tu. Gràcies per fer-me sempre costat i entendre'm en tot moment. Per fi arriba el final d'una etapa, i el començament d'una altra.

Table of Contents

Abbreviations and acronyms	1
Summary	7
CHAPTER 1. General Introduction	13–47
1.1. Glycosphingolipids	15
1.1.1. Structure of glycosphingolipids	15
1.2. The discovery of KRN7000	17
1.2.1. KRN7000 and NKT cells	18
1.2.2. Interaction of KRN7000 with CD1d and TCR	20
1.3. Structure-Activity relationship studies on KRN7000	23
1.3.1. Modifications on the sugar head and glycosidic bond	24
1.3.2. Modification at the ceramide moiety	27
1.4. Synthesis of KRN7000 - Literature methods	33
1.5. Importance of fluorine in Medicinal Chemistry	40
1.5.1 The effect of fluorine on physicochemical properties of bioactive molecules	41
1.5.2. Role in ligand-protein interactions	44
CHAPTER 2. Antecedents and General Objectives	49–57
CHAPTER 3. Synthesis of KRN7000 analogues with a high degree of fluorination	59-106
3.1. Objectives	61
3.2. Retrosynthetic analysis and background	62
3.2.1. Retrosynthetic analysis	62
3.2.2. Background	63
3.3. Synthesis of a KRN7000 analogue fluorinated at acyl chain	72
3.3.1. Synthesis of non fluorinated amine intermediate 7	72
3.3.2. Synthesis of fluorinated acid, acylation and deprotection	76
3.4. Synthesis of a KRN7000 analogue fluorinated at sphingoid base	78

3.4.1. Introduction of fluorinated chain via Wittig olefination	78
3.4.2. Introduction of fluorinated chain via Cross Metathesis	82
3.4.3. Synthesis of amine intermediates	93
3.4.4. Last steps: Acylation, CM and deprotection	101
3.5. Synthesis of a KRN7000 analogue fluorinated at both lipid chains	103
3.6. Conclusions	105

CHAPTER 4. Synthesis of KRN7000 analogues with a low degree of fluorination at the acyl chain	109-121
4.1. Introduction	111
4.2. Objectives and Retrosynthetic analysis	114
4.3. Results and discussion	115
4.3.1. Synthesis of polyfluorinated acids	115
4.3.2. <i>N</i> -Acylation and total deprotection	119
4.4. Conclusions	121

CHAPTER 5. Synthesis of conformationally rigid KRN7000 analogues	123-146
5.1. Introduction	125
5.1.1. Conformational restriction as a powerful tool in drug design	125
5.1.2. Unexpected cyclization process during the synthesis of fluorinated analogues of KRN7000	126
5.1.3. 1,3-Dipolar cycloaddition	127
5.2. Antecedents	130
5.3. Objectives and Retrosynthetic analysis	131
5.4. Results and discussion	134
5.4.1. Synthesis of pyrrolidine intermediates	134
5.4.2. Acylation and/or deprotection steps	142
5.5. Conclusions	146

CHAPTER 6. Highly Reactive 2-Deoxy-2-iodo-D-allo and D-Gulopyranosyl Sulfoxide Donors Ensure β-Stereoselective Glycosylations with Steroidal Aglycones	149-169
6.1. Introduction	151
6.1.1. Stereoselective synthesis of 2-deoxyglycosides	152
6.1.2. Glycosylation through glycosyl sulfoxides	155
6.2. Objectives	161
6.3. Results and discussion	163
6.4. Conclusions	169
CHAPTER 7. Preliminar Biological Evaluation of the Synthesized KRN7000 analogues	171-187
7.1. Introduction and Objectives	173
7.2. Results and Discussion	175
7.2.1. Binding affinity of glycolipids to mouse CD1d protein	175
7.2.2. Computer simulation of TCR-glycolipid-CD1d interaction	178
7.2.3. <i>In vitro</i> assays with human iNKT cells	183
7.3. Conclusions	186
CHAPTER 8. General Conclusions	189-194
CHAPTER 9. Experimental Section	197-288
9.1. General Considerations	199
9.2. General Procedures	200
9.3. Compound Characterization	207

Abbreviations and Acronyms

A

Ac	Acetyl
AIBN	Azobisisobutyronitrile
Ar	Aryl
atm	Atmosphere(s)

B

Bn	Benzyl
Boc	<i>tert</i> -Butyl carbamate
b.p.	Boiling point
Bu	<i>n</i> -Butyl
Bz	Benzoyl

C

Calc.	Calculated
cat	Catalyst
CM	Cross Metathesis
Conv.	Conversion
COSY	Proton homonuclear correlation
Cy	Cyclohexyl

D

d	Doublet
2D	Two dimensional
DCM	Dichloromethane
dd	Doublet of doublets
ddd	Doublet doublet of doublets
DIAD	Diisopropyl azodicarboxylate
DIPEA	<i>N,N</i> -Diisopropylethylamine
DMAP	4-Dimethylaminopyridine
DMF	<i>N,N</i> -Dimethylformamide
DMSO	Dimethyl sulfoxide
DPPA	Diphenylphosphoryl azide

Abbreviations and Acronyms

DTBMP	2,6-Di- <i>tert</i> -butyl-4-methylpyridine
E	
EDC	1-Ethyl-3-(3-dimethylaminopropyl) carbodiimide
equiv	Equivalent(s)
ESI-TOF	Electrospray ionization-time of flight
Et	Ethyl
EXSY	Exchange Spectroscopy
EWG	Electron withdrawing group
F	
FTIR	Fourier transform infrared spectroscopy
H	
h	Hour(s)
HFIP	1,1,1,3,3,3-Hexafluoro-2-propanol
HMBC	Heteronuclear Multiple Bond Correlation
HOBt	Hydroxybenzotriazole
HRMS	High-resolution Mass Spectrometry
HSQC	Heteronuclear Single-Quantum Correlation
Hz	Hertz
I	
<i>i</i> -Pr	Isopropyl
IR	Infrared
J	
<i>J</i>	Coupling constant
L	
L	Ligand
LHMDS	Lithium bis(trimethylsilyl)amide
M	

m	Multiplet
Me	Methyl
m.p.	Melting point
Ms	Mesyl
MS	Molecular Sieves
m/z	Mass under charge
N	
NHC	<i>N</i> -heterocyclic carbene
NMR	Nuclear magnetic resonance
NOESY	Nuclear Overhauser Effect Spectroscopy
Nu	Nucleophile
O	
ovn	Overnight
P	
Ph	Phenyl
ppm	Parts per million
Py	Pyridine
Q	
q	Quartet
quant	Quantitative
quint	Quintet
R	
rt	Room temperature
ROESY	Rotating frame overhauser effect spectroscopy
S	
s	Singlet
T	

Abbreviations and Acronyms

t	Triplet
Tf	Trifluoromethylsulfonyl
Tf ₂ O	Trifluoromethylsulfonyl anhydride
THF	Tetrahydrofuran
TLC	Thin layer chromatography
TS	Transition state
Ts	Tosyl
U	
UV/Vis	Ultraviolet/visible

Summary

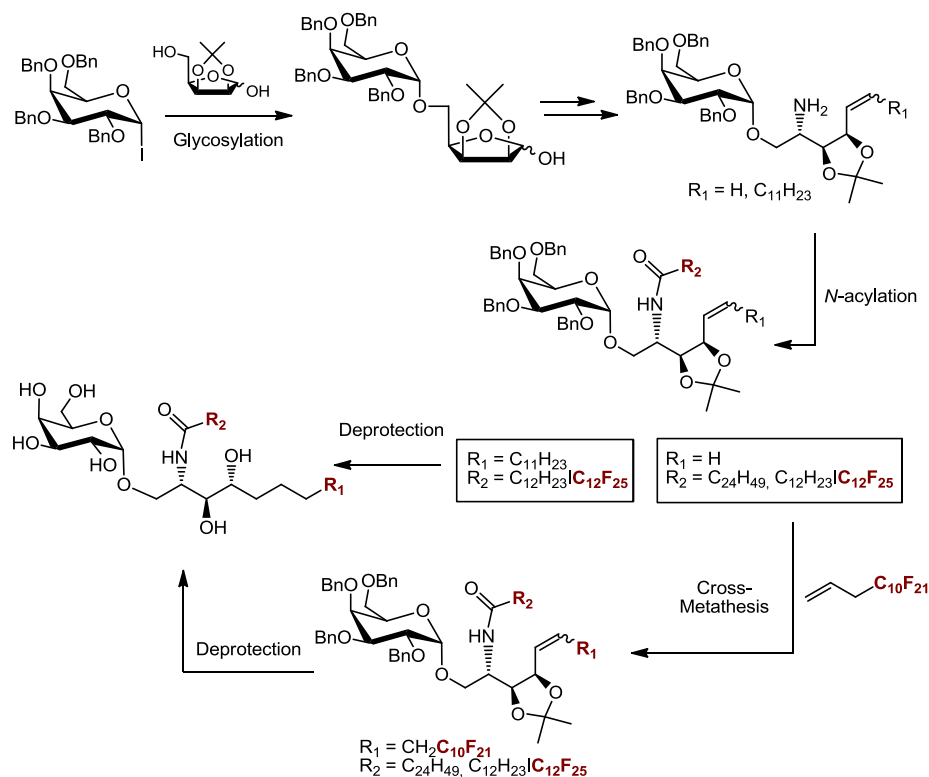
KRN7000 (α -GalCer) is a synthetic glycosphingolipid that upon interaction with CD1d proteins is capable of activating invariant natural killer T (iNKT) cells. NKT cells are a subset of lymphocytes involved in the immune response for a large number of pathological conditions such as infections, autoimmunity and cancer. When activated by KRN7000, NKT cells produce a variety of anti-inflammatory (T_H2) cytokines, such as interleukin-4 (IL-4), and pro-inflammatory (T_H1) cytokines, such as interferon- γ (IFN- γ). These cytokines produce different biological responses depending on their nature. Pro-inflammatory cytokines (T_H1 -type cytokines) activate cellular immune responses to fight against tumors or viral/bacterial/parasitic infections (T_H1 response). Instead, immunomodulatory cytokines (T_H2 -type cytokines) are responsible for the activation of lymphocytes and the production of immunoglobulins and antibodies, desired for the treatment of autoimmune diseases. KRN7000 stimulates both T_H1 and T_H2 responses indiscriminately while a biased response is desired because of the antagonistic nature of both types of cytokines. For this reason, extensive research has been focused on the synthesis of new KRN7000 analogues capable of stimulating selective responses. In this regard, it is believed that T_H1 response is certainly favoured by stabilization of the KRN7000-CD1d-NKT complex whereas moderate destabilization leads to T_H2 response. In this sense, it has been recently demonstrated that polyfluorinated chains produce stronger interactions with hydrophobic cavities of proteins than its hydrocarbon counterparts.

Within this context, this thesis aims the synthesis of different KRN7000 analogues bearing fluoroalkyl chains at ceramide moiety. We

Summary

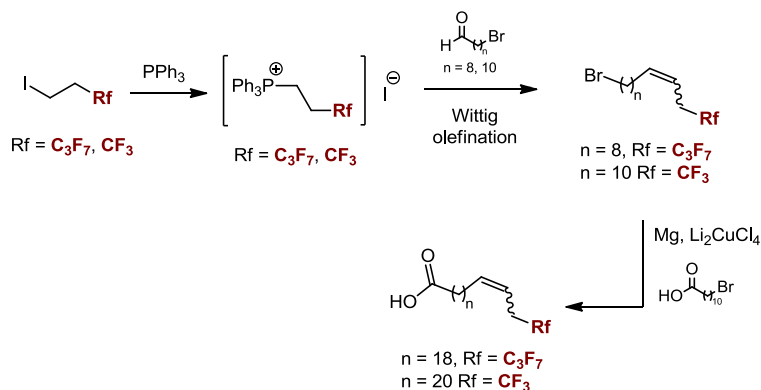
hypothesized that this structural modification would modulate the ligand-CD1d binding affinity, leading to biased cytokine responses.

KRN7000 analogues bearing highly fluorinated acyl chain and/or sphingoid base moieties were synthesized. These results are presented in Chapter 3. Their preparation was accomplished following an adapted version of the total synthesis developed by Panza *et al.* and the strategy of Yen and co-workers (Scheme 1). Key steps involve: 1- Initial α -selective glycosylation. 2- Introduction of fluorinated acyl chain via *N*-acylation. 3- Introduction of fluorinated sphingoid base fragment via CM reaction.



Scheme 1. General approach for the preparation of fluorinated KRN7000 analogues.

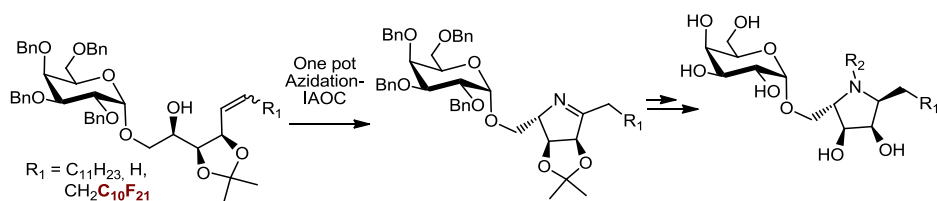
The same synthetic approach was again used, in Chapter 4, for the synthesis of KRN7000 analogues bearing low fluorinated acyl chains. The major challenge of this chapter was the synthesis of long carboxylic acids bearing short fluoroalkyl moieties (C_3F_7 and CF_3) at the end of chain (Scheme 2). The synthesis of such acids was achieved via initial formation of long ω -perfluoropropyl and trifluoromethyl alkyl bromides which then underwent Cu-catalyzed coupling with ω -bromo carboxylic acids.



Scheme 2. Synthesis of long carboxylic acids bearing short, terminal fluoroalkyl units.

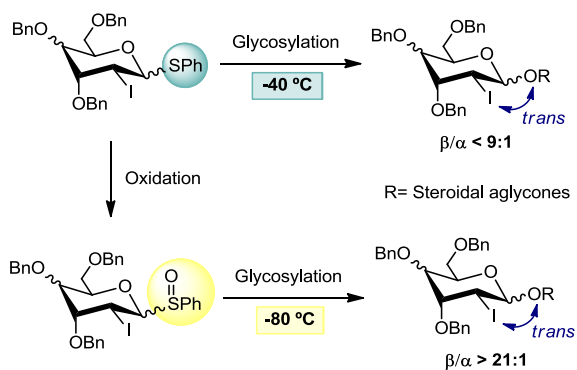
The research described in Chapter 5 aroused from an unexpected reactivity found in Chapter 3. We observed that cyclic imines could be obtained from hydroxyalkene intermediates via one pot azidation-1,3-dipolar cycloaddition (IAOC) sequence (Scheme 3). This reactivity enabled access to the synthesis of conformationally rigid KRN7000 analogues.

Summary



Scheme 3. Synthesis of conformationally restricted KRN7000 analogues via one pot azidation-IAOC.

The topic studied in Chapter 6 was in line with a previous methodology, developed by our group, for the synthesis of 2-deoxy- β -glycosides. The last step of the strategy dealt with 1,2-*trans*-stereoselective glycosylation controlled by a bulky iodine atom at C-2 position of thioglycosyl donors. Although this methodology proceeded with excellent diastereoselectivities with simple alcohols, more "challenging" steroidal acceptors required higher reaction temperatures, which ultimately decreased the β -stereoselectivity. Therefore our aim was to explore the feasibility of utilizing 2-deoxy-2-iodo-pyranosyl sulfoxides instead of the corresponding sulfides as convenient acceptors that permit activation at very low temperature, ensuring a precise kinetic control for a complete 1,2-*trans* stereoselective glycosylation promoted by the neighboring bulky iodine (Scheme 4).



Scheme 4. Glycosylation of thioglycosides vs sulfoxides.

Finally, Chapter 7 dealt with the biological evaluation of the previously synthesized KRN7000 analogues. Binding affinity towards mouse CD1d protein as well as human iNKT cell stimulation experiments are described in this chapter. Furthermore, molecular dynamic simulations of the interaction between the glycolipid and mouse CD1d and TCR receptor of mouse iNKT cells are also presented.

CHAPTER 1

GENERAL INTRODUCTION

1.1. GLYCOSPHINGOLIPIDS

Glycosphingolipids (GSLs) are essential components of the cell plasma membrane present in various tissues and in neuronal cells. They play a key role in the regulation of a variety of biological processes like cell division, growth, proliferation, signalling, regeneration or apoptosis and they also participate in cell-to-cell recognition and communication. Additionally, GSLs act as mediators between cell and various external agents (toxins, viruses or bacteria). As a result, they are considered valuable biomarkers of a number of pathologies and thus, their activity have been studied in relation to cancer, HIV microbial infection, diabetes, Alzheimer's, or Parkinson's disease.¹

1.1.1. Structure of glycosphingolipids

GSL are composed of a hydrophilic sugar head connected to a hydrophobic ceramide fragment (Figure 1.1). This ceramide moiety, in turn, consists of a long-chain aminoalcohol (sphingoid base), in amide-linkage to a fatty acid.

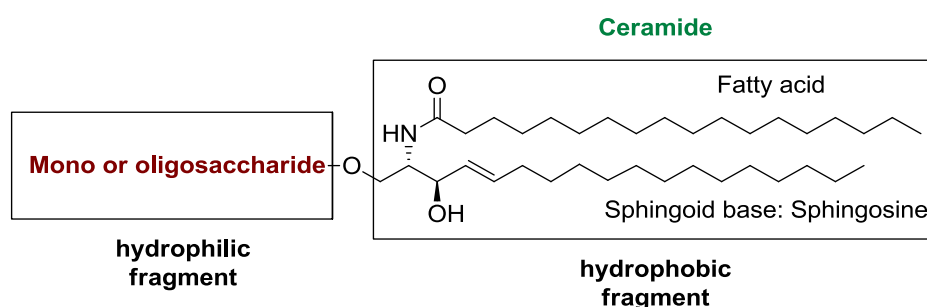


Figure 1.1. General structure of a glycosphingolipid.

¹ Varki, A.; Cummings, R.D.; Esko, J. D.; Stanley, P.; Hart, G.; Aebi, M.; Darvill, A.; Kinoshita, T.; Packer, N.H.; Prestegard, J.J.; Schnaar, R.L.; Seeberger, P.H. *Essentials of Glycobiology*. 3rd Edition, Cold Spring Harbor Laboratory Press, New York, 2015.

General Introduction

A large number of GSL species, differing in both sugar and ceramide fragments are known to exist in vertebrate cell membranes. Some of them are highlighted in Figure 1.2.

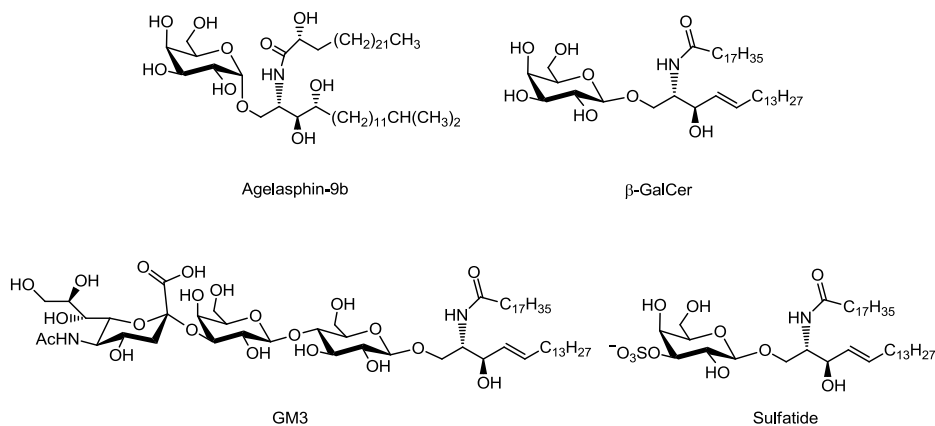


Figure 1.2. Some significant GSLs.

Among all structural variations present in ceramide fragment, generally, three main sphingoid bases can be found in nature: Sphingosine, Sphinganine and Phytosphingosine (Figure 1.3).

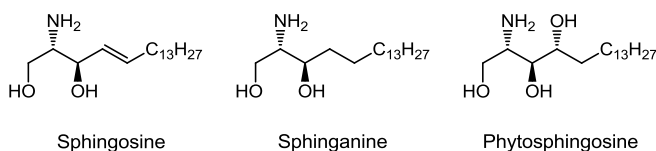


Figure 1.3. Main sphingoid bases found in nature.

The nature of the carbohydrate fragment is also widely varied. In fact, major GSL classifications are based on the nature of sugar units and divide them as neutral (non-charged sugars) like agelasphin 9b and β-galactosylceramide (β-GalCer) or acidic (sialylated or sulphated carbohydrates) such as GM3 or 3-Sulfogalactosylceramide (Sulfatide) (Figure 1.2).

1.2. THE DISCOVERY OF KRN7000

In 1993, the Kirin Brewery co.² reported the isolation of a set of GSLs from the Japanese marine sponge *Agelas mauritianus*, showing antitumoral activity. Interestingly, structural elucidation of these compounds, named Agelasphins, revealed the presence of α -galactose head as common feature linked to different ceramides (Figure 1.4A). At that time, it was the first characterization of α -configured galactosyl ceramides extracted from natural sources. Since this discovery, subsequent structure-activity relationship studies³ culminated in the production of KRN7000, a potent antitumoral agent (Figure 1.4B).

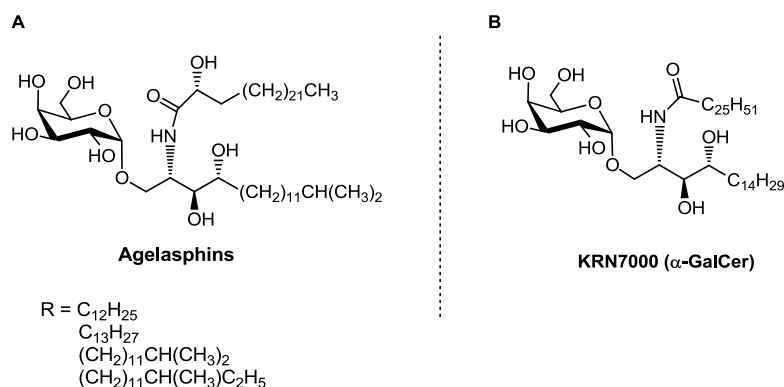


Figure 1.4. A) Agelasphins from *Agelas mauritianus*. B) Synthetic α -GalCer (KRN7000).

The structure of this encouraging GSL consisted in a galactose polar head α -linked to a ceramide fragment, composed, in turn, of a phytosphingosine moiety bearing a N-linked hexacosanoic fatty acid chain. After extense research, KRN7000, also known as α -GalCer,

² (a) Natori, T.; Morita, M.; Akimoto, K.; Koezuka, Y. *Tetrahedron* **1994**, *50*, 2771-2784. (b) Natori, T.; Koezuka, Y.; Higa, H. *Tetrahedron Lett.* **1993**, *34*, 5591-5592.

³ (a) Motoki, K.; Kobayashi, E.; Uchida, T.; Fukushima, H.; Koezuka, Y. *Bioorg. Med. Chem. Lett.* **1995**, *5*, 705-710. (b) Morita, M.; Motoki, K.; Akimoto, K.; Natori, T.; Sakai, T.; Sawa, E.; Yamaji, K.; Koezuka, Y.; Kobayashi, E.; Fukushima, H. *J. Med. Chem.* **1995**, *38*, 2176-2187.

General Introduction

showed promising bioactivities against diverse pathologies⁴ and in 2001 entered in Phase-I clinical trials for cancer immunotherapy.⁵

1.2.1. KRN7000 and iNKT cells

Despite its known potential in tumor growth prevention, KRN7000 does not present direct cytotoxicity against tumor cells. Instead, its bioactivity is based on its ability to stimulate invariant Natural Killer T (iNKT) cells,⁶ a subset of lymphocytes involved in the immune response for a large number of pathological conditions such as infections, autoimmunity and cancer.⁷

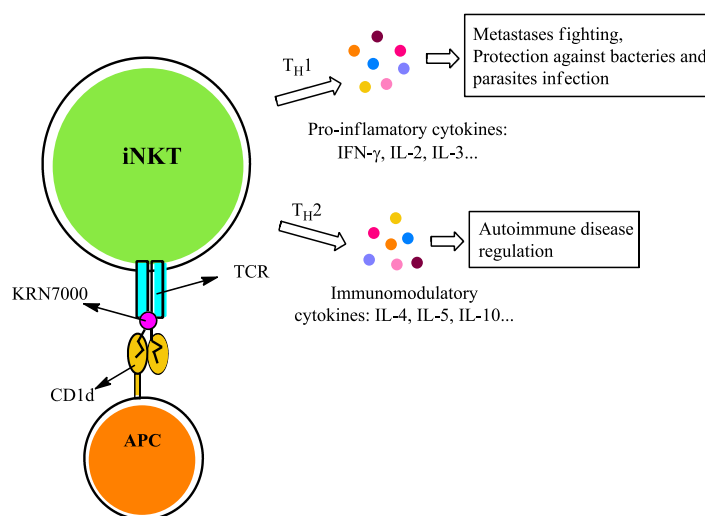


Figure 1.5. Simplified representation for iNKT cell activation by KRN7000.

⁴ Yu, K. O. A.; Porcelli, S. A. *Immunol. Lett.* **2005**, *100*, 42-55 and references therein.

⁵ (a) For a recent review compiling the clinical data for cancer immunotherapy of KRN7000, see: Schneiders, F. L.; Scheper, R. J.; von Blomberg, B. M. E.; Woltman, A. M.; Janssen, H. L. A.; van den Eerthegh, A. J. M.; Verheul, H. M. W.; de Gruijl, T. D.; van der Vliet, H. J. *Clin. Immunol.* **2011**, *140*, 130-141. (b) For more information, visit the website <http://www.alphagalcer.net/index.html> (last visit the 27th of July 2017).

⁶ (a) Kitamura, H.; Iwakabe, K.; Yahata, T.; Nishimura, S-I.; Ohta, A.; Ohmi, Y.; Sato, M.; Takeda, K.; Okumura, K.; Van Kaer, L.; Kawano, T.; Taniguchi, M.; Nishimura, T. *J. Exp. Med.* **1999**, *189*, 1121-1127. (b) Kobayashi, E.; Motoki, K.; Yamaguchi, Y.; Uchida, T.; Fukushima, H.; Koezuka, Y. *Bioorg. Med. Chem.* **1996**, *4*, 615-619.

⁷ For a general review describing basic information of NKT cells, see: Bendelac, A.; Savage, P. B.; Teyton, L. *Annu. Rev. Immunol.* **2007**, *25*, 297-336.

The mechanism for such activation involves two consecutive cellular recognitions. Firstly, KRN7000 binds to CD1d, a protein situated on the surface of antigen presenting cells (APC) such as dendritic cells, macrophages, and B cells (Figure 1.5). Then, this binary complex is recognized by the T cell receptor (TCR) of iNKT cells to form a ternary complex. This last interaction is considered to activate the iNKT cells and triggers the secretion of massive amounts of different cytokines, which are signalling molecules responsible for the final immune outcome. These cytokines are categorized as T_H1 - and T_H2 -type, depending on their response upon release. Pro-inflammatory cytokines (T_H1 -type cytokines) such as IFN- γ , IL-2 or IL-3 activate cellular immune responses to fight against tumors, or viral/bacterial/parasitic infections (T_H1 response). Instead, immunomodulatory cytokines (T_H2 -type cytokines) as IL-4, IL-5, IL-10 or IL-13 are responsible for the activation of lymphocytes and the production of immunoglobulins and antibodies, desired for the treatment of autoimmune diseases.

It is important to note that both T_H1 and T_H2 responses have antagonistic effects, which means that, for example, IFN- γ inhibits a T_H2 phenotype in the same way as IL-4 deactivates a T_H1 one.⁸ For this reason, an appropriate cytokine secretion pattern is crucial for the development of an efficient type of immune response to a particular antigenic challenge. In this sense, despite the potent bioactivity shown by KRN7000, its indiscriminate production of both T_H1 and T_H2 -type cytokines limits its therapeutical use.

The mechanism that determines the cytokine profile secretion upon activation of iNKT cells is still not well understood. Apparently, the

⁸ Godfrey, D. I.; Kronenberg, M. *J. Clin. Invest.* **2004**, *114*, 1379-1388.

General Introduction

cytokine release process generated by KRN7000 is time dependent.⁹ Initially, iNKT cells produce detectable amounts of both IL-4 (T_H2) and IFN- γ (T_H1) within 2 h of stimulation. Then, after approximately 16 h of stimulation no IL-4 production is observed while high production of IFN- γ is maintained until at least 72 h.

In this sense, a strong hypothesis is that T_H1/T_H2 polarisation is closely related to the half-life of the ternary complex (TCR-KRN700-CD1d). In fact structure-activity relationship (SAR) studies (see section 1.3), have lead to the synthesis of KRN7000 analogues providing highly stable complexes, which proved to favour a T_H1 response. Conversely, biased T_H2 responses have been observed for ligands forming less stable complexes. Nevertheless, the stability of the ternary complex should not be seen as the only responsible for cytokine polarisation and many other aspects should also be taken into consideration. For example, the nature of the antigen presenting cell (APC) carrying the CD1d-glycolipid complex also seems to play a role in this sense.¹⁰

1.2.2. Interaction of KRN7000 with CD1d and TCR

The publication of the crystallographic data of human and mouse binary (CD1d-ligand) and ternary (TCR-ligand-CD1d) complexes with KRN7000 and other analogues provided crucial insights about their interaction nature. Additionally, posterior reported molecular dynamic

⁹ Crowe, N. Y.; Uldrich, A. P.; Kyparissoudis, K.; Hammond, K. J. L.; Hayakawa, Y.; Sidobre, S.; Keating, R.; Kronenberg, M.; Smyth, M.; Godfrey, D. I. *J. Immunol.* **2003**, *171*, 4020–4027.

¹⁰ (a) Im, J. S.; Tapinos, N.; Chae, G. T.; Illarionov, P. A.; Besra, G. S.; DeVries, G. H.; Modlin, R. L.; Sieling, P. A.; Rambukkana, A.; Porcelli, S. A. *J. Immunol.* **2006**, *177*, 5226–5235. (b) Schmieg, J.; Yang, G.; Franck, R. W.; Van Rooijen, N.; Tsuji, M. *USA.* **2005**, *102*, 1127–1132. (c) Bezbradica, J. S.; Stanic, A. K.; Matsuki, N.; Bour-Jordan, H.; Bluestone, J. A.; Thomas, J. W.; Unutmaz, D.; Van Kaer, L.; Joyce, S. *J. Immunol.* **2005**, *174*, 4696–4705.

(MD) simulations of the recognition process also proved helpful in this field.¹¹

1.2.2.1. Binary complex (CD1d-KRN7000)

CD1d is a protein associated with a b2-microglobulin (b2m) present in antigen presenting cells (APC) such as dendritic cells, macrophages, and B cells. Human and mouse CD1d proteins present few differences in their amino acid sequences. Thus, for an easy understanding, in this manuscript, human nomenclature will be principally used and the mouse one will be placed in brackets, if different.

This protein contains a C-terminal part, composed of sheets in two layers and a N-terminal domain, with two hydrophobic pockets (A' and C' (or F' for mouse)). The crystal structure of CD1d-KRN7000 complex¹² revealed that the lipidic chains of KRN7000 are loaded into the hydrophobic pockets of CD1d protein, stabilized by the hydrophobic interactions with their amino acid residues (Figure 1.6 A). On the other hand, the sugar moiety is positioned on the surface of CD1d protein ready to interact with TCR. The X-ray structure data and MD simulations¹³ indicated the presence of a stabilizing proton bond network involving polar aminoacid residues of CD1d (Asp151 (Asp153), Asp80 and Thr154 (Thr156)) with heteroatoms of both the carbohydrate moiety (1'-O, 2'-OH and 3'-OH) and ceramide fragment (2-NH, 3-OH and 4-OH) of KRN7000 (Figure 1.6 B).

¹¹ For detailed reviews, see: (a) Laurent, X.; Bertin, B.; Renault, N.; Farce, A.; Speca, S.; Milhomme, O.; Millet, R.; Desreumaux, P.; Hénon, E.; Chavatte, P. *J. Med. Chem.* **2014**, *57*, 5489–5508. (b) Tashiro, T. *Biosci. Biotechnol. Biochem.* **2012**, *76*, 1055-1067.

¹² (a) Koch, M.; Stronge, V. S.; Shepherd, D.; Gadola, S. D.; Mathew, B.; Ritter, G.; Fersht, A. R.; Besra, G. S.; Schmidt, R. R.; Jones E. Y.; Cerundolo, V. *Nat. Immunol.* **2005**, *6*, 819–826. (b) Zajonc, D. M.; Cantu III, C.; Mattner, J.; Zhou, D.; Savage, P. B.; Bendelac, A.; Wilson, Y. A.; Teyton, L. *Nat. Immunol.* **2005**, *6*, 810–818.

¹³ Hénon, E.; Dauchez, M.; Haudrechy, A.; Banchet, A. *Tetrahedron*, **2008**, *64*, 9480–9489.

General Introduction

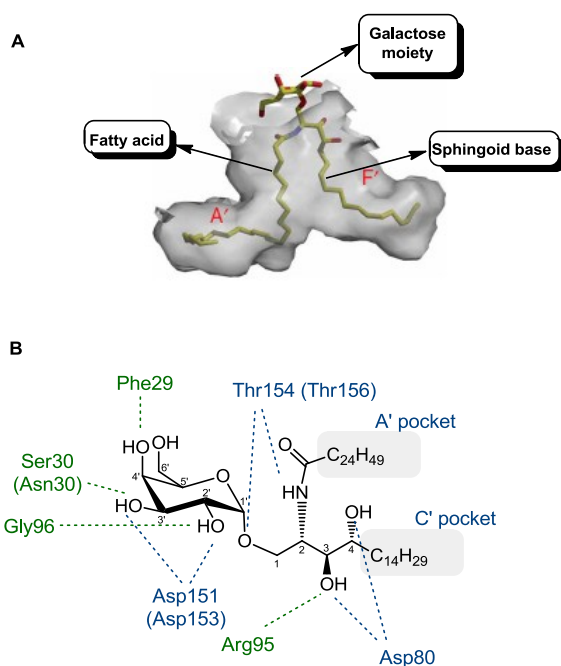


Figure 1.6. A) Model of mouse CD1d-KRN7000 binary complex.¹⁴ B) Schematic representation of Hydrogen-Bonding Network of KRN7000 with human TCR (in green) and human CD1d (in blue). Aminoacids of mouse CD1d and TCR are placed in parenthesis if different.^{11b}

1.2.2.2. Ternary complex (TCR-KRN7000-CD1d)

The crystal structure of the ternary complex was published in 2007 by Borg *et al.*¹⁵ and also provided important information for the understanding of iNKT cell activation mechanism. The interactions mediated by TCR occur through three of its six CDRs (Complementarity Determining Regions). It was found that TCR effectively interacts with sugar head of KRN7000 (2'-OH, 3'-OH, 4'-OH) although an hydrogen bond with 3-OH moiety of sphingosine was also observed (Figure 1.6).

¹⁴ Zajonc, D. M.; Cantu, C., III; Mattner, J.; Zhou, D.; Savage, P. B.; Bendelac, A.; Wilson, I. A.; Teyton, L. *Nat. Immunol.* **2005**, *6*, 810-818.

¹⁵ Borg, N. A.; Wun, K. S.; Kjer-Nielsen, L.; Wilce, M. C. J.; Pellicci, D. G.; Koh, R.; Besra, G. S.; Bharadwaj, M.; Godfrey, D. I.; McCluskey, J.; Rossjohn, J. *Nature.* **2007**, *448*, 44-49.

Interestingly, it was also suggested that additional strong stabilizing forces occur between TCR and CD1d helices. The critical role of the TCR-CD1d interactions was also highlighted by Nadas *et al.*,¹⁶ who showed, via computational simulations, that the deletion of some aa residues such as Asp80 (CD1d), Arg95 (TCR) or Glu83 (TCR) provoked major impact on TCR binding affinity.

1.3. STRUCTURE-ACTIVITY RELATIONSHIP STUDIES ON KRN7000

Since the discovery of KRN7000, intensive research have been focused on its structural modification in order to generate new analogues with a cytokine biased response and provide more information for a correct understanding of the iNKT cell activation mechanism. In this sense, a large number of structure-activity relationship (SAR) studies have been described, successfully revealing critical structural patterns that effectively polarise the immune response toward a T_H1 or T_H2 response.¹¹

The structural alterations can be divided in four groups: substitution and variation of the sugar (1), modification of the configuration and the nature of the glycosidic bond (2), modification of the polar portion of the ceramide (3) and variation on the lipid chains (4) (Figure 1.7).

¹⁶ Nadas, J.; Li, C.; Wang, P. G. *J. Chem. Inf. Model.* **2009**, *49*, 410–423.

General Introduction

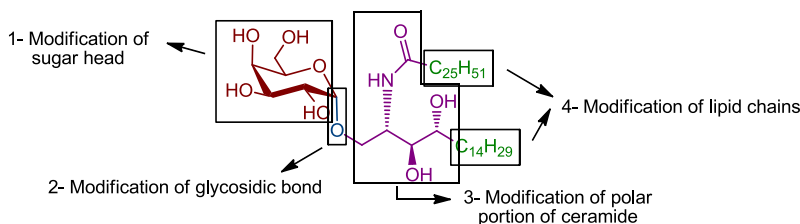


Figure 1.7. Structural modifications for synthesis of KRN7000 analogues.

1.3.1. Modifications on the sugar head and glycosidic bond

Initial SAR studies of KRN7000 were focused on its carbohydrate fragment. From the extensive data obtained, some conclusions were drawn. Firstly, different sugar heads¹⁷ such as glucose, mannose or fucose were tested being the original galactopyranoside the most potent analogue. Disaccharide heads were also tested providing unsuccessful results. Furthermore, it was concluded that α -configuration is a structural requirement for iNKT cell activation since most β -pyranosides were almost inactive. More recently, nonglycosidic analogues bearing noncyclic heads such as threitol¹⁸ have been synthesized showing a T_H1 response but being less potent than KRN7000 (Figure 1.8).

Modifications on the different hydroxyl groups of the galactose head were posteriorly studied (Figure 1.8).¹⁹ From the results, it seemed

¹⁷ (a) Kawano, T.; Cui, J.; Koezuka, Y.; Toura, I.; Kaneko, Y.; Motoki, K.; Ueno, H.; Nakagawa, R.; Sato, H.; Kondo, E.; Koseki, H.; Taniguchi, M. *Science*, **1997**, *278*, 1626–1629. (b) Kobayashi, E.; Motoki, K.; Yamaguchi, Y.; Uchida, T.; Fukushima, H.; Koezuka, Y. *Bioorg. Med. Chem.* **1996**, *4*, 615–619. (c) Motoki, K.; Kobayashi, E.; Uchida, T.; Fukushima, H.; Koezuka, Y. *Bioorg. Med. Chem. Lett.* **1995**, *5*, 705–710. (d) Motoki, K.; Morita, M.; Kobayashi, E.; Uchida, T.; Akimoto, K.; Fukushima, H.; Koezuka, Y. *Biol. Pharm. Bull.* **1995**, *18*, 1487–1491.

¹⁸ (a) Reddy, B. G.; Silk, J. D.; Salio, M.; Balamurugan, R.; Shepherd, D.; Ritter, G.; Cerundolo, V.; Schmidt, R. R. *ChemMedChem*, **2009**, *4*, 171–175. (b) Silk, J. D.; Salio, M.; Reddy, B. G.; Shepherd, D.; Gileadi, U.; Brown, J.; Masri, S. H.; Polzella, P.; Ritter, G.; Besra, G. S.; Jones, E. Y.; Schmidt, R. R.; Cerundolo, V. *J. Immunol.* **2008**, *180*, 6452–6456.

¹⁹ For some selected examples, see: (a) Raju, R.; Castillo, B. F.; Richardson, S. K.; Thakur, M.; Severins, R.; Kronenberg, M.; Howell, A. R. *Bioorg. Med. Chem. Lett.* **2009**, *19*, 4122–4125. (b) Xia, C.; Zhang, W.; Zhang, Y.; Chen, W.; Nadas, J.; Severin, R.; Woodward, R.; Wang, B.; Wang, X.; Kronenberg, M.; Wang, P. G. *ChemMedChem*, **2009**, *4*, 1810–1815. (c) Wu, D.; Xing, G.-W.; Poles, M. A.; Horowitz, A.; Kinjo, Y.; Sullivan, B.; Bodmer-Narkevitch, V.; Plettenburg, O.; Kronenberg, M.;

clear that 2' hydroxyl moiety was critical for iNKT cell recognition since any replacement or suppression completely inhibited activation. Similarly, removal or substitution of 3' or 4' hydroxyl groups resulted in decrease of activity or complete inhibition. In these cases, however, analogues bearing sulfonyl²⁰ and phenylethyl ether²¹ moieties at positions 3 and 4 respectively showed similar activities as KRN7000.

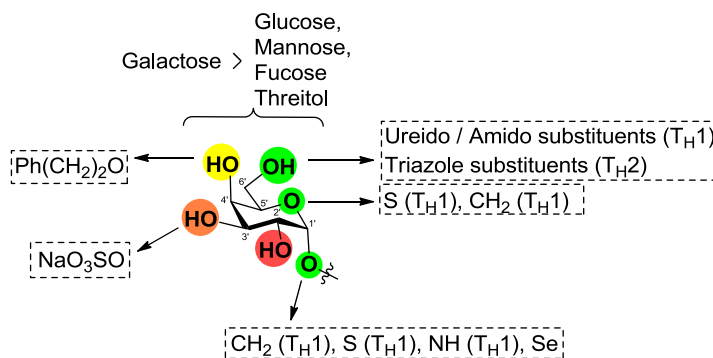


Figure 1.8. Representation of the relative effect of the substitution at different positions in the sugar moiety (red for the less tunable, green for the most tunable) and some relevant examples.

On the other hand, a huge family of analogues bearing different substituents at position 6' have been synthesized providing, most of them, satisfactory results. A relevant example was "Nu- α -GalCer"²² bearing an ureido group in this position, which showed a T_H1 polarized

Tsuji, M.; Ho, D. D.; Wong, C-H. *Proc. Natl. Acad. Sci. USA.* **2005**, *102*, 1351–1356. (d) Barbieri, L.; Costantino, V.; Fattorusso, E.; Mangoni, A.; Basilico, N.; Mondani, M.; Taramelli, D. *Eur. J. Org. Chem.* **2005**, 3279–3285. (e) Barbieri, L.; Costantino, V.; Fattorusso, E.; Mangoni, A.; Aru, E.; Parapini, S.; Taramelli, D. *Eur. J. Org. Chem.* **2004**, 468–473. (f) Miyamoto, K.; Miyake, S.; Yamamura, T. *Nature.* **2001**, *413*, 531–534.

²⁰ (a) Franchini, L.; Matto, P.; Ronchetti, F.; Panza, L.; Barbieri, L.; Costantino, V.; Mangoni, A.; Cavallari, M.; Mori, L.; De Libero, G. *Bioorg. Med. Chem.* **2007**, *15*, 5529–5536. (b) Xing, G-W.; Wu, D.; Poles, MA.; Horowitz, A.; Tsuji, M.; Ho, DD.; Wong, C-H. *Bioorg. Med. Chem.* **2005**, *13*, 2907–2916.

²¹ Zhang, W.; Xia, C.; Nadas, J.; Chen, W.; Gu, L.; Wang, P. G. *Bioorg. Med. Chem.* **2011**, *19*, 2767–2776.

²² Trappeniers, M.; Beneden, K. V.; Decruy, T.; Hillaert, U.; Linclau, B.; Elewaut, D.; Calenbergh, S. *V. J. Am. Chem. Soc.* **2008**, *130*, 16468–16469.

General Introduction

response (Figure 1.9). Crystallographic data²³ of TCR-"Nu- α -GalCer"-CD1d showed that the ligand is further stabilized by the interaction of the carbonyl group of the ureido moiety with Thr159 residue of CD1d. Otherwise, a set of 6'-triazole substituted analogues were also reported exhibiting modest T_H2 response.²⁴ As commented before, there is no observed contacts between 6'-OH and CD1d or TCR. Instead, it is exposed to solvent and thus allows the fit of bulky groups.^{12,14}

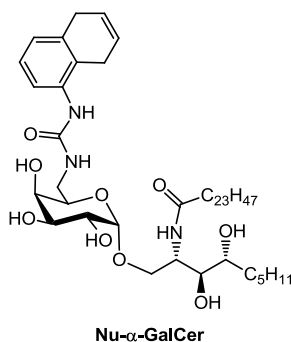


Figure 1.9. Structure of Nu- α -GalCer.

The configuration and nature of the glycosidic bond have also been investigated showing apparently contrasting results. As commented before, α -configuration was required for iNKT cell activation. However, the substitution of the anomeric oxygen atom by others gave intriguing results. For example, α -C-GalCer²⁵ induced a highly potent release of T_H1-type cytokines in mice, whereas it resulted inactive in human cells.²⁶ On the contrary, the S-analogue of KRN7000 proved inactive in mice²⁷

²³ Aspeslagh, S.; Li, Y.; Yu, E. D.; Pauwels, N.; Trappeniers, M.; Girardi, E.; Decruy, T.; Beneden, K. V.; Venken, K.; Drennan, M.; Leybaert, L.; Wang, J.; Franck, R. W.; Calenbergh, S. V.; Zajonc, D. M.; Elewaut, D. *EMBO J.* **2011**, *30*, 2294–2305.

²⁴ Jervis, P. J.; Graham, L. M.; Foster, E. L.; Cox, L. R.; Porcelli, S. A.; Besra, G. S. *Bioorg. Med. Chem. Lett.* **2012**, *22*, 4348–4352.

²⁵ For a review of α -C-GalCer, see: Franck, R. W.; Tsuji, M. *Acc. Chem. Res.* **2006**, *39*, 692–701.

²⁶ Li, X.; Chen, G.; Garcia-Navarro, R.; Franck, R. W.; Tsuji, M. *Immunology.* **2008**, *127*, 216–225.

²⁷ (a) Dere, R. T.; Zhu, X. *Org. Lett.* **2008**, *10*, 4641–4644. (b) Blauvelt, M. L.; Khalili, M.; Jaung, W.; Paulsen, J.; Anderson, A. C.; Brian Wilson, S.; Howell, A. R. *Bioorg. Med. Chem. Lett.* **2008**, *18*, 6374–6376.

but has been recently reported to generate a T_H1 response in humans.²⁸ Finally the α -Se-GalCer²⁹ counterpart has also been recently synthesized but its biological behaviour has not been tested yet.

1.3.2. Modifications at the ceramide moiety

1.3.2.1. Modifications on the polar part

Modifications on the polar part of ceramide were quite useful for determining the key role of this fragment in the activation of iNKT Cells (Figure 1.10). For instance, a complete loss of activity was detected when both hydroxyl groups at positions 3 and 4 were removed.³⁰ This lack of activity was in agree with the aforementioned crystallographic data^{12,14} and MD simulations¹³ which showed interactions of both 3-OH and 4-OH moieties with amino acids residues of either CD1d and TCR crystal structures. The hydroxyl moiety in position 3 proved to be more crucial than the one at C-4 since 3-deoxy analogue³¹ showed reduced activity while 4-deoxy analogue³² exhibited activity equivalent to KRN7000. Similarly, when hydroxyl groups were replaced by amino moieties, dramatic to moderate lowering of activity was observed.³³

Linclau and co-workers provided an interestingly T_H1 biased analogue in which both the hydroxyl and proton moieties in position 4

²⁸ Hogan, A. E.; O'Reilly, V.; Dunne, M. R.; Dere, R. T.; Zeng, S. G.; O'Brien, C.; Amu, S.; Fallon, P. G.; Exley, M. A.; O'Farrelly, C.; Zhu, X.; Doherty, D. G. *Clin. Immunol.* **2011**, *140*, 196–207.

²⁹ McDonagh, A. W.; Mahon, M. F.; Murphy, P. V. *Org. Lett.* **2016**, *18*, 552–555.

³⁰ Sidobre, S.; Hammond, K. J. L.; Bénazet-Sidobre, L.; Maltsev, S. D.; Richardson, S. K.; Ndonge, R. M.; Howell, A. R.; Sakai, T.; Besra, G. S.; Porcelli, S. A.; Kronenberg, M. *Proc. Natl. Acad. Sci.* **2004**, *101*, 12254–12259.

³¹ Baek, D. J.; Seo, J.-H.; Lim, C.; Kim, J. H.; Chung, D. H.; Cho, W.-J.; Kang, C.-Y.; Kim, S. *Med. Chem. Lett.* **2011**, *2*, 544–548.

³² (a) Lacône, V.; Hunault, J.; Pipelier, M.; Blot, V.; Lecourt, T.; Rocher, J.; Turcot-Dubois, A.-L.; Marionneau, S.; Douillard, J.-Y.; Clément, M.; Le Pendu, J.; Bonneville, M.; Micouin, L.; Dubreuil, D. *J. Med. Chem.* **2009**, *52*, 4960–4963. (b) Ndonge, R. M.; Izmirian, D. P.; Dunn, M. F.; Yu, K. O. A.; Porcelli, S. A.; Khurana, A.; Kronenberg, M.; Richardson, S. K.; Howell, A. R. *J. Org. Chem.* **2005**, *70*, 10260–10270.

³³ Trappeniers, M.; Chofoor, R.; Aspeslagh, S.; Li, Y.; Linclau, B.; Zajonc, D. M.; Elewaut, D.; Calenbergh, S. V. *Org. Lett.* **2010**, *12*, 2928–2931.

General Introduction

were replaced by fluorine atoms.³⁴ The authors suggested that the introduction of fluorine atoms might increase the proton donor ability of the vicinal 3-OH group, which is expected to enhance its interaction with Asp-80 (CD1d). This stronger binding affinity would be the responsible for the T_H1 biased response.

The same authors³⁵ also used this last reasoning in order to modulate the interaction of the 2-NH moiety of KRN7000 with Thr 154 (CD1d). With this purpose, they inserted two fluorine atoms in α position to the amide carbonyl group. This fluorination should again increase the proton binding donor ability of 2-NH moiety obtaining thus more stable CD1d-glycolipid complex leading to a T_H1 biased response. However, a slightly T_H2 selective response was observed for this new analogue. This unexpected behaviour was attributed to a possible conformational change of the amido moiety, induced by fluorine atoms, which could perturb the hydrogen-bonding network required for stable complex formation.

A number of studies have also been addressed to the modification of the 2-amido moiety. Some relevant examples are the substitution of the amide by ester³⁶ or sulphonamide³⁷ structures both of which resulted in T_H2 biased responses. Similarly, triazole-containing KRN7000 analogues³⁸ induced preferential release of IL-4 versus IFN- γ . On the

³⁴ Leung, L.; Tomassi, C.; Van Beneden, K.; Decruy, T.; Elewaut, D.; Elliott, T.; Al-Shamkhani, A.; Ottensmeier, C.; Van Calenbergh, S.; Werner, J.; Williams, T.; Linclau, B. *Org. Lett.* **2008**, *10*, 4433–4436.

³⁵ Leung, L.; Tomassi, C.; Van Beneden, K.; Decruy, T.; Trappeniers, M.; Elewaut, D.; Gao, Y.; Elliott, T.; Al-Shamkhani, A.; Ottensmeier, C.; Werner, J. M.; Williams, A.; Van Calenbergh, S.; Linclau, B. *ChemMedChem*. **2009**, *4*, 329–334.

³⁶ Shiozaki, M.; Tashiro, T.; Koshino, H.; Nakagawa, R.; Inoue, S.; Shigeura, T.; Watarai, H.; Taniguchi, M.; Mori, K. *Carbohydr. Res.* **2010**, *345*, 1663–1684.

³⁷ Tashiro, T.; Hongo, N.; Nakagawa, R.; Seino, K.; Watarai, H.; Ishii, Y.; Taniguchi, M.; Mori, K. *Bioorg. Med. Chem.* **2008**, *16*, 8896–8906.

³⁸ Lee, T.; Cho, M.; Ko, S.-Y.; Youn, H.-J.; Baek, D. J.; Cho, W.-J.; Kang, C.-Y.; Kim, S. *J. Med. Chem.* **2007**, *50*, 585–589.

contrary, thioamido, ureo and carbamate replacements lead to T_{H1} -biased analogues.³⁹

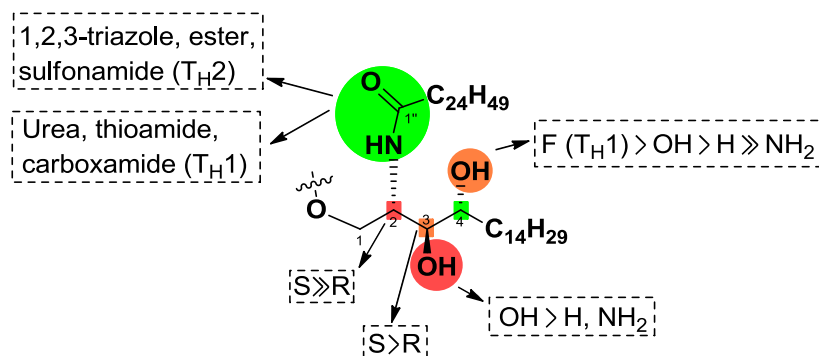


Figure 1.10. Representation of the relative effect of the substitution at different positions in the sugar moiety (red for the less changeable, green for the most changeable) and some relevant examples.

These results highlight the role of 2-amido moiety in iNKT cell stimulation since structural changes lead to different iNKT cell activations and are in agree with the reported crystal structures^{12,14} and MD studies¹³ which manifested the involvement of NH group in a strong H-bonding network (Figure 1.6, B).

Finally, alterations on the sphingoid backbone configuration and its biological impact have also been tested.⁴⁰ From the results it seems that natural configuration (2*S*, 3*S*, 4*R*) of phytosphingosine is the most active one since any change provided no improvements. Stereochemical modifications in position 2 were more detrimental than in position 3, while inversion of configuration in position 4 produced the lowest impact.

1.3.2.2. Modifications on the lipid chain

³⁹ Wojno, J.; Jukes, J.-P.; Ghadbane, H.; Shepherd, D.; Besra, G. S.; Cerundolo, V.; Cox, L. R. *ACS Chem. Biol.* **2012**, *7*, 847–855.

⁴⁰ Park, J.-J.; Lee, J. H.; Ghosh, S. C.; Bricard, G.; Venkataswamy, M. M.; Porcelli, S. A.; Chung, S.-K. *Bioorg. Med. Chem. Lett.* **2008**, *18*, 3906–3909.

General Introduction

SAR studies on the lipidic chains of KRN7000 have resulted in the discovery of analogues with attractive biased cytokine production, revealing their pivotal role in iNKT cell activation process. In fact, OCH,⁴¹ a truncated KRN7000 analogue (Figure 1.11), was the first one to induce a T_H2-biased response, although its activity in humans was relatively weak. Its structure mainly differs from that of KRN7000 in its reduced sphingosine chain length (from C18 to C9).

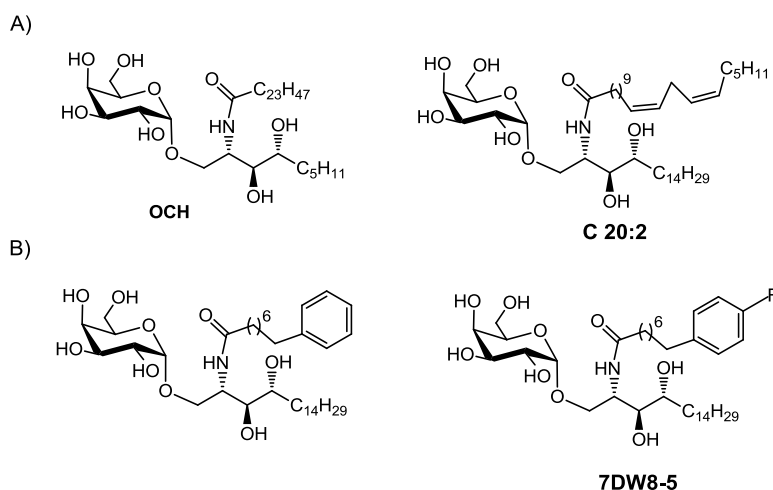


Figure 1.11. Examples of structural modifications of KRN7000 leading to a A) T_H2 response or B) T_H1 response.

Since then, various studies⁴² focused on the effect of modulating the length of sphingosine and acyl chains on iNKT cell activation. The results showed a general tendency in which longer chains (up to C26 for acyl chain and C14 for sphingoid base) lead to potent T_H1 responses, while shorter ones result in lower activation levels with preferential T_H2

⁴¹ Miyamoto, K.; Miyake, S.; Yamamura, T. *Nature*. **2001**, *413*, 531–534.

⁴² (a) Toba, T.; Murata, K.; Nakanishi, K.; Takahashi, B.; Takemoto, N.; Akabane, M.; Nakatsuka, T.; Imajo, S.; Yamamura, T.; Miyake, S.; Annoura, H. *Bioorg. Med. Chem. Lett.* **2007**, *17*, 2781–2784. (b) Goff, R. D.; Gao, Y.; Mattner, J.; Zhou, D.; Yin, N.; Cantu, C.; Teyton, L.; Bendelac, A.; Savage, P. B. *J. Am. Chem. Soc.* **2004**, *126*, 13602–13603.

cytokine release. McCarthy *et al.*⁴³ confirmed the tremendous effect of the lipid chain length on both the ligand affinity for CD1d protein as well as the subsequent recognition by iNKT cells. They effectively showed that the CD1d-ligand dissociation rates increased while shortening either acyl or sphingosine chains. Interestingly, they also observed that while the truncation of phytosphingosine fragment reduced the binding with TCR receptor, the length of acyl chain barely altered the iNKT TCR binding affinity. This result explained the lower levels of cytokine production by "OCH". The authors suggested that the different positioning of the shorter chain of OCH in CD1d groove might alter either the position of the sugar head and/or cause a shift on the CD1d helices making more difficult the posterior TCR recognition. Subsequent MD simulations⁴⁴ of TCR-OCH-CD1d interaction supported the last hypothesis showing a variation of carbohydrate orientation as well as deviation of CD1d amino acid residues making more difficult the binding with TCR.

Lipid chain shortening is not the unique known modification leading to a T_H2 response. Indeed, it was found that the incorporation of one or two double bonds ("C 20:2" analogue in Figure 1.11 A) in the acyl fragment of KRN7000 while maintaining considerable chain length, led to a stronger T_H2 profile than "OCH" with higher activation levels.⁴⁵ In contrast, the same compound with a truncated sphingosine chain was only as potent as "OCH".⁴⁶ These results could be difficultly explained in terms of energetic behaviour of the ternary complex since

⁴³ McCarthy, C.; Shepherd, D.; Fueire, S.; Stronge, V. S.; Koch, M.; Illarionov, P. A.; Bossi, G.; Salio, M.; Denkberg, G.; Reddington, F.; Tarlton, A.; Reddy, B. G.; Schmidt, R. R.; Reiter, Y.; Griffiths, G. M.; Van der Merwe, P. A.; Besra, G. S.; Jones, E. Y.; Batista, F. D.; Cerundolo, V. *J. Exp. Med.* **2007**, *1131*–1144.

⁴⁴ Hénon, E.; Dauchez, M.; Haudrechy, A.; Banchet, A. *Tetrahedron*. **2008**, *64*, 9480–9489.

⁴⁵ Yu, K. O. A.; Im, J. S.; Molano, A.; Dutronc, Y.; Illarionov, P. A.; Forestier, C.; Fujiwara, N.; Arias, I.; Miyake, S.; Yamamura, T.; Chang, Y.-T.; Besra, G. S.; Porcelli, S. A. *Proc. Natl. Acad. Sci.* **2005**, *102*, 3383–3388.

⁴⁶ Velmourougane, G.; Raju, R.; Bricard, G.; Im, J. S.; Besra, G. S.; Porcelli, S. A.; Howell, A. R. *Bioorg. Med. Chem. Lett.* **2009**, *19*, 3386–3388.

General Introduction

the rigid acyl chain of "C 20:2" is expected to fit the curved CD1d cavity stabilizing the CD1d-ligand-TCR complex and hence providing T_H1-biased response, instead of the T_H2 obtained. Therefore, additional aspects might contribute to the polarization of iNKT cell stimulation. Although interesting explanations have been suggested in this sense,⁴⁷ the nature of this behaviour still remains unclear.

A described lipid modification leading to selective and potent T_H1 response is the incorporation of an aromatic group at the end of truncated acyl or sphingosine chains (Figure 1.11 B).⁴⁸ Interestingly, compounds bearing a phenyl ring at the acyl chain exhibited remarkable enhanced binding affinities towards CD1d protein than KRN7000.^{48c,e} Concretely, the analogue bearing a F atom in *para* position of the aromatic ring,^{48c} (Figure 1.11, 7DW8-5) showed a 100-fold higher affinity for both human and mouse CD1d compared to KRN7000. In addition it also proved to stimulate higher amounts of IFN- γ release than KRN7000, showing enhanced adjuvant effect in HIV and malaria vaccines in mice and recently entered in phase I clinical trials.⁴⁹ Computational studies^{48d,g} showed that phenyl rings at the acyl chain undergo interactions with some aromatic amino acid residues (Tyr73, Trp40 or Phe70) at the A' channel of CD1d, as well as Van der Waals contacts with non aromatic residues such as Cys12, Gln14, Leu100 and Ala102. In addition, the

⁴⁷ Bai, L.; Constantinides, M. G.; Thomas, S. Y.; Reboulet, R.; Meng, F.; Koentgen, F.; Teyton, L.; Savage, P. B.; Bendelac, A. *J. Immunol.* **2012**, *188*, 3053-3061.

⁴⁸ (a) Wu, T.-N.; Lin, K.-H.; Wu, Y.-T.; Huang, J.-R.; Hung, J.-T.; Wu, J.-C.; Chen, C.-Y.; Chu, K.-C.; Lin, N.-H.; Yu, A. L.; Wong, C.-H. *ACS Chem. Biol.* **2016**, *11*, 3431-3441. (b) Wu, T.-N.; Lin, K.-H.; Chang, Y.-J.; Huang, J.-R.; Cheng, J.-Y.; Yu, A. L.; Wong, C.-H. *Proc. Natl. Acad. Sci.* **2011**, *108*, 17275-17280. (c) Li, X.; Fujio, M.; Imamura, M.; Wu, D.; Vasana, S.; Wong, C.-H.; Ho, D. D.; Tsuji, M. *Proc. Natl. Acad. Sci.* **2010**, *107*, 13010-13015. (d) Schiefner, A.; Fujio, M.; Wu, D.; Wong, C.-H.; Wilson, I. A. *J. Mol. Biol.* **2009**, *394*, 71-82. (e) Liang, P.-H.; Imamura, M.; Li, X.; Wu, D.; Fujio, M.; Guy, R. T.; Wu, B.-C.; Tsuji, M.; Wong, C.-H. *J. Am. Chem. Soc.* **2008**, *130*, 12348-12354. (f) Chang, Y.-J.; Huang, J.-R.; Tsai, Y.-C.; Hung, J.-T.; Wu, D.; Fujio, M.; Wong, C.-H.; Yu, A. L. *Proc. Natl. Acad. Sci.* **2007**, *104*, 10299-10304. (g) Fujio, M.; Wu, D.; Garcia-Navarro, R.; Ho, D. D.; Tsuji, M.; Wong, C.-H. *J. Am. Chem. Soc.* **2006**, *128*, 9022-9023.

⁴⁹ (a) Padte, N. N.; Li, X.; Tsuji, M.; Vasana, S. *Clin. Immunol.* **2011**, *140*, 142-151. (b) For updated information, visit the website: <http://www.alphagalcer.net/index.html> (last visit the 27th of July 2017).

fluorine atom in analogue 7DW8-5 showed further contact with backbone carbonyls of the peptide bonds between residues Cys12, Leu13, and Gln14 in an orthogonal disposition.

In summary, as shown in this section, modification of KRN7000 lipid chains has emerged as a powerful tool for tuning the iNKT cell activation. Apparently the nature of lipidic chains might play key role in the stability of TCR-glycolipid-CD1d complex and thus in the final profile of the released cytokines.

1.4. SYNTHESIS OF KRN7000 - LITERATURE METHODS

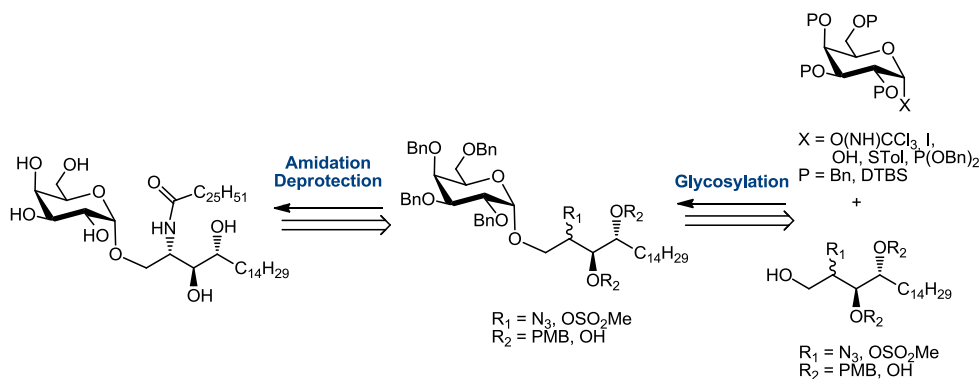
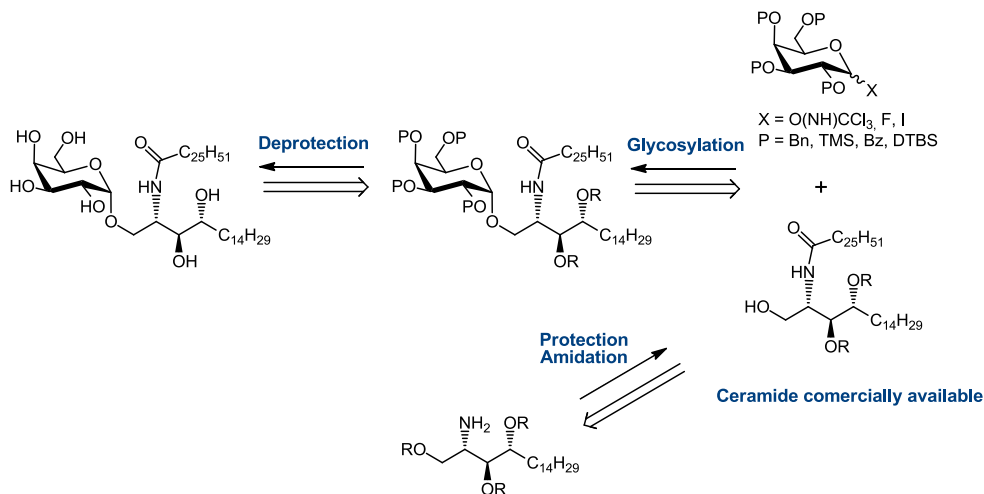
Being a compound with a promising biological activity, KRN7000 has received increasing attention since its discovery. Therefore, different synthetic procedures to obtain this GSL have been published. It is widely accepted that selective formation of α -configured glycosydic bond has been the more challenging step in most of the described KRN syntheses. For this reason, the reported syntheses can be classified into three categories depending on the stage in which glycosylation is performed:⁵⁰ A) total construction of ceramide moiety, followed by coupling with the sugar⁵¹ (Scheme 1.1); B) glycosylation of sphingosine backbone, and

⁵⁰ Banchet-Cadeddu, A.; Hénon, E.; Dauchez, M.; Renault, J-H.; Monneaux, F.; Haudrechy, A. *Org. Biomol. Chem.* **2011**, *9*, 3080–3104.

⁵¹ (a) Boutureira, O.; Morales-Serna, J. A.; Díaz, Y.; Matheu, M. I.; Castellón, S.; *Eur. J. Org. Chem.* **2008**, *11*, 1851-1854. (b) Du, W.; Kulkarni, S. S.; Gervay-Hague, J. *Chem. Commun.* **2007**, 2336-2338. (c) Kimura, A.; Imamura, A.; Ando, H.; Ishida, H.; Kiso, M. *Synlett* **2006**, 2379-2382. (d) Xia, C.; Yao, O.; Schümann, J.; Rossy, E.; Chen, W.; Zhu, L.; Zhang, W.; De Libero, G.; Wang, P. G. *Bioorg. Med. Chem. Lett.* **2006**, *16*, 2195-2199. (e) Kim, S.; Song, S.; Lee, T.; Jung, S.; Kim, D. *Synthesis*, **2004**, *6*, 847-850. (f) Koezuka, Y.; Kirin Brewery Company Ltd *EU Patent WO98/29534*, **1999**. (g) Takikawa, H.; Muto, S.- E.; Mori, K. *Tetrahedron*, **1998**, *54*, 3141-3150. (h) Morita, M.; Sawa, E.; Yamaji, K.; Sakai, T.; Natori, T.; Koezuka, Y.; Fukushima, H.; Akimoto, K. *Biosci. Biotechnol. Biochem.* **1996**, *60*, 288-292. (i) Morita, M.; Natori, T.; Akimoto, K.; Osawa, T.; Fukushima, H.; Koezuka, Y. *Bioorg. Med. Chem. Lett.* **1995**, *5*, 699-704.

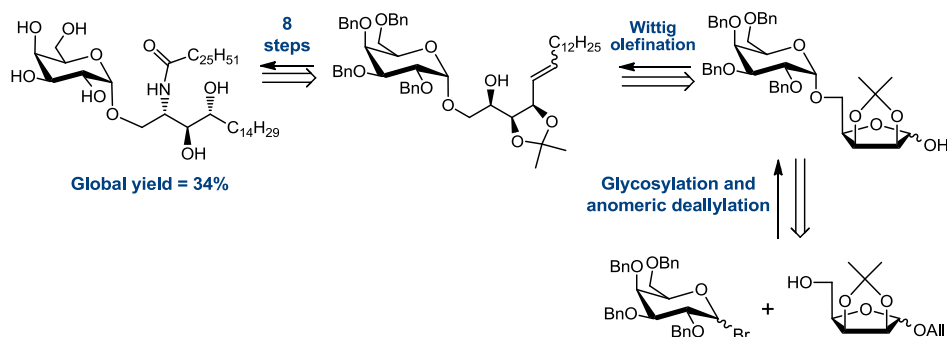
General Introduction

subsequent *N*-acylation⁵² (Scheme 1.2); C) Ceramide formation after glycosylation⁵³ (Scheme 1.3).



⁵² (a) Enders, D.; Terteryan, V.; Paleček, J. *Synthesis*, **2010**, *17*, 2979-2984. (b) Ding, N.; Li, C.; Liu, Y.; Zhang, Z.; Li, Y. *Carbohydr. Res.* **2007**, *342*, 2003-2013; (c) Luo, S.-Y.; Kulkarni, S. S.; Chou, C.-H.; Liao, W.-M.; Hung, S.-C. *J. Org. Chem.* **2006**, *71*, 1226-1229; (d) Lee, A.; Farrand, K. J.; Dickgreber, N.; Hayman, C. M.; Jürs, S.; Hermans, I. F.; Painter, G. F. *Carbohydr. Res.* **2006**, *341*, 2785-2798; (e) Fan, G.-T.; Pan, Y.-S.; Lu, K.-C.; Cheng, Y.-P.; Lin, W.-C.; Lin, S.; Lin, C.-H.; Wong, C.-H.; Fanga, J.-M.; Lin, C.-C. *Tetrahedron*, **2005**, *61*, 1855-1862; (f) Du, W.; Gervay-Hague, J. *Org. Lett.* **2005**, *7*, 2063-2065; (g) Plettenburg, O.; Bodmer-Narkevitch, V.; Wong, C.-H. *J. Org. Chem.* **2002**, *67*, 4559-4564; (h) Figueroa-Pérez, S.; Schmidt, R. R. *Carbohydr. Res.* **2000**, *328*, 95-102.

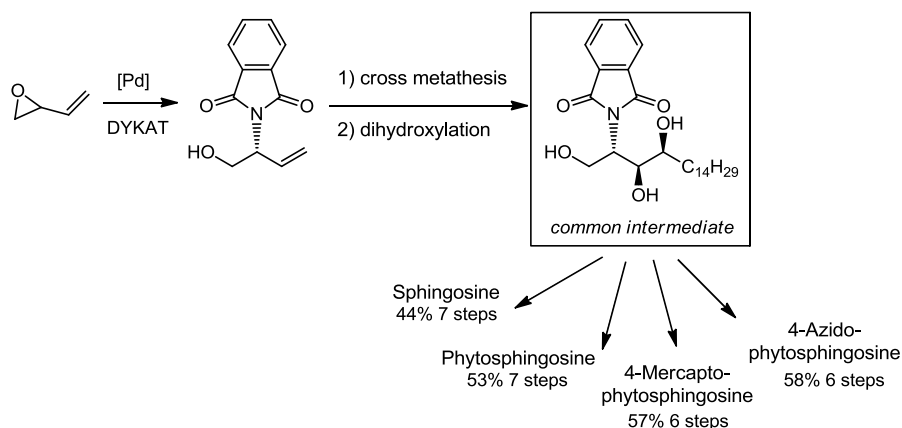
⁵³ (a) Yen, Y. F.; Kulkarni, S. S.; Chang, C. W.; Luo, S. Y. *Carbohydr. Res.* **2013**, *368*, 35-39. (b) Michieletti, M.; Bracci, A.; Compostella, F.; De Libero, G.; Mori, L.; Fallarini, S.; Lombardi, G.; Panza, L. *J. Org. Chem.* **2008**, *73*, 9192-9195. (c) Tsujimoto, T.; Ito, Y. *Tetrahedron Lett.* **2007**, *48*, 5513-5516.



Scheme 1.3. Approach C for the synthesis of KRN7000.

KRN7000 syntheses following pathway **A** or **B** are characterized by the direct glycosylation of ceramide or phytosphingosine derivatives respectively (Scheme 1.1 and Scheme 1.2). Since both compounds are commercially available, these approaches represent the most straightforward methodologies for the synthesis of KRN7000. However, it should be noted that the expensive nature of the starting materials and the general scientific interest for the synthesis of KRN7000 analogues bearing structural modifications on lipid portion prompted researchers towards the preparation of Sphingosine or Ceramide structures and related compounds. Many syntheses have been reported starting from chiral compounds such as D-allosamine, L-arabitol, D-galactose, or D-lyxose among others.^{11b} Alternatively, our group developed an efficient asymmetric 6,7-step synthesis of different sphingoid bases in good yields (44%-58%) (Scheme 1.4). These compounds were obtained from a common intermediate, prepared from butadiene monoepoxide, by a synthetic sequence involving enantioselective allylic substitution, cross-metathesis, and dihydroxylation.

General Introduction



Scheme 1.4. Asymmetric divergent synthesis of different sphingoid bases from butadiene monoepoxide.

As commented before, selective α -glycosylation step is considered the biggest hurdle in the KRN7000 synthesis. Several methodologies have been tested by tuning both glycosyl donor and acceptor properties.⁵⁴ In this sense, it has been shown that glycosylation of sphingosine derivatives (method B) has generally provided higher yields than direct coupling of ceramide moiety (method A) regardless of the glycosyl donor used. It is believed that lower nucleophilicity of 1-hydroxyl group of ceramide moiety because of amide-hydroxyl H-bonding interactions is the responsible for its reduced reactivity.⁵⁵ Furthermore, Xia *et al.*^{51d} showed that the protecting groups on ceramide moiety (method A) strongly influenced the stereoselectivity of the process, apparently by modulating its nucleophilicity. In this way OBn protected ceramides generated β -glycolipid while when electronwithdrawing OBz groups were used α -selectivity was observed.

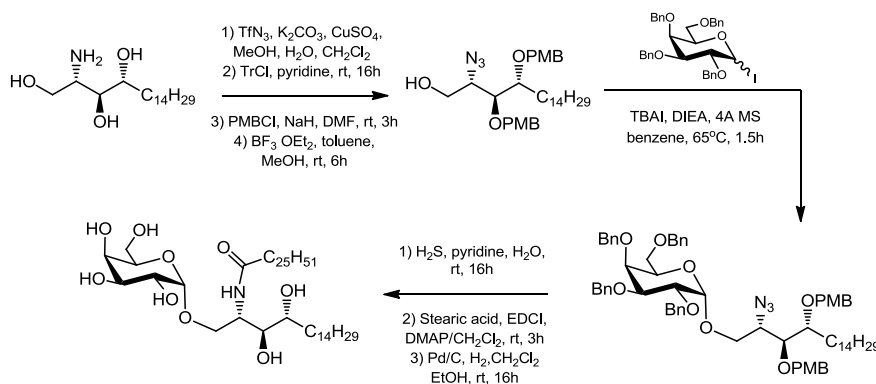
Regarding the glycosyl donor, trichloroacetimidate^{51c,d,e,52g,h} and iodide^{51a,b,52f} leaving groups have provided the most successful results.

⁵⁴ Tashiro, T. *Biosci. Biotechnol. Biochem.* **2012**, *76*, 1055–1067.

⁵⁵ (a) Polt, R.; Szabo, L.; Treiberg, J.; Li, Y.; Hruby, V. J. *J. Am. Chem. Soc.* **1992**, *114*, 10249-10258.
(b) Schmidt, R. R.; Zimmermann, P. *Angew. Chem. Int. Ed. Engl.* **1986**, *25*, 725-726.

Others such as 1-OH free galactoside, thiogalactoside, phosphite, phosphate or acetate have also been tested, generally resulting in lower yields and/or poor stereoselectivities.^{11b}

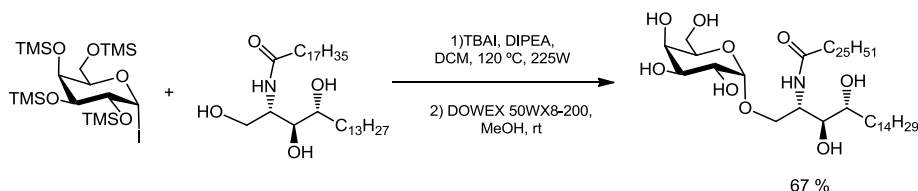
One interesting example of α -stereoselective glycosylation was developed by Gervay-Hague and Du^{51b,52c} making use of glycosyl iodides. This method has proved to be the highest efficient protocol to date for α -glycosylation in the context of KRN7000 preparation. They applied this methodology to the direct glycosylation of 2-azidosphingosine (method B) derivative providing excellent yields and total stereoselectivities (Scheme 1.5).



Scheme 1.5. Synthetic route to KRN7000 employing galactosyl iodides.

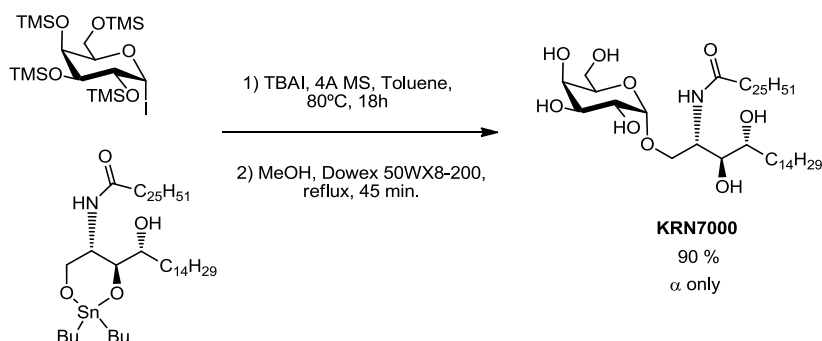
In an effort to provide a more straightforward pathway for KRN7000 preparation, the same authors applied this protocol for the direct glycosylation of ceramide (Scheme 1.6). However, this time, harsh conditions, with the use of high temperatures and MW irradiation were required for achieving a modest 67% yield.

General Introduction



Scheme 1.6. Direct glycosylation of Ceramide via glycosyl iodides.

In this regard, our group achieved excellent yields in ceramide glycosylation, by combining the high stereoselectivity of galactosyl iodides with the enhanced ceramide nucleophilicity by the use of stannyl ethers (Scheme 1.7).⁵⁶

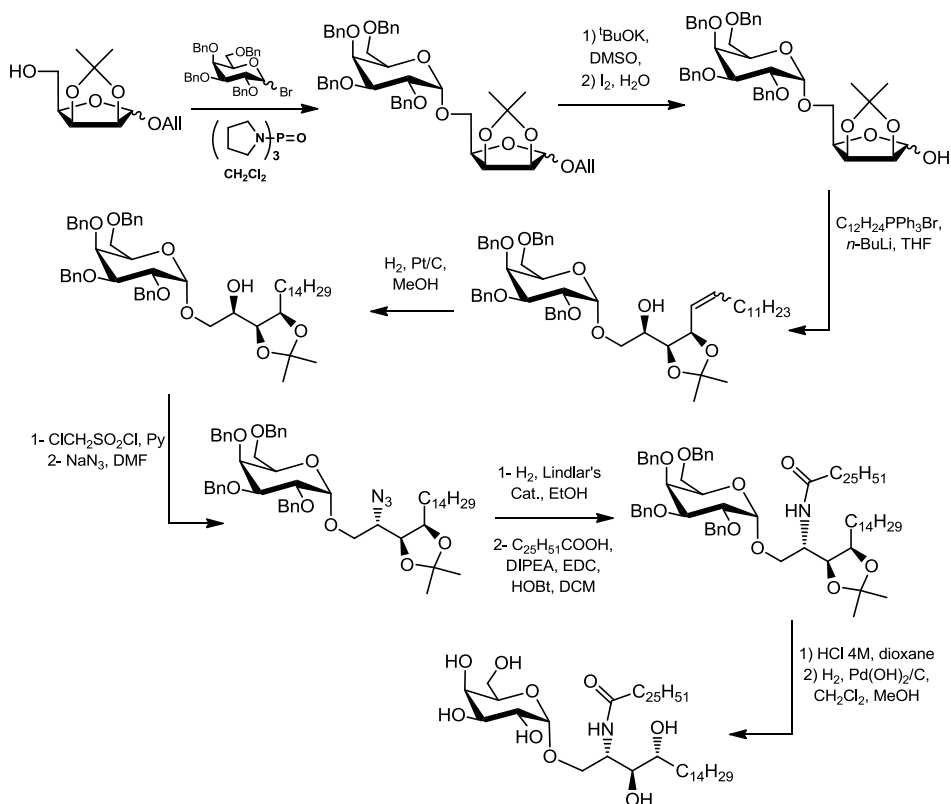


Scheme 1.7. Direct glycosylation of Ceramide via TBAI-mediated glycosylation of stannyl ethers with per-O-silylated galactosyl iodides.

The third methodology (Scheme 1.3) is a more divergent pathway, therefore allowing easier access to lipid-modified KRN7000 analogues. Although this strategy was initially developed in 2007 by Tsujimoto and Ito,^{53c} Panza *et al.*^{53b} developed an improved version one year later. This synthesis is based in the construction of a key disaccharide intermediate, which is subsequently opened in order to introduce the lipidic chains (Scheme 1.8). The disaccharide was obtained from glycosylation of allyl 2,3-O-isopropylidene-D-lyxofuranoside with tetra-O-benzyl-D-galactosyl

⁵⁶ Boutureira, O.; Morales-Serna, J. A.; Díaz, Y.; Matheu, M. I.; Castellón, S. *Eur. J. Org. Chem.* **2008**, *11*, 1851–1854.

bromide in the presence of activating agent tri(1-pyrrolidine)phosphine oxide. The expected α -anomer was obtained in 95% yield along with traces of the β -anomer. After deallylation, Wittig reaction allows the introduction of different lipid chains bearing wide diversity of functional groups. Thus, the furanosidic ring of the disaccharide was opened with the aid of a phosphonium salt and after reduction of the created double bond, the introduction of the azide moiety was performed with NaN_3 . Subsequent reduction of the azide, *N*-acylation of the amine and full deprotection afforded the targeted KRN7000 in a 40% overall yield.

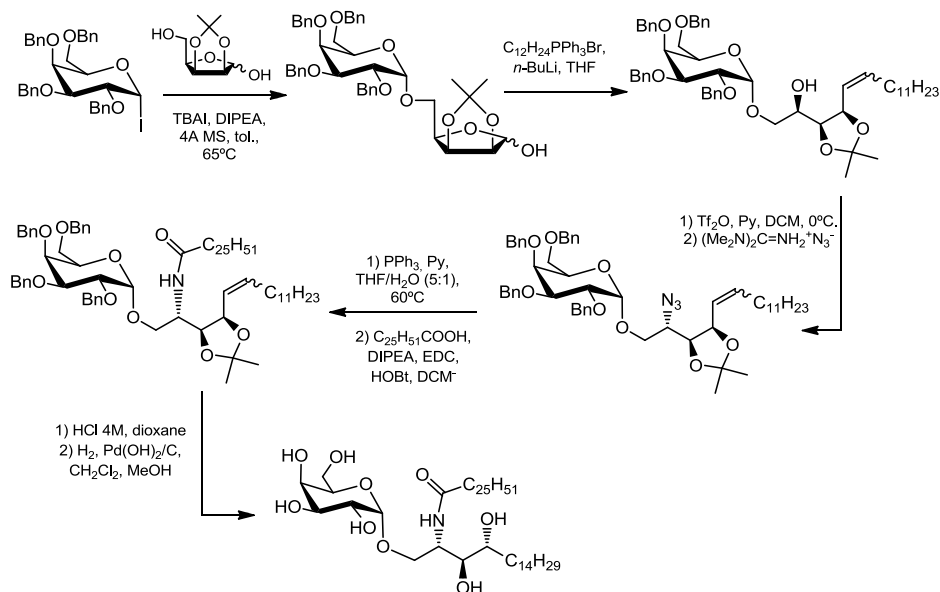


Scheme 1.8. Synthetic approach to KRN7000 by Panza *et al.*

Shortly after this protocol, Yen *et al.*^{53a} developed a shorter version in which the main modification was the use of Gervay Hague's

General Introduction

glycosylation methodology through glycosyl iodides. By this way, complete α -stereoselectivity was achieved in a 63 % yield. Furthermore, the lack of anomeric protection reduced the number of protecting-deprotecting steps. Then, next steps are similar to Panza's strategy: Wittig olefination, azidation, reduction, *N*-acylation and final deprotection afforded KRN7000 in 34% overall yield (Scheme 1.9). As far as we are concerned, this methodology is, to date, the shortest one starting from non-expensive materials.



Scheme 1.9. Synthetic approach to KRN7000 by Yen *et al.*

1.5. IMPORTANCE OF FLUORINE IN MEDICINAL CHEMISTRY

Fluorine chemistry has become a hot topic in many areas of chemical sciences and in the last 20 years it has grown in importance, especially in the field of medicinal chemistry. Some fluorinated minerals such as fluorite (CaF_2) and fluoroapatite ($\text{Ca}_5(\text{PO}_4)_3\text{F}$) are widely present

in nature. However, fluorine-containing organic molecules are scarce in naturally occurring compounds. Despite this fact and although pharmaceuticals are normally inspired by nature, nowadays about 25% of all pharmaceuticals on the market contain fluorine moieties and this number is continuously increasing.⁵⁷

1.5.1. The effect of fluorine on physicochemical properties of bioactive molecules

Although the effect of fluorine on the biological activity of drug-like compounds is generally difficult to predict, introduction of fluorine into a molecule can productively influence conformation, pKa, intrinsic potency, membrane permeability, metabolic pathways and pharmacokinetic properties.⁵⁸ Some of these properties are briefly commented in subsequent sections.

1.5.1.1. Metabolic stability

Oxidation of lipophilic compounds by liver enzymes usually limits their bioavailability (% of the dose reaching the circulatory system). For this reason, high metabolic stability of bioactive compounds is usually requested. The high strength of the C–F bond makes organofluorine compounds more stable towards oxidation than their non-fluorinated analogues. Consequently, and since the van der Waals radius of fluorine (1.47 Å) is intermediate to that of oxygen (1.52 Å) and hydrogen (1.2 Å), F atom is frequently used as an isostere of hydrogen and of hydroxyl groups.

1.5.1.2. pKa and lipophilicity

⁵⁷ Wang, J.; Sánchez-Roselló, M.; Aceña, J. L.; del Pozo, C.; Sorochinsky, A. E.; Fustero, S.; Soloshonok, V. A.; Liu, H. *Chem. Rev.* **2014**, *114*, 2432-2506.

⁵⁸ For key reviews see: (a) Gillis, E. P.; Eastman, K. J.; Hill, M. D.; Donnelly, D. J.; Meanwell, N. A. *J. Med. Chem.* **2015**, *58*, 8315-8359. (b) Swallow, S. *Prog. Med. Chem.* **2015**, *54*, 65-133 (c) Purser, S.; Moore, P. R.; Swallow, S.; Gouverneur, V. *Chem. Soc. Rev.* **2008**, *37*, 320-330; (d) Hagmann, W. K. *J. Med. Chem.* **2008**, *51*, 4359-4369; (e) Kirk, K. L. *J. Fluorine Chem.* **2006**, *127*, 1013-1029.

General Introduction

The pK_a of a drug has a strong effect on its absorption process (permeability) and thus, on its bioavailability. Fluorine is the most electronegative atom in the periodic table. When suitably situated, it greatly affects the acidity-basicity properties of neighbouring functional groups such as alcohols, amines, amides or carboxylic acids (Table 1.1).

Table 1.1. pK_a of acetic acid and ethylamine derivatives at 25 °C in water.^{58a}

Compound	pK _a	Compound	pK _a
CH ₃ COOH	4.76	CH ₃ CH ₂ NH ₂	10.58
CH ₂ F ₂ COOH	2.60	CH ₂ FCH ₂ NH ₂	9.19
CHF ₂ COOH	1.40	CHF ₂ CH ₂ NH ₂	7.45
CF ₃ COOH	0.51	CF ₃ CH ₂ NH ₂	5.40

In this regard, drugs bearing basic functionalities such as nitrogen-containing groups are often troubled by low bioavailability. Introduction of fluorine atoms adjacent to the basic group decreases its basicity, thus enhancing the bioavailability of the compound.

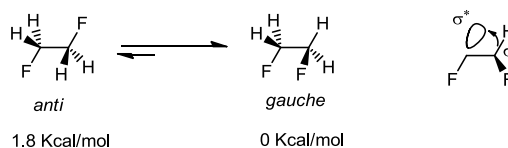
Permeability of a drug is also highly dependent of its lipophilicity, which is usually expressed by a partition coefficient (log P) between 1-octanol and water. High lipophilicities are required for a bioactive molecule to pass through the cell membrane. However, excess of lipophilicity could result in poor solubility and thus incomplete absorption following an oral administration. Most orally administered drugs have log P between 1 and 5. In this sense, fluorine has been used for drug lipophilicity modulation. Böhm and co-workers⁵⁹ observed general slightly higher lipophilicities upon H/F replacement in a series of organic molecules. However, they also concluded that this should not be used as a general rule since some exceptions were observed.

⁵⁹ Böhm, H.-J.; Banner, D.; Bendels, S.; Kansy, M.; Kuhn, B.; Müller, K.; Obst-Sander, U.; Stahl, M. *ChemBioChem* **2004**, *5*, 637–643.

1.5.1.3. Molecular conformation

The introduction of fluorine atoms can modulate the preferred conformation of a molecule either by electronic or steric effects. Regarding the steric effects, the influence of fluorine is expected to be marginal since its van der Waals radius (1.47 Å) is similar to the one of hydrogen atom (1.20 Å). However, the volume of a trifluoromethyl group is roughly twice than that of a methyl group. For this reason, the introduction of a CF₃ group could change the geometry of the molecule.

On the other hand, the electronic properties of fluorine could also modulate conformation of a compound. For example, 1,2-difluoroethane adopts a *gauche* conformation instead of the less sterically demanding *anti* conformation (Scheme 1.10). This observation is explained by reinforcing hyperconjugative interactions in which the $\sigma_{\text{C-H}}$ bonding orbital donates electronic density to the adjacent $\sigma^*_{\text{C-F}}$ anti-bonding orbital.



Scheme 1.10 Stabilization of the *gauche* conformation of 1,2-difluoroethane by hyperconjugation effect.

1.5.2. Role in ligand-protein interactions

Introduction of fluorine into bioactive molecules is also known to affect their noncovalent interactions with other molecules, such as proteins, modulating therefore, their ligand-protein binding affinities.^{58b,60} Understanding of the nature of such interactions has recently received

⁶⁰ Muller, K.; Faeh, C.; Diederich, F. *Science* **2007**, *317*, 1881-1886.

General Introduction

increased attention. Thus, detailed theoretical and experimental investigations indicate that fluorine is able to establish specific intermolecular interactions.⁶¹ On the other hand, it is also known that fluorocarbons are more hydrophobic than hydrocarbons. Therefore, H/F replacement has also been studied in order to exploit the high hydrophobicity of fluorinated compounds, for obtaining stronger ligand-protein binding energies.⁶²

1.5.2.1. Specific intermolecular interactions

Molecular recognition processes between ligands and their hosts (usually proteins) are based on the existence of attractive interactions. Among them, hydrogen bonds are by far the most important ones. However, other non-covalent interactions such as ion-ion or ion-dipole interactions are known to contribute to the binding affinity.⁶³

The large number of ligand-protein crystal structures now available in the literature (PDB and CSD databases), have greatly contributed to the understanding of the recognition processes at atomic level. Observation, in these crystal structures, of several short contacts between fluorine atoms present in ligands with aminoacid residues of proteins have prompted increasing attention on the role of fluorine in drug-protein interactions.

Despite the described low tendency of organic fluorine to undergo hydrogen bonds, short contacts between fluorine and HX moieties (where X=O,N,S) have been observed in the PDB and CSD databases.⁶⁴

⁶¹(a) Xing, L.; Keefer, C.; Brown, M. F. *J. Fluorine Chem.* **2017**, DOI: 10.1016/j.jfluchem.2016.12.013. (b) Pollock, J.; Borkin, D.; Lund, G.; Purohit, T.; DygudaKazimierowicz, E.; Grembecka, J.; Cierpicki, T. *J. Med. Chem.* **2015**, *58*, 7465-7474. (c) Zhou, P.; Zou, J.; Tian, F.; Shang, Z. *J. Chem. Inf. Model.* **2009**, *49*, 2344-2355.

⁶² Mecinović, J.; Snyder, P. W.; Mirica, K. A.; Bai, S.; Mack, E. T.; Kwant, R. L.; Moustakas, D. T.; Héroux, A.; Whitesides, G. M. *J. Am. Chem. Soc.* **2011**, *133*, 14017-14026.

⁶³ Bissantz, C.; Kuhn, B.; Stahl, M. *J. Med. Chem.* **2010**, *53*, 5061-5084.

⁶⁴ Carosati, E.; Sciabola, S.; Crucia, G. *J. Med. Chem.* **2004**, *47*, 5114-5125.

Despite its weak nature (-3 Kcal/mol at most), changes in binding modes and increases in binding affinities have been attributed to these interactions.⁵⁹

Orthogonal multipolar interactions in which fluorine atoms interact with the carbon atom of carbonyl moieties (typically amides) in aminoacid residues are also frequently observed in ligand-protein crystal structures.⁶⁵ These attractive C-F...C=O interactions have received detailed attention in the last years and are characterized by a close orthogonal contact between the two dipolar moieties. A nice example of this kind of interactions was reported by Diederich and co-workers⁶⁶ in their study of fluorinated thrombin inhibitors. The authors observed a 5-fold increase in inhibitor potency upon hydrogen to fluorine exchange which was partially attributed to orthogonal multipolar interactions between the C-F group and a backbone amide carbonyl group. Further recent studies have concluded that the gain on free energy associated to C-F...C=O interactions are modest (0.3 to 0.6 Kcal/mol) and they may not be considered the sole responsible for the gain in binding affinities observed compared to the non-fluorinated analogues.⁶⁷

Within this context, a recent publication⁶⁸ reported the first experimental study of the energies of fluorine bonding in a protein-ligand complex in the absence of solvent. The authors compared activation energies (E_a) for the dissociation of a set of differently fluorinated analogues of stearic acid from β -lactoglobulin protein (Figure 1.12).

⁶⁵ Paulini, R.; Müller, K.; Diederich, F. *Angew. Chem. Int. Ed.* **2005**, *44*, 1788-1805 and references therein.

⁶⁶ Olsen, J. A.; Banner, D. W.; Seiler, P.; Wagner, B.; Tschopp, T.; Obst-Sander, U.; Kansy, M.; Müller, K.; Diederich, F. *ChemBioChem* **2004**, *5*, 666-675.

⁶⁷ (a) Xing, L.; Keefer, C.; Brown, M. F. *J. Fluorine Chem.* **2017**, in press. DOI: 10.1016/j.jfluchem.2016.12.013. (b) Pollock, J.; Borkin, D.; Lund, G.; Purohit, T.; Dyguda-Kazimierowicz, E.; Grembecka, J.; Cierpicki, T. *J. Med. Chem.* **2015**, *58*, 7465-7474.

⁶⁸ Liu, L.; Jalili, N.; Baergen, A.; Ng, S.; Bailey, J.; Derda, R.; Klassen, J. S. *J. Am. Soc. Mass Spectrom.* **2014**, *25*, 751-757.

General Introduction

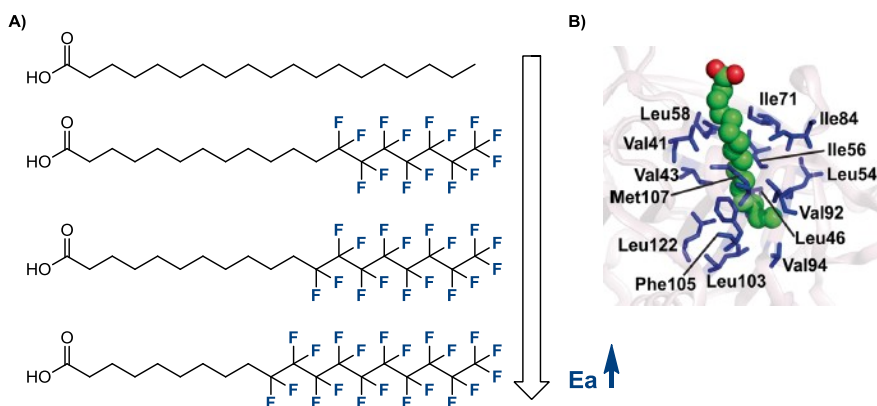


Figure 1.12. A) Increasing fluorination degree in stearic acid analogues leading to higher E_a . B) Amino acid residues involved in fluorine bonding with stearic acid analogues.

They concluded that the average energetic contribution of each CF_2 group to E_a (1.1 Kcal/mol) was larger than the one for each CH_2 moieties (0.8 Kcal/mol). MD simulations of the system pointed fluorine bonding to NH and NH_2 ($\text{F}\cdots\text{HN}-$) moieties present in the amino acid residues of the protein, as the responsible for the higher binding energies of fluorinated analogues.

1.5.2.2. Hydrophobic effect

Generally, the interaction of hydrophobic ligands with proteins is entropically favourable due to the release of water molecules encapsulated in receptor or desolvation of the ligand.⁶⁹ This phenomenon is due to the so-called hydrophobic effect,⁷⁰ which is generally explained as the negative entropy of solvation of hydrophobic solutes in water because of the tendency of the water molecules to "order" around the solute. Therefore, hydrophobic compounds tend to aggregate forcing

⁶⁹ Biffinger, J. C.; Kim, H. W.; DiMugno, S. G. *ChemBioChem* **2004**, *5*, 622–627

⁷⁰ For a general review of hydrophobicity concept, see: Sarkar, A.; Kellogg, G. E. *Curr. Top. Med. Chem.* **2010**, *10*, 67–83.

water molecules to form one larger “cage” structure around the combined solutes, whose surface area will be smaller than the combined surface areas of isolated solutes. This process maximizes the amount of free "disordered" water molecules and thus the entropy.

In this context, although being both hydrophobic in nature, fluoroalkyl compounds have much lower water solubilities than their hydrocarbon counterparts.⁷¹ This greater hydrophobicity has been attributed to the higher molecular cross-sectional area of fluoroalkyl (28.3 Å) compared to alkyl (18.9 Å) leading to increased free-energy penalties for hydration.⁷² For this reason, ligand perfluoroalkylation have become an interesting strategy to exploit the hydrophobic effect in order to increase ligand-protein binding energies. Whitesides *et al.*⁷³ extensively studied this effect in the binding affinities of perfluoroalkyl-containing benzenesulfonamides towards CA II enzyme. The authors showed that fluorinated ligands presented higher interactions than their hydrocarbon counterparts. Furthermore, they exclusively attributed this difference to the greater hydrophobic surface area of the fluorinated analogues.

⁷¹ Krafft, M. P.; Riess, J. G. *J. Polym. Sci.* **2007**, *45*, 1185-1198.

⁷² Dalvi, V. H.; Rossky, P. J. *Proc. Natl. Acad. Sci. U. S. A.* **2010**, *107*, 13603-13607.

⁷³ (a) Mecinović, J.; Snyder, P. W.; Mirica, K. A.; Bai, S.; Mack, E. T.; Kwant, R. L.; Moustakas, D. T.; Héroux, A.; Whitesides, G. M. *J. Am. Chem. Soc.* **2011**, *133*, 14017-14026. (b) Gao, J.; Qiao, S.; Whitesides, G. M. *J. Med. Chem.* **1995**, *38*, 2292-2301.

CHAPTER 2

ANTECEDENTS AND GENERAL OBJECTIVES

As mentioned before, incorporation of fluorine atoms in bioactive molecules with different purposes has gained increasing interest in medicinal chemistry. KRN7000 has not been an exception and to date, several analogues bearing at least one fluorine atom have been reported.

For example, galactose 2-OH,¹ 3-OH or 4-OH² moieties were formally replaced by fluorine atoms in order to gain insights into the role of these hydroxyl groups in TCR binding affinity (compounds **I**, **II** and **III** in Figure 2.1). Since fluorine atoms are described to undergo a range of different interactions with protein structures (see Chapter 1), the authors also aimed to test the ability of these fluorine atoms to participate in the H-bond network of the KRN7000 polar head. However, the 2-deoxy-2-fluoro analogue (**I**, Figure 2.1) showed complete lack of activity while the 3-fluoro and 4-fluoro derivatives (**II** and **III**, Figure 2.1) still presented some NKT cell stimulation although at lower extent than KRN7000.

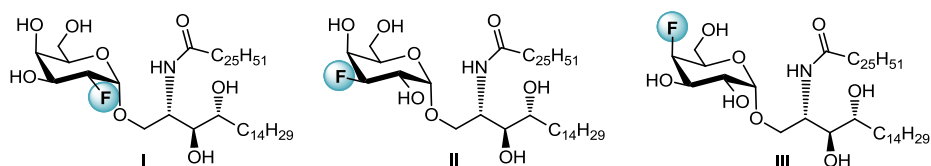


Figure 2.1. KRN7000 analogues fluorinated at galactose head.

Similarly, Hunault and co-workers³ provided evidences for the importance of sphingosine 3-OH moiety by its replacement by one or two F atoms (compounds **IV** and **V** in Figure 2.2). Both fluoro- and difluoro-analogues showed lower activities than KRN7000, highlighting the vital

¹ Barbieri, L.; Costantino, V.; Fattorusso, E.; Mangoni, A.; Basilico, N.; Mondani, M.; Taramelli, D. *Eur. J. Org. Chem.* **2005**, 3279-3285.

² Raju, R.; Castillo, B. F.; Richardson, S. K.; Thakur, M.; Severins, R.; Kronenberg, M.; Howell, A. R. *Bioorg. Med. Chem. Lett.* **2009**, 19, 4122-4125.

³ Hunault, J.; Diswall, M.; Frison, J.-C.; Blot, V.; Rocher, J.; Marionneau-Lambot, S.; Oullier, T.; Douillard, J.-Y.; Guillaume, S.; Saluzzo, C.; Dujardin, G.; Jacquemin, D.; Graton, J.; Le Questel, J.-Y.; Evain, M.; Lebreton, J.; Dubreuil, D.; Le Pendu, J.; Pipelier, M. *J. Med. Chem.* **2012**, 55, 1227-1241.

Antecedents and General Objectives

role of this hydroxyl group in the NKT cell stimulation process and the incapacity of fluorine atoms to restore the native H-bonding network.

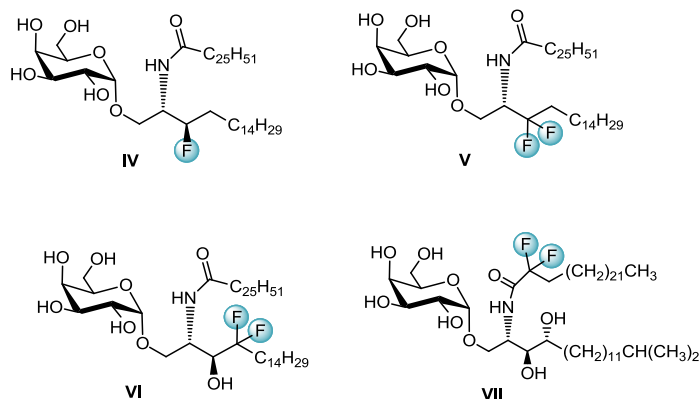


Figure 2.2. KRN7000 analogues fluorinated at polar part of ceramide moiety.

Due to its high electronegativity, fluorine has also been used for modulating H-bond character of vicinal moieties such as OH⁴ or NH.⁵ Indeed, Linclau. *et al.*⁴ synthesized a T_H1 biased KRN7000 analogue by incorporating a difluoromethylene group in α position to the 3-OH functionality (compound **VI** in Figure 2.2). The authors suggested that the CF₂ moiety might effectively enhance the 3-OH hydrogen bond donor ability, increasing interactions with specific CD1d amino acid residues and thus leading to a T_H1 biased response. However, when the same strategy was used for improving the 2-amido NH hydrogen bond donor ability, an unexpected T_H2 biased stimulation was observed (compound **VII** in Figure 2.2).⁵ This unexpected activity was attributed to a possible conformational change of the amido moiety induced by fluorine atoms,

⁴ Leung, L.; Tomassi, C.; Van Beneden, K.; Decruy, T.; Elewaut, D.; Elliott, T.; Al-Shamkhani, A.; Ottensmeier, C.; Van Calenbergh, S.; Werner, J.; Williams, T.; Linclau, B. *Org. Lett.* **2008**, *10*, 4433–4436.

⁵ Leung, L.; Tomassi, C.; Van Beneden, K.; Decruy, T.; Trappeniers, M.; Elewaut, D.; Gao, Y.; Elliott, T.; Al-Shamkhani, A.; Ottensmeier, C.; Werner, J. M.; Williams, A.; Van Calenbergh, S.; Linclau, B. *ChemMedChem* **2009**, *4*, 329–334.

which could perturb the hydrogen-bonding network required for stable complex formation.

As already commented in the previous chapter, analogue 7DW8-5 (Figure 2.3), bearing a terminal phenyl ring with a F atom in *para* position exhibited great CD1d binding affinity as well as a potent T_H1 cytokine release. This analogue is currently under evaluation in phase I clinical trials.⁶ From computational studies⁷ it was found that F atom undergoes multipolar interactions with carbonyl moieties of the peptide bonds between residues Cys12, Leu13, and Gln14. These interactions might therefore contribute to its enhanced CD1d binding affinity. Since then, a series of analogues presenting similar fluorinated aromatic rings have been synthesized showing strong T_H1 responses. Some examples are described in Figure 2.3.

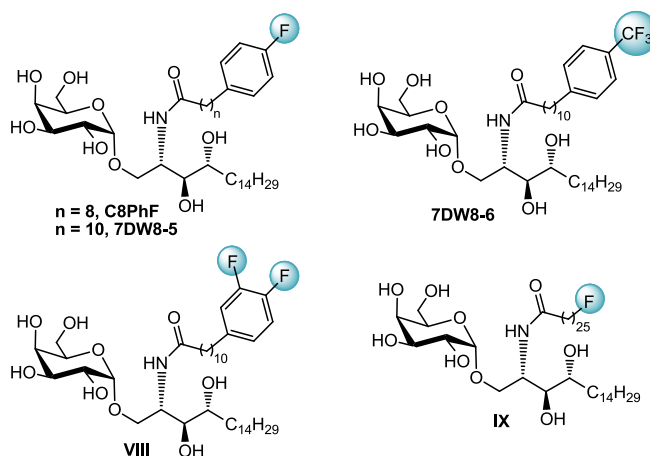


Figure 2.3. KRN7000 analogues fluorinated at acyl chains.

⁶ (a) Li, X.; Huang, J.; Kaneko, I.; Zhang, M.; Iwanaga, S.; Yuda, M.; Tsuji, M. *Expert Rev. Vaccines*. **2017**, 73-80. (b) Xu, X.; Hegazy, W. A.; Guo, L.; Gao, X.; Courtney, A. N.; Kurbanov, S.; Liu, D.; Tian, G.; Manuel, ER; Diamond, D. J.; Hensel, M.; Metelitsa, L. S. *Cancer Res*. **2014**, 74, 6260-6270. (c) Padte, N. N.; Li, X.; Tsuji, M.; Vasani, S. *Clin. Immunol.* **2011**, 140, 142-151. (d) For updated information, visit the website: <http://www.alphagalcer.net/index.html> (last visit the 27th of July 2017).

⁷ Schiefner, A.; Fujio, M.; Wu, D.; Wong, C. H.; Wilson, I. A. *J. Mol. Biol.* **2009**, 394, 71-82.

Antecedents and General Objectives

Very recently, Hossain and co-workers⁸ have synthesized a KRN7000 analogue in which the only modification consisted in a sole H/F replacement at the end of the C25 acyl chain (compound **IX** in Figure 2.3). Interestingly, despite the minimal structural change, this analogue showed a high T_H1 biased response comparable to some of the previously commented aromatic analogues.

From these bibliographic data it is quite apparent that any replacement of hydroxyl moieties (2'-OH, 3'-OH, 4'-OH or 3-OH) by fluorine atoms reduces NKT cell activation levels presumably because of perturbation of the ligand-CD1d hydrogen bond network. On the other hand, insertion of F atoms at ceramide moiety have provided successful results. Apparently, the presence of fluorine units at acyl chains is special of interest, since they seem to greatly stabilize ligand-CD1d complex leading to potent T_H1 biased outcomes. In this regard, and as previously informed in Chapter 1, it has been recently demonstrated that perfluorinated chains produce stronger interactions with hydrophobic cavities of proteins than its hydrocarbon counterparts.

Within this context, and the current knowledge of the beneficial effects of F introduction into organic molecules in ligand-protein recognition processes (e.g. specific fluorine interactions with protein amino acid residues, enhanced hydrophobicity, etc.) already detailed in Chapter 1, the main objective contemplated in the present PhD work is to accomplish the synthesis of KRN7000 analogues of general structure **IX** (Figure 2.4) bearing different degree of fluorination at ceramide fragment.

⁸ Hossain, M. I., Hanashima, S., Nomura, T., Lethu, S., Tsuchikawa, H., Murata, M., Kusaka, H., Kita, S., and Maenaka, K. *Bioorg. Med. Chem.* **2016**, *24*, 3687–3695.

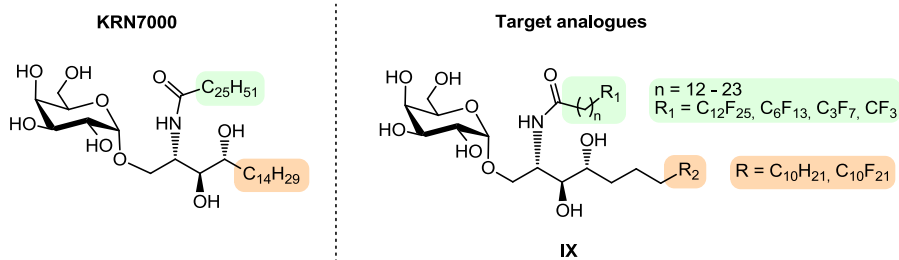


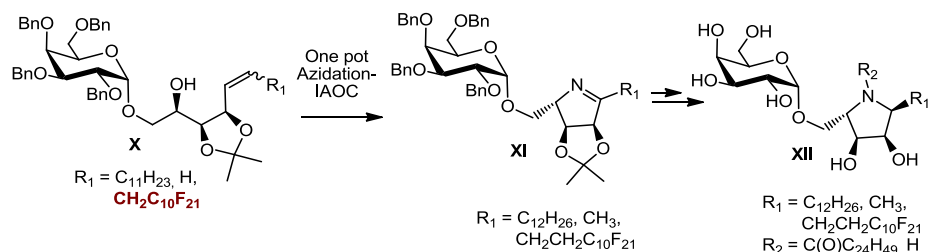
Figure 2.4. Target analogues of KRN7000 with different degree of fluorinated at sphingoid base and/or acyl chain.

These and additional ongoing objectives, aroused during the elaboration of the present work, are distributed in different chapters as follows:

- The research described in Chapter 3 aims to synthesize KRN7000 analogues bearing highly fluorinated acyl chain and/or sphingoid base moieties (Figure 2.4). The major issue to overcome in the preparation of such compounds is the introduction of long fluoroalkyl chains into KRN7000 backbone. In this sense, different strategies such as Wittig olefination, CM coupling as well as radical pathways will be explored.
- The research described in Chapter 4 aims the synthesis of KRN7000 analogues containing a low degree of fluorination on acyl chain (Figure 2.4, analogues bearing CF₃, C₃F₇ and C₆F₁₂ fragments). This time the major challenge would be the synthesis of long carboxylic acids bearing short fluorinated units.
- The research described in Chapter 5 aroused from an unexpected reactivity observed in Chapter 3, where we found that hydroxyalkenes **X** could be converted in pyrroline derivatives **XI** via one pot azidation-1,3-dipolar cycloaddition (Scheme 2.1). These compounds were seen as potential precursors of conformationally restricted KRN7000 analogues **XII**. Therefore, the aim of Chapter 5 is

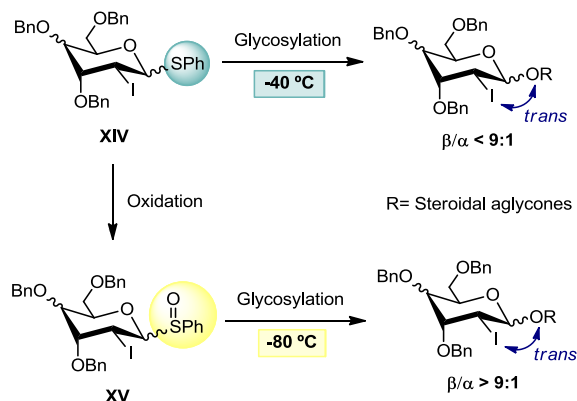
Antecedents and General Objectives

to explore the feasibility of applying this methodology for the synthesis of conformationally restricted KRN7000 analogues.



Scheme 2.1. Synthesis of conformationally rigid KRN7000 analogues via one pot azidation-IAOC.

d) The research described in Chapter 6 deals with the synthesis of a different kind of glycosides, 2-deoxy steroidal glycosides, in an effort to upgrade a previous work performed in our group. The specific objective of this chapter is to improve the stereoselectivity of the glycosylation step, by replacing 2-iodo glycosyl sulphides by their more reactive sulfoxide counterparts. The latter might permit activation at very low temperature, ensuring a precise kinetic control for a complete 1,2-*trans* stereoselective glycosylation assisted by the neighboring bulky iodine (Scheme 2.2).



Scheme 2.2. Glycosylation of thioglycosides vs. sulfoxides.

- e) Finally, the research described in Chapter 7, deals with the preliminar biological evaluation of the synthesized KRN7000 analogues. The two main objectives are: A) To study the interaction process of each lipid with mouse CD1d protein either experimentally and with the aid of molecular dynamic simulations; B) To evaluate the ability of our KRN7000 analogues for stimulating human NKT cells.

CHAPTER 3

SYNTHESIS OF KRN7000 ANALOGUES WITH A HIGH DEGREE OF FLUORINATION

3.1. OBJECTIVES

The main goal in this chapter is to synthesize the three highly fluorinated analogues of KRN7000 shown in Figure 3.1. All compounds maintain the core structure of KRN7000 (galactose head α -glycosylated to ceramide moiety) but the alkyl lipidic chains have been replaced by fluoroalkyl ones. Compound **1** contains a highly fluorinated acyl chain ($C_{12}F_{25}$), while in analogue **2** a $C_{10}F_{21}$ fragment is present at the sphingoid base moiety. Finally, **3** bears perfluoroalkyl groups in both lipidic chains.

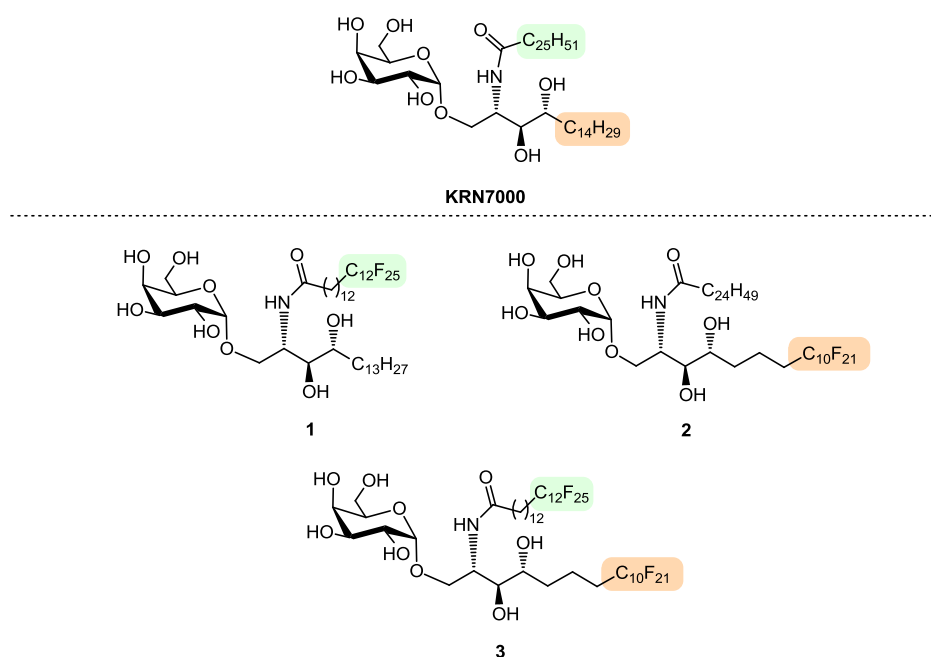
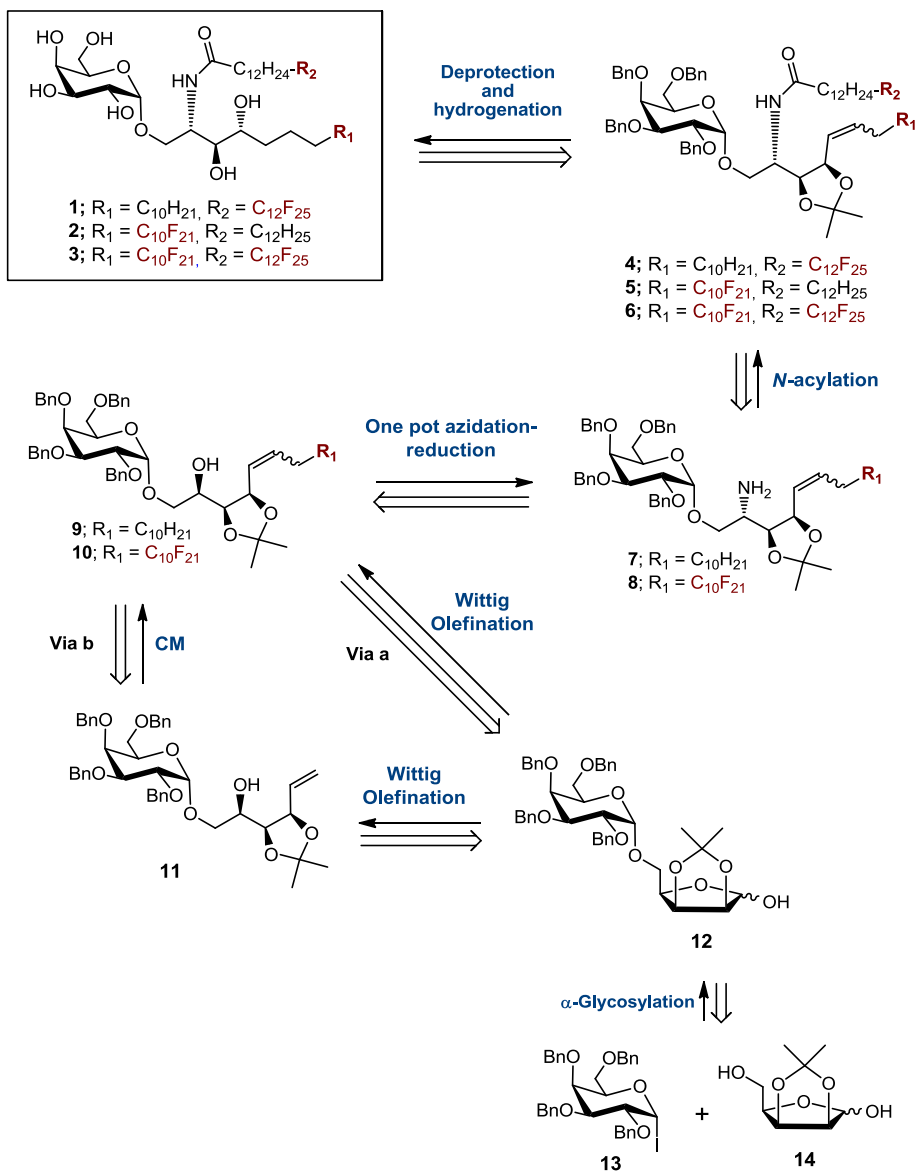


Figure 3.1. Target polyfluorinated KRN7000 analogues.

Synthesis of KRN7000 analogues with a high degree of fluorination.

3.2. RETROSYNTHETIC ANALYSIS AND BACKGROUND

3.2.1. Retrosynthetic analysis



Scheme 3.1. Retrosynthetic analysis of fluorinated analogues **1**, **2** and **3**.

A diversity- oriented synthesis of these analogs was envisioned as shown in Scheme 3.1, following an adapted version of total synthesis developed by Panza *et al.*,¹ and the strategy of Yen and co-workers.² These approaches avoid the difficulties of glycosylation reaction on ceramide acceptors or that of sphingosine, used in different published synthesis of KRN7000, through a key disaccharide precursor **12** with the desirable phytosphingosine stereochemistry already installed in the D-lyxose unit. The insertion of the fluorinated or hydrocarbon fragment corresponding to the sphingoid base could be achieved via direct Wittig reaction (via a, Scheme 3.1) or by consecutive Wittig and Cross-metathesis (CM) processes (via b, Scheme 3.1). The incorporation of the different acyl chains (fluorinated or not) would be possible through the introduction of an azide group, via Mitsunobu reaction, azide reduction and subsequent acylation.

3.2.2. Background

3.2.2.1. Fluoroalkylation via Wittig reaction

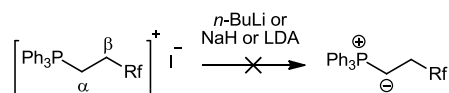
Wittig reaction is a widely used methodology for chain elongation of carbohydrates at reducing end, taking advantage of the carbonyl functionality present in the open form of the carbohydrate. Notwithstanding the endless and varied bibliography of Wittig transformations, only few examples with fluoroalkyl phosphonium salts have been reported to date and to the best of our knowledge there are no precedents for their reaction with sugars.

¹ Michieletti, M.; Bracci, A.; Compostella, F.; De Libero, G.; Mori, L.; Fallarini, S.; Lombardi, G.; Panza, L. *J. Org. Chem.* **2008**, *73*, 9192-9195.

² Yen, Y. F.; Kulkarni, S. S.; Chang, C. W.; Luo, S. Y. *Carbohydr. Res.* **2013**, *368*, 35-39.

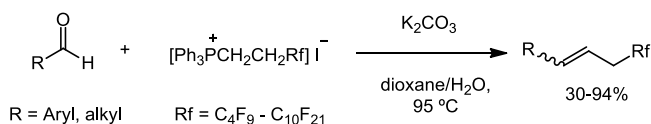
Synthesis of KRN7000 analogues with a high degree of fluorination.

First examples were reported by Escoula *et al.*^{3a} and Cecutti *et al.*^{3b} Both publications described Wittig reactions of different aldehydes with fluorinated phosphonium salts. Interestingly the authors claimed that the use of strong bases such as *n*-BuLi, LDA or NaH resulted unsuccessful since indiscriminate deprotonation at α and β positions of phosphonium salts occurred, preventing the formation of the expected ylide (Scheme 3.2). This unexpected reactivity was attributed to the strong electron-withdrawing character of the perfluorinated chain which is prone to acidify the protons at β position of the phosphorous atom.



Scheme 3.2. Deprotonating susceptible positions of fluoroalkyl phosphonium salts preventing the formation of target ylides.

In the same study, successful olefinations were finally achieved through an alternative Wittig procedure in which K_2CO_3 was used as soft base in H_2O /dioxane at 95 °C (Scheme 3.3). This methodology has been used, since then, for most of the reported similar transformations.⁴

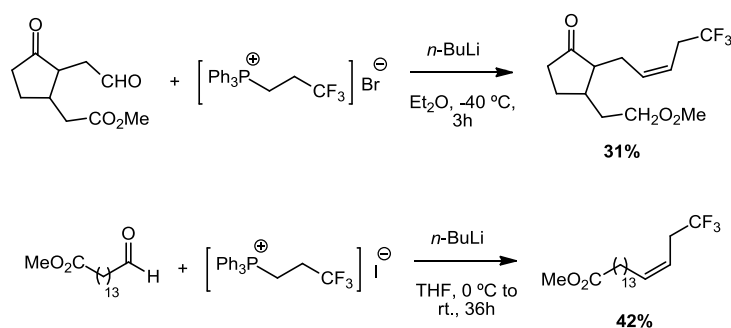


Scheme 3.3. Wittig reactions with fluoroalkyl phosphonium salts with simple aldehydes using soft K_2CO_3 base.

³ (a) Cecutti, C.; Rico, I.; Lattes, A.; Novelli, A.; Rico, A.; Marion, G.; Graciaa, A.; Lachaise, J. *Eur. J. Med. Chem.* **1989**, *24*, 485-492. (b) Escoula, B.; Rico, I.; Laval, J. P.; Lattes, A. *Synth. Commun.* **1985**, *15*, 35-38.

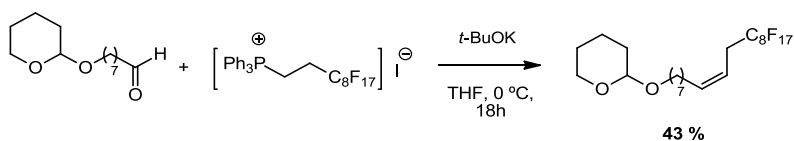
⁴ For examples using this methodology, see: (a) Saiz-Poseu, J.; Sedo, J.; García, B.; Benaiges, C.; Parella, T.; Alibes, R.; Hernando, J.; Busque, F.; Ruiz-Molina, D. *Adv. Mater.* **2013**, *25*, 2066-2070. (b) Boswell, P. G.; Anfang, A. C.; Bühlmann, P. *J. Fluorine Chem.* **2008**, *129*, 961-967. (c) Kaleta, Z.; Tárkányi, G.; Gömöry, Á.; Kálmán, F.; Nagy, T.; Soós, T. *Org. Lett.* **2006**, *8*, 1093-1095. (d) Rocaboy, C.; Gladysz, J. A. *Org. Lett.* **2002**, *4*, 1993-1996. (e) Rocaboy, C.; Rutherford, D.; Bennett, B. L.; Gladysz, J. A. *J. Phys. Org. Chem.* **2000**, *13*, 596-603.

In spite of these studies, further uses of *n*-BuLi in Wittig reactions with fluorinated phosphonium salts have been reported in the literature. In this sense, during the synthesis of trifluoromethyl derivatives of Jasmonate⁵ and Ganglioside GM1,⁶ Wittig olefinations with triphenyl(3,3,3-trifluoropropyl) phosphonium salt were conducted using *n*-BuLi under "typical" Wittig conditions. However, low and moderate olefination yields were obtained (Scheme 3.4).



Scheme 3.4. Wittig olefinations with triphenyl(3,3,3-trifluoropropyl) phosphonium salt using *n*-BuLi as base.

Munteanu and co-workers,⁷ provided another example in which Wittig olefination with a highly fluorinated phosphonium salt ($\text{Ph}_3\text{PCH}_2\text{CH}_2\text{C}_8\text{F}_{17}\text{I}$) was performed using potassium *t*-butoxide as base, in THF at 0°C. The reaction afforded the target olefinated compound in moderate 43% yield (Scheme 3.5).



Scheme 3.5. Wittig olefination from a highly fluorinated phosphonium salt using *t*-BuOK as a base.

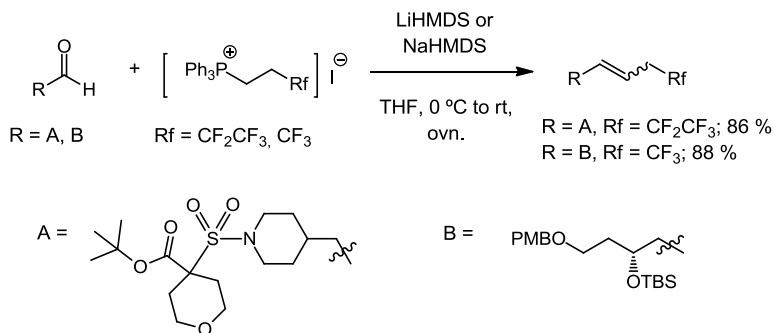
⁵ Kiyota, H.; Saitoh, M.; Oritani, T.; Yoshihara, T. *Phytochemistry*, **1996**, *42*, 1259-1262.

⁶ Liu, Z.; Kumar, K. *Synthesis* **2010**, 1905-1908.

⁷ G.W. Buchanan, R.; Smits, E.; Munteanu, *J. Fluorine Chem.* **2003**, *119*, 207–209.

Synthesis of KRN7000 analogues with a high degree of fluorination.

Finally, excellent olefination yields have been reported by using NaHMDS and LiHMDS bases again under "typical" Wittig conditions (Scheme 3.6).⁸



Scheme 3.6. Reported Wittig reactions using LiHMDS or NaHMDS bases.

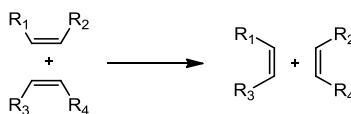
In summary, from these bibliographic data, it became apparent that the election of a proper base is key for the success in Wittig olefinations with fluoroalkyl phosphonium salts. In this regard, strong bases such as *n*-BuLi, LDA or NaH should be avoided being preferred the use of weaker bases as LiHMDS, NaHMDS or even K₂CO₃.

3.2.2.2. Fluoroalkylation via Cross Metathesis reaction

Olefin cross metathesis (CM)⁹ is a catalytic process through which two alkylidene fragments undergo bond reorganization, leading to the formation of a new olefinic compound. This process involves both the cleavage and the formation of C-C bonds (Scheme 3.7).

⁸ (a) Nicolau, K. C.; Pulukuri, K. K.; Rigol, S.; Heretsch, P.; Yu, R.; Grove, I. C.; Hale, C. R. H.; ElMarrouni, A.; Fetz, V.; Brönstrup, M.; Aujay, M.; Sandoval, J.; Gavriluyk, J. *J. Am. Chem. Soc.* **2016**, *138*, 6550–6560. (b) Barta, T. E.; Becker, D. P.; Bedell, L. J.; Boehm, T. L.; Brown, D. L.; Carroll, J. N.; Chen, Y.; Fobian, Y.; Freskos, J. N.; Gasielki, A. F.; WO2003091247 A2, 2003.

⁹ Grubbs, R. H.; Wenzel, A. G.; O'Leary, D. J.; Khosrau, E. *Handbook of Metathesis*, Wiley – VCH, Weinheim, **2015**, 245-248.



Scheme 3.7. General CM transformation.

Typical catalysts for CM reaction are Ru-based catalysts¹⁰ such as Grubbs 1st and 2nd Generation (G-I and G-II) and Hoveyda-Grubbs 2nd Generation (HG-II) catalysts (Figure 3.2).

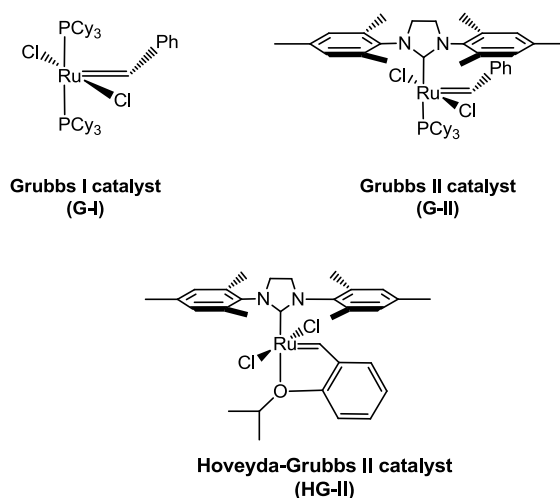


Figure 3.2. Some relevant Ru catalysts for OM.

These compounds exhibit an impressive activity in metathesis applications since they are stable to decomposition by moisture and air, and more importantly, compatible with several functional groups. For this reason, olefin CM is a powerful tool for the formation of carbon-carbon double bonds and therefore it has been used in the synthesis of many organic compounds.¹¹ Particularly of interest for our purposes, CM

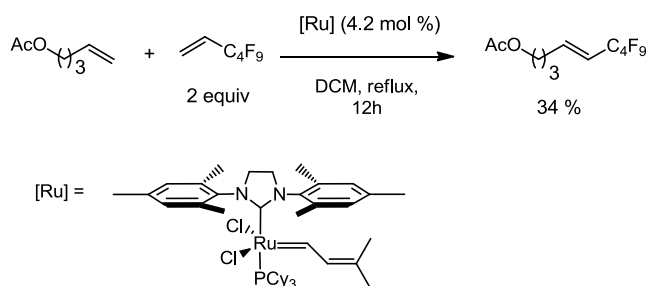
¹⁰ Samojłowicz, C.; Bieniek, M.; Grela, K. *Chem. Rev.* **2009**, *109*, 3708-3742.

¹¹ For some applications of metathesis reaction, see: (a) Prunet, J. *Eur. J. Org. Chem.* **2011**, 3634-3647. (b) Aljarilla, A.; López, J. C.; Plumet, J. *Eur. J. Org. Chem.* **2010**, 6123-6143. (c) Binder, J. B.; Raines, R. T. *Curr. Opin. Chem. Biol.* **2009**, *12*, 767-773.

Synthesis of KRN7000 analogues with a high degree of fluorination.

reaction with electron-deficient fluorinated olefins has emerged as a feasible methodology for fluoroalkylation of organic compounds.¹²

The first precedent of Ru-catalyzed CM with fluorinated olefins was reported in 2000 by Grubbs *et al.*¹³ In this isolated example, 2 equivalents of perfluorobutylethylene were reacted with 1 equivalent of 5-hexenyl-1-acetate affording the desired alkene in a modest 34% yield (Scheme 3.8).



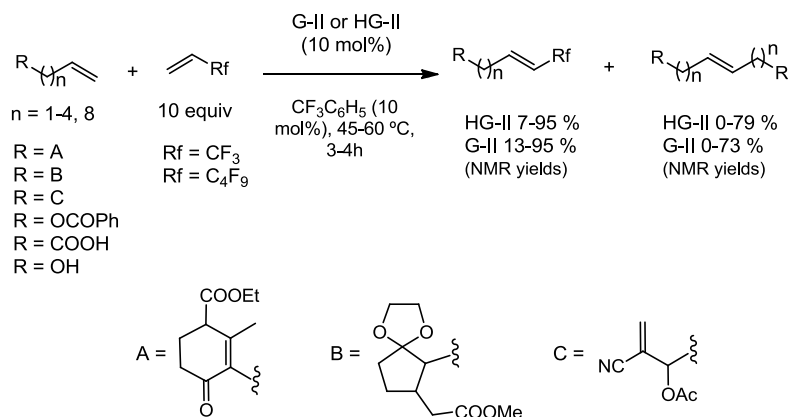
Scheme 3.8. First reported example of CM reaction with perfluoroalkylethylenes.

Blechert *et al.* provided, in 2001, the first study of CM reactions with such electron poor fluorinated olefins.¹⁴ The authors concluded that, at least, 10 equivalents of (perfluoroalkyl)ethylenes were required in order to overcome dimerisation of the more electron-rich counterpart and achieve high yields. Nevertheless, in most cases, homodimer product was also obtained, although the fluoroolefin formation was generally favoured. Regarding the catalyst, G-I was totally inactive and HG-II proved more effective than G-II. Furthermore, the use of α,α,α -trifluorotoluene was required in order to overcome solubility problems (Scheme 3.9).

¹² Fustero, S.; Simón-Fuentes, A.; Barrio, P.; Haufe, G. *Chem. Rev.* **2015**, *115*, 871-930.

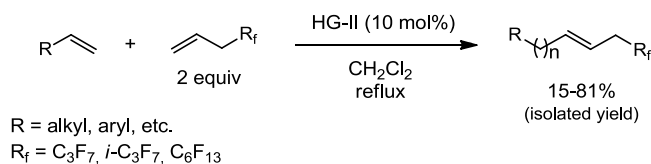
¹³ Chatterjee, A. K.; Morgan, J. P.; Scholl, M.; Grubbs, R. H. *J. Am. Chem. Soc.* **2000**, *122*, 3783-3784.

¹⁴ Imhof, S.; Randl, S.; Blechert, S. *Chem. Commun.* **2001**, 1692-1693.



Scheme 3.9. CM reactions with (perfluoroalkyl)ethylenes.

Later, in 2008, Kotora and co-workers¹⁵ published a further CM study in which the previously used (perfluoroalkyl)ethylenes were replaced by (perfluoroalkyl)propenes (Scheme 3.10). In this case, reasonable perfluoroalquene/substrate ratios (2:1) proved enough for achieving high metathesis yields using HG-II catalyst in refluxing DCM. This enhanced reactivity was attributed to the presence of the methylene unit between the double bond and the fluorinated moiety. This spacer diminishes the CF_2 inductive effect on the olefin, and thus, its electron deficient character. This methodology was applied to a huge variety of compounds including terpenes and one example of 1-allylglycoside affording poor to good yields. It is important to note that, in this study, no homodimerization of the starting materials was observed in isolable amounts.

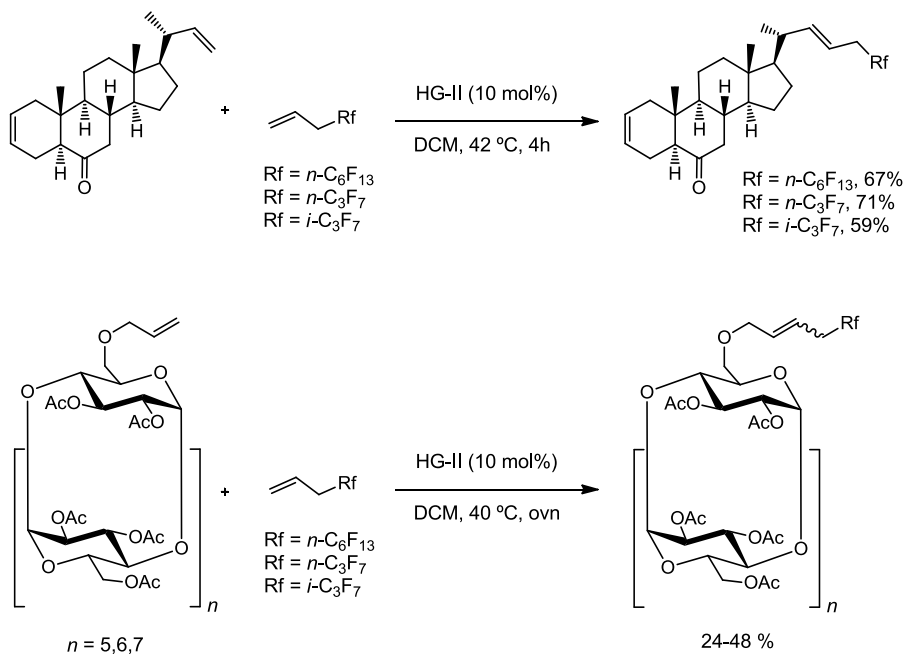


Scheme 3.10. CM with (perfluoroalkyl)propenes.

¹⁵ Eignerová, B.; Dračínský, M.; Kotora, M. *Eur. J. Org. Chem.* **2008**, 4493-4499.

Synthesis of KRN7000 analogues with a high degree of fluorination.

This successful work was then applied to the synthesis of polyfluorinated analogues of natural products such as brassinosteroids¹⁶ and β -cyclodextrins¹⁷ (Scheme 3.11).



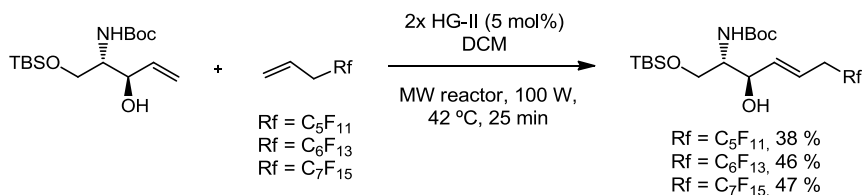
Scheme 3.11. Synthesis of polyfluorinated analogues of natural products via CM reaction.

Interestingly, the methodology was also used for the synthesis of fluorinated sphingosine analogues, but in this case, MW irradiation was required in order to increase chemical yields¹⁸ (Scheme 3.12).

¹⁶ Eignerová, B.; Slavíková, B.; Buděšinský, M.; Dračínský, M.; Klepetářová, B.; Št'astná, E.; Kotora, M. *J. Med. Chem.* **2009**, *52*, 5753-5757.

¹⁷ Řezanka, M.; Eignerová, B.; Jindřich, J.; Kotora, M. *Eur. J. Org. Chem.* **2010**, 6256-6262.

¹⁸ Prchalová, E.; Votruba, I.; Kotora, M. *J. Fluorine Chem.* **2012**, *141*, 49-57.



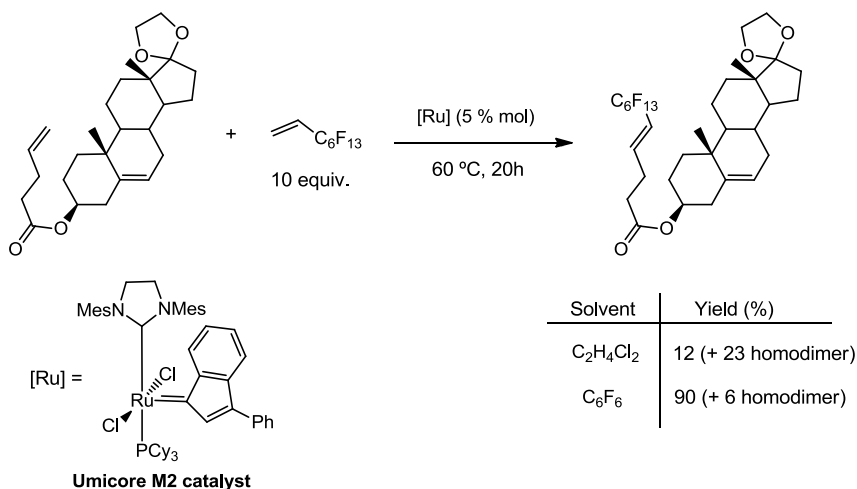
Scheme 3.12. Synthesis of spingosine analogues fluorinated at the non-polar fragment.

An important contribution to the CM field was brought by Grela and co-workers¹⁹ who observed that CM yields could be enhanced by the use of fluorinated aromatic solvents (FAHs). FAHs were used instead of "classical" solvents in specially demanding CM reactions, providing substantial improvements in reaction yields. In particular, an example of CM with (perfluorohexyl)ethylene showed an outstanding increase in yield from 12 to 90% when dichloroethane was replaced by perfluorobenzene.²⁰ The authors suggested the formation of π - π stacking interactions between the electron donating N-aromatic substituents of the catalysts and the electron poor molecules of the fluorinated solvent which might stabilize the 14-electron Ru species. This higher stability of the propagating species might be the responsible for the enhanced catalyst activity observed. The only drawback of this methodology is once again, the need for a tenfold excess of the perfluoroalkyl ethene with respect to the substrate in order to minimise the homo-coupling of the latter (Scheme 3.13).

¹⁹ Samojłowicz, C.; Bieniek, M.; Pazio, A.; Makal, A.; Woźniak, K.; Poater, A.; Cavallo, L.; Wójcik, J.; Zdanowski, K.; Grela, K. *Chem. Eur. J.* **2011**, *17*, 12981-12993.

²⁰ Samojłowicz, C.; Bieniek, M.; Zarecki, A.; Kadyrov, R.; Grela, K. *Chem. Commun.* **2008**, 6282-6284.

Synthesis of KRN7000 analogues with a high degree of fluorination.



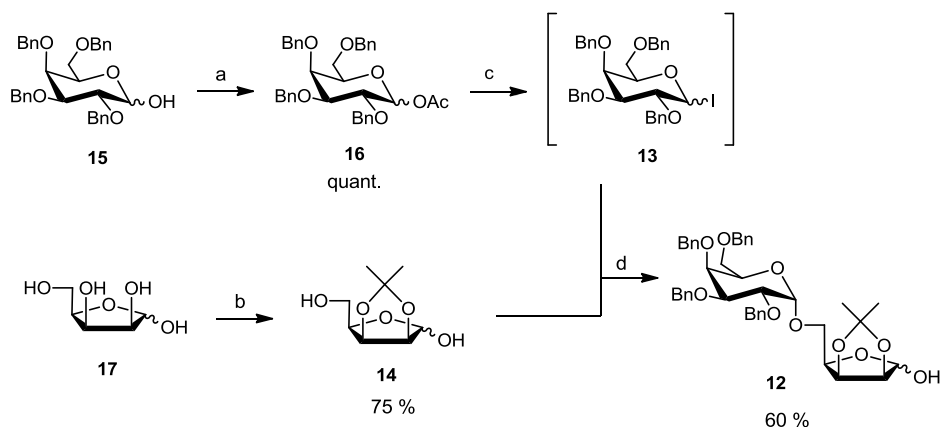
Scheme 3.13. Example of FAHs effect in CM reaction with perfluoroalkylethylenes.

To conclude, in contrast to Wittig olefination, Cross metathesis reaction with fluoroolefins has been extensively used for the introduction of highly fluorinated fragments into diverse complex organic molecules, although low yields are sometimes observed.

3.3. SYNTHESIS OF A KRN7000 ANALOGUE FLUORINATED AT ACYL CHAIN

3.3.1. Synthesis of non fluorinated amine intermediate 7

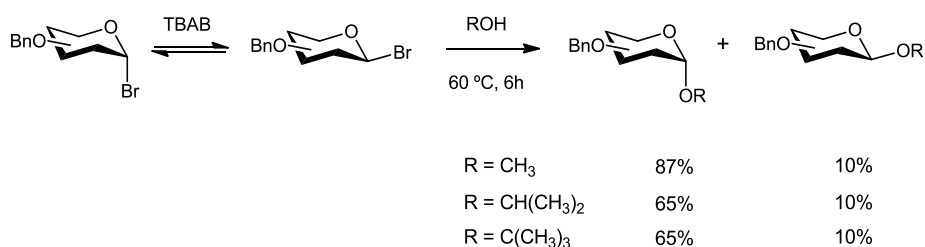
The synthesis of fluorinated analogues presented in this chapter began by the preparation of disaccharide intermediate **12**, through α -selective glycosylation via glycosyl iodides (Scheme 3.14). For this purpose, the commercially available protected galactopyranose **15** was acetylated at anomeric position. Treatment of **15** with Ac₂O in presence of NEt₃ afforded 2,3,4,6-tetra-O-benzyl-D-galactopyranosyl acetate **16** quantitatively. Next, selective protection of both secondary alcohol groups of D-lyxofuranose **17** was achieved in 75% yield via reaction with sulfuric acid in acetone.



a) Ac_2O , NEt_3 , DCM, rt, 2 h; b) H_2SO_4 , acetone, rt, overnight; c) TMSI, MgO, 0 °C, 0.5h; d) DIPEA, TBAI, 4 Å MS, toluene, 65 °C, 1 h.

Scheme 3.14. Synthesis of 2,3-O-isopropylidene-5-O-(2,3,4,6-tetra-O-benzyl- α -D-galactopyranosyl)-D-lyxofuranose **12**.

α -Selective glycosylation via glycosyl halides was first reported by Lemieux *et al.*²¹ In this reaction, a first continuous equilibrium between α -glycosyl halide and its more reactive β anomer, followed by a rate determining $\text{S}_{\text{N}}2$ -like O-glycoside formation, afforded α -linked disaccharides with high stereoselectivities (Scheme 3.15).



Scheme 3.15. Halide ion catalyzed glycosylation with simple alcohols.

The diastereoselectivity of this process may be dictated by the relative energies of the two possible diastereomeric transition states as defined by the Curtin–Hammett principle (Figure 3.3). In this situation, the

²¹ Lemieux, R. U.; Hendricks, K. B.; Stick, R. V.; James, K. J. *Am. Chem. Soc.* **1975**, *97*, 4056-4062.

Synthesis of KRN7000 analogues with a high degree of fluorination.

α and β glycosyl halides are in rapid equilibrium, and the product distribution is determined by the absolute difference between the two energy barriers to α or β products.

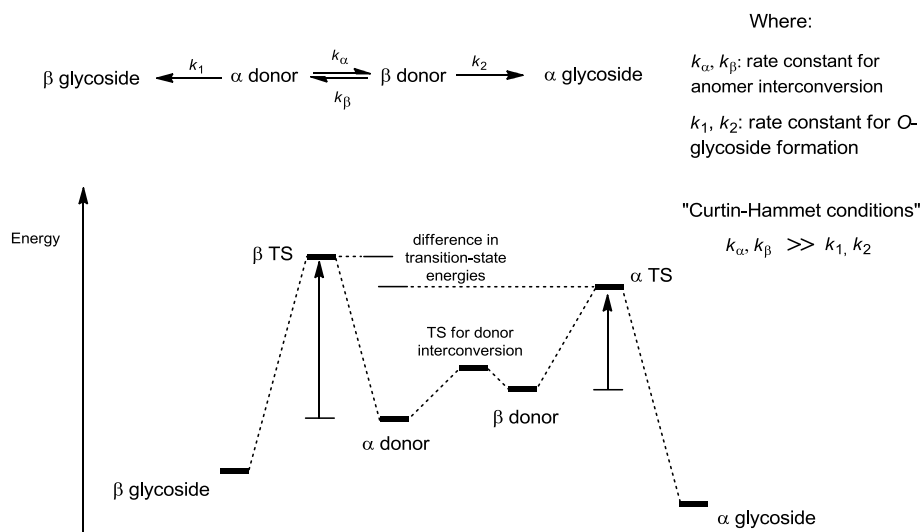
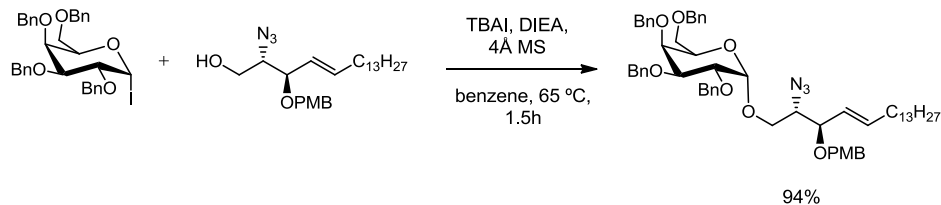


Figure 3.3. Curtin-Hammett situation for S_N2 -like glycosylation.²²

Gervay-Hague and Du²³ applied this methodology to the total synthesis of KRN7000. They found that complete α -stereoselectivity was achieved by using glycosyl iodides as glycosyl donors and TBAI as anomerisation source (Scheme 3.16).



Scheme 3.16. Stereoselective S_N2 -like glycosylation reaction via glycosyl halides for the synthesis of KRN7000.

²² Cumpstey, I. *Org. Biomol. Chem.* **2012**, *10*, 2503–2508.

²³ Du, W.; Gervay-Hague, J. *Org. Lett.* **2005**, *7*, 2063–2065.

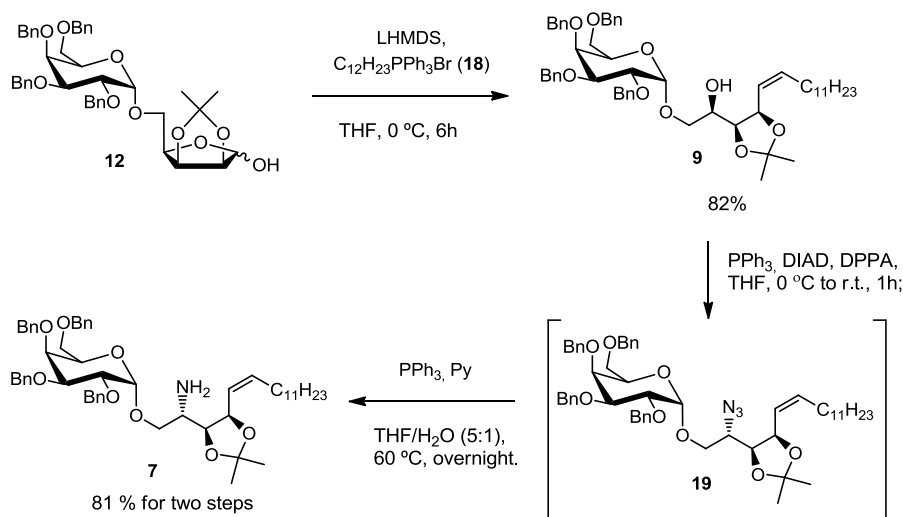
In this way, our galactosyl acetate **16** was treated with TMSI in presence of MgO yielding 2,3,4,6-tetra-*O*-benzyl-*D*-galactopyranosyl iodide **13**, which was then used *in situ* as glycosyl donor in the subsequent glycosylation step (Scheme 3.14). MgO acts as a Lewis base to sequester the TMSOAc generated during the iodination reaction which could revert the reaction to the initial glycosyl acetate.²⁴ Glycosylation reaction was performed with acceptor **14** using DIPEA as a base and TBAI as halogen anomerisation source, affording 2,3-*O*-isopropylidene-5-*O*-(2,3,4,6-tetra-*O*-benzyl- α -*D*-galactopyranosyl)-*D*-lyxofuranose **12** as the sole anomer in a good 60% yield. The anomeric configuration of the disaccharide was confirmed by ¹H NMR and HSQC. The ¹H NMR spectrum showed a coupling constant ($J_{1,2'} = 3.3$ Hz), typical for axial-equatorial couplings. Furthermore, undecoupled HSQC spectrum showed a $J_{C,H}$ of 171 Hz (values around 170 Hz for $J_{H,C}$ indicates an equatorial proton at C-1, while $J_{H,C}$ values around 160 Hz are typical for axial protons).²⁵

From disaccharide **12**, the hydrocarbon sphingoid base was introduced via Wittig reaction. Thus, compound **12** was treated under standard Wittig conditions using LiHMDS as a base and dodecyltriphenylphosphonium bromide **18** in THF to afford alkene **9** in 82% yield (Scheme 3.17). *Cis* alkene was obtained as a major product together with traces of *trans* compound. This fact was confirmed since the signal corresponding to H-6 in the minor product showed a coupling constant of 15.3 Hz, typical for *trans* alkenes. Coupling constants for the *cis* olefin were not observable since signals corresponding to H-5 and H-6 appeared together as a multiplet.

²⁴ Dabideen, D. R.; Gervay-Hague, J. *Org. Lett.* **2004**, 6, 973–975.

²⁵ Bubb, W. A. *Concepts Magn. Reson. Part A* **2003**, 19A, 1-19.

Synthesis of KRN7000 analogues with a high degree of fluorination.



Scheme 3.17. Preparation of **7** from **12** via Wittig olefination and one pot azidation-reduction.

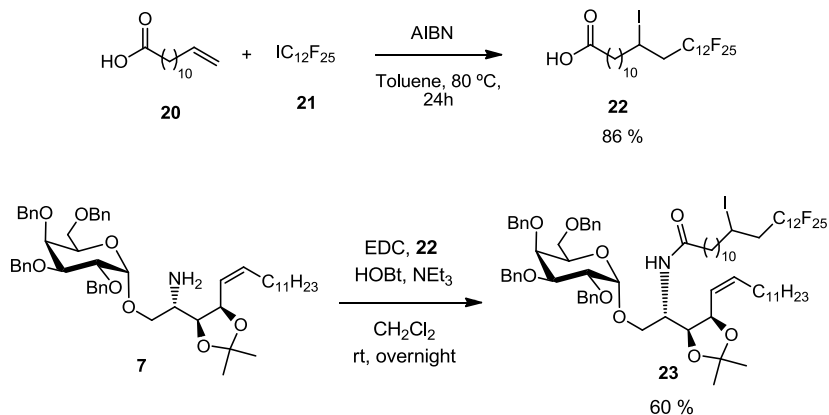
Subsequent Mitsunobu azidation using DPPA as nucleophilic azide source in presence of PPh_3 and DIAD rendered azido compound **19** with total conversion (as determined by TLC). Crude azide was then treated with PPh_3 in THF/ H_2O 5:1 affording the corresponding amine **7** in 81% yield. Compound formation was evidenced by the appearance of a typical signal for protons in α position to amino group at 3.02 ppm corresponding to H-2 in its 1H NMR spectrum.

3.3.2. Synthesis of fluorinated acid, acylation and deprotection

With key amine intermediate **7** in hand, we were then able to introduce the fluorinated acyl chain via acylation with the corresponding polyfluorinated carboxylic acid. For this purpose, **22** was synthesized via AIBN mediated radical perfluoroalkylation²⁶ of olefinic compound **20** with perfluorododecyl iodide **21** (Scheme 3.18). It is important to mention that the iodine atom present in acid **22** would be subsequently removed together with the benzyl groups in the final hydrogenolysis step of the

²⁶ Brace, N.O. *J. Fluorine Chem.* **1999**, *93*, 1-25.

synthesis. Further acylation was performed in presence of EDC and HOBT as coupling agents furnishing fluorinated amide **23** in 60% yield.

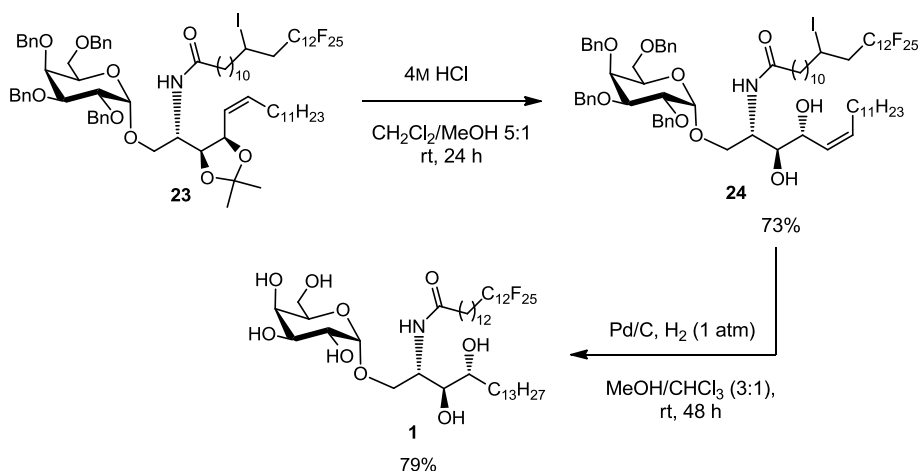


Scheme 3.18. Synthesis of polyfluorinated carboxylic acid **22** and subsequent acylation of amine **7**.

Finally, having constructed the glycolipid core structure, total deprotection remained as the final stage of the synthesis. Isopropylidene removal was achieved via acidic hydrolysis of **23** with a 4M solution of HCl affording **25** in 73% yield (Scheme 3.19).

Further hydrogenolysis using an excess of Pd/C, under hydrogen atmosphere (1 atm) during 48 h furnished the desired KRN7000 analogue **1** in 79% yield. The removal of iodine atom was confirmed by the shift of the signal corresponding to H-12", from 4.23 ppm to the field of aliphatic protons (1.5-1.2 ppm), in the ¹H NMR spectrum. Similarly, the disappearance of all the AB systems corresponding to benzylic protons as well as the olefinic signals, in ¹H NMR spectrum, evidenced the complete removal of all benzylic groups and the reduction of the double bond moiety.

Synthesis of KRN7000 analogues with a high degree of fluorination.



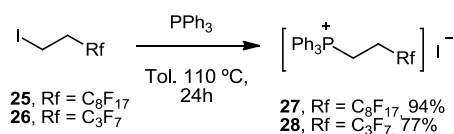
Scheme 3.19. Total deprotection of **23** to target KRN7000 analogue **1**.

3.4. SYNTHESIS OF A KRN7000 ANALOGUE FLUORINATED AT SPHINGOID BASE

The synthesis of target analogue **2**, fluorinated at sphingoid base, started from previously synthesized disaccharide intermediate **12**. Following the retrosynthesis previously described, introduction of the proper fluoroalkyl fragment was initially attempted through Wittig-type methodology from this substrate (Scheme 3.1, via A).

3.4.1. Introduction of fluorinated chain via Wittig olefination

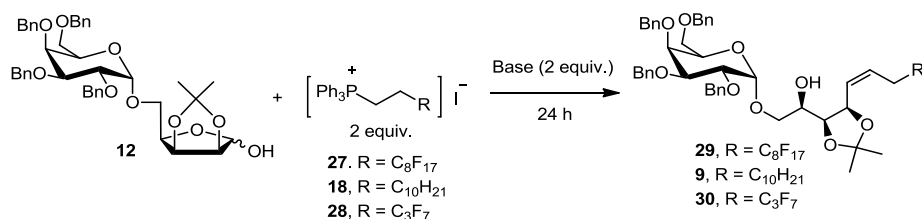
Highly fluorinated triphenyl phosphonium iodide **27** was prepared in high yield, by reaction of the corresponding iodide **25** with triphenylphosphine (Scheme 3.20).



Scheme 3.20. Synthesis of phosphonium salts **27** and **28** from perfluorodecyl iodides.

Phosphonium salt **28**, bearing a shorter fluoroalkyl chain, was also synthesized in order to discern a possible effect of the fluoroalkyl length in the Wittig olefination outcome. Furthermore, previously obtained olefination result with non fluorinated phosphonium salt **18** (Scheme 3.17) was also used for comparison with results for fluorinated phosphonium salts (Table 3.1).

Table 3.1. Tested reaction conditions for Wittig olefination of **12** with fluoroalkyl-containing phosphonium salts.

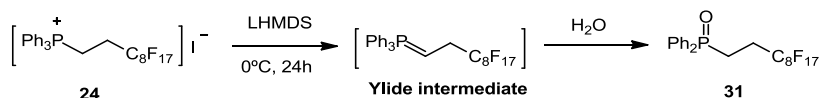


Entry	R	Base	Conditions ^a	Conversion of 27/28 ^b	Products (Yield %) ^c
1	C ₈ F ₁₇	LHMDS	A	> 99 ^d	12 (89)
2	C ₈ F ₁₇	<i>t</i> -BuOK	A	55 ^e	12 (32) ^f
3	C ₈ F ₁₇	K ₂ CO ₃	B	40 ^e	12 (91)
4 ^g	C ₈ F ₁₇	K ₂ CO ₃	B	88 ^e	12 (89)
5	C ₁₀ H ₂₁	LHMDS	A	n.d.	12 (0); 9 (82)
6	C ₃ F ₇	LHMDS	A	> 99 ^h	12 (10); 30 (67)

^a Conditions A: THF, 0 °C; Conditions B: H₂O/dioxane (5:1), 95 °C. ^b Determined by ³¹P NMR spectroscopy. ^c Isolated yields. ^d Complete conversion to Ph₂P(O)CH₂CH₂C₈F₁₇ **31** (Scheme 3.21) was observed by ³¹P NMR. ^e Mixture of P-containing compounds was observed by ³¹P NMR. ^f An unseparable complex mixture was obtained in addition to **31**. ^g After 24 h of reaction, additional 2 equivalents of base were added and the reaction was stirred again for 24 h. ^h A 6:4 mixture of triphenylphosphine oxide and **31** was observed by ³¹P NMR.

Synthesis of KRN7000 analogues with a high degree of fluorination.

First olefination attempt was performed with fluorinated phosphonium salt **27** using "classical" Wittig conditions (Table 3.1, entry 1). Disaccharide **12** was, thus, reacted with **27** in THF at 0 °C, using LHMDS as base. Unfortunately, after 24 h of reaction, no conversion of starting material **12** was observed by TLC. Interestingly, phosphonium salt **27** was not detected in the crude ^1H NMR spectrum. Further ^{31}P NMR spectrum analysis of the crude reaction revealed the total conversion of **27** (25.1 ppm) into **31** (30.7 ppm) (Scheme 3.21). The structure of **31** was confirmed by MS analysis. Formation of diphenyl phosphonium oxides such as **31** are described to occur through hydrolysis of the corresponding ylides.²⁷ Therefore, from this result we hypothesized that successful ylide formation occurred during the reaction but since being not capable of reacting with disaccharide **12**, it underwent hydrolysis during the work-up process.



Scheme 3.21. Hydrolysis of fluorinated phosphonium ylide in Wittig olefination.

Replacement of LHMDS by *t*-BuOK as base did not provide better results (Table 3.1, entry 2). Instead, it resulted in partial conversion of **12** into an unseparable mixture of presumable elimination products. Although the presence of a set of fluorine signals in ^{19}F NMR spectrum of the mixture revealed the insertion of fluoroalkyl chain, the desired product **29** was not identified. In contrast to the assay corresponding to entry 1, ^{31}P NMR spectrum of the crude mixture revealed only partial conversion of **27** into a mixture of the previously observed alkyl phosphine oxide **31** (30.7 ppm) among other unidentified P-containing species.

²⁷ Kolodiaznyi, O. I. *Phosphorus Ylides: Chemistry and application in organic synthesis*, Wiley – VCH, Weinheim, **1999**.

Further attempt was performed using "non classical" Wittig conditions. In this reaction, a mixture of disaccharide **12** and phosphonium salt **27** was heated at 95 °C in H₂O/dioxane using K₂CO₃ as base (Table 3.1, entry 3). This time 91% of starting compound **12** was recovered after purification. ³¹P NMR spectrum of the crude showed unreacted phosphonium salt **27** as well as **31** as major components of a mixture of P-containing species. No further improvements were observed when the mixture was heated for additional 24h adding extra amount of base (Table 3.1, entry 4). In this occasion, almost complete disappearance of **27** was observed by ³¹P NMR spectrum, but no detectable amounts of Wittig reaction were observed.

Again, all these results suggested that although initial ylide formation occurred, this specie did not react with our substrate **12**, and due to the known instability of such ylides, it finally decomposed.

It should be noted that, previously in this chapter, disaccharide **12** underwent efficient coupling with dodecyltriphenylphosphonium bromide **18**, the non-fluorinated counterpart of **27**. This reaction was performed in THF, at 0 °C and using LHMDS as base affording 82% of the olefinated compound **9** (Table 3.1, entry 5 and Scheme 3.17).

Interestingly, the use of the same "standard" conditions for olefination of **12** with phosphonium salt **28**, bearing a shorter fluoroalkyl chain, also proved successful (Table 3.1, entry 6). In this reaction, introduction of a C₃F₇-containing fragment was successfully achieved furnishing olefinated compound **30** in good 67% yield.

Although more information would be required for a more accurate conclusion, these results pointed "high" fluorinated phosphonium salt **27** as the responsible for the lack of reactivity observed, presumably because of its low solubility in the tested system.

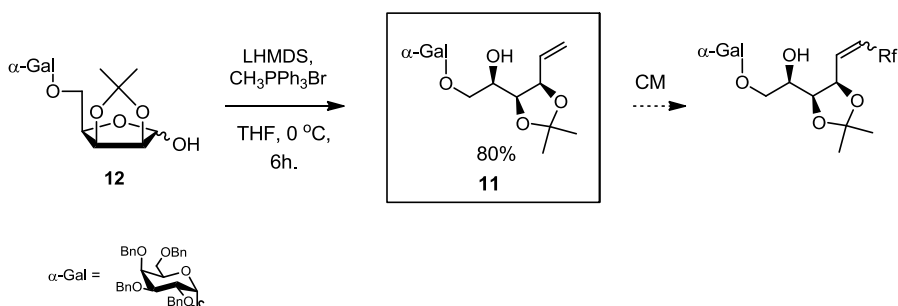
Synthesis of KRN7000 analogues with a high degree of fluorination.

In view of the unsuccessful results and the limited information available in the bibliography for fluoroalkylation via Wittig-type methodology, we decided to move to the alternative CM strategy (Scheme 3.1, via B).

3.4.2. Introduction of fluorinated chain via Cross Metathesis

As commented before, CM reaction was selected as a feasible alternative to Wittig reaction for the fluorination of KRN7000 sphingoid base moiety.

With the aim of conducting the study of CM reaction with fluorinated olefins, disaccharide **12** was initially transformed into terminal olefin **11** via LHMDS-promoted Wittig olefination with methyltriphenyl phosphonium bromide (Scheme 3.22). Product obtaining was confirmed by the presence, in the ^1H NMR spectrum, of two doublets at 5.24 and 5.18 ppm corresponding to the terminal olefinic protons of the molecule, showing both of them coupling signals (COSY) with the internal olefinic proton with constants of 17.2 Hz for *trans* proton and 10.1 Hz for *cis* proton.

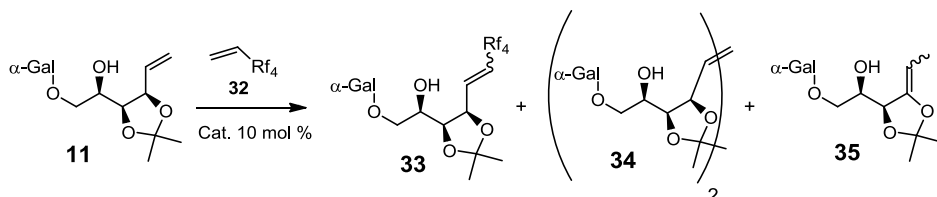


Scheme 3.22. Synthesis of the olefinic intermediate **11** for further CM studies.

Initial investigations began by reproducing the conditions reported by Blechert *et al.*¹⁴ Accordingly, our terminal olefin **11** was reacted with

10 equiv. of perfluorobutylethylene **32** in the presence of HG-II catalyst and 1 eq. of α,α,α -trifluorotoluene (Table 3.2, entry 1).

Table 3.2. CM attempts of olefin **11** with perfluorobutylethylene **32**.



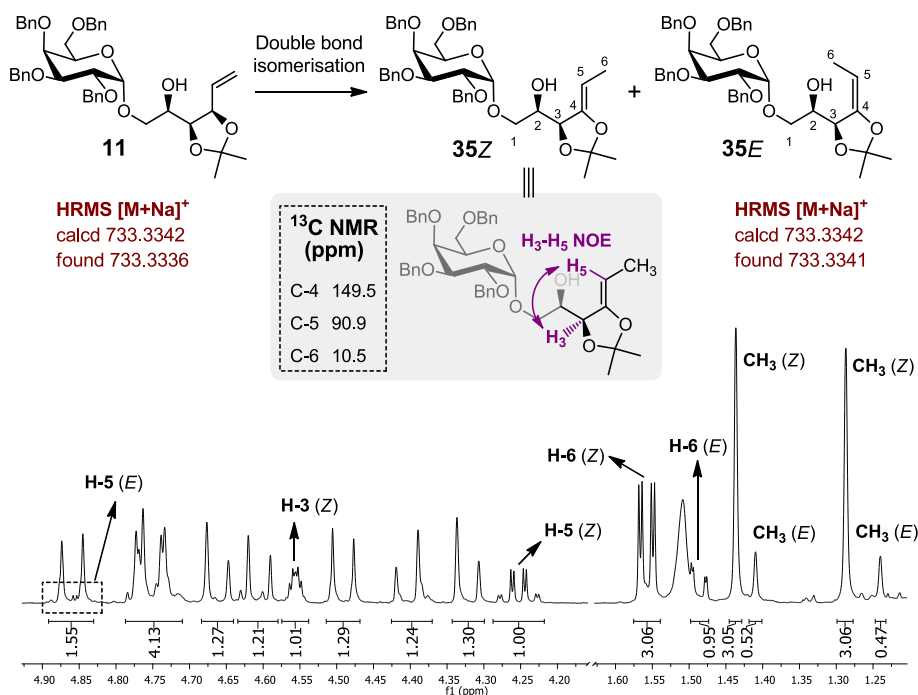
Entry ^a	32 equiv.	Catalyst	Solvent	T (°C)	t (h)	Yield (%) ^b			
						11	33	34	35
1 ^c	10	HG-II	-	40	72	35	-	43	10
2	2	HG-II	CH ₂ Cl ₂	40	48	38	-	54	-
3	2	G-II	CH ₂ Cl ₂	40	48	42	-	45	-
4 ^d	2	G-II	CH ₂ Cl ₂	40	48	47	-	46	-
5	10	G-II	C ₆ F ₅ CF ₃	50	48	42	-	34	8
6	10	HG-II	C ₆ F ₅ CF ₃	50	48	42	-	29	23
7	10	Umicore M2	C ₆ F ₅ CF ₃	50	48	63	-	30	5

^a α -Gal refers to 2,3,4,6-tetra-O-benzyl- α -D-galactopyranosyl; ^b Isolated yields; ^c 1 equiv. of α,α,α -trifluorotoluene was added to the mixture to solubilise the catalyst in **32**; ^d 2 equiv. of fluorinated olefin and 10 mol% of catalyst were added in two portions every 24h.

Unfortunately, no cross product was observed and homodimerized product **34** was obtained instead, in a 43% yield. The ¹H NMR spectrum unambiguously confirmed the formation of homodimer **34** because of the presence of a sole olefinic signal at 5.91 ppm integrating for only one proton atom. The symmetric nature of this compound made

Synthesis of KRN7000 analogues with a high degree of fluorination.

both olefinic protons equivalent. Furthermore the absence of signals in ^{19}F NMR discarded coupling with the fluorinated olefin **32**. In addition, a different derivative was also obtained from this experiment. Initial analysis of its ^1H spectrum showed no apparent olefinic signals. However, ^{13}C NMR spectrum clearly showed a peak in the zone of olefinic protons (149.5 ppm) corresponding to C-4 (Scheme 3.23), which resulted to be a quaternary carbon atom (as determined by HSQC assay). Further analysis by HMBC experiment, revealed the coupling between C-4 and two proton signals at 4.25 ppm (H-5) and 1.55 ppm (H-6) integrating for one and three proton atoms respectively.

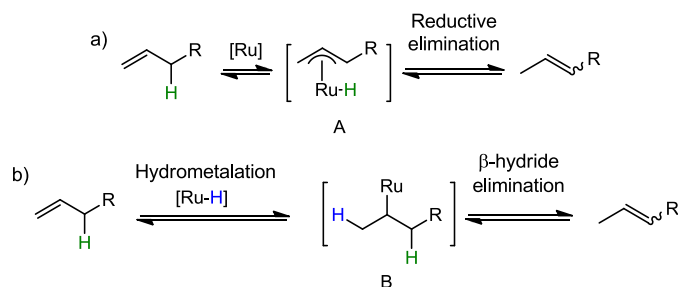


Scheme 3.23. Double bond isomerisation and key spectroscopic data for identification of **35**.

Finally, mass spectrum analysis revealed a m/z which fitted with the starting olefin **11**. All these data suggested that this new compound, **35**, was the result of isomerisation of the terminal olefin into the more

stable internal one (Scheme 3.23). The double bond stereochemistry was elucidated by NOESY experiments, which indicated the presence of a 85:15 *Z/E* mixture.

Olefin isomerisation of double bonds have been widely reported as a side reaction during metathesis conditions.²⁸ Two main different rationalizations have been described for this process. The first one lies in a π -allyl mechanism which involves the initial formation of π -allyl intermediate **A** and subsequent reductive elimination (Scheme 3.24, a). The second mechanism requires the presence of an initial Ru-H specie which undergoes hydrometalation to the double bond moiety leading to σ -alkyl complex **B**. Finally, β -hydride elimination gives the internal olefinated product (Scheme 3.24, b).



Scheme 3.24. Simplified proposed mechanisms for metal catalyzed olefin isomerisation. a) π -Allyl hydride mechanism. b) Hydrometalation / β -hydride elimination mechanism.

Particularly, the formation of Ru-H species during metathesis reaction has gained importance during the last years. Involvement in olefin isomerisation of different ruthenium hydride complexes accessible from decomposition of G-I and G-II catalyst has been suggested in the bibliography (Figure 3.4).²⁹ Percy *et al.*³⁰ even observed **Ru-H 3** complex

²⁸ Schmidt, B. *Eur. J. Org. Chem.* **2004**, 1865-1880 and references therein.

²⁹ (a) Hong, S. H.; Wenzel, A. G.; Salguero, T. T.; Day, M.W.; Grubbs, R. H. *J. Am. Chem. Soc.* **2007**, *129*, 7961-7968. (b) Hong, S. H.; Day, M. W.; Grubbs, R. H. *J. Am. Chem. Soc.* **2004**, *126*, 7414-7415. (c) Trnka, T. M.; Morgan, J. P.; Sanford, M. S.; Wilhelm, T. E.; Scholl, M.; Choi, T.-L.; Ding, S.; Day, M. W.; Grubbs, R. H. *J. Am. Chem. Soc.* **2003**, *125*, 2546-2558. (d) Dinger, M. B.;

Synthesis of KRN7000 analogues with a high degree of fluorination.

during ring closing metathesis. However, isomerisation activities of these complexes have been recently reported to be marginally when compared to the one observed with G-II catalyst under the same CM conditions.³¹

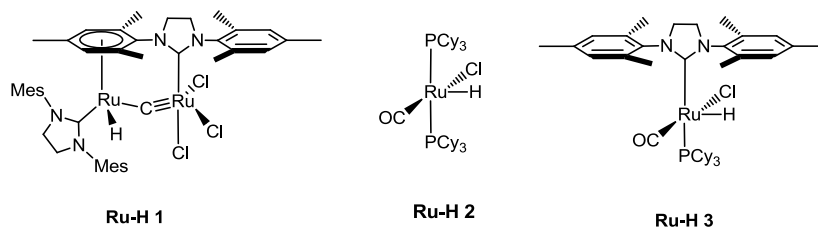


Figure 3.4. Reported Ru-H species observed from G-I and G-II catalyst decomposition.

In this sense, a recent report³² evidenced the presence of Ru nanoparticles (NPs) in commercially available G-II catalyst as well as its formation during CM reaction using the same catalyst. These NPs appeared to considerably contribute to olefin isomerisation during CM reaction. All these observations make clear that a proper characterization of reactive intermediates and decomposed catalysts are vital for a future understanding of olefin isomerization mechanism.

Back to our CM study with perfluorobutylethylene **32**, no cross product was neither observed when the reaction was carried out in DCM as solvent using either HG-II or G-II catalysts (Table 3.2, entries 2-3). In these cases, homodimerization took place exclusively, affording **34** in 54% and 45% yields, respectively. No significant improvement in the conversion was neither observed when catalyst G-II was added in two portions separated by a 24 h period (Table 3.2, entry 4).

Mol, J. C. *Eur. J. Inorg. Chem.* **2003**, 2827-2883. (e) Dinger, M. B.; Mol, J. C. *Organometallics* **2003**, *22*, 1089-1095.

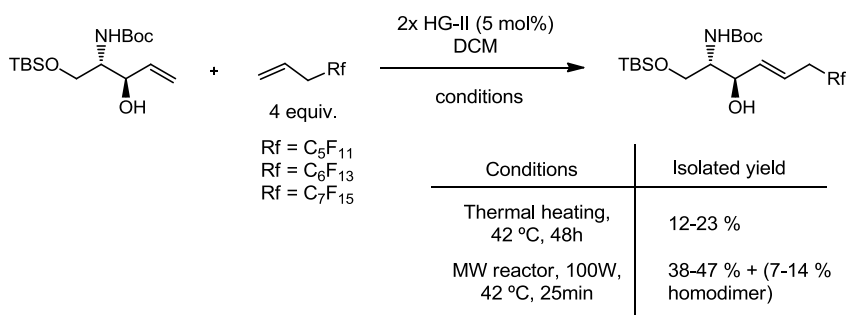
³⁰ Ashworth, I. W.; Hillier, I. H.; Nelson, D. J.; Percy, J. M.; Vincent, M. A. *Eur. J. Org. Chem.* **2012**, 5673-5677.

³¹ Higman, C. S.; Plais, L.; Fogg, D. E. *ChemCatChem* **2013**, *5*, 3548-3551.

³² Higman, C. S.; Lanterna, A. E.; Marin, M. L.; Scaiano, J. C.; Fogg, D. E. *ChemCatChem* **2016**, *8*, 2446-2449.

In contrast to the aforementioned Grela's results,²⁰ the use of perfluorotoluene as solvent in our cross metathesis reaction did not provide better results (Table 3.2, entries 5-7). Instead, homocoupling and isomerisation products **34** and **35** were again obtained in different yields depending on the catalyst used. Umicore M2 catalyst (Table 3.2, entry 7) is a modified G-II catalyst and it was used in order to mimic Grela's conditions showed in Scheme 3.13.

In light of the disappointing results showed above, further experiments under microwave (MW) irradiation³³ were carried out. Among the benefits of MW-assisted heating, the dramatic shortening of reaction times and even altered product distribution are the main profits of this enabling technology. Concretely, Prchalová *et al.*¹⁸ took advantage of this useful technique to increase yields of CM with perfluoroalkylpropenes in their synthesis of fluorinated analogues of sphingosines. Although the isolated yields were moderate and also homodimer product was obtained, the yield increments obtained in this work resulted interesting for us (Scheme 3.25).



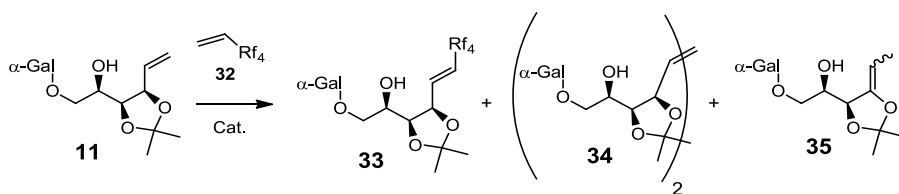
Scheme 3.25. Described yield enhancement by the use of MW irradiation in the synthesis of fluorinated sphingosines.

³³ For general reviews on microwave-assisted synthesis, see: (a) Caddick, S.; Fitzmaurice, R. *Tetrahedron* **2009**, *65*, 3325-3355. (b) Kappe, C. O.; Dallinger, D. *Mol. Divers.* **2009**, *13*, 71-193. (c) Kappe, C.O. *Chem. Soc. Rev.* **2008**, *37*, 1127-1139. (d) Dallinger, D.; Kappe, C. O. *Chem. Rev.* **2007**, *107*, 2563-2591. (e) De la Hoz, A.; Díaz-Ortiz, A.; Moreno, A. *Chem. Soc. Rev.* **2005**, *34*, 164-178. (f) Kappe, C. O. *Angew. Chem. Int. Ed. Engl.* **2004**, *43*, 6250-6284. (g) Perreux, L.; Loupy, A. *Tetrahedron* **2001**, *57*, 9199-9223.

Synthesis of KRN7000 analogues with a high degree of fluorination.

In addition, a recent publication by Grela *et al.*³⁴ showed impressive enhancements in challenging metathesis transformations by combining the previously mentioned beneficial effect of fluorinated aromatic solvents (FAHs) in CM reaction¹⁹ with the advantageous MW irradiation. These recent reports, prompted us to explore this avenue (Table 3.3).

Table 3.3. CM assays between olefins **11** and **32** under MW irradiation.



Entry ^a	Catalyst	Solvent	t (min)	Yield (%) ^b			
				11	33	34	35
1	HG-II	CH ₂ Cl ₂	20 + 150	80	-	16	-
2	HG-II	C ₆ F ₅ CF ₃	20 + 180	13	-	-	78
3	G-II	C ₆ F ₅ CF ₃	20 + 20	24	-	24	46
4	Umicore M2	C ₆ F ₅ CF ₃	20 + 20	28	-	16	49
5 ^c	G-II	C ₆ F ₅ CF ₃	20 + 20	25	-	43	23
6 ^d	HG-II	C ₆ F ₅ CF ₃	20 + 20	No reaction			

^a α -Gal refers to 2,3,4,6-tetra-O-benzyl- α -D-galactopyranosyl; All reactions were performed in a sealed vessel under MW irradiation (200W) at 50°C. 10 equiv. of **32** and 10 mol % of catalyst were added in two portions every period of time indicated. ^b Isolated Yields. ^c 10 mol % of (Cy)₃P(O) were added to the mixture. ^d 10 mol % of 2,6-dichloro-1,4-benzoquinone were added to the mixture.

³⁴ Samojłowicz, C.; Borré, E.; Mauduit, M.; Grela, K. *Adv. Synth. Catal.* **2011**, *353*, 1993-2002.

Initial attempts of CM under MW irradiation were performed with HG-II catalyst in DCM (Table 3.3, entry 1). Unfortunately, no significant improvements were observed when compared to thermal conditions. On the other hand, the combination of MW irradiation with perfluorotoluene as solvent promoted impressive changes in reaction course (Table 3.3, entries 2-6). Although considerable reduction of reaction times was observed, the product distribution was totally inverted in favour to isomerised product **35**. In fact, single formation of **35** was observed when HG-II was used as catalyst in perfluorotoluene (Table 3.3, entry 2) while amounts of homodimer **34** were also observed with G-II and Umicore M2 catalysts (Table 3.3, entries 3-4). The higher reaction time used for entry 2 was an attempt to check the reactivity of **35** towards CM as it could also become an interesting product. Certainly, no reaction progress was observed by TLC after 40 min of reaction.

As mentioned before, isomerisation side reactions during metathesis conditions have been described in the literature. In consequence, several reports of isomerisation inhibition by the use of additives have also been highlighted.³⁵ In this way, different additives were tested with our reaction conditions but all failed to completely inhibit isomerisation process. Tricyclohexylphosphine oxide proved to reduce isomerisation rate when it was catalytically added to the reaction catalyzed by G-II in perfluorotoluene (Table 3.3, entry 5). Nevertheless, homodimerisation and isomerization took place and no cross product was observed. On the other hand, the use of 2,6-dichloro-1,4-benzoquinone under similar conditions resulted in total suppression of catalyst activity and no reaction was observed (Table 3.3, entry 6).

³⁵ For some isomerization inhibition additives, see: (a) Schulz, M. D.; Atkinson, M. B. J.; Elsey, R. J.; Thuo, M. M. *Transit. Met. Chem.* **2014**, *39*, 763-767. (b) Gimeno, N.; Formentín, P.; Steinke, J. H. G.; Vilar, R. *Eur. J. Org. Chem.* **2007**, 918-924. (c) Hong, S. H.; Sanders, D. P.; Lee, C.W.; Grubbs, R. H. *J. Am. Chem. Soc.* **2005**, *127*, 17160-17161. (d) Bourgeois, D.; Pancrazi, A.; Nolan, S.; Prunet, J. *J. Organomet. Chem.* **2002**, *643*, 247-252

Synthesis of KRN7000 analogues with a high degree of fluorination.

Although further isomerisation inhibitors could have been tested, from these results it became apparent that perfluorobutylethylene **32** was not reactive enough to undergo cross metathesis with our terminal olefin **11**, neither catalyzed by G-II, HG-II nor Umicore M2 catalysts. The low electron density in the double bond of **32** (because of inductive effect of difluoromethylene groups) would probably be the main responsible for this lack of reactivity. In addition, the modest yields obtained for homodimer product **34** also suggested some impediment of our substrate towards CM reaction (*e. g.* sterical hindrance provided by isopropylidene structure next to the double bond moiety).

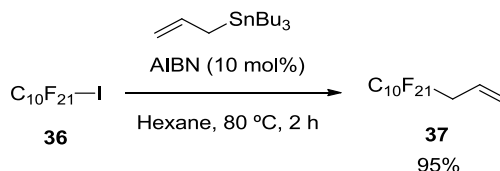
In view of the discouraging results of CM with perfluoroalkylethylenes showed above, we decided to move to their more reactive counterparts, perfluoroalkylpropenes.¹⁵ As previously outlined, the methylene spacer between the fluorinated chain and the double bond moiety could provide greater reactivity to such olefins by attenuating the inductive effect of CF₂ groups on the double bond moiety. It should be noted that this modification might be irrelevant for our biological purposes since the final product would still bear a polyfluorinated chain at the sphingoid base.

3-Perfluorodecylprop-1-ene **37** was selected as the model fluoroalkyl allyl derivative maintaining a high fluorination grade and having almost the same chain length as the phytosphingosine moiety present in KRN7000 (we assumed that one methylene unit less would not suppose a problem for our biological purposes).

Although perfluoroalkylpropenes are not commercially available, they are readily accessible via Keck radical allylation.³⁶ In this way,

³⁶ Ryu, I.; Kerimerman, S.; Niguma, T.; Minakata, S.; Komatsu, M.; Luo, Z.; Curran, D. P. *Tetrahedron Lett.* **2001**, *42*, 947-950.

perfluorodecyl iodide **36** was converted into **37** in a 95% yield upon treatment with allyltributyltin in the presence of AIBN as radical initiator (Scheme 3.26).



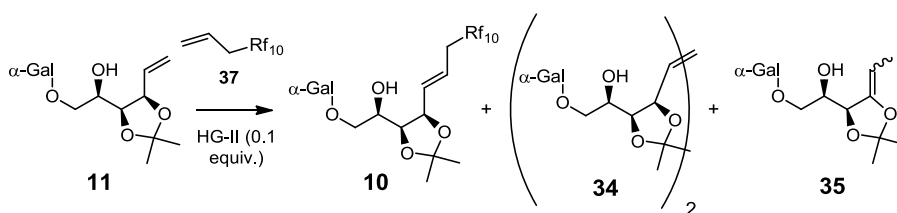
Scheme 3.26. Synthesis of 3-perfluorodecylprop-1-ene **37** via Keck radical allylation.

Initial attempts of olefin metathesis with 3-perfluorodecylprop-1-ene **37** were performed under MW irradiation because of the higher conversions observed in the previous CM studies. In addition, HG-II was selected as the catalyst since it proved the most efficient in the literature of perfluoroalkylpropenes (Table 3.4). To our delight and for the first time, the desired cross product **10** was obtained in 27% yield following a "2+2" strategy (fluorinated olefin and catalyst were added in two portions during the stipulated time) in DCM (Table 3.4, entry 1). This result was encouraging since the desired product was obtained in a greater proportion than the dimer one **34** (6%) and no isomerisation was observed. Moreover, the low yield obtained was mainly due to a low conversion (62% of starting material **11** was recovered).

In order to improve conversion, the solvent was changed from DCM to perfluorotoluene (conversions were increased using this methodology in the preceding CM study). However, undesired isomerised olefin **35** was obtained as the major product (66% yield) and just traces of cross product **10** were observed (Table 3.4, entry 2). This result along with the ones previously obtained in Table 3.3 suggested that both MW irradiation and perfluorotoluene solvent may somehow favour isomerisation reaction front CM.

Synthesis of KRN7000 analogues with a high degree of fluorination.

Table 3.4. Optimization of CM reaction of **11** with 3-perfluorodecylprop-1-ene **37**.



Entry ^a	37 equiv.	Solvent	t	Yield (%) ^b			
				11	10	34	35
1 ^c	2 + 2	CH ₂ Cl ₂	(20 + 20) min	62	27	6	-
2	2	C ₆ F ₅ CF ₃	20 min	15	Traces	11	66
3 ^d	2	C ₆ F ₅ CF ₃	20 min	15	32	16	28
4 ^e	2	C ₆ F ₅ CF ₃	20 min	19	40	18	17
5 ^{c,e,f}	2 + 2	C ₆ F ₅ CF ₃	(24 + 24) h	-	76	18	-

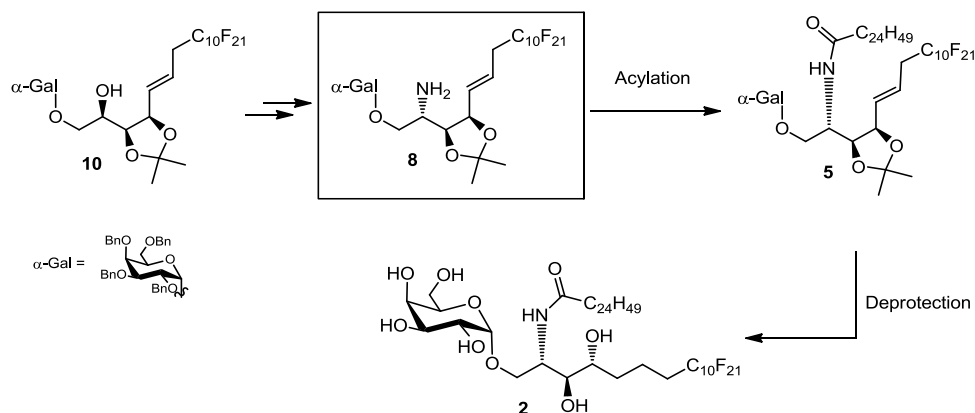
^a α -Gal refers to 2,3,4,6-tetra-O-benzyl- α -D-galactopyranosyl; The reaction was performed in a sealed tube under MW irradiation (200W) at 40 °C unless otherwise indicated. ^b Isolated yields. ^c Extra 0.1 equiv. of catalyst were added every addition of **37**. ^d 10 mol % of (Cy)₃P(O) was added to the mixture. ^e 10 mol % of benzoic acid was added to the mixture. ^f The reaction was performed under thermal heating, instead of MW irradiation.

Initial attempts for isomerisation suppression were performed by using the aforementioned known isomerisation inhibitors. However, although higher CM yields were observed, all additives failed in preventing isomerisation process (Table 3.4, entries 3-4). Even so, the yield for the cross product **10** was increased up to 40% in the presence of benzoic acid (Table 3.4, entry 4). Fortunately, isomerisation was totally suppressed when the latter conditions were performed under thermal heating, instead of MW irradiation. In this reaction, the desired cross product **10** was obtained in 76% yield (Table 3.4, entry 5).

Taken together, these results evidenced the higher reactivity in CM conditions of perfluoroalkylpropenes, such as **37** compared to the corresponding ethylenes, such as **32**. The reduced electronic density at the double bond moiety of **32** might be the main responsible for such different reactivity. In addition, despite the enhanced conversions in reduced times provided by MW irradiation, in comparison to thermal heating, this methodology did not provide successful results in our CM conditions. Insetad, it seemed to favour isomerisation process over CM reaction, especially in perfluorotoluene as solvent. Finally, optimal polyfluoroalkylation of **11** was achieved via CM reaction with **37** in perfluorotoluene as solvent.

3.4.3. Synthesis of amine intermediates

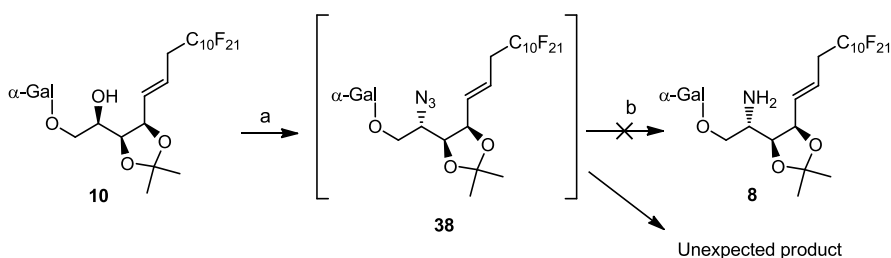
Having finally obtained the desired fluorinated olefin **10** in good yield, we next moved on to the formation of key amine intermediate **8**, which would allow the subsequent acylation and deprotection affording target analogue **2**. (Scheme 3.27).



Scheme 3.27. Synthetic pathway from **10** to **2**.

Synthesis of KRN7000 analogues with a high degree of fluorination.

Conversion of alcohol **10** into amine **8** was expected to proceed, as previously occurred in this chapter, by one-pot Mitsunobu azidation - Staudinger azide reduction. However, this time, such transformation proved unsuccessful (Scheme 3.28). Alcohol **10** was reacted under Mitsunobu azidation conditions, using DPPA as nucleophilic azide source in presence of PPh₃ and DIAD in THF, affording azide **38** (observed by TLC). Unfortunately, treatment of crude azide under Staudinger conditions did not afford the desired amine. Instead, it led to the formation of a new and unexpected derivative as the only product.



a) PPh₃, DIAD, DPPA, THF, 0°C to rt, 1h; b) PPh₃, Py, THF/H₂O (5:1), 60°C, 12h

Scheme 3.28. Unexpected product formation under Staudinger conditions from **38**.

Accurate spectroscopic analysis of this new derivative suggested the formation of pyrroline derivative **39**, which was then confirmed by MS (Figure 3.5). Key spectroscopic evidences for its structural elucidation are here highlighted:

In the ¹H NMR spectrum:

- No double bond proton signals were observed.
- All proton signals of the molecule were identified except from H-5.
- Great chemical shift of H-2 from \approx 3.0 ppm (expected amine **8**) ppm to 4.19 ppm, indicated the presence of an alternative moiety instead of free amine.

In the ^{13}C NMR spectrum:

- A new signal at 175.6 ppm corresponding to a quaternary centre (HSQC) was observed, which was attributed to C-5 suggesting the presence of an imine moiety.

In HMBC spectrum:

- Correlation of C-5 with H-2, H-3, H-4 and H-6 evidenced the pyrroline ring structure.

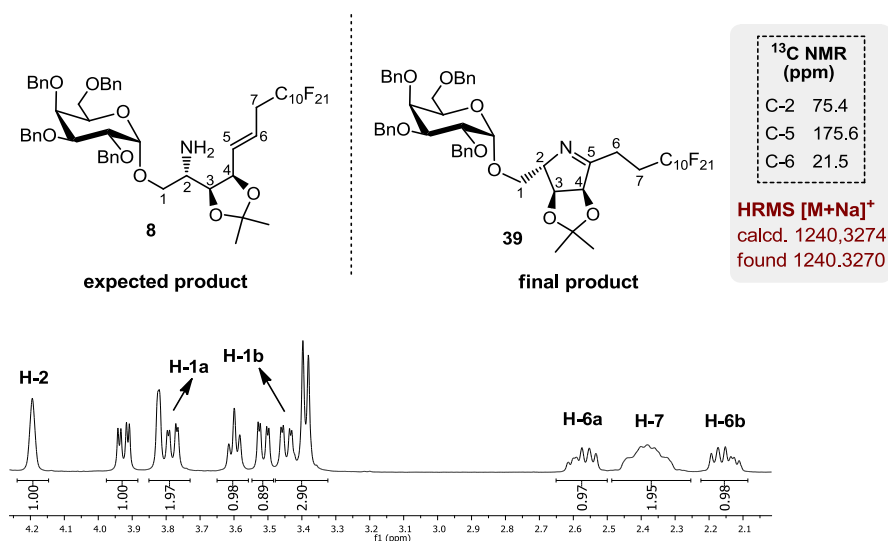


Figure 3.5. Structures of expected amine **8** and obtained imine **39** and selected region of ^1H NMR spectrum of **39**.

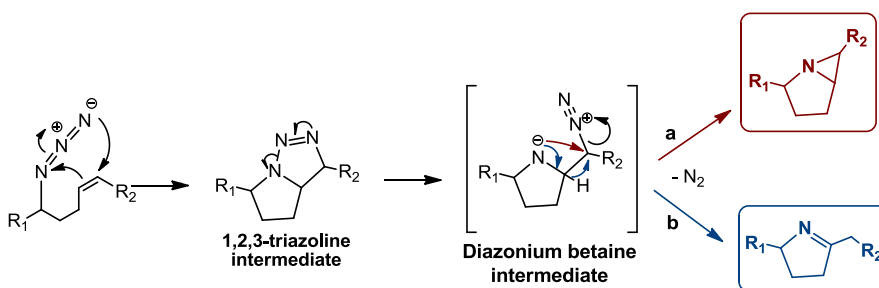
On the basis of the bibliographic data, intramolecular 1,3 dipolar cycloaddition between azide and double bond moieties of **38** was the suggested mechanism for this transformation. This side reaction was subtly pointed by Yu and Luo and co-workers³⁷ as well as by Panza and

³⁷ Sawant, R. C.; Hung, J.-T.; Chuang, H.-L.; Lin, H.-S.; Chen, W.-S.; Yu, A.-L.; Luo, S.-Y. *Eur. J. Org. Chem.* **2013**, 7611–7623.

Synthesis of KRN7000 analogues with a high degree of fluorination.

co-workers³⁸ in their synthesis of KRN7000 analogues, but the final product was not identified.

Intramolecular azide-olefin 1,3 dipolar cycloaddition (IAOC) was firstly studied by Logothetis.³⁹ This report described thermal decomposition of several organic azides containing unsaturations two, three, four and five bonds away from azide moiety, being cyclic imines and bicyclic aziridines the major products identified. A widely accepted mechanism^{39,40} for this transformation is showed in Scheme 3.29. First, a triazoline intermediate is formed by a 1,3-dipolar cycloaddition⁴¹ between azide and double bond moieties. Then, triazoline undergoes heterolytic cleavage of the N-N bond to produce a diazonium betaine intermediate which finally ends either with the direct formation of bicyclic aziridines via nucleophilic displacement (Scheme 3.29, via a) or with a initial proton migration and subsequent imine formation (Scheme 3.29, via b).



Scheme 3.29. Proposed mechanism for transformation of olefinic azides into imines and aziridines.

It is noteworthy that to our knowledge, this is the first time that this kind of by-product is isolated and characterized in the context of reported KRN7000 synthesis.

³⁸ Michieletti, M.; Bracci, A.; Compostella, F.; Libero, G. De; Mori, L.; Fallarini, S.; Lombardi, G.; Panza, L. *J. Org. Chem.* **2008**, *73*, 9192-9195.

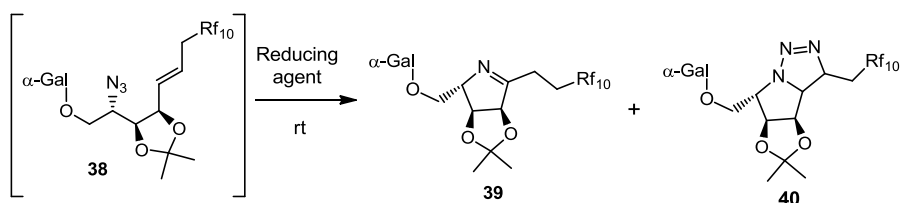
³⁹ Logothetis, A. L. *J. Am. Chem. Soc.* **1965**, *87*, 749-754.

⁴⁰ Reddy, D. S.; Judd, W. R.; Aubé, J. *Org. Lett.* **2003**, *5*, 3899-3902.

⁴¹ For detailed characteristics of 1,3-dipolar cycloaddition, see: Huisgen, R. *Proc. Chem. Soc.* **1961**, 357-369.

Since this transformation was favoured by temperature, milder azide reduction conditions were investigated in order to continue with the synthesis of the target KRN7000 analogue (Table 3.5). Unfortunately, all attempts for azide reduction failed.

Table 3.5. Attempts for reduction of azide moiety in **38**



Entry ^a	Reducing agent	Solvent	Time (h)	Yield (%) ^b		
				38	39	40
1	Lindlar cat., H ₂	EtOH	12	31	traces	62
2	Zn, NH ₄ Cl	THF/MeOH/ H ₂ O (3:1:1)	5	No reaction		
3	Zn, NH ₄ Cl, AcOH	THF/MeOH/ H ₂ O (3:1:1)	48	10	78	-

^a α -Gal refers to 2,3,4,6-tetra-O-benzyl- α -D-galactopyranosyl. Azide **38** refers to the crude mixture obtained from azidation of **10**. ^b Isolated Yields.

Firstly, mild hydrogenation with Lindlar catalyst^{38,42} in EtOH was tested (Table 3.5, entry 1). However, after 12 h of reaction, a 62% of triazolone derivative **40** was obtained together with traces of imine compound **39**. Key ¹H NMR data for triazolone structure elucidation (Figure 3.6) are here highlighted:

- Signals of protons H-5 and H-6 did not appear in the zone of olefinic protons. This fact suggested the loss of the

⁴² Murata, K.; Toba, T.; Nakanishi, K.; Takahashi, B.; Yamamura, T.; Miyake, S.; Annoura, H. *J. Org. Chem.* **2005**, *70*, 2398–2401.

Synthesis of KRN7000 analogues with a high degree of fluorination.

alkene moiety in the starting material and in consequence, that a 1,3-dipolar cycloaddition process took place.

- The signal corresponding to H-5 appeared at 3.44 ppm integrating for 1H. This fact indicated an sp^3 character of position 5, instead of the sp^2 hybridization observed for imine **39**.
- However, correlation of this signal with H-3, H-4 and H-2 observed by HMBC experiment suggested a ring structure similar to **39**.
- H-6 signal was, in turn, identified as a multiplet at 5.11 ppm, integrating for 1H. The high chemical shift observed for this signal revealed the electron-withdrawing effect of a near substituent.

All these observations fitted with the formation of triazoline intermediate **40**. Further MS analysis finally confirmed this hypothesis.

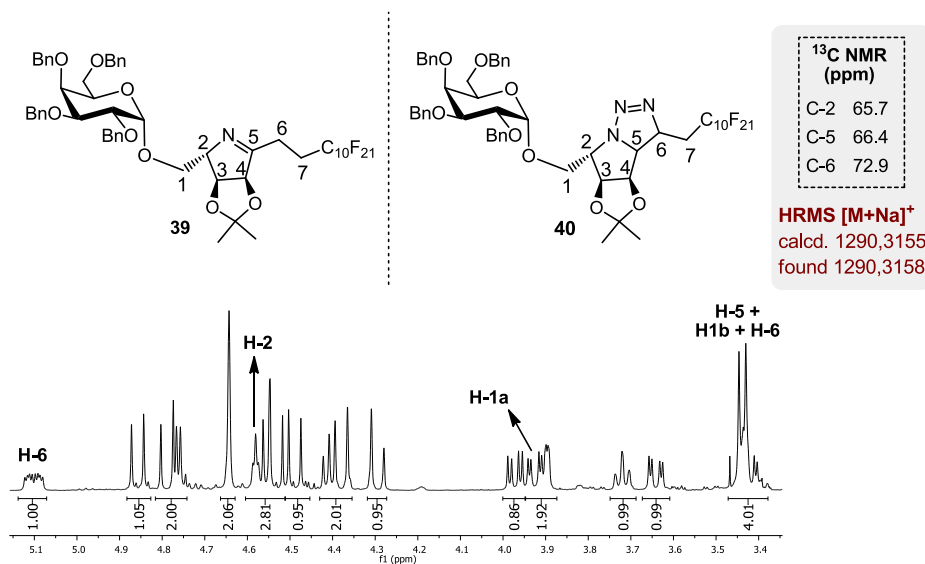
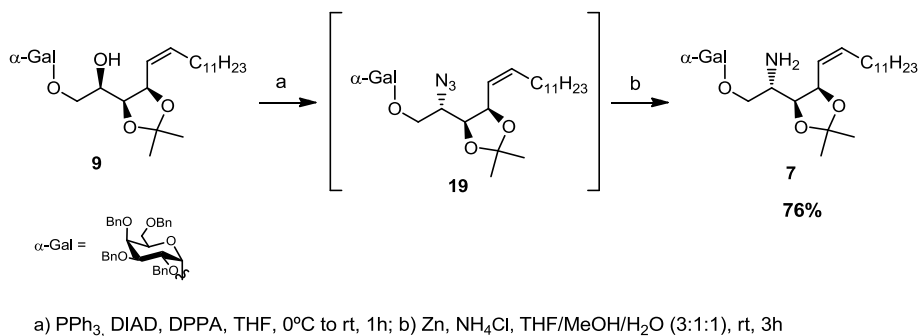


Figure 3.6. Structures of imine **39** and obtained triazoline **40** and selected region of ¹H NMR spectrum of **40**.

As commented before, triazoline species are intermediates in IAOC reactions. In this sense, it seems that under this reaction conditions, azido-alkene **38** underwent 1,3-dipolar cycloaddition affording triazoline **40** which was not able to undergo further ring opening under the tested conditions (Scheme 3.29).

Further azide reduction attempt was performed using Zn and ammonium chloride as reducing agents (Table 3.5, entry 2).⁴³ This time, no reaction progress was observed by TLC after 5 h of reaction. Forcing the reaction conditions by adding acetic acid, did not yield the desired amine. Instead, pyrroline derivative **39** was again obtained in 78% yield together with unreacted starting material **38** (10%, Table 3.5, entry 3). In contrast to the last result, equal treatment to **19**,⁴⁴ bearing an alkyl chain instead of the perfluorinated one, did afford the expected amine **7** in a good 76% yield (Scheme 3.30).



Scheme 3.30. Azide reduction of **19** in Zn/NH₄Cl system.

These results denoted that, for **38**, 1,3-dipolar cycloaddition reaction was much more favourable than azide reduction. The different behaviour observed for alkyl azide **19** and fluoroalkyl azide **38** could

⁴³ (a) Rai, A. N.; Basu, A. *Org. Lett.* **2004**, *6*, 2861-2863. (b) Lin, W.; Zhang, X.; He, Z.; Gong, L.; Mi, A. *Synth. Commun.* **2002**, *32*, 3279-3284.

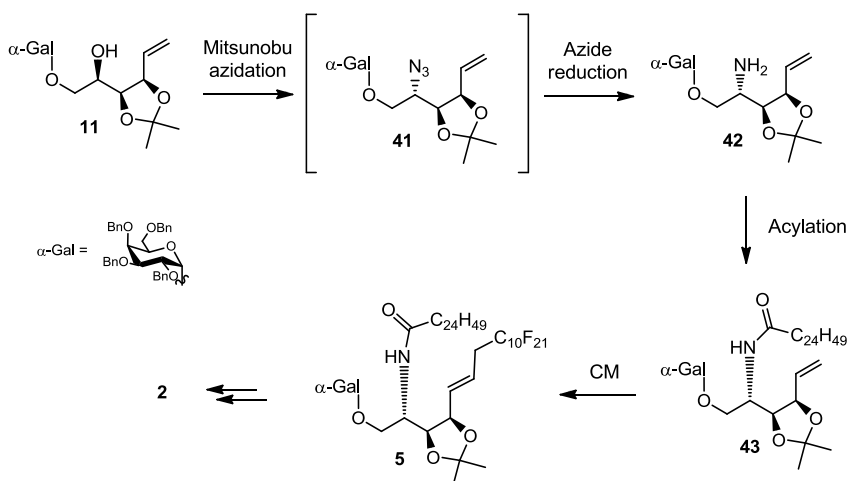
⁴⁴ Azide **19** was previously synthesized, in this chapter, during the synthesis of KRN7000 analogues fluorinated at fatty acid chain. It should be noted that this compound was readily reduced under Staudinger conditions.

Synthesis of KRN7000 analogues with a high degree of fluorination.

either rely on the cis/trans orientation of the double bond or on the inductive electronic effect of the olefin substituents.

At this point, in order to avoid coexistence of azide moiety and fluorinated alkene chain, we decided to explore the feasibility of introducing the fluorinated fragment after azide reduction.

A reorganization of the synthetic plan was, thus, envisioned in which terminal olefin **11** would undergo Mitsunobu azidation, instead of CM, and further treatment under Staudinger conditions would provide amine **42** still bearing the terminal double bond moiety. Finally, it was expected that acylation of **42** previous to CM would provide better coupling results because of the known low tolerance of Grubbs catalysts for free amine groups (Scheme 3.31).⁴⁵



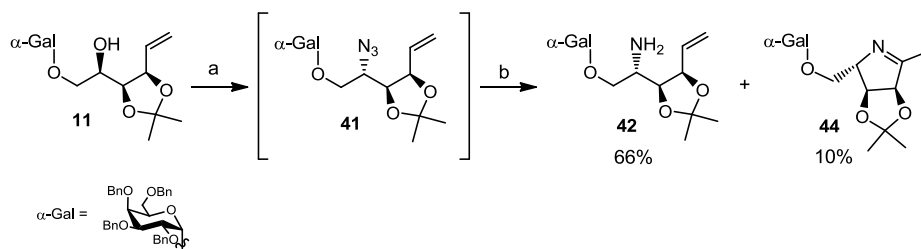
Scheme 3.31. New reorganized synthetic plan for obtaining KRN7000 analogue **2**.

In this way, **11** was subjected to Mitsunobu azidation conditions and the crude azide was then reduced. This time milder Zn/NH₄Cl

⁴⁵ Wilson, G. O.; Porter, K. A.; Weissman, H.; White, S. R.; Sottos, N. R.; Moore, J. S. *Adv. Synth. Catalysis* **2009**, *351*, 1817-1825.

reducing conditions were used instead of Staudinger ones with the aim of avoiding possible 1,3-dipolar cycloaddition (Scheme 3.32).

Fortunately, azide **41** was readily reduced affording 66% yield of amine **42**. However, it should be noted that 10% yield of imine subproduct **44** was also observed indicating the susceptibility of azide intermediate **41** to undergo 1,3-dipolar cycloaddition. The formation of **42** was evidenced by the presence, in the ^1H NMR spectrum, of a signal at 3.00 ppm corresponding to H-2 bearing the amino group. On the other hand, the structure of imine byproduct **44** was also confirmed by NMR spectroscopy by the appearance of a singlet at 1.84 ppm in ^1H NMR spectrum, corresponding to H-6, as well as the appearance in ^{13}C of the signal at 175.4 ppm, corresponding to the carbon of imine group, which was previously detected in compound **39**.



a) PPh_3 , DIAD, DPPA, THF, 0°C to rt., 1h b) Zn, NH_4Cl , THF/MeOH/ H_2O (3:1:1), r.t., 3h.

Scheme 3.32 One pot azidation-reduction of **11**.

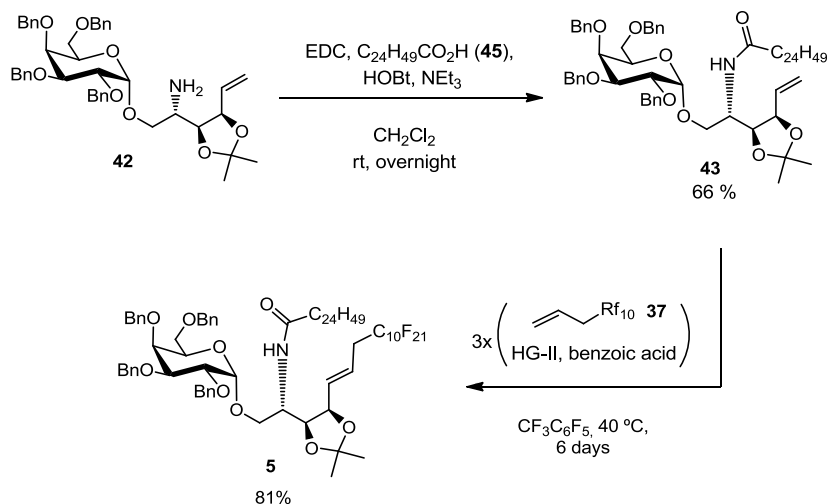
With amine intermediate **42** in hand, we finally focused our efforts on completing the synthesis of sphingoid base-fluorinated analogue of KRN7000.

3.4.4. Last steps: Acylation, CM and deprotection.

N-acylation of **42** with commercially available pentacosanoic acid **45** in the presence of EDC·HCl and HOBt as coupling agents was

Synthesis of KRN7000 analogues with a high degree of fluorination.

accomplished affording amide **43** in 66% yield (Scheme 3.33). Then, it was subjected to CM reaction with 3-perfluorodecylprop-1-ene **37** under the previously optimized CM conditions. Up to 6 days of reaction with successive additions of fluorinated olefin (2 equiv.), HG-II (5 mol%) and benzoic acid (5 mol%) every 48 h were required to obtain **5** in 81% yield. The longer reaction times as well as higher catalyst and olefin partner loadings needed to reach good yield, were presumably due to the high bulkiness of **43** provided by its long acyl chain.

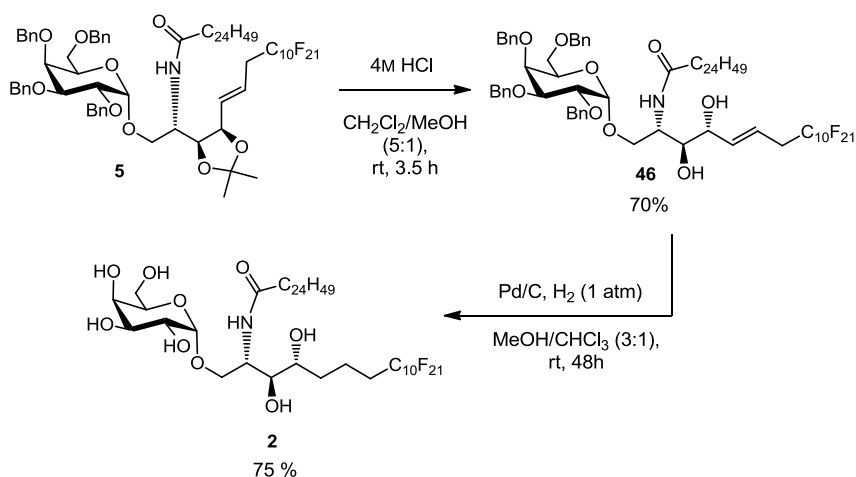


Scheme 3.33. Acylation of amine **42** with pentacosanoic acid **45** and subsequent fluoroalkylation via CM reaction.

Once having built the structural core of glycolipid **5**, removal of all protecting groups remained as the final stage to target KRN7000 fluorinated analogue **2**.

Firstly, isopropylidene moiety present in sphingoid base was removed via acidic hydrolysis. Thus, **5** was treated with 4M hydrochloric acid in DCM/MeOH (5:1) during 3.5 h affording 70% yield of the desired free diol product **46** (Scheme 3.34).

Then, double bond reduction and removal of all carbohydrate benzyl groups were accomplished in one step, via hydrogenolysis over palladium on carbon. Compound **46** was reacted with hydrogen gas (1 atm) and an excess of Pd/C for 48 h at r.t. leading to compound **2** in 75% yield. The disappearance of all the AB systems corresponding to benzylic protons as well as the aromatic and olefinic signals, in ^1H NMR spectrum, evidenced the complete removal of all benzylic groups and the reduction of the double bond moiety.



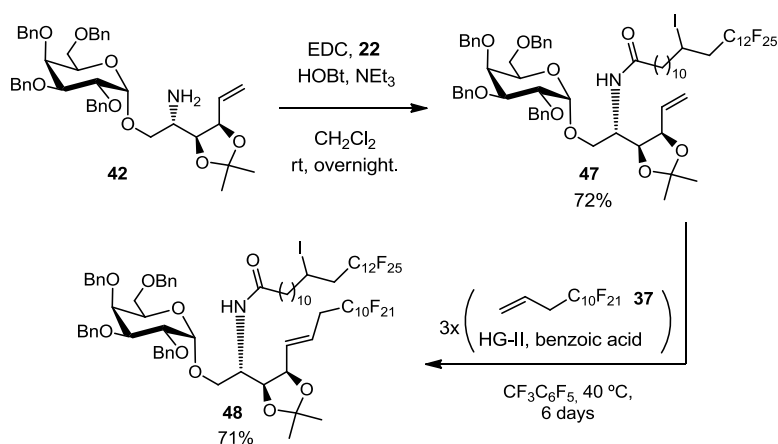
Scheme 3.34. Total deprotection of **5** to target KRN7000 analogue **2**.

3.5. SYNTHESIS OF A KRN7000 ANALOGUE FLUORINATED AT BOTH LIPID CHAINS.

The synthesis of this analogue was performed using the methodologies described before. In this sense, starting from amine intermediate **42**, acylation with previously synthesized fluorinated acid **22** furnished **47** in 72% yield (Scheme 3.35).

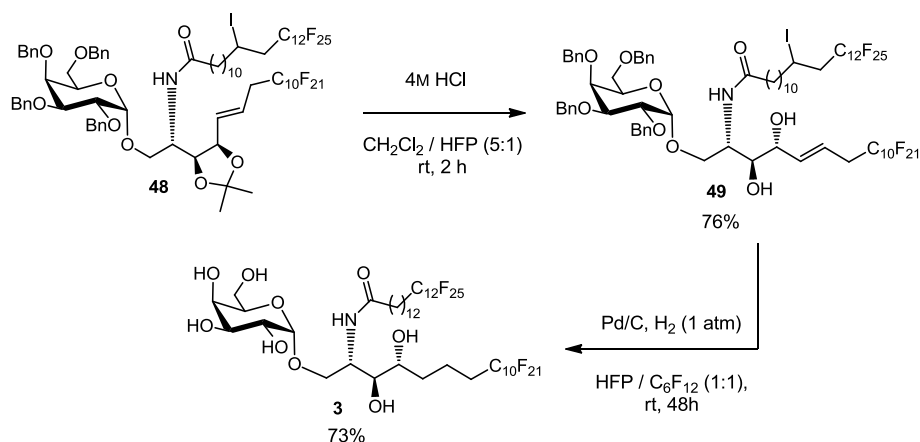
Synthesis of KRN7000 analogues with a high degree of fluorination.

The introduction of the second fluoroalkyl chain was performed again, by CM reaction. Compound **47** was thus reacted with perfluorodecylpropene **37** using HG-II catalyst and in the presence of benzoic acid to avoid isomerisation of the terminal double bond. As occurred before, 6 days of reaction and 3 successive additions of fluorinated olefin, HG-II and benzoic acid were required for reaching a good yield.



Scheme 3.35. N-acylation of **42** with **22** and subsequent fluoroalkylation via CM reaction.

To conclude the synthesis, acidic hydrolysis and Pd/C hydrogenolysis were performed (Scheme 3.36). This time, fluorinated solvents such as hexafluoroisopropanol (HFP) were required in order to solubilise the highly fluorinated glycolipid. In this manner, **48** underwent acidic hydrolysis in DCM/HFP (5:1) system as solvent affording **49** in 76% yield. Further hydrogenolysis was performed in HFP/C₆F₁₂ (1:1) system using an excess of Pd/C under 1 atm of H₂ furnishing **3** in 73% yield.



Scheme 3.36. Total deprotection of **48** to target KRN7000 analogue **3**.

3.6. CONCLUSIONS

In conclusion, analogues **1**, **2** and **3** bearing long fluoroalkyl fragments at sphingoid base and/or acyl chain have been successfully synthesized in 14%, 13% and 9% overall yields, respectively.

AIBN-mediated radical perfluoroalkylation of double bonds proved successful for the synthesis of polyfluorinated carboxylic acid **22**, which allowed the synthesis of **1**, bearing a polyfluorinated acyl chain.

On the other hand, introduction of fluoroalkyl moiety at sphingoid base resulted more problematic. Wittig olefination with fluorinated phosphonium salts as well as CM reaction with perfluoroalkylethylene **32** proved unsuccessful in our system. Instead, introduction of the fluorinated chain was finally achieved in good yield via CM coupling with perfluoroalkylpropene **37**. Unfortunately, reduction of fluorinated azidoalkene **38** resulted unsuccessful since intramolecular azide-alkene 1,3-dipolar cycloaddition took place. For this reason, a reorganization of the synthetic pathway was envisioned in which CM reaction was performed

| *Synthesis of KRN7000 analogues with a high degree of fluorination.*

after acylation step. This change resulted in longer CM reaction times as well as the use of more equivalents of fluorinated olefin **37**. However, the final CM yields were maintained good. These reactions enabled access to **2** and **3**, bearing fluoroalkyl chains at sphingoid base and at both lipid chains respectively.

CHAPTER 4

SYNTHESIS OF KRN7000 ANALOGUES WITH A LOW DEGREE OF FLUORINATION AT THE ACYL CHAIN

4.1. INTRODUCTION

In the previous chapter we investigated the introduction of long perfluoroalkyl chains to ceramide fragment of KRN7000 with the aim of evaluating its biological outcome. In this sense, it should be noted that notwithstanding the known beneficial effects of fluorine in medicinal chemistry, the presence of such kind of polyfluorinated chains (longer than C_3F_7) in biologically active systems is still in its infancy. To date, only few drug candidates bearing long perfluoroalkyl fragments have been synthesized, presenting totally different biological behaviour from that of the parent compounds.¹ This fact makes difficult to predict the biological outcome resulting from the introduction of such long fluoroalkyl chains in bioactive molecules. Some examples are here highlighted (Figure 4.1).

Clavamamol H is an aminoalcohol with a long carbon chain presenting cytotoxicity against some cancer cell lines. Analogues replacing its lipid fragment by a fluoroalkyl were synthesized presenting different bioactivities.² While both fluorinated and hydrogenated compounds presented similar activity levels, their action mechanism was completely different. Original Clavamamol H provoked apoptosis towards cancer cells, while instead, its fluoroalkyl-containing counterpart induced necrosis. The authors hypothesized that the increased rigidity of fluorinated chains or their already reported different level of cell wall penetration could be the main responsible for such behaviour.

¹ For a recent review on synthesized bioactive molecules bearing long perfluoroalkyl chains, see: Prchalová, E.; Štěpánek, O.; Smrček, S.; Kotora, M. *Future Med. Chem.* **2014**, *6*, 1201-1229.

² Prchalová, E.; Votruba, I.; Kotora, M. *J. Fluorine Chem.* **2012**, *141*, 49-57.

KRN7000 analogues with a low degree of fluorination at the acyl chain.

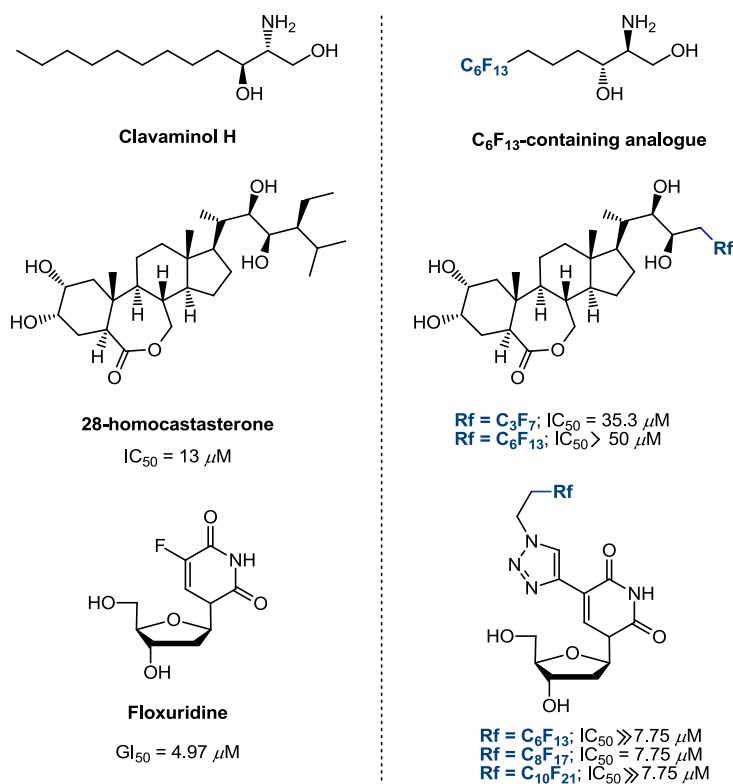


Figure 4.1. Selected examples of long fluoroalkyl-containing drugs and their bioactivities.

Another example are the fluorinated brassinosteroids reported by Eignerová and co-workers.³ This time, introduction of fluoroalkyl chains reduced drug cytotoxicity towards cancer cells. In fact, its activity was decreased as the fluoroalkyl length was increased. It should be mentioned, however, that any fluorinated analogue presented cytotoxicity against normal cells.

On the other hand, perfluoroalkylation of anticancerous drug Floxuridine resulted in successful results.⁴ Interestingly, it was shown that minor changes on the fluoroalkyl length produced major differences

³ Eignerová, B.; Slavíková, B.; Buděšinský, M.; Dračínský, M.; Klepetářová, B.; Št'astná, E.; Kotora, M. *J. Med. Chem.* **2009**, *52*, 5753-5757.

⁴ Park, S. M.; Yang, H.; Park, S.-K.; Kim, H. M.; Kim, B. H. *Bioorg. Med. Chem. Lett.* **2010**, *20*, 5831-5834.

in bioactivity. While the analogue bearing a perfluorooctyl fragment displayed similar activity (1.6-fold less) than the original drug, both perfluorodecyl or perfluorohexyl analogues presented substantially decreased activity. Nevertheless, all fluoroalkylated analogues showed amazing selectivity toward cancer cells front normal ones. Instead, Fluoxuridine presented serious toxicity against both.

As mentioned before, the therapeutical effect that could provide the incorporation of perfluoroalkyl fragments in drugs and how it could enhance its activity is still poorly understood. Furthermore, the potential or real toxicity, low solubility in either water or common organic solvents and unknown routes of the metabolism for the polyfluorinated compounds in living systems are some issues that hampers the interest of medicinal chemists for such kind of compounds.⁵

On the other hand, introduction of low fluorinated units such as one single fluorine atom, trifluoromethyl moieties and at a lower extent, pentafluoroethyl fragments are commonplace in medicinal chemistry.⁶ Some advantages of short fluorine-containing units compared to long perfluoroalkyl chains are enhanced solubility and flexibility. These conditions are quite important in medicinal chemistry and could make the difference in the physiological media. Therefore, although investigations on the application of the beneficial effects of long perfluoroalkyl chains in drug design field should be explored in greater detail in the near future, it seems that nowadays the incorporation of shorter fluoroalkyl units is more promising.

⁵ Kannan K. *Environ. Chem.* **2011**, *8*, 333-338.

⁶ Wang, J.; Sánchez-Roselló, M.; Aceña, J. L.; del Pozo, C.; Sorochinsky, A. E.; Fustero, S.; Soloshonok, V. A.; Liu, H. *Chem. Rev.* **2014**, *114*, 2432-2506.

KRN7000 analogues with a low degree of fluorination at the acyl chain.

4.2. OBJECTIVES AND RETROSYNTHETIC ANALYSIS

In line with Chapter 3, the main goal herein is to synthesize a new set of KRN7000 analogues differing on their fluorination degree at the acyl chain (Figure 4.2). Compounds **50**, **51** and **52** would bear perfluorohexyl, perfluoropropyl and trifluoromethyl moieties, respectively.

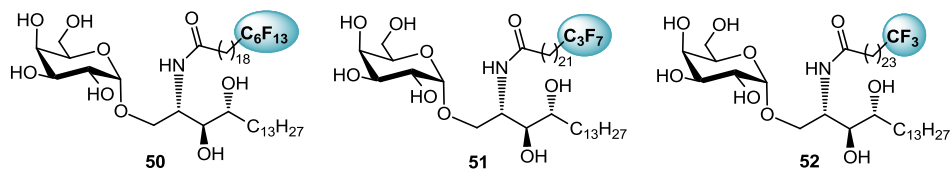
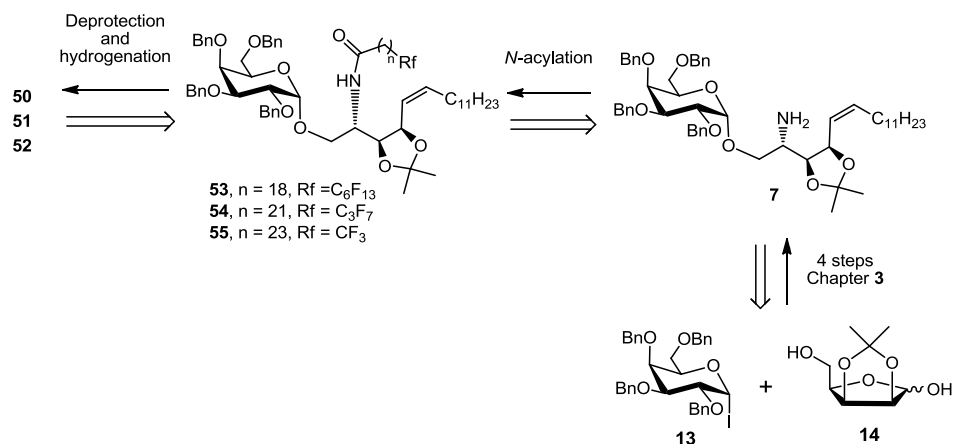


Figure 4.2. Target KRN7000 analogues bearing low fluorinated acyl chains.

The synthetic route used is adapted from the one used in Chapter 3. Therefore, introduction of different fluorinated acyl chains would be performed via *N*-acylation from common amine intermediate **7**, which was previously prepared in Chapter 3 from galactosyl iodide **13** and lyxofuranose derivative **14** (Scheme 4.1).



Scheme 4.1. Synthesis of target KRN7000 analogues **50**, **51** and **52** bearing low fluorinated acyl chains, from common amine intermediate **7**.

4.3. RESULTS AND DISCUSSION

4.3.1. Synthesis of polyfluorinated acids

The present synthesis began by the preparation of a set pentacosanoic acid analogues (**56**, **57** and **58**) containing decreasing number of fluorine atoms at the end of the lipid chain, while maintaining the same chain length (Figure 4.3).

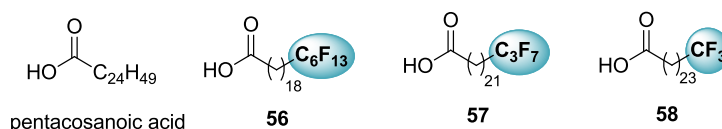
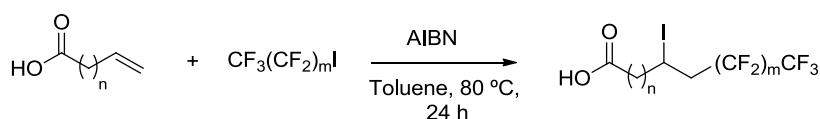


Figure 4.3. Selected carboxylic acids with different fluorination grades.

A widely used methodology for the synthesis of carboxylic acids bearing perfluoroalkyl fragments is the direct AIBN mediated radical perfluoroalkylation⁷ of ω -unsaturated carboxylic acids with commercially available perfluoroalkyl iodides (Scheme 4.2).



Scheme 4.2. Perfluoroalkylation of terminal alkenes via AIBN mediated radical reaction.

However, the high temperatures (refluxing toluene) used in this reaction, makes it presumably poorly suitable for the synthesis of "low" fluorinated carboxylic acids which require highly volatile perfluoroalkyl iodides as starting materials (Table 4.1).

For this reason, while perfluorohexyl-containing carboxylic acid **56** could be synthesized via such AIBN radical reaction, an alternative

⁷ Brace, N.O. *J. Fluorine Chem.*, **1999**, 93, 1-25.

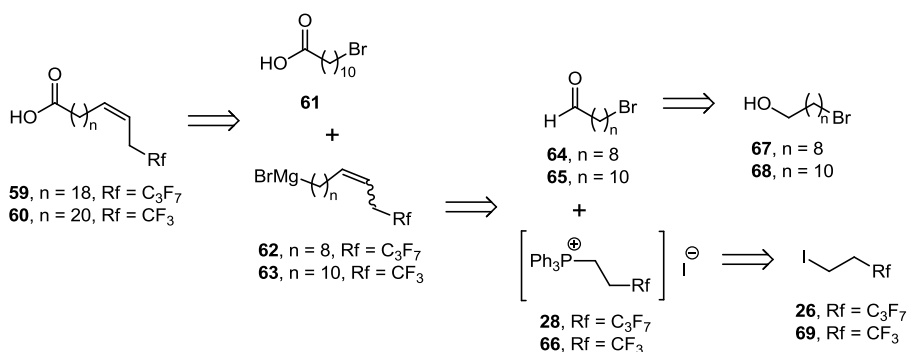
KRN7000 analogues with a low degree of fluorination at the acyl chain.

approach was envisioned for the synthesis of the resting carboxylic acids **57** and **58** bearing C₃F₇ and CF₃ moieties respectively.

Table 4.1. Reported boiling points of some commercially available perfluoroalkyl iodides.

C _n F _{2n+1} I	bp (°C) ^a
n	
1	- 22.5
2	12-13
3	41
4	67
5	95
6	117
7	137-138

In this sense, we proposed a retrosynthetic pathway involving a Cu-catalyzed coupling of ω-bromo acid **61** with the Grignard reagents **62** and **63** which in turn could be obtained via Wittig olefination of the corresponding ω-bromo aldehydes **64** and **65** and low fluorinated phosphonium salts **28** and **66** (Scheme 4.3).

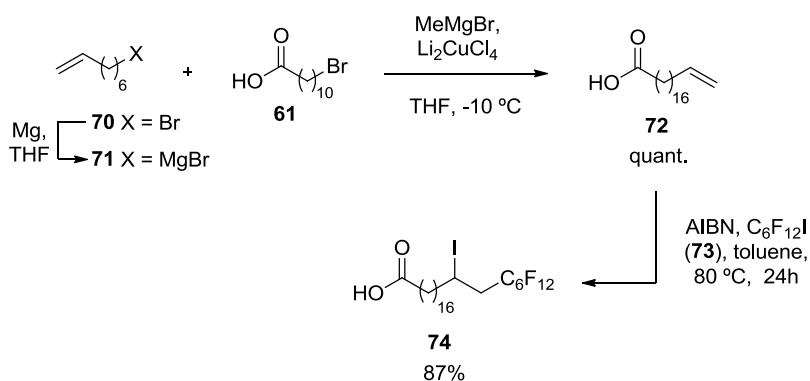


Scheme 4.3. Retrosynthetic strategy for the preparation of low fluorinated carboxylic acids **59** and **60**.

It should be noted that although in previous chapter, Wittig olefination proved an unsuccessful methodology for introduction of long perfluoroalkyl chains, it worked well for shorter fluoroalkyl chains, such as

28.⁸ We reasoned that double bond in acids **59** and **60** could be hydrogenated, once being introduced in the KRN7000 core, in the last hydrogenolysis step of the synthesis.

We initially dealt with the preparation of perfluorohexyl-containing acid **74** via AIBN mediated radical fluoroalkylation (Scheme 4.4). Previous synthesis of docos-18-enoic acid **72** was required because of its lack of commercial availability. Thus, 11-bromoundecanoic acid **61** was reacted with freshly prepared Grignard reagent **71** in the presence of Li_2CuCl_4 . The reaction afforded the corresponding acid **72** in quantitative yield. Subsequent treatment with perfluorohexyl iodide **73** in the presence of AIBN gave 19-perfluorohexyl-18-iodononadecanoic acid **74** in 87 % yield. Introduction of fluoroalkyl fragment was confirmed by the appearance, in ^{19}F NMR spectra, of a set of signals corresponding to the perfluorohexyl chain. Again, iodine atom was thought to be removed, along with benzyl protecting groups, in the last hydrogenolysis step.



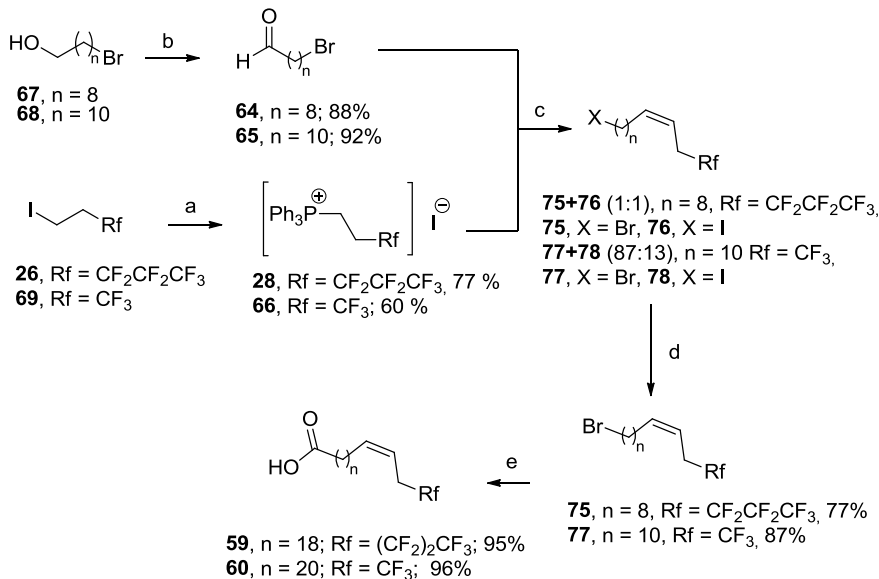
Scheme 4.4. Synthesis of fluorinated acid **74** via AIBN mediated radical perfluoroalkylation.

Regarding the synthesis of the low fluorinated carboxylic acids **59** and **60**, we began by the preparation of aldehydes **64** and **65** in 88% and

⁸ See Chapter 3, section 3.4.1.

KRN7000 analogues with a low degree of fluorination at the acyl chain.

92% yields respectively, via Swern oxidation of commercially available alcohols **67** and **68** (Scheme 4.5).



a) 1) (COCl)₂, DMSO, DCM, -78°C, 30 min; 2) NEt₃ -78°C to rt, 30 min; b) PPh₃, toluene, reflux, 24h; c) KHMDS, THF, 0°C, overnight; d) TBAB, THF, rt, overnight; e) 1) Mg, I₂, THF, 80 °C, 2h, 2) **61**, EtMgBr, THF, 0°C, 0.5 h. 3) Li₂CuCl₄ 0.02 eq, THF, -20 °C to rt, 5h.

Scheme 4.5. Synthesis of long polyfluoroalkyl acids **59** and **60**.

Concurrently, fluorinated phosphonium salt **66** was synthesized in 60% yield via treatment of the corresponding iodide **69** with PPh₃ in refluxing toluene. Phosphonium salt **28** was prepared in Chapter 3.⁸

Wittig condensation of aldehyde **64** and phosphonium salt **28** was performed at 0 °C in THF and using KHMDS as a base. Unexpectedly, the reaction afforded an equimolar and unseparable mixture of the desired polyfluoroalkyl bromide **75** and its iodide counterpart **76**. The latter compound presumably arose from S_N2 displacement of bromide either in the starting material **64** or final product **75**, by the iodide anion of phosphonium salt **28**. Nevertheless, smooth treatment of the mixture with

TBAB at rt afforded pure bromide **75** in 77 % yield for two steps. Product obtaining was confirmed by ^{19}F NMR spectroscopy with the appearance of three signals at -80.6, -114.2 and -127.5 ppm corresponding to CF_3 , CF_2CH_2 , and CF_2CF_3 respectively. Z olefin was obtained as a sole isomer, as evidenced by vicinal coupling constant of double bond protons ($J_{9,10} = 10.7$ Hz).

Analogously, Wittig reaction of aldehyde **65** with phosphonium salt **66** afforded a mixture of bromide and iodide products **77** and **78** in a 87:13 ratio which, after reacting with TBAB, gave rise to bromide **77** as a sole Z isomer in 87% yield over two steps.

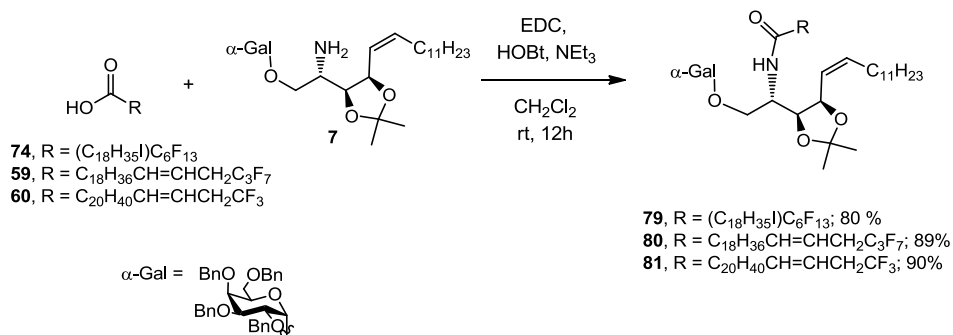
Finally, **75** was reacted with Mg in refluxing THF, yielding the corresponding Grignard reagent which was directly condensed with 11-bromoundecanoic acid **61** in the presence of Li_2CuCl_4 and EtMgBr. The reaction afforded the desired perfluoropropyl-containing carboxylic acid **59** in 95% yield. Analogous procedure with bromide **77** gave acid **60** in 96% yield.

4.3.2. N-Acylation and total deprotection

With the desired fluorinated acids **74**, **59** and **60** in hand, we next focused our attention on acylation of previously prepared key amine intermediate **7**⁹ (Scheme 4.6). In this way, amide **79** was obtained in 80% yield upon the reaction of amine **7** with 19-perfluorohexyl-18-iodononadecanoic acid **74** in presence of EDC·HCl and HOBT as coupling agents. Similarly, acylation with acids **59** and **60** afforded the corresponding amide compounds **80** (89%) and **81** (90%).

⁹ Amine compound **7** was prepared in chapter **3** during the synthesis of fluorinated analogue **1**

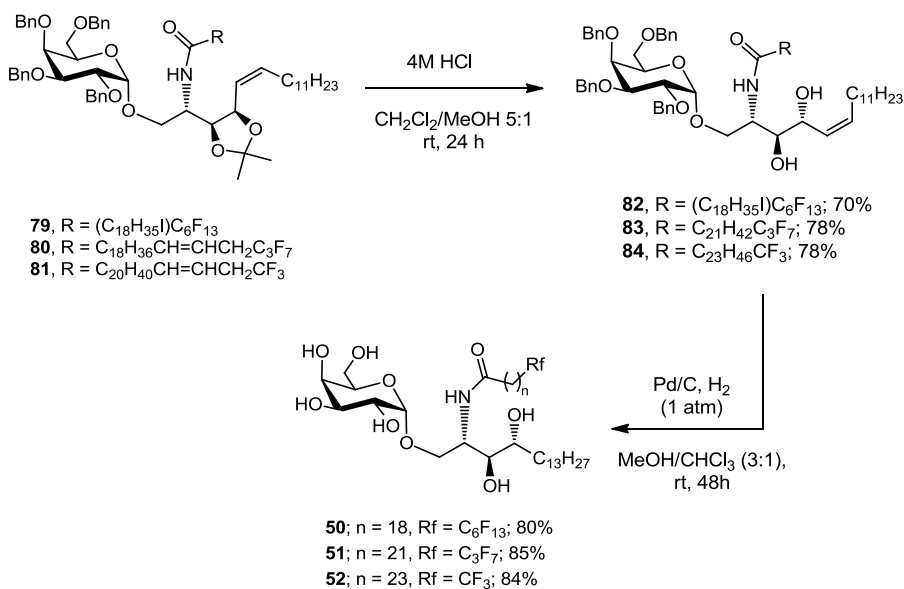
KRN7000 analogues with a low degree of fluorination at the acyl chain.



Scheme 4.6. Acylation of **7** with carboxylic acids **74**, **59** and **60**.

The present synthesis of KRN7000 analogues **50**, **51** and **52** finished with total deprotection of the molecule. This last stage was divided in two steps: 1) Acidic hydrolysis of the isopropylidene moiety and 2) Hydrogenolysis reaction to remove all benzylic groups and iodine atoms in the molecule as well as to reduce the double bond functionality.

In this way, glycosphingolipids **79**, **80** and **81** were equally treated with 4M hydrochloric acid at rt during 24 h affording the corresponding free diols **82** (70% yield), **83** (78% yield) and **84** (78% yield) (Scheme 4.7). Further hydrogenolysis of **82**, **83** and **84** was performed using an excess of Pd/C, under hydrogen atmosphere (1 atm), during 48 h. The reaction furnished the desired KRN7000 analogues **50** (80%), **51** (85%) and **52** (84%). Removal of iodine atom was confirmed by the shift, in the ¹H NMR spectrum, of the signal corresponding to H-12", from 4.23 ppm to the field of aliphatic protons. Similarly, the disappearance of all the AB systems corresponding to benzylic protons as well as the aromatic and olefinic signals, in ¹H NMR spectrum, evidenced the complete removal of all benzylic groups and the reduction of the double bond moiety.



Scheme 4.7. Last total deprotecting steps to afford analogues **50**, **51** and **52**.

4.4. CONCLUSIONS

In conclusion, KRN7000 analogues **50**, **51** and **52** bearing C₆F₁₃, C₃F₇ and CF₃ moieties respectively have been synthesized in 18%, 23% and 23% overall yields.

Acid **74**, incorporating a C₆F₁₃ fragment was synthesized via AIBN-mediated radical perfluoroalkylation. In contrast, the preparation of acids **59** and **60** bearing perfluoropropyl and trifluoromethyl groups required a longer synthetic pathway. In this sense, Li₂CuCl₄ catalyzed coupling of ω-bromo carboxylic acids with long ω-perfluoropropyl and trifluoromethyl alkyl bromides **75** and **77**, prepared via Wittig olefination, provided access to the desired carboxylic acids.

CHAPTER 5

SYNTHESIS OF CONFORMATIONALLY RIGID KRN7000 ANALOGUES

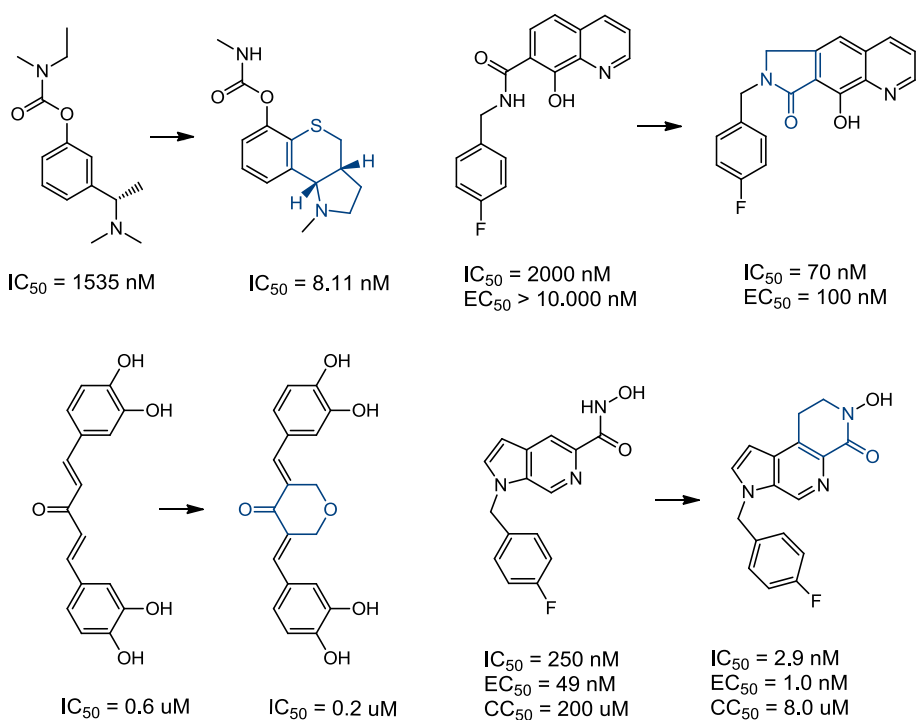
5.1. INTRODUCTION

5.1.1. Conformational restriction as a powerful tool in drug design.

The success (or not) in interaction between a ligand and a protein is mediated by an equilibrium of several thermodynamic parameters. The loss of entropy that suffer flexible ligands when bind to a protein is an unfavourable process which, if not overcome, may reduce the drug potency. In order to minimize the entropy penalties and improve the binding affinity of a ligand, a successful strategy is to limit its conformational flexibility. Therefore, conformational restriction of biologically active compounds has been widely used in modern drug design to increase their potency by stabilizing favourable binding conformations.¹ A common strategy for conformational restriction is the incorporation of cyclic structures in the drug core. Some selected examples are here highlighted (Scheme 5.1).

¹ Fang, Z.; Song, Y.; Zhan, P.; Zhang, Q.; Liu, X. *Future Med. Chem.* **2014**, *6*, 885–901.

Synthesis of conformationally rigid KRN7000 analogues.

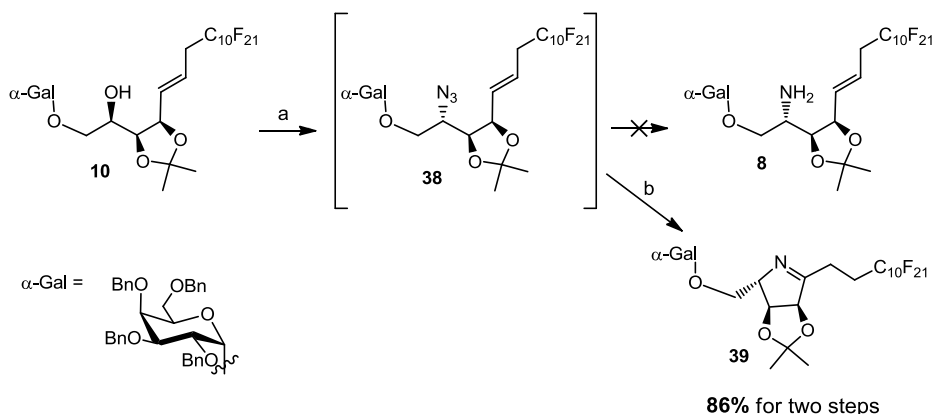


Scheme 5.1. Improvement of biological properties by ligand conformational restriction.

5.1.2. Unexpected cyclization process during the synthesis of fluorinated analogues of KRN7000.

During our synthesis of fluorinated analogues of KRN7000 described in Chapter 3, an unexpected formation of cyclic imine **39** was observed (Scheme 5.2). The reaction occurred while our efforts were focused on the conversion of alcohol **10** to the corresponding amine **8** via one pot Mitsunobu azidation - Staudinger reduction. We hypothesized that cyclization occurred through azide intermediate **38** leading to imine **39** in 86% yield for two steps.

In fact, a similar side reaction has been suggested in previous synthesis of KRN7000 and analogues.² However, the side products were not identified. For this reason, we decided to explore the behaviour of this reaction. Moreover, pyrroline derivative **39** was considered as a product particularly interesting being a potential precursor of conformationally restricted KRN7000 analogues.



a) PPh₃, DIAD, DPPA, THF, 0°C to rt, 1h; b) PPh₃, Py, THF/H₂O (5:1), 60°C, 12h

Scheme 5.2. Unexpected formation of cyclic imine **39** from alcohol **10** during one pot Mitsunobu azidation - Staudinger reduction.

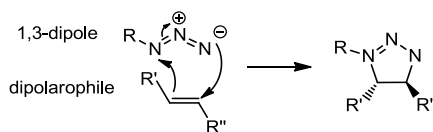
5.1.3. 1,3-Dipolar cycloaddition

Cycloaddition reaction of 1,3-dipoles to dipolarophiles is a widely known reaction described in detail by Huisgen in 1963.³ As reported by the author, this process occurs by a concerted mechanism in which the two new bonds are formed simultaneously, therefore leading to a stereoselective *cis* addition (Scheme 5.3).

² (a) Sawant, R. C.; Hung, J.-T.; Chuang, H.-L.; Lin, H.-S.; Chen, W.-S.; Yu, A.-L.; Luo, S.-Y. *Eur. J. Org. Chem.* **2013**, 7611–7623. (b) Michieletti, M.; Bracci, A.; Compostella, F.; De Libero, G.; Mori, L.; Fallarini, S.; Lombardi, G.; Panza, L. *J. Org. Chem.* **2008**, *73*, 9192-9195.

³ Huisgen, R. *Angew. Chem., Int. Ed. Engl.* **1963**, *2*, 565-632.

Synthesis of conformationally rigid KRN7000 analogues.



Scheme 5.3. General mechanism for 1,3-dipolar cycloaddition between azides (1,3-dipole) and alkenes (dipolarophile).

Further developments in this area conducted 1,3-dipolar cycloaddition to become a powerful method for the synthesis of a diverse array of five-membered heterocyclic rings.⁴ Consequently, it has been widely used for the synthesis of natural products and many other interesting heterocyclic containing compounds either by an intermolecular⁵ or intramolecular⁶ fashion.

5.1.3.1. Intramolecular azide-olefin 1,3-dipolar cycloaddition (IAOC).

Intramolecular azide-olefin cycloaddition (IAOC) is a subset of 1,3-dipolar cycloaddition in which the azide moiety behaves as the 1,3-dipole and the double bond acts as the dipolarophile. Although the immediate products of this reaction are 1,2,3-triazolines, these compounds generally evolve through nitrogen extrusion affording imines and/or aziridines (Scheme 5.4). In fact, triazoline isolation is usually a difficult challenge due to its rapid decomposition. For this reason, the synthetic interest of

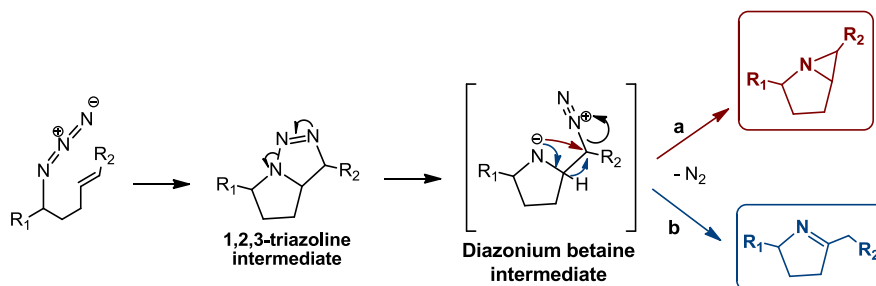
⁴ Padwa, A. In *1,3-Dipolar Cycloaddition Chemistry*; Padwa, A. Ed.; Wiley-Intersciences: New York, **1984**, 2, 277.

⁵ For some reviews on intermolecular applications of 1,3-dipolar cycloadditions see: (a) Koumbis, A. E.; Gallos, J. K. *Curr. Org. Chem.* **2003**, 7, 585–628; (b) Gallos, J. K.; Koumbis, A. E. *Curr. Org. Chem.* **2003**, 7, 397–425; (c) Koumbis, A. E.; Gallos, J. K. *Curr. Org. Chem.* **2003**, 7, 771–797; (d) Jones, R. C.; Martin, J. N. In *Synthetic Applications of 1,3-Dipolar Cycloaddition Chemistry toward Heterocycles and Natural Products*; Padwa, A., Pearson, W. H., Eds.; Wiley & Sons: New York, NY, **2002**.

⁶ For some reviews on intramolecular applications of 1,3-dipolar cycloadditions see: (a) Menon, R. S.; Nair, V. Intramolecular 1,3-dipolar cycloadditions of alkenes, alkynes, and allenes In *Comprehensive Organic Synthesis II*; Knochel, P., Ed.; Elsevier: Amsterdam, The Netherlands, **2014**; 1281–1341; (b) Burrell, A. J.; Coldham, I. *Curr. Org. Synth.* **2010**, 7, 312–331; (c) Nair, V.; Suja, T. D. *Tetrahedron* **2007**, 63, 12247–12275. (c) Wade, P.A. Intramolecular 1,3-Dipolar Cycloadditions. In *Comprehensive Organic Synthesis*; Trost, B.M.; Fleming, I., Eds.; Pergamon: Oxford, UK, **1991**, Vol. 4, 1111–1168.

azide-alkene 1,3 dipolar cycloaddition generally pivots around the formation of either imines or aziridines.

A widely accepted mechanism for IAOC⁷ involves the formation of a diazonium betaine intermediate followed by a 1,2 proton migration and imine formation (Scheme 5.4, path a) or direct nucleophilic displacement of molecular nitrogen to yield aziridine species (Scheme 5.4, path b). Alternatively, Erba *et al.* have recently proposed (based on theoretical calculations) a concerted mechanism in which imines and/or aziridines are directly formed from triazoline intermediate without the formation of any ionic intermediate.⁸



Scheme 5.4. Proposed mechanism for triazoline decomposition to aziridines and imines via diazonium betaine intermediate.

Although imines and aziridines are frequently obtained indiscriminately as a mixture, numerous examples leading selectively to imines⁹ or aziridines¹⁰ as intermediates in the synthesis of alkaloids and

⁷ (a) Logothetis, A. L. *J. Am. Chem. Soc.* **1965**, *87*, 749–754; (b) Reddy, D. S.; Judd, W. R.; Aubé, J. *Org. Lett.* **2003**, *5*, 3899–3902.

⁸ Contini, A.; Erba, E. *RSC Adv.* **2012**, *2*, 10652–10660.

⁹ For representative examples, see: (a) de Miguel, I.; Velado, M.; Herradón, B.; Mann, E. *Adv. Synth. Catal.* **2013**, *355*, 1237–1242; (b) de Miguel, I.; Herradón, B.; Mann, E. *Adv. Synth. Catal.* **2012**, *354*, 1731–1736; (c) Hui, B. W.-Q.; Chiba, S. *Org. Lett.* **2009**, *11*, 729–732; (d) Pearson, W.H.; Suga, H. *J. Org. Chem.* **1998**, *63*, 9910–9918; (e) Choi, J.-R.; Han, S.; Cha, J. K. *Tetrahedron Lett.* **1991**, *32*, 6469–6472; (f) Bennett, R. B., III; Choi, J. R.; Montgomery, W. D.; Cha, J. K. *J. Am. Chem. Soc.* **1989**, *111*, 2580–2852.

¹⁰ For a few examples, see: (a) Guo, Z.; Schultz, A. G. *Tetrahedron Lett.* **2004**, *45*, 919–921; (b) Ducray, R.; Cramer, N.; Ciufolini, M.A. *Tetrahedron Lett.* **2001**, *42*, 9175–9178.

Synthesis of conformationally rigid KRN7000 analogues.

other structurally interesting molecules have been described in the bibliography.

5.2. ANTECEDENTS

To our knowledge, there is only one reported synthesis of conformationally restricted analogues of KRN7000. The authors reported eight analogues showing two of them (RCAI-18 and RCAI-51) remarkable and moderate bioactivities, respectively (Figure 5.1).¹¹ The main structural features of these compounds are azetidine or pyrrolidine rings in their sphingosine backbones with one hydroxyl less compared to phytosphingosine chain of KRN7000.

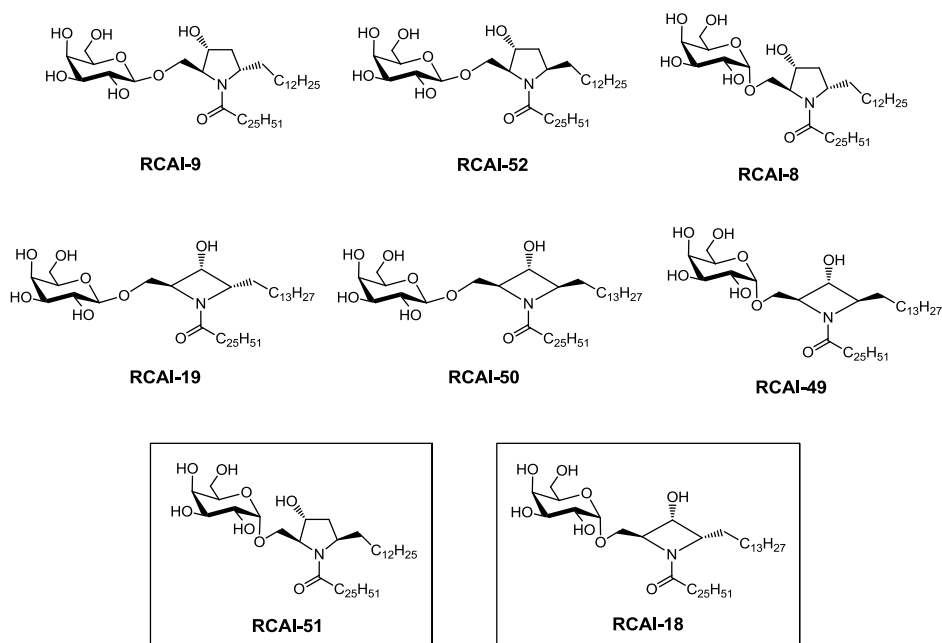
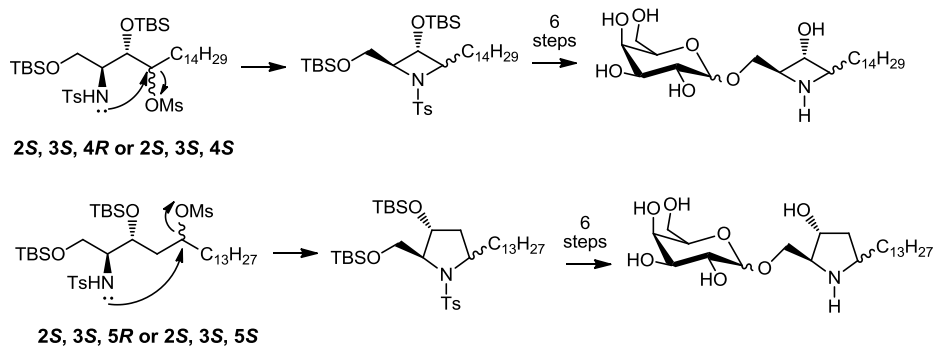


Figure 5.1. Described conformationally restricted KRN7000 analogues.

¹¹ Fuhshuku, K.-I.; Hongo, N.; Tashiro, T.; Masuda, Y.; Nakagawa, R.; Seino, K.-I.; Taniguchi, M.; Mori, K. *Bioorg. Med. Chem.* **2008**, *16*, 950-964.

The key cyclization step in this synthesis (Scheme 5.5) consisted in an intramolecular S_N2 displacement of the tosyl protected amino group in position 2 to the mesylate moiety placed in positions 4 (for azepane synthesis) or 5 (for pyrrolidine synthesis). In this way, starting from 2,4- and 2,5-aminoalcohols presenting different stereochemistries at C-4/C-5, four diastereomeric azepane and pyrrolidine compounds were obtained. Finally, glycosylation of each diastereoisomer afforded separable mixtures of α and β isomers leading thus, to 8 different analogues.



Scheme 5.5. Synthetic scheme for the formation of 8 different conformationally rigid analogues.

5.3. OBJECTIVES AND RETROSYNTHETIC ANALYSIS

The main objective of this chapter is to get insight into the divergent synthesis of the conformationally restricted KRN7000 analogues shown in Figure 5.2.

Synthesis of conformationally rigid KRN7000 analogues.

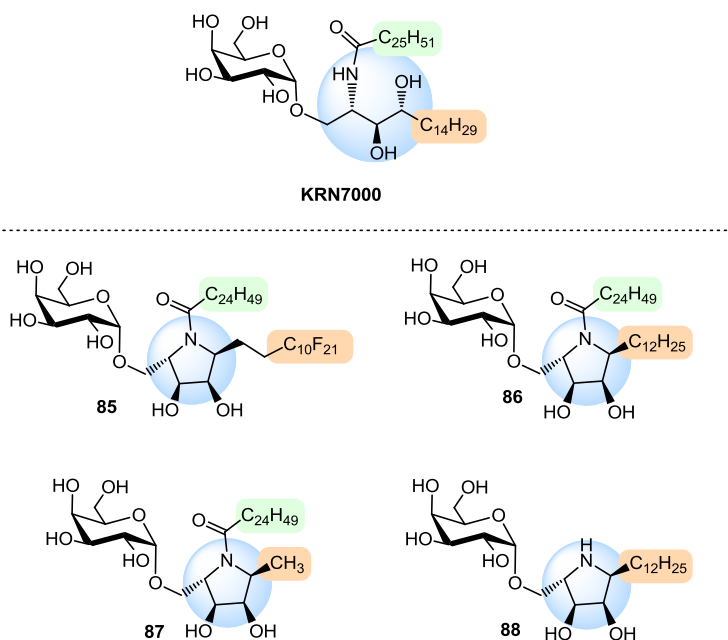
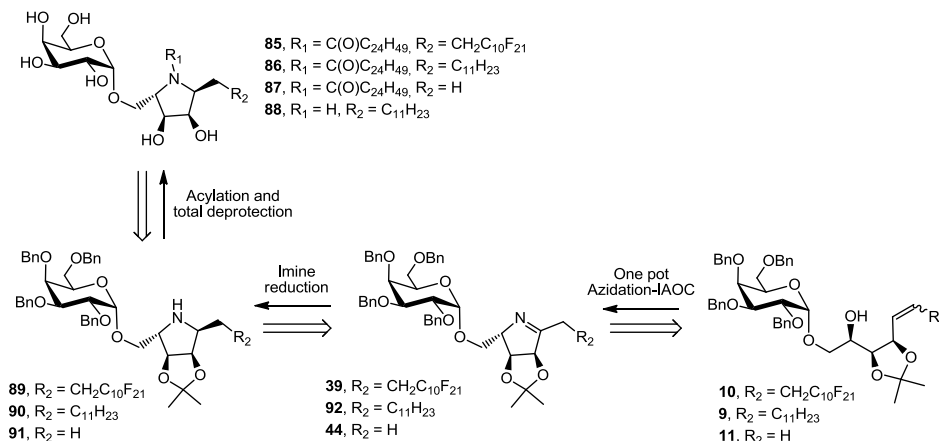


Figure 5.2. Target conformationally rigid KRN7000 analogues.

Compound **85** could arise from the unexpectedly obtained pyrroline **39** bearing a fluorinated sphingoid base. To determine the importance of fluorinated fragment in this analogues, compound **86**, being the cyclic counterpart of KRN7000 without presenting further structural modifications, was also targeted.

On the other hand, product **87** is a single lipidic chain derivative bearing a truncated phytosphingosine moiety. Analogue **88**, is the complementary single lipidic chain derivative having the original sphingoid base fragment of KRN7000 but lacking of acyl chain. This compound is in fact a cyclic analog of α -galactosyl phytosphingosine (α -psychosine), the product resulting from *in vivo* degradation of KRN7000. α -Galactosyl phytosphingosine, as recently demonstrated, stimulates

cytokine release from NKT cells.¹² Comparison of the mode of interaction of the latter analogues with the protein CD1d could provide light on the independent importance of the two lipid chains in such interaction.



Scheme 5.6. Retrosynthetic plan for conformationally restricted KRN7000 analogues **85-88**.

These target products would be accessible from the corresponding pyrrolidine derivatives **89-91** via acylation and/or total deprotection (Scheme 5.6). Compounds **89-91** could be obtained by selective reduction of the corresponding cyclic imines **39**, **92** and **44**, accessible in turn by the key one pot azidation-intramolecular azide-olefin cycloaddition (IAOC) from the hydroxy-alkene products **10**, **9** and **11** respectively. It should be noted that differently to the previously commented Mori's *et al.* methodology described for conformationally restricted KRN7000 analogues, our approach provide access to pyrrolidine rings bearing both hydroxyl groups at positions 3 and 4, which in the case of KRN7000 are known to be involved in the strong H-network with Asp-80 of CD1d.¹³

¹² Deng, S.; Kain, L.; Pereira, C. S.; Mata, S.; Macedo, M. F.; Bendelac, A.; Teyton, L.; Savage, P. B. *Chem. Sci.* **2017**, *8*, 2204-2208.

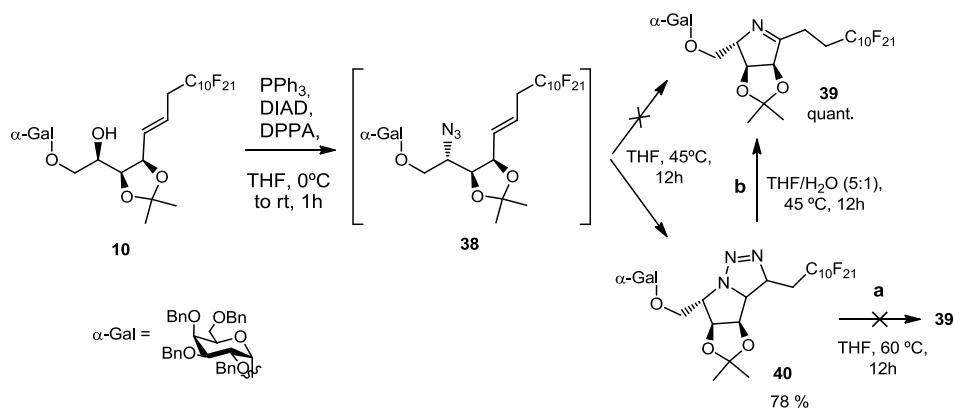
¹³ Hénon, E.; Dauchez, M.; Haudrechy, A.; Banchet, A. *Tetrahedron*, **2008**, *64*, 9480-9489.

5.4. RESULTS AND DISCUSSION

5.4.1. Synthesis of pyrrolidine intermediates

Initial IAOC investigations began by the reproduction and optimization of the previously unwanted formation of **39**. This product was obtained, in Chapter 3, via one pot Mitsunobu azidation-Staudinger reduction, in a 86% yield (Scheme 5.2). However, for our current purposes, the reaction was performed avoiding the reducing conditions in order to optimize its formation (Scheme 5.7). Thus, hydroxy-alkene **10** was reacted under standard Mitsunobu conditions affording crude azide **38** (observed by TLC). The crude mixture was then heated at 45 °C in THF for 12 h to undergo IAOC reaction. As indicated before, in this last step, PPh₃, H₂O and Py reagents were not added to the system since they apparently had no role in the cyclization process. Furthermore the temperature was decreased to 45 °C in order to test milder conditions. Surprisingly, although complete conversion to a sole product was observed by TLC, the analysis of the ¹H NMR spectrum of the pure product, revealed the formation of triazoline **40**¹⁴ instead of the desired imine **39**.

¹⁴ Compound **40** was fully characterized in Chapter 3.



Scheme 5.7. Optimization of conditions for conversion of **10** into **39**.

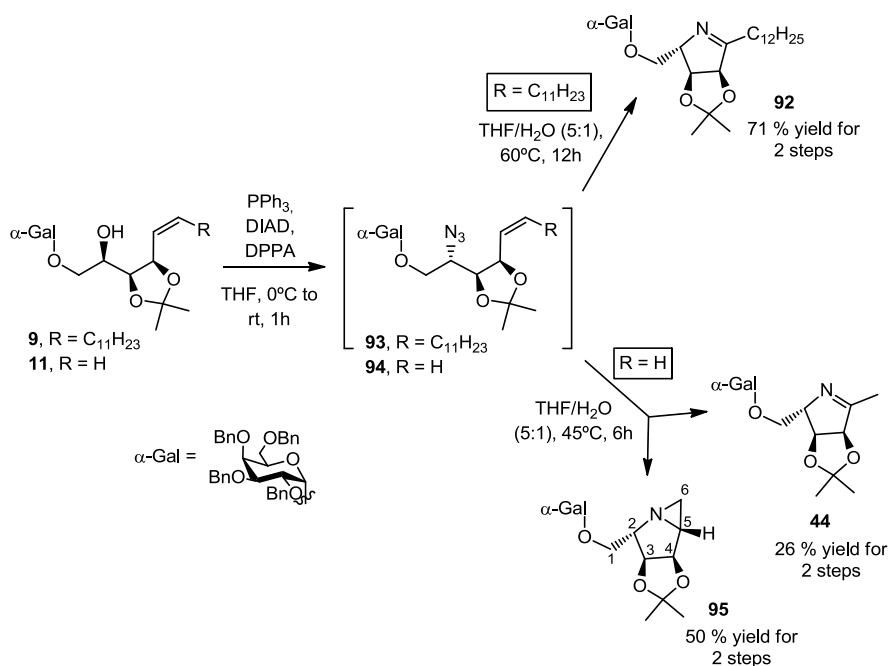
Since, as described above, this kind of species are intermediates in IAOC reactions, triazoline **40** was again heated, this time, at 60 °C, in order to force the nitrogen extrusion. However, no conversion was observed after 24 h of reaction (Scheme 5.7 via a). Interestingly, we found that upon the addition of some amount of water to the mixture (final reaction solvent: THF/H₂O 5:1), quantitative formation of desired cyclic derivative **39** was accomplished in 12h at 45 °C (Scheme 5.7 via b). The vital role of H₂O in our system contrasted with the literature data¹⁵ since a wide range of solvents have been used for this kind of transformations (e.g. toluene, THF, MeOH, DMF). However, it should be mentioned that in most of the reported examples the process is performed at higher temperatures (100 °C) than the employed in our case. At such temperatures the importance of the solvent might be diminished.

Having found favourable conditions for one pot azidation-IAOC of **10**, we next focused our attention on exploring the reactivity of non

¹⁵ For some recent examples, see: (a) de Miguel, I.; Velado, M.; Herradón, B.; Mann, E.; *Tetrahedron* **2016**, *72*, 4617-4625. (b) Moynihan, L.; Chadda, R.; McArdle, P.; Murphy, P. V. *Org. Lett.* **2015**, *17*, 6226-6229. (c) Rambla, M.; Durore, L.; Chabaud, L.; Guillou, C. *Eur. J. Org. Chem.* **2014**, 7716-7720. (d) de Miguel, I.; Velado, M.; Herradón, B.; Mann, E. *Adv. Synth. Catal.* **2013**, *355*, 1237-1242.

Synthesis of conformationally rigid KRN7000 analogues.

fluorinated hydroxy-alkenes **9** and **11**. To our delight, **9** underwent cyclization upon heating the previously obtained azide **93** at 60 °C in THF/H₂O (5:1) for 12 h. The reaction furnished **92** in 71% yield for two steps (Scheme 5.8). As occurred with its fluorinated counterpart, disappearance, in ¹H NMR spectra, of olefinic signals along with the apparition of a peak at 178.6 ppm (C=N), in ¹³C NMR spectra, confirmed the imine formation.



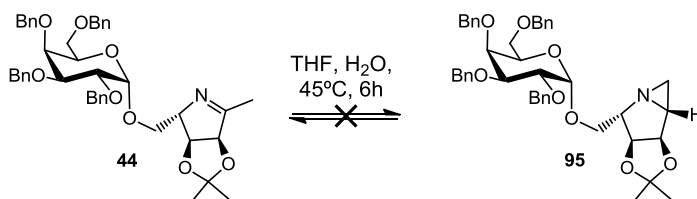
Scheme 5.8. One pot azidation-IAOC reactions of **9** and **11**.

On the other hand, the formation of imine **44**¹⁶ from alcohol **11** proved more problematic (Scheme 5.8). Although total conversion was reached in 6 h when the azide **94** was treated analogously to its fluorinated counterpart **38**, a mixture of two products was observed this time. Expected imine **44** was obtained in low 26% yield along with a new product. The unknown compound was identified as aziridine **95** since

¹⁶ Imine compound **44** was also obtained in Chapter 3 as side reaction product from reduction of azide **94**.

typical doublets at 1.91 and 1.72 ppm corresponding to H-6 protons of the aziridine appeared in the ^1H NMR spectrum of the pure product. Aziridine formation was then confirmed by HRMS. The stereochemistry of **95** was assigned by NOESY NMR experiment where a NOE crosspeak was observed between H-2 and H-5. As commented before, aziridines are also usual products of IAOC from azido-alkenes. However, as far as we are concerned, there are no reported explanations for the selective formation of imines or aziridines via this reaction.

A set of experiments were carried out for a better understanding of the product distribution observed. Firstly, in order to discard the formation aziridine **95** from imine **44** or *vice versa*, both isolated compounds were subjected to cycloaddition conditions (Scheme 5.9). However, heating pure compounds in separate flasks for 6h, resulted in total recovery of the unreacted starting materials refusing the hypothesis of product interconversion during cycloaddition reaction.¹⁷

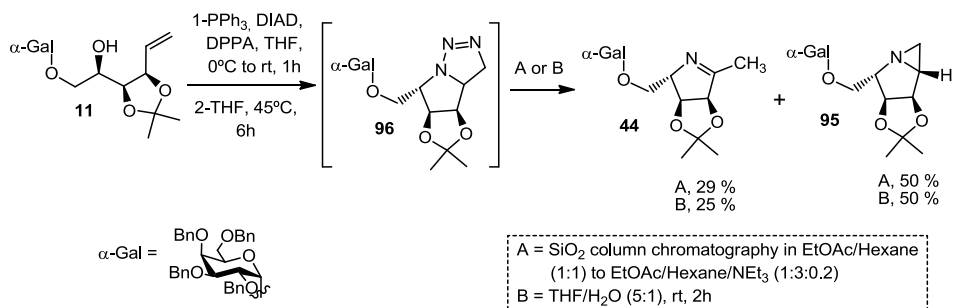


Scheme 5.9. Frustrated attempt for interconversion between **44** and **95**.

Furthermore, in an attempt to confirm the formation of both products from the same triazoline intermediate **96**, the isolation of the latter and subsequent ring opening was analysed as a two-step procedure (Scheme 5.10).

¹⁷ Similar experiment was also carried out in: Kim, S.; Lee, Y. M.; Lee, J.; Lee, T.; Fu, Y.; Song, Y.; Cho, J.; Kim, D. *J. Org. Chem.* **2007**, *72*, 4886-4891.

Synthesis of conformationally rigid KRN7000 analogues.



Scheme 5.10. Triazoline formation followed by A) purification of the crude by silica column chromatography or B) stirring of the crude in THF/H₂O solution.

In this experiment, hydroxy-alkene **11** was again treated under standard Mitsunobu azidation conditions and the resulting crude was then heated at 45 °C for 6 h in anhydrous THF. The presence of water in the media was avoided in order to stop the reaction at the formation of triazoline intermediate **96**. Although the analysis of the crude spectroscopical data revealed the successful formation of triazoline **96** as major product (by comparison with the spectroscopical data previously obtained for triazoline **40**) upon SiO₂ column chromatography afforded compounds **44** and **95** in 29% and 50% isolated yields respectively (Scheme 5.10, conditions A). This fact suggested that the reaction was promoted by the acidic nature of silica gel. A similar result was observed, when the crude triazoline was stirred for 2 h in THF/H₂O (5:1) at rt (Scheme 5.10, conditions B).

Two main conclusions were drawn from these results. The first one is that both imine and aziridine compounds aroused from the same triazoline intermediate **96**. In addition, although similar SiO₂-mediated evolution of triazoline intermediates to imine and aziridine species are exemplified in the literature,¹⁸ the unstability of triazoline **96** contrasted

¹⁸For some examples of silica-mediated triazoline ring opening, see: (a) Zhou, Y.; Murphy, P. V. *Org. Lett.* **2008**, *10*, 3777-3780. (b) Rambla, M.; Duroure, L.; Chabaud, L.; Guillou, C. *Eur. J. Org. Chem.* **2014**, 7716-7720. (c) Hassner, A.; Amarasekara, A. S.; Andisik, D. *J. Org. Chem.* **1988**, *53*, 27-30.

with the observed for its fluorinated counterpart **40**, which was easily purified without any evidences of decomposition. The high unstability of **96** also became evident by its total ring opening in solution during 2 h at rt (Scheme 5.10, conditions B), while conversion of fluorinated triazoline **40** required heating at 45 °C during 12 h (Scheme 5.7).

In an additional experiment, crude triazoline **96** was dissolved in THF- d_8 /D $_2$ O (5:1) in order to monitor its ring opening by ^1H NMR spectroscopy (Figure 5.3). In this study, several ^1H spectra were recorded at rt every 2 minutes. As a result, we observed the total disappearance of signal corresponding to H-5 in triazoline **96** in 30 minutes and the simultaneous apparition of signals corresponding to CH $_3$ moiety in **44** and H-5 in **95**.

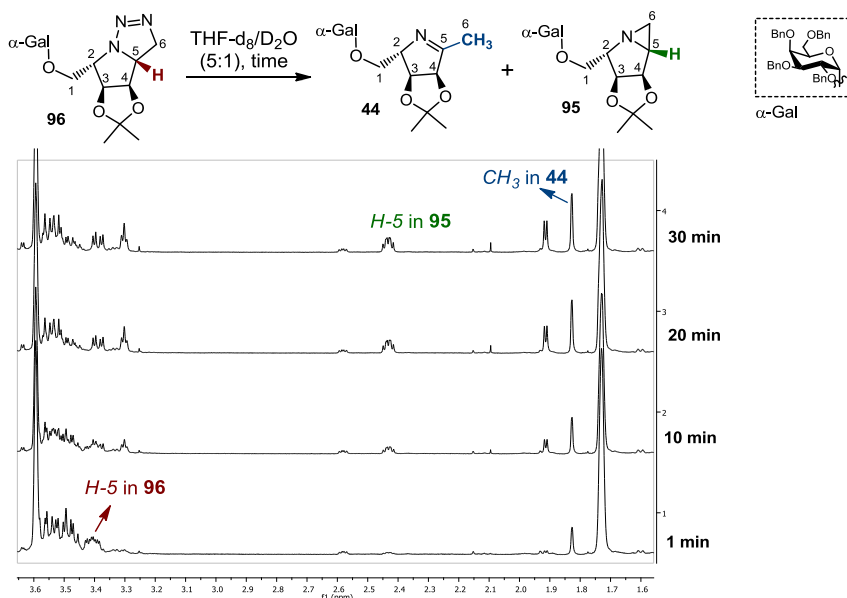


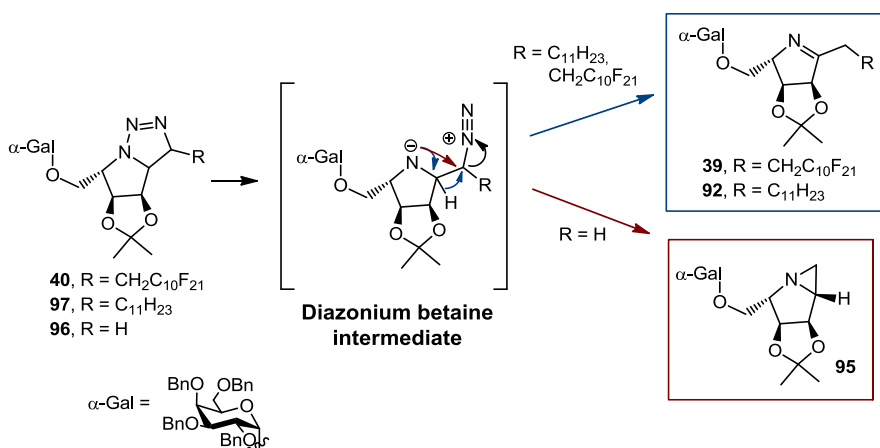
Figure 5.3. Selected region of the ^1H NMR spectrum (THF- d_8 /D $_2$ O (5:1), 400 MHz) of **96** ring opening recorded at different times.

All these results pointed triazoline **96** as the mutual reaction intermediate for the formation of both imine **44** and aziridine **95**.

Synthesis of conformationally rigid KRN7000 analogues.

Furthermore, the distinct product distribution observed for its ring opening compared to the one showed by non-terminal triazolines (**40** and **97** in Scheme 5.11) might be determined mainly by the nature of the triazoline intermediates, not by product interconversion.

In this sense, assuming the Logothetis proposed mechanism⁷ for triazoline decomposition commented before, a tentatively reasonable explanation for the different product distribution observed for cycloaddition of **40** and **97** compared to **96** could be suggested (Scheme 5.11). When R = H, the diazonium betaine intermediate obtained from the triazoline derivative evolves via nucleophilic displacement of nitrogen rendering aziridine **95** as major product. Instead, when R = perfluoroalkyl or alkyl chain, due to the higher steric hindrance, the nucleophilic attack is difficulted and the diazonium intermediate undergoes preferably a 1,2-H shift leading exclusively imine **39** or **92** respectively.

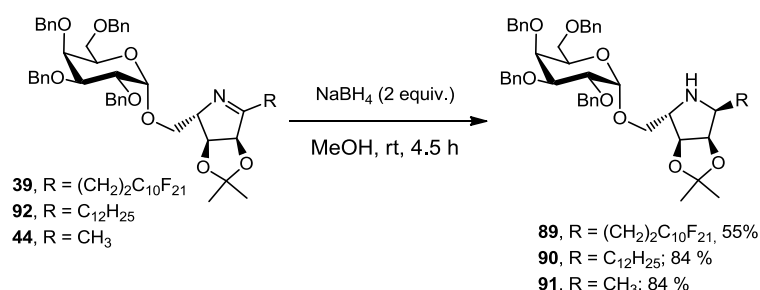


Scheme 5.11. Different product distribution, in IAOC reaction, depending on the triazoline substituents.

These results shed some light on the formation of imine and aziridines in IAOC reaction. However, to the best of our knowledge, there are no studies reporting optimal conditions for obtaining imine or aziridine

selectively. For this reason, we decided to go on with the synthesis from imine **44**, in spite the low yield obtained.

Having cyclic imines **39**, **92** and **44** in hand, we next moved to the synthesis of conformationally rigid analogues. NaBH₄ mediated imine reduction in methanol afforded, in a complete stereoselective way, pyrrolidines **89** (55%), **90** (84%) and **91** (84%) (Scheme 5.12). Reduction by using NaBH₃CN or PtO₂/H₂ were also tested but a mixture of diastereoisomers or partial debenzylation were respectively observed.



Scheme 5.12. Imine reduction with NaBH₄.

Elucidation of the stereochemistry at C-5 in the pyrrolidine rings of **89**, **90** and **91** was performed by NOESY experiments. Key NOE correlation peaks between H-5 and H-1 indicated a *trans* relationship between H-5 and H-2 in the three obtained products. Furthermore, NOESY spectrum analysis of the opposed diastereoisomer **98** (obtained during optimization of imine reduction conditions) showed a NOE cross-peak between H-6 and H-1 indicating a *cis* relationship between H-2 and H-5 (Figure 5.4). In addition, vicinal coupling constant values of **89**, **90** and **91** also proved helpful for their conformational analysis. Concretely, the marginal H2-H3 coupling constant value ($J_{2,3} \approx 0$ Hz) indicated a dihedral angle of 90° between them. Taken together, the spectroscopical data suggested a ^NE conformation for pyrrolidines **89**, **90** and **91** (Figure 5.4).

Synthesis of conformationally rigid KRN7000 analogues.

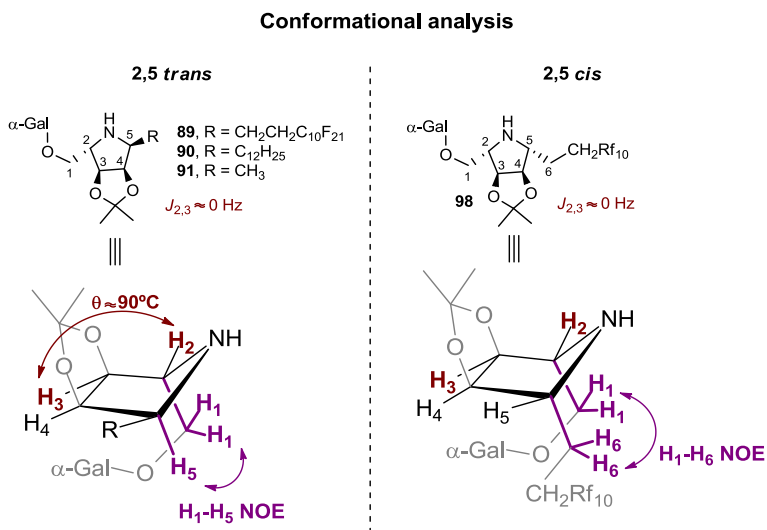
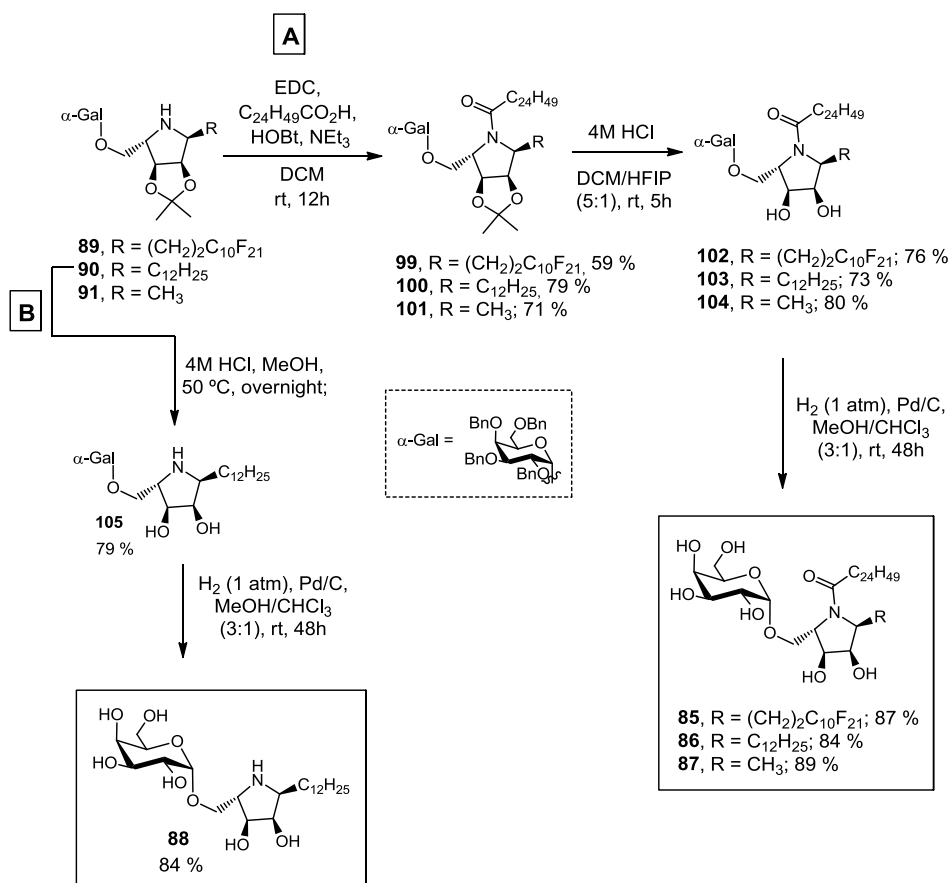


Figure 5.4. Proposed ^NE conformation of pyrrolidine ring in **89**, **90**, **91** and **98** on the basis of the observed NOE correlation peaks and *J* values.

5.4.2. Acylation and/or deprotection steps

With amines **89**, **90** and **91** in hand we next focused on the final obtaining of the target KRN7000 analogues (Scheme 5.13). Acylation of the three amino compounds with pentacosanoic acid, were carried out in DCM using EDC and HOBT as coupling agents (Scheme 5.13, A). The reactions afforded amides **99**, **100** and **101** in 59 %, 79 % and 71% yield respectively.

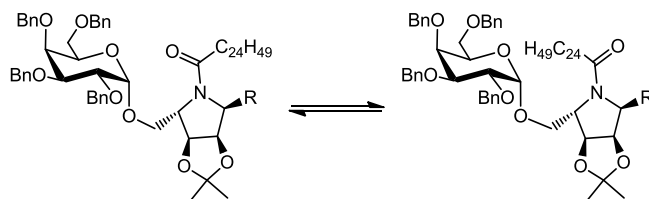


Scheme 5.13. Final steps for synthesis of KRN7000 analogues **85**, **86**, **87** and **88**.

Interestingly, the ¹H and ¹³C NMR spectra of **101** showed clear desdoublement of all peaks. Similar effect was observed for **100** but not for fluorinated amide **99**. While the formation of diastereoisomers upon acylation seemed improbable, *N*-acyl functionalization of pyrrolidines is generally known to induce the formation of rotamers (*Z* and *E*) due to a slow interconversion between them. This fact is due to the pseudo double bond character of the C-N bond (Scheme 5.14).¹⁹

¹⁹ Kleinpeter, E. *J. Mol. Struct.* **1996**, *380*, 139–156.

Synthesis of conformationally rigid KRN7000 analogues.



Scheme 5.14. Representation of *N*-acylated pyrrolidine rotamers in equilibrium.

This effect became more evident in the three amides upon acidic hydrolysis of isopropylidene moiety (Scheme 5.13, A, second step). The ^1H spectra of **102**, **103** and **104** clearly showed the presence of two sets of signals. At this time, the presence of rotamers in **102** was easily demonstrated by ^1H variable temperature (VT) NMR (with temperatures ranging from rt to 112 °C) and NOESY experiments.

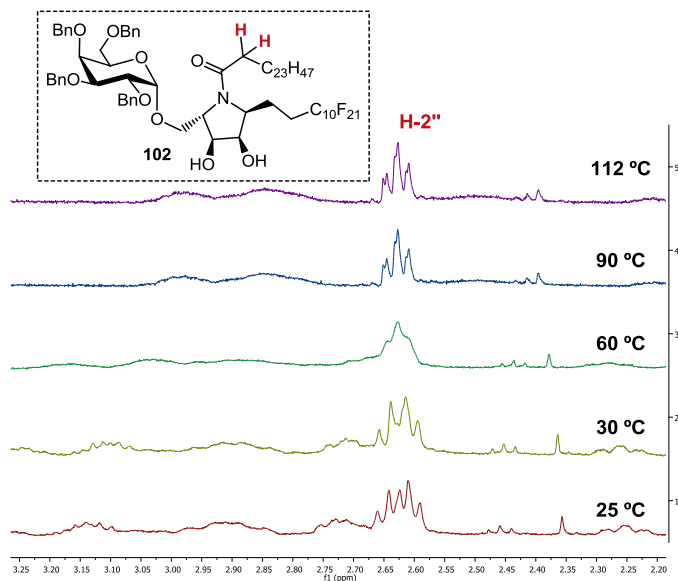


Figure 5.5. Selected region of the ^1H VT-NMR spectrum (CDCl_3 , 400 MHz) of **102** showing a coalescence temperature of about 90°C.

A coalescence temperature of around 90 °C was observed in ^1H VT-NMR experiment (Figure 5.5). In addition, 2D NOESY spectra

showed NOE correlation peaks of the same sign as the diagonal peaks. This fact is indicative of rotamers in slow interconverting conformations on the NMR time scale, since the "true" NOE cross peaks are of opposite sign compared to the diagonal peaks (Figure 5.6). Although VT-NMR is the preferred method for distinguishing equilibrating rotamers from non-equilibrating diastereoisomers, the use of chemical exchange NMR experiments such as 1D NOE, NOESY (EXSY) or ROESY have gained popularity due to their operational simplicity.²⁰

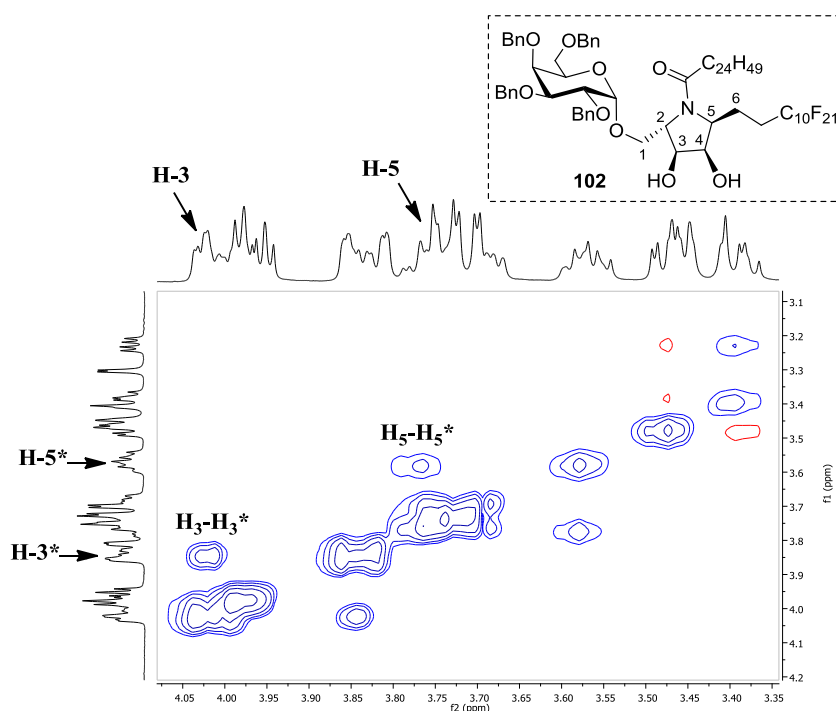


Figure 5.6. Selected region of the NOESY spectrum (CDCl_3 , 376.5 MHz) of **103**.

Back to the synthetic sequence, direct isopropylidene hydrolysis of pyrrolidine **90** was also performed in order to access to KRN7000 analogue **88**, lacking of acylic chain (Scheme 5.13, B). The reaction was

²⁰ (a) Hu, D. X.; Grice, P.; Ley, S. V. *J. Org. Chem.* **2012**, *77*, 5198–5202. (b) Wang, J.-P.; Lin, W.; Wray, V.; Lai, D.; Proksch, P. *Tetrahedron Lett.* **2013**, *54*, 2492–2496.

Synthesis of conformationally rigid KRN7000 analogues.

performed with 4M hydrochloric acid in MeOH at 50 °C affording the desired product **105** in 79% yield.

Having built the core structure of conformationally rigid target analogues, the total removal of benzyl protecting groups via Pd/C hydrogenolysis remained as the final step. In this way, compounds **102**, **103**, **104** and **105** were treated with H₂ (1 atm) in the presence of Pd/C giving rise to the final KRN7000 analogues **85** (87%), **86** (84%), **87** (89%) and **88** (84%). A complete disappearance of benzylic proton signals, in the ¹H NMR spectrum of the isolated products, evidenced the total deprotection. Mass spectroscopy provided further confirmation for the obtaining of analogues.

5.5. CONCLUSIONS

Based on a previously reported KRN7000 synthesis², a facile 6-7-step pathway for pyrrolidine containing KRN7000 analogues have been established. The key step of the synthesis is a one pot Mitsunobu azidation-IAOC from hydroxy-alkenes. This reaction has provided high reaction yields for compounds **9** and **10**. Unfortunately, in the case of terminal olefin **11**, mixtures of imine and aziridine species were observed, affording a low 26% yield of the desired imine product **44**.

Due to the easy access to hydroxy-alkene compounds differently substituted at double bond moiety, this synthesis enable access to a huge library of pyrrolidine containing KRN7000 analogues. In this work, the synthesized analogues possess perfluoroalkyl (**85**), alkyl (**86**) and methyl (**87**) moieties at the pyrrolidine side chain. Furthermore, an analogue bearing no acyl chain (**88**) has also been prepared.

UNIVERSITAT ROVIRA I VIRGILI
SYNTHESIS OF FLUORINATED ANALOGS OF KRN7000
David Collado Fernández

CHAPTER 6

HIGHLY REACTIVE 2-DEOXY-2- IODO-D-ALLO AND D- GULOPYRANOSYL SULFOXIDE DONORS ENSURE β - STEREOSELECTIVE GLYCOSYLATIONS WITH STEROIDAL AGLYCONES

6.1. INTRODUCTION

2-Deoxy- and 2,6-dideoxyglycosides are valuable structural units frequently present in bioactive natural products and clinical agents, such as antitumor drugs (anthracyclines, aureolic acids, calicheamicin, esperamicin), antibiotics (erythromycins, orthosomycins), cardiac glycosides (digitoxine) and antiparasitic agents (avermectins).¹ Specially, cardiac glycosides, in which the aglycone has an steroidal structure are applied in medicine for the treatment of congestive cardiac insufficiency, as antiarrhythmic drugs and as anticancer agents (Figure 6.1).²

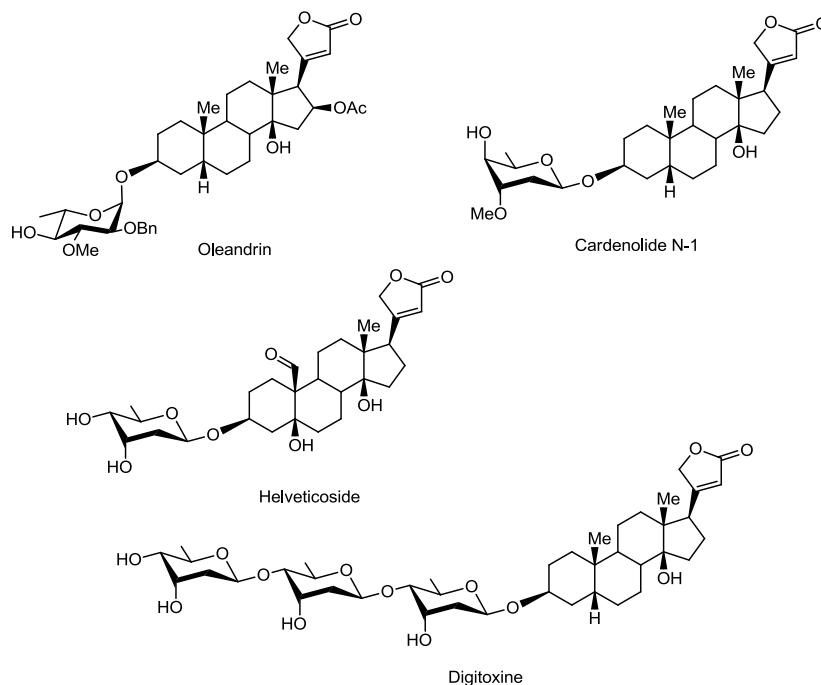


Figure 6.1. Examples of cardiac glycosides.

¹ (a) De Lederkremer, R. M.; Marino, C. *Adv. Carbohydr. Chem. Biochem.* **2007**, *61*, 143-216. (b) Kennedy, J. F.; White, C. A. In *Bioactive Carbohydrates in Chemistry, Biochemistry, and Biology*, Chichester, Ellis Horwood, 1983

² For key reviews see: (a) Ziff, O. J.; Kotecha, D. *Trends. Cardiovasc Med.* **2016**, *26*, 585-595; (b) Kumar, A.; De, T.; Mishra, A.; Mishra, A. *Pharmacogn Rev.* **2013**, *7*, 131-139; (c) Slingerland, M.; Cerella, C.; Guchelaar, H. J.; Diederich, M.; Gelderblom, H. *Invest. New Drugs* **2013**, *31*, 1087-1094 (d) Schoner, W.; Scheiner-Bobis, G. *Am. J. Cardiovasc. Drugs* **2007**, *7*, 173-189.

Glycosyl Sulfoxides Ensure β -Stereoselective Glycosylations with Steroidal Aglycones

These carbohydrate fragments are essential for the biological activities of such clinically important molecules. In fact, removal of the glycosidic part can cause the loss of efficiency and/or specificity as it is involved in the pharmacokinetic properties of the drug.³

Deoxysugars are also important components of lipopolysaccharides, glycoproteins and glycolipids where they play key role in cell-cell interactions, serve as targets for toxins, antibodies and microorganisms and participate in biochemical and bioorganic processes including active transmembrane transport, stabilization of protein folding and enzymatic inhibition.⁴

6.1.1. Stereoselective synthesis of 2-deoxyglycosides

Due to the biological relevance of 2-deoxyglycosides, researchers have focused their attention into the development of methods for the efficient and stereoselective construction of such compounds.⁵ Moreover, since many 2-deoxy sugars are not readily isolable from natural sources in enough quantities, their chemical synthesis is important.

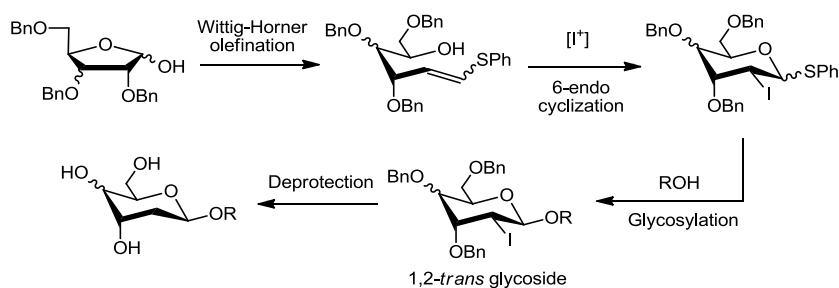
It should also be noted that most of the above deoxyglycosides, and especially cardiac glycosides (e.g. Cardenolide N-1, Oleandrin and Helveticoside, Figure 6.1), are usually composed of uncommon glycosyl moieties including *gulo*- and *allo*-configured pyranoses. While these sugars are nicely produced in nature, recent chemical glycosylation approaches are still inefficient for the synthesis of 2-deoxy- β -glycosides

³ Kren, V.; Martínková, L. *Curr. Med. Chem.* **2001**, *8*, 1303-1328.

⁴ (a) Albrecht, H. P. In *Naturally Occurring Glycosides*, Ikan, R.; Ed.; Wiley, Chichester, 1999; b) Weymouth-Wilson, A.C. *Nat. Prod. Rep.* **1997**, *14*, 99-110 c) Kirschning, A.; Bechtold, A. F.-W.; Rohr, J. *Top. Curr. Chem.* **1997**, *188*, 1-84; d) Allen, H. J.; Kisailus, E. C. Eds.; *Glycoconjugates: Composition, Structure and Function*, Marcel Dekker, New York, 1992.

⁵ (a) Zeng, J.; Xu, Y.; Wang, H.; Meng, L.; Wan, Q. *Sci. China Chem.* **2017**, Ahead of print. (b) Borovika, A.; Nagorny, P. *J. Carbohydr. Chem.* **2012**, *31*, 255-283. (c) Hou, D.; Lowary, T. L. *Carbohydr. Res.* **2009**, *344*, 1911-1940.

featuring such particular configurations. In this regard, our group developed a synthetic approach for the synthesis of 2-deoxy-2-iodoglycosides, especially effective for the production of *gulo* and *allo* pyranosides (Scheme 6.1).⁶



Scheme 6.1. Strategy to access to 2-deoxypyranosides from furanoses.

The resulting configuration is predefined by the starting furanose, *ribo* and *xylo*, serving as configurational templates for *allo* and *gulo* pyranosides respectively. After olefination of the starting furanose, the sulfanyl alkene is subjected to a stereochemical determining cyclization/glycosylation sequence. The cyclization occurs affording thioglycosides with complete stereoselectivity by virtue of the so-called *inside alkoxy effect*,⁷ leading to the iodine at C-2 always *cis* to the neighbouring alkoxy group. Subsequent glycosylation is controlled by the presence of a temporary iodine group which favours the formation of 1,2-*trans* glycosides and can be removed in the last step of the synthesis. The glycosylation stereoselectivity is explained as follows: After the activation of a thiophenyl donor, an oxocarbenium intermediate is produced (Figure 6.2). Among all the possible conformational

⁶ (a) Kövér, A.; Boutureira, O.; Matheu, M. I.; Díaz, Y.; Castellón, S. *J. Org. Chem.* **2014**, *79*, 3060-3068. (b) Rodríguez, M. A.; Boutureira, O.; Matheu, M. I.; Díaz, Y.; Castellón, S. *Eur. J. Org. Chem.* **2007**, 2470-2476. (c) Rodríguez, M. A.; Boutureira, O.; Arnés, X.; Díaz, Y.; Matheu, M. I.; Castellón, S. *J. Org. Chem.* **2005**, *70*, 10297-10310.

⁷ (a) Halter, J.; Strassner, T.; Houk, K. N. *J. Am. Chem. Soc.* **1997**, *119*, 8031-8034; (b) Houk, K.N.; Moses, S.R.; Wu, Y.-D.; Rondan, N.G.; Jäger, V.; Schohe, R.; Fronczek, F.R. *J. Am. Chem. Soc.* **1984**, *106*, 3880-3882; (c) Stork, G.; Kahn, M. *Tetrahedron Lett.* **1983**, *24*, 3951-3954.

Glycosyl Sulfoxides Ensure β -Stereoselective Glycosylations with Steroidal Aglycones

intermediates, the most prevalent half-chair conformations are 3H_4 and 4H_3 . When the iodine is positioned in axial (*manno* configuration) the lowest transition state is derived from the 4H_3 conformation in which the nucleophile approaches from the bottom face, thus avoiding steric repulsion with the bulky I group. On the other hand, when I is in equatorial (*gluco* configuration), the favoured TS is displayed with the nucleophile attacking from the top face to produce the β -glycosylated product.

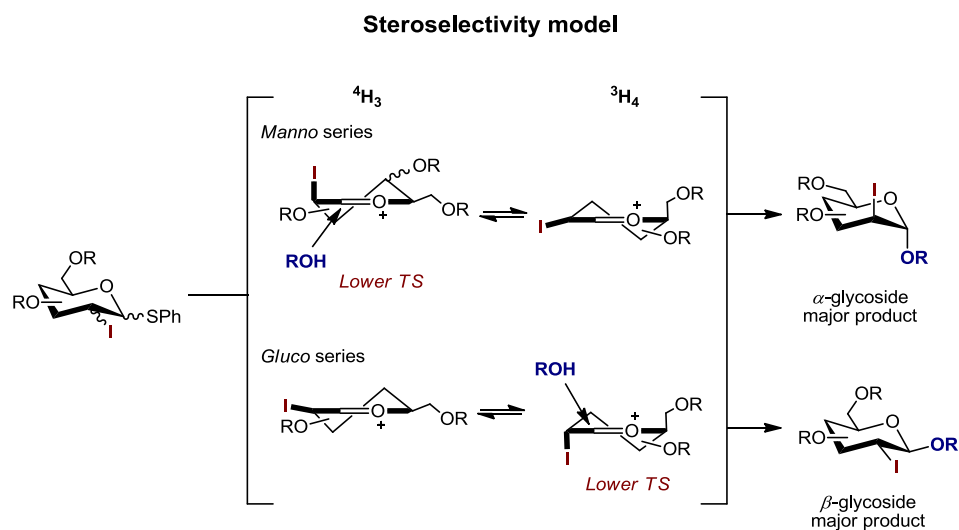
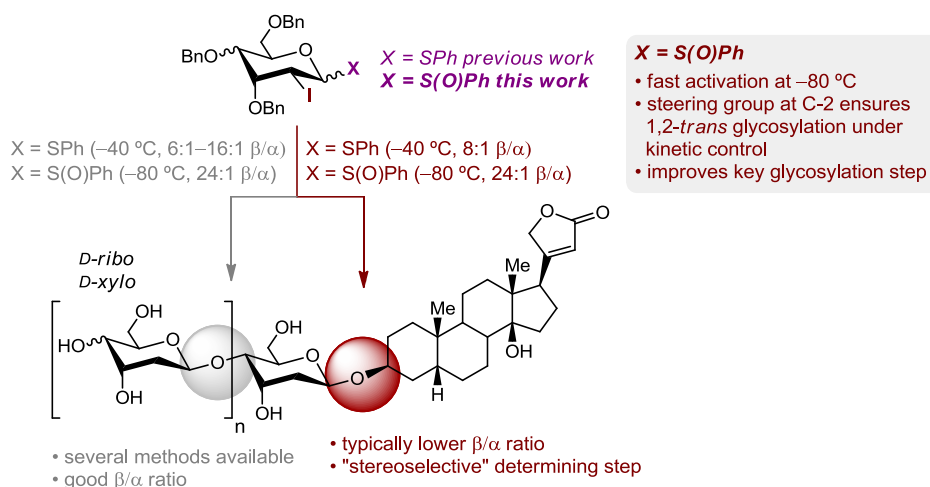


Figure 6.2. Proposed model to explain the stereoselectivity in the glycosylation of 2-deoxy-2-iodoglycosyl donors.

In the latter step, we observed that challenging glycosylations using steroidal aglycones required higher reaction temperatures, which ultimately decreased the β -stereoselectivity.^{6c} For this reason, we reasoned that prior oxidation of the thiophenyl donors to the corresponding glycosyl sulfoxides would enhance the reactivity to enable activation at lower temperature (Scheme 6.2).



Scheme 6.2. Scope and Limitations of the Stereoselective Synthesis of β -Steroidal Glycosides of *D-ribo* and *D-xyl*o Configurations – Using Sulfoxides to Improve Key Aglycone Glycosylation Step.

6.1.2. Glycosylation through glycosyl sulfoxides

Anomeric glycosulfonyl donors are characterized by being highly reactive compounds at very low temperatures. They are usually accessible from the corresponding glycosulfides by means of conventional oxidizing agents such as H_2O_2 ⁸ or *m*-CPBA⁹ among others.¹⁰ An additional strategy is the use of electrophilic Selectfluor reagent in MeCN/ H_2O .¹¹ This methodology may involve the initial formation of a fluoro-sulfonium cation which is then trapped by water providing the sulfoxide (Scheme 6.3).

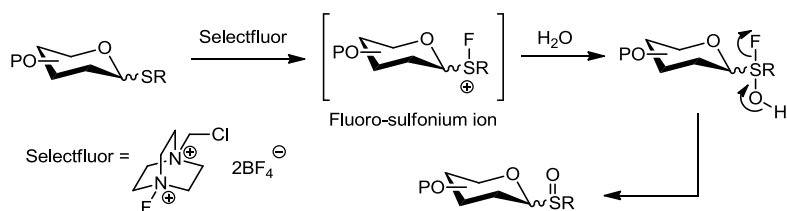
⁸ (a) Misbahi, K.; Lardic, M.; Ferrières, V.; Noiret, N.; Kerbal, A.; Plusquellec, D. *Tetrahedron:Asymmetry* **2001**, *12*, 2389-2393. (b) Ravikumar, K. S.; Zhang, Y. M.; Bégué, J.-P.; Bonnet-Delpon, D. *Eur. J. Org. Chem.* **1998**, 2937-2940. (c) Kakarla, R.; Dukina, R. G.; Hatzenbuehler, N. T.; Hui, Y. W.; Sofia, M. J. *J. Org. Chem.* **1996**, *61*, 8347-8349.

⁹ (a) Agnihotri, G.; Misra, A. K. *Tetrahedron Lett.* **2005**, *46*, 8113-8116. (b) Crich, D.; Mataka, J.; Sun, S.; Lam, K.-C.; Rheingold, A. L.; Wink, D. J. *Chem. Commun.* **1998**, 2763-2764. (c) Kahne, D.; Walker, S.; Cheng, Y.; Van Engen, D. *J. Am. Chem. Soc.* **1989**, *111*, 6881-6882.

¹⁰ Aversa, M. C.; Barattucci, A.; Bonaccorsi, P. *Tetrahedron* **2008**, *64*, 7659-7683.

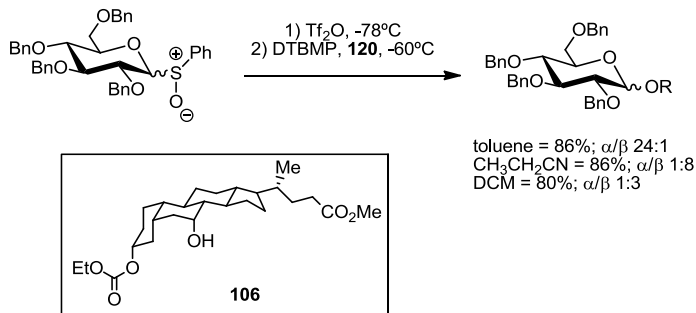
¹¹ Vincent, S. P.; Burkart, M. D.; Tsai, C.-Y.; Zhang, Z.; Wong, C.-H. *J. Org. Chem.* **1999**, *64*, 5264-5279.

Glycosyl Sulfoxides Ensure β -Stereoselective Glycosylations with Steroidal Aglycones



Scheme 6.3. Oxidation of glycosyl sulfides to the corresponding sulfoxides via Selectfluor in the presence of MeCN/H₂O.

The effectiveness of such glycosyl donors towards challenging glycosylations was initially reported by Kahne and co-workers^{9c} who, after several trials, managed challenging glycosylation of deoxycholic ester derivative **106** (Scheme 6.4). In this reaction, Tf₂O was used as activator and DTBMP as acid scavenger affording high yields of glycoside in different solvents.



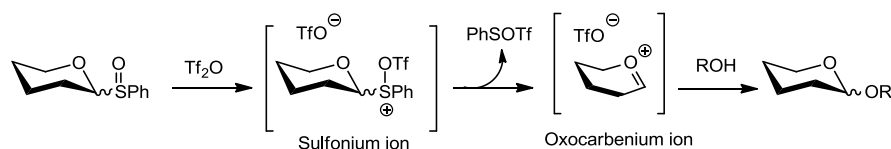
Scheme 6.4. Challenging glycosylation of deoxycholic ester **106** through glycosyl sulfoxides.

Since then, this methodology has been successfully applied to a wide variety of acceptors such as acetamides, phenols, hydroxylamines and tertiary alcohols among others.^{10,12}

¹² For a recent review, see: Fascione, M. A., Brabham, R., & Turnbull, W. B. *Chem. Eur. J.* **2016**, *22*, 3916-3928.

6.1.2.1. Mechanistic studies

A simple representation of the glycosylation mechanism through glycosyl sulfoxides is shown in Scheme 6.5. Initial reaction of sulfoxide oxygen with triflic anhydride affords sulfonium ion. Subsequent release of phenylsulfenyl triflate specie produces the oxocarbenium ion which is then trapped by a glycosyl acceptor to form the glycoside.



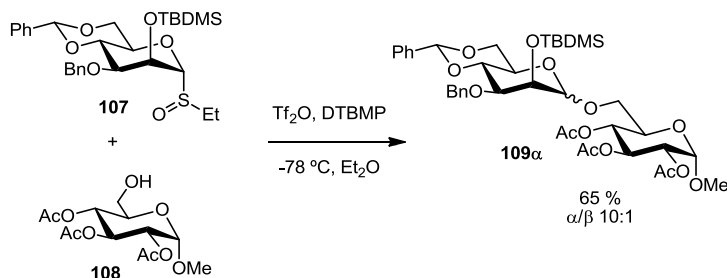
Scheme 6.5. Simple representation of glycosulfoxide glycosylation.

Nevertheless, various experimental observations during glycosylation reactions uncovered higher levels of reaction complexity. For example, while glycosylation experiments on mannopyranosides,¹³ Crich and co-workers discovered that complete shift on α/β stereoselectivities could be achieved depending on the order of the addition of the glycosyl acceptor and promoter. Thus, when a previously prepared mixture of donor **107** and acceptor **108** was treated with triflic anhydride, α -mannopyranoside **109 α** was obtained preferentially. (Scheme 6.6, A). In contrast, when glycosyl sulfoxide **107** was activated with triflic anhydride prior to addition of acceptor, the reaction afforded β -mannopyranoside **109 β** selectively (Scheme 6.6, B).

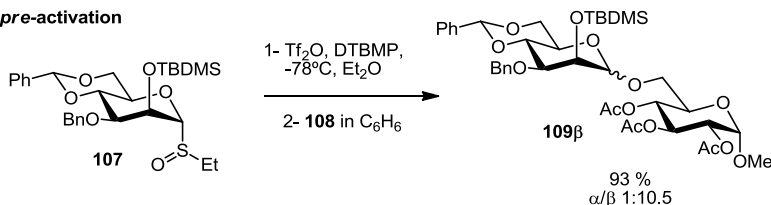
¹³ Crich, D.; Sun, S. *J. Org. Chem.* **1996**, *61*, 4506-4507.

Glycosyl Sulfoxides Ensure β -Stereoselective Glycosylations with Steroidal Aglycones

A) *In situ* activation



B) *pre-activation*

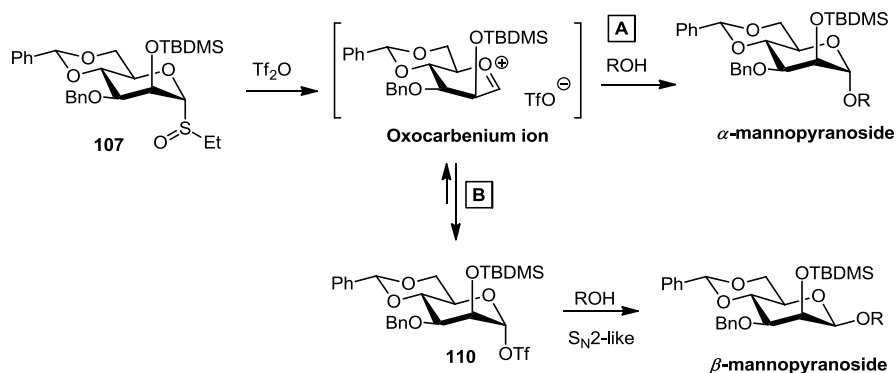


Scheme 6.6. Opposed glycosylation stereoselectivities obtained with: A) *in situ* activation or B) *pre-activation*.

The proposed mechanistic hypothesis¹⁴ for explaining this observation involved the formation of glycosyl triflate intermediate **110** during the reaction (Scheme 6.7). In this way, when donor activation occurs in the presence of glycosyl acceptor, oxocarbenium ion reacts with the latter leading to α -glycoside (Scheme 6.7, A). Instead, when oxocarbenium specie is formed "prior" to acceptor addition, it is trapped by triflate anion affording α -glycosyl triflate **110** which then reacts in a S_N2-like fashion with the added acceptor yielding β -mannopyranoside (Scheme 6.7, B). Formation of glycosyl triflate intermediate **110** was evidenced by low-temperature NMR studies of the glycosylation process.¹⁵

¹⁴ Crich, D.; Sun, S. *J. Org. Chem.* **1997**, *62*, 1198-1199;

¹⁵ Crich, D.; Sun, S. *J. Am. Chem. Soc.* **1997**, *119*, 11217-11223.



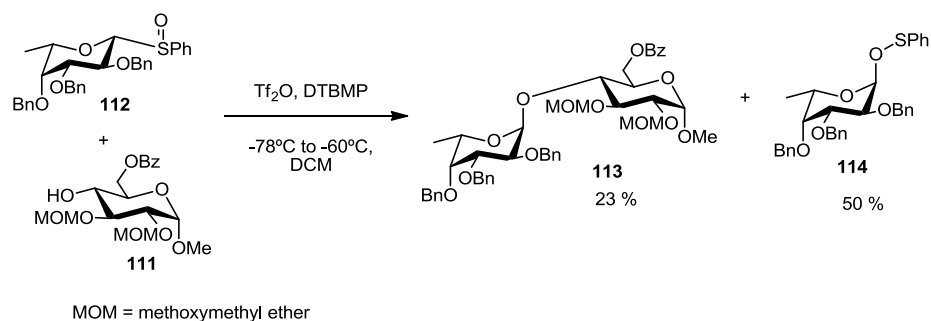
Scheme 6.7. Mechanism proposal for the selective formation of α - or β -mannopyranosides depending on the order of reagent addition.

An additional unusual reactivity was also reported by Kahne *et al.* during glycosylation of alcohol **111** with sulfoxide **112** (Scheme 6.8).¹⁶ The authors noticed that although complete consumption of sulfoxide at -78°C was observed, only little amount of glycoside **113** was formed. However, subsequent warming of the reaction mixture resulted in the production of higher amounts of **113**. This finding suggested the initial sulfoxide evolution to a more stable intermediate, which might lead to final glycosylated product. When the reaction was stopped at low temperatures, glycoside **113** was isolated in a 23% yield along with high quantities (50 %) of sulfenated compound **114**. Next, preparation of the same glycosyl sulfenate **114** from the corresponding glycosyl sulfoxide was achieved using catalytic triflic anhydride. For this reason and the fact that similar glycosyl sulfenates had been previously used as glycosyl donors in glycosylation reactions,¹⁷ the authors pointed **114** as the putative reactive intermediate in the the synthesis of disaccharide **113** under the conditions assayed.

¹⁶ Gildersleeve, J.; Pascal, R. A.; Kahne, D. *J. Am. Chem. Soc.* **1998**, *120*, 5961-5969.

¹⁷ Ferrier, R. J.; Furneaux, R. H.; Tyler, P. C. *Carbohydr. Res.* **1977**, *58*, 397-404.

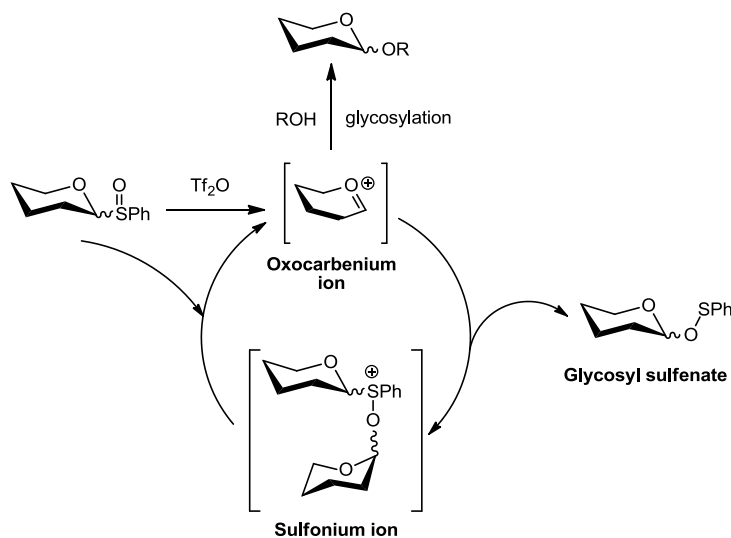
Glycosyl Sulfoxides Ensure β -Stereoselective Glycosylations with Steroidal Aglycones



Scheme 6.8. Formation of glycosyl sulfenate **114** during glycosylation through glycosyl sulfoxides.

In view of these evidences, the authors suggested a mechanistic proposal in which after activation of the starting sulfoxide, the glycosylation of oxocarbenium ion thus formed with a second molecule of glycosyl sulfoxide takes place (Scheme 6.9). This reaction leads to a sulfonium-linked ionic disaccharide which subsequently evolves releasing the glycosyl sulfenate and regenerating oxocarbenium ion. This ion could afford the glycoside by reaction with the glycosyl acceptor or generate again the glycosyl sulfonate.

It should be noted that formation of glycosyl sulfenates are not always observed during sulfoxide glycosylation reaction. This means that there could be substantial differences in the kinetic accessibility to the different sulfenates.



Scheme 6.9. Proposed mechanism for the formation of glycosyl sulfenates from glycosyl sulfoxides.

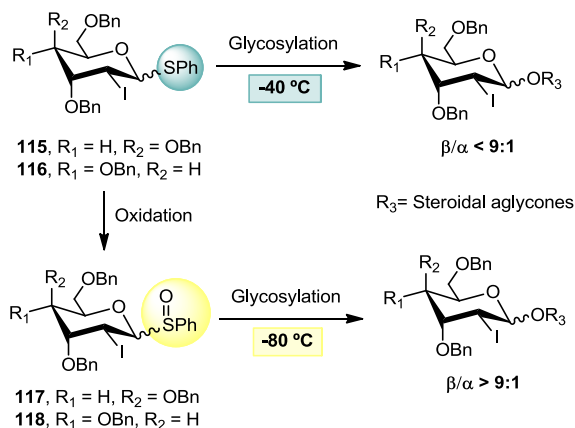
In conclusion, three different active intermediate species could be generated from a glycosyl sulfoxides: the oxocarbenium ion, the anomeric triflate or the corresponding sulfenate. The relative formation of such species depends on both the nature of glycosyl sulfoxide as well as the order of addition of the reagents. Other factors like the solvent could also affect the reaction outcome. The presence or absence of each intermediate might affect the stereochemistry and the yield of the glycosylation reaction.

6.2. OBJECTIVES

This chapter is in line with previous work performed in our group entailing glycoside formation through a Wittig/cyclization/glycosylation sequence from furanosides (Scheme 6.1). Our aim herein is to improve the stereochemical outcome of the last glycosylation step by oxidation of thioglycosides **115** and **116** to the corresponding sulfoxides **117** and **118**.

Glycosyl Sulfoxides Ensure β -Stereoselective Glycosylations with Steroidal Aglycones

We hypothesized that highly reactive 2-deoxy-2-iodo-pyranosyl sulfoxides might permit activation at very low temperature, ensuring a precise kinetic control for a complete 1,2-*trans* stereoselective glycosylation, promoted by the neighbouring bulky iodine atom (Scheme 6.10).



Scheme 6.10. Oxidation of thiophenyl glycosyl donor to the corresponding sulfoxide and subsequent glycosylation of "challenging" steroidal acceptors at $-80\text{ }^\circ\text{C}$.

Furthermore, this strategy will be used for the synthesis of β -stereoisomerically enriched biologically interesting cardiac glycosides **119** and **120** (Figure 6.3).

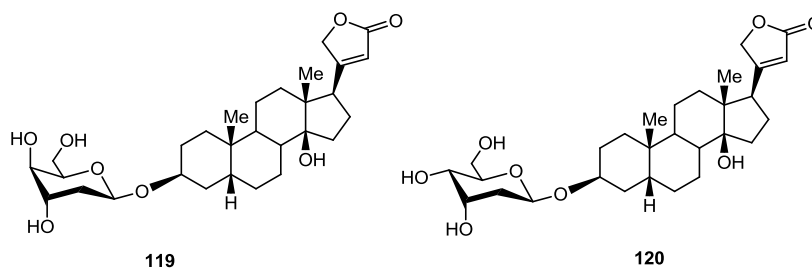


Figure 6.3. Target digitoxigenyl 2-deoxy- β -D-gulo- and *allo*-pyranosides **119** and **120**.

6.3. RESULTS AND DISCUSSION

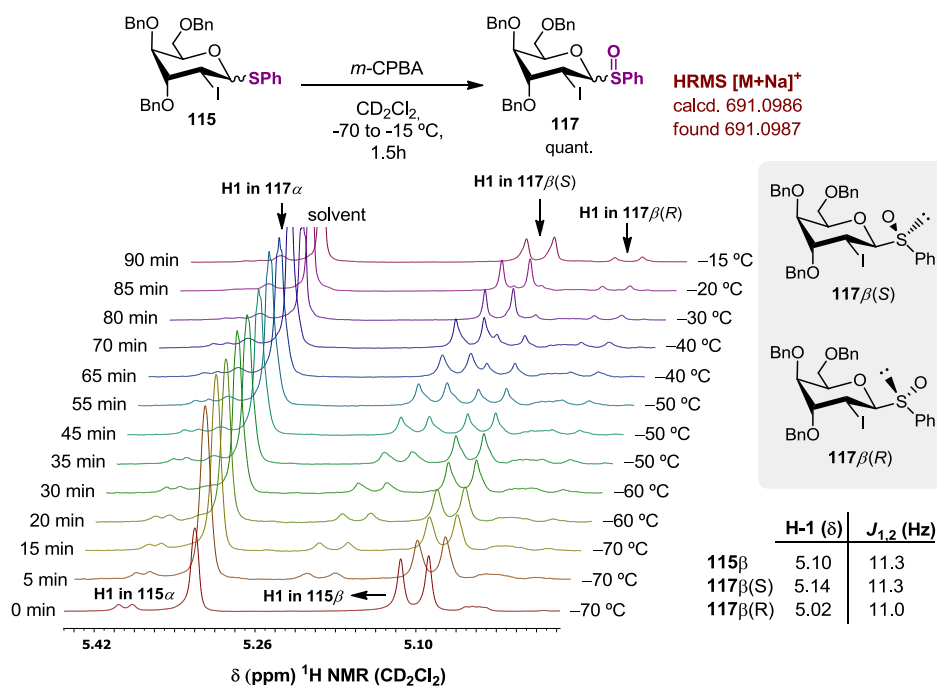
Initial oxidation studies of glycosyl sulphide **115** (Scheme 6.10) were performed using *m*-CPBA as the oxidant agent in dichloromethane from -80 °C to -50 °C. Fortunately, complete conversion to a sole product was observed by TLC in 60 min. However, after basic work-up and column chromatography a complex mixture was observed. We hypothesized that the high reactivity of 2-deoxy-glycosyl sulfoxide **117** evaded its isolation undergoing decomposition during purification process.

To verify sulfoxide formation, oxidation was monitored by ¹H NMR in CD₂Cl₂ (Scheme 6.11). The signal peak at 5.1 ppm corresponding to H-1 proton of **115** β anomer was gradually converted into two new doublets displaying at 5.14 and 5.02 ppm, presumably assigned to the known two stereoisomeric forms of sulfoxides **117** β (S) and **117** β (R)¹⁸ respectively with a 88:12 d.r. Although the signal of **117** β (S) was gradually shifting upfield upon warming from -70 to -20 °C, the $\Delta\delta$ of 0.2 ppm between the two stereoisomers was in accordance of previously reported diastereomeric sulfoxides.¹⁹ The generation of **117** was further confirmed by mass analysis.

¹⁸ Sanhueza, C. A.; Arias, A. C.; Dorta, R. L.; Vázquez, J. T. *Tetrahedron: Asymmetry* **2010**, *21*, 1830-1832 and references therein.

¹⁹ Taniguchi, T.; Asahata, M.; Nasu, A.; Shichibu, Y.; Konishi, K.; Monde, K.; *Chirality*, **2016**, *28*, 534-539.

Glycosyl Sulfoxides Ensure β -Stereoselective Glycosylations with Steroidal Aglycones

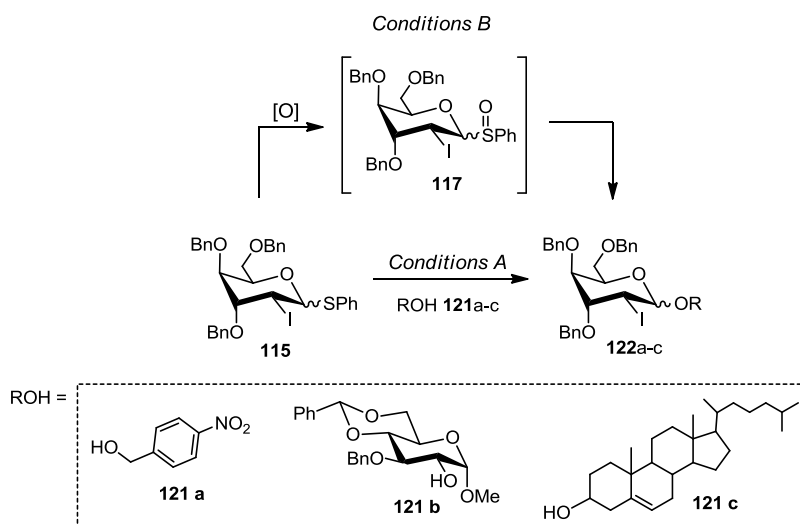


Scheme 6.11. ^1H NMR monitoring of the oxidation of **115**.

Since sulfoxide isolation proved problematic, we reasoned that glycosylation studies would be conducted using crude sulfoxide **117** without further isolation.

Next, glycosylation with decreasing nucleophilicity on the aglycone was explored comparing the selectivities obtained of activation of **115** (data obtained from published results)^{6c} with the ones of **117** (Table 6.1). In this way, glycosyl sulfide **116** was again treated with *m*-CPBA in DCM from -80 °C to -50 °C till complete conversion was observed. Then, the benzoic acid residue was neutralized with NaHCO_3 and the precipitate was removed by filtration under Ar atmosphere. The resulting sulfoxide was then added to a flask containing *p*-nitrobenzyl alcohol **121a** and DTBMP in DCM at -80°C followed by Tf_2O addition (Table 6.1, entry 2).

Table 6.1. Comparison between direct glycosylation from glycosyl sulphide **115** or glycosylation via its previous oxidation to sulfoxide **117**.



Entry	Acceptor	Conditions ^a	Time (h)	Yield (%) ^b	β/α ratio ^c
1	121a	<i>A</i> ^d	4	122a , 72	30:1
2		<i>B</i>	0.5	122a , 80	40:1
3	121b	<i>A</i>	3	122b , 61	16:1
4		<i>B</i>	0.5	122b , 69	24:1
5	121c	<i>A</i>	3	122c , 66	8:1
6		<i>B</i>	0.5	122c , 63	21:1

^a*Conditions A*: **115** (1 mmol), acceptor (2 mmol) and 4Å MS in CH₂Cl₂ (4 mL) at -80 °C. Then, addition of NIS (3 mmol) and TfOH (0.2 mmol) at -40 °C unless otherwise indicated. *Conditions B*: **115** (1 mmol), *m*-CPBA (1 mmol) and 4Å MS in CH₂Cl₂ (30 mL) at -80°C to -50°C. Then, NaHCO₃ (5 mmol), filtration and addition of acceptor (2 mmol), DTBMP (3 mmol), 4Å MS and Tf₂O (2 mmol) at -80 °C. ^bIsolated yield. ^cCalculated by integration of anomeric protons. ^dReaction was carried out at -80°C.

To our delight total conversion of sulfoxide **117** was observed by TLC in 30 min. ¹H NMR analysis of crude revealed the successful

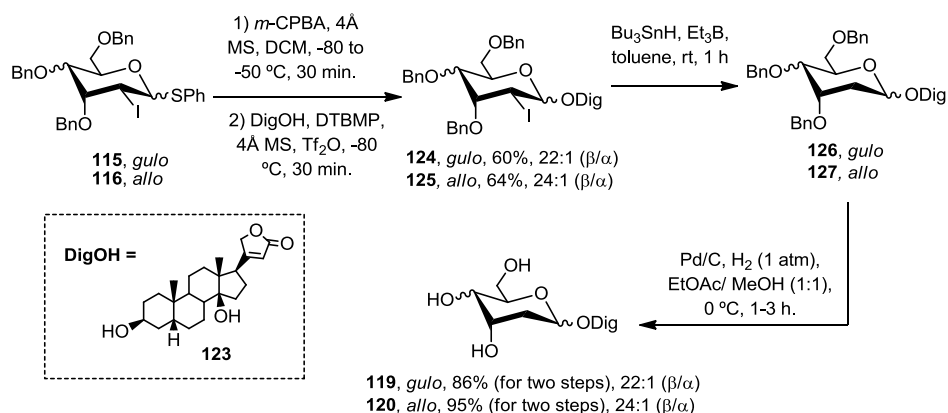
Glycosyl Sulfoxides Ensure β -Stereoselective Glycosylations with Steroidal Aglycones

formation of glycoside **122a** in a d.r. of 40:1 (β/α). Posterior column chromatography provided **122a** in a 80% yield proving the effectiveness of the *m*-CPBA oxidation/glycosylation sequence methodology. Comparison with previously reported results of glycosylation with the thiosulfide counterpart **115**^{6c} (Table 6.1, entry 1) evidenced drastic shortening of reaction time while maintaining similar stereoselectivities.

Glycosylation using sulfide **115** with secondary methyl glucoside alcohol **121b** required higher reaction temperatures (-40°C) and therefore, the β -stereoselectivity was decreased (Table 6.1, entry 3). On the contrary, glycosylation with sulfoxide **117** effectively allowed reaction at low reaction temperatures (-80°C) affording, in reduced reaction time, slightly higher stereoselectivity (Table 6.1, entry 4).

However, the best improvement in stereoselectivity was observed with glycosylation of challenging steroidal aglycone **121c** (Table 6.1, entries 5-6). While direct activation of **115** at -40°C afforded reduced stereoselectivities compared to previous glycosylations, oxidation of **115** to **117** followed by coupling with **121c** at -80°C maintained excellent α/β ratio. Therefore, glycosylation with **121c** reached a comparable level of stereocontrol only when sulfoxide was used as the glycosyl donor. Combination of the iodine stereodirecting group and the lower reaction temperature enabled by the reactive sulfoxide ensured excellent kinetic control with steroidal aglycones.

With this results in hand, we decided to take advantage of this strategy for the synthesis of 2-deoxy cardiac glycosides **119** and **120**. For this purpose, steroidal digitoxigenin acceptor **123** would be glycosylated with *gulo*- and *allo*-thiopyranosides **115** and **116** respectively (Scheme 6.12).



Scheme 6.12. Synthesis of digitoxygenyl 2-deoxy- β -*gulo* and -*allo* pyranosides **119** and **120**.

Oxidation/glycosylation sequence of **115** and **116** with digitoxigenin **123** afforded the desired 2-deoxy-2-iodoglycosides **124** and **125** with 22:1 and 24:1 β/α ratios respectively and good yields.

Their structures were confirmed by NMR experiments including ¹H, ¹³C, HSQC, ¹H-coupled HSQC, HMBC, NOESY, and COSY (Figure 6.4, A).

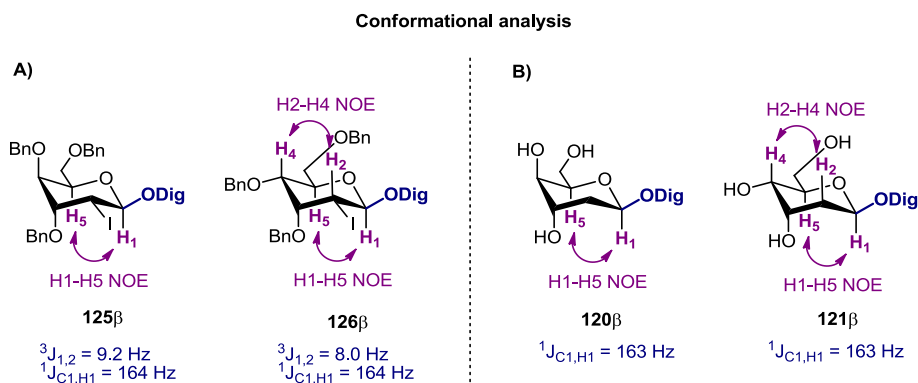


Figure 6.4. Conformational analysis of: A) **125 β** and **126 β** ; B) **120 α** and **121 β** .

The high value of vicinal coupling constants of **124 β** ($J_{1,2} = 9.2$ Hz) and **125 β** ($J_{1,2} = 8.0$ Hz) and the heteronuclear coupling constant value $J_{C_1-H_1}$ of 164 Hz for both products indicate a relative trans-diaxial

disposition between H-1 and H-2. On the other hand, key NOE contacts between H-1 and H-5 in **124 β** and between H-1 and H-5 and H-2 and H-4 for **125 β** , suggest a 4C_1 conformation for both compounds.

Posterior iodine removal in **124** was performed using radical deiodination with Bu_3SnH/Et_3B system affording 2-deiodo derivative **126**. However, 1H NMR analysis after column chromatography showed the presence of traces of some aromatic protons abnormally deshielded, resembling to that of benzoate groups. Concretely, proton signal at 8.05 ppm corresponding to aromatic protons at *ortho* position suggested some extent of oxidation of benzyl groups into benzoate. Although the formation of benzoate-containing compounds was not confirmed by MS analysis, oxidation of benzyl groups under Bu_3SnH/Et_3B conditions have been previously observed in our group.²⁰

Due to the problematic removal of such impurities from our desired compound **126**, we decided to treat the mixture with H_2 in the presence of Pd/C in order to remove benzyl protecting groups for an easier purification step. The reaction was performed at 0°C and was cautiously monitored by TLC in order to avoid possible reduction of the digitoxigenin double bond moiety. Fortunately, no double bond reduction was observed by 1H NMR spectroscopy and the desired Digitoxigenyl 2-deoxy-D-*gulo*-pyranoside **119** was recovered in 86% yield over two steps. Analogous treatment of 2-iodo-*allo*-glycoside **125** afforded **120** in 95% yield for the two steps. Again, complete structural elucidation was performed with 1H , ${}^{13}C$, HSQC, 1H -coupled HSQC, HMBC, NOESY, and COSY experiments (Figure 6.4, B). Formation of the desired steroidal glycosides was finally confirmed by MS analysis.

²⁰ Mestre, J. Ph.D. Thesis, URV, Tarragona, 2017.

6.4. CONCLUSIONS

In conclusion, the present work upgrades the previous reported methodology for the stereoselective synthesis of 2-deoxyglycosides, improving the glycosylation control using challenging steroidal aglycones. The enhanced reactivity of glycosyl sulfoxides and the presence of an equatorial I permitted the precise formation of complex 2-deoxy- β -glycosides **119** and **120** with excellent β/α stereoselectivities (22:1 and 24:1 respectively) after removal of the temporary directing element.

CHAPTER 7

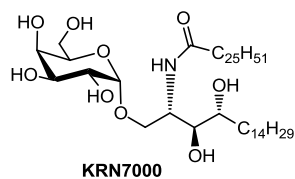
PRELIMINAR BIOLOGICAL EVALUATION OF THE SYNTHESIZED KRN7000 ANALOGUES

7.1. INTRODUCTION AND OBJECTIVES

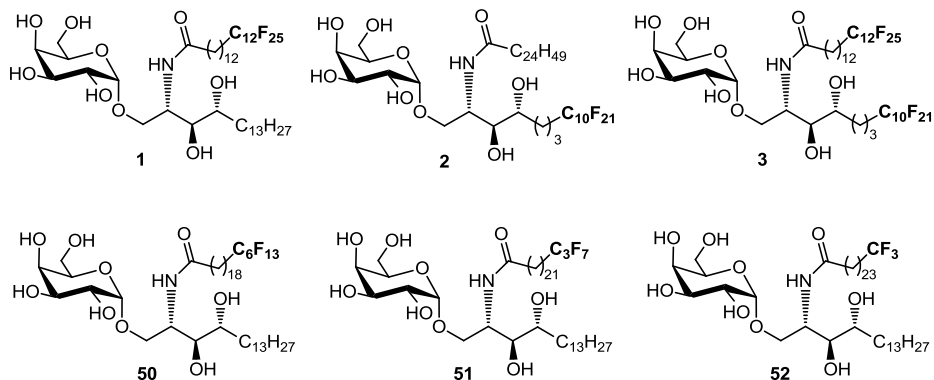
As commented in Chapter 1, the therapeutical effect of KRN7000 resides in its ability to stimulate iNKT cells. This activation occurs through the initial binding of KRN7000 to CD1d protein of antigen presenting cells, forming a glycolipid-CD1d binary complex. Then, this complex is recognized by T cell receptors (TCR) on the surface of iNKT cells, forming a CD1d-glycolipid-TCR ternary complex that ultimately activates iNKT cells. Upon activation, iNKT cells secrete T_H1 (such as $IFN-\gamma$) and T_H2 (such as IL-4) type cytokines, leading to different biological responses. Since T_H1 and T_H2 cytokines are believed to antagonize each other biological effects, a biased cytokine secretion is desired. In this sense, it is believed that the stability of both binary and ternary complexes plays an important role in both the potency and selectivity of cytokine release.

For this reason, the two main objectives of the present chapter are the following: A) To experimentally evaluate the binding affinity of our previously synthesized KRN7000 analogues (Figure 7.1) for mouse CD1d protein. Further molecular dynamic simulations of glycolipid-CD1d interaction will provide useful information at molecular level. B) To evaluate the ability of our compounds for stimulating human iNKT cells.

Preliminar biological evaluation of the synthesized KRN7000 analogues



A) Fluorinated analogues



B) Conformationally rigid analogues

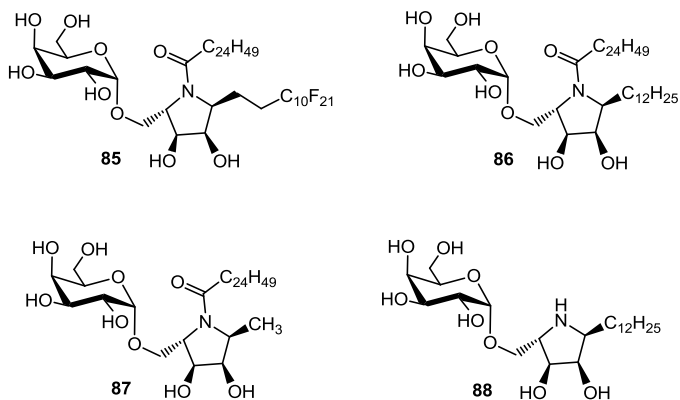


Figure 7.1. Synthesized KRN7000 analogues. A) Fluorinated analogues. B) Conformationally rigid analogues.

7.2. RESULTS AND DISCUSSION

7.2.1. Binding affinity of glycolipids to mouse CD1d protein

In the context of a collaboration with Dr. Miquel Mulero (Department of Biochemistry and Biotechnology, University Rovira i Virgili), direct assessment of binding affinity of our designed KRN7000 analogues against CD1d protein, independent of subsequent TCR recognition, was performed via a cell-free competitive binding ELISA test.¹ This assay consists in the use of a biotinylated 18:1 PE lipid as an indicator for the competition with increasing concentrations of the target glycolipid (including KRN7000) in binding to immobilized mouse CD1d proteins. The results are expressed as half maximal inhibitory concentration (IC₅₀) values.

We first investigated the conformationally restricted derivatives **86**, **87** and **88** as shown in Figure 7.2. In general terms, comparing the IC₅₀ values of KRN7000 (11.21 μ M) with the one of its cyclic analogue containing the two aliphatic chains, **86** (14.87 μ M), it seems that conformational restriction of the ceramide moiety does not have a huge impact in the ligand binding affinity. In contrast, an unexpected result aroused from the sphingoid base truncated analogue **87**, which presented remarkable enhanced affinity compared to both **86** and KRN7000. This result contrasts with a previous report² which showed that the shortening of either acyl or sphingoid base chains in KRN7000 reduces the stability of mouse CD1d-lipid complex.

¹ Shiratsuchi, T.; Schneck, J.; Kawamura, A.; Tsuji, M. *J Immunol Methods* **2009**, *345*, 49-59.

² Oki, S.; Chiba, A.; Yamamura, Y.; Miyake, S. *J. Clin. Invest.* **2004**, *113*, 1631-1640.

Preliminar biological evaluation of the synthesized KRN7000 analogues

CONFORMATIONALLY RESTRICTED KRN7000 ANALOGUES

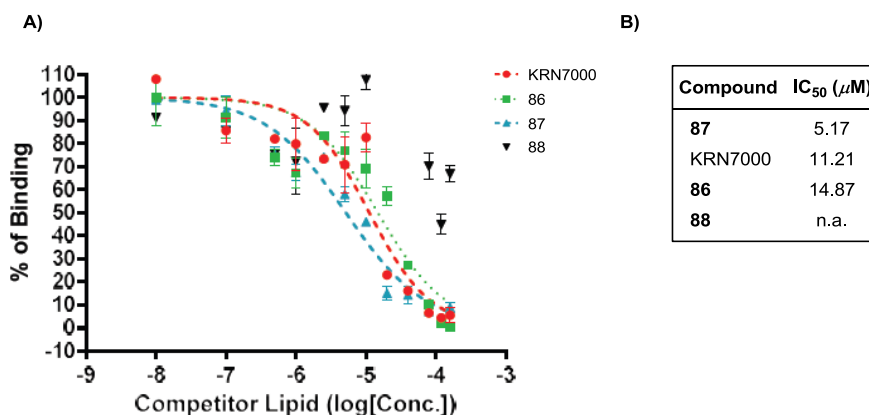


Figure 7.2. Results of the competition ELISA assay for conformationally restricted analogues. A) Representation of % of binding front log[conc.] for the different glycolipids. B) Half maximal inhibitory concentration (IC₅₀) values for each glycolipid.

Although highly speculative, a possible explanation could arise from different ligand positioning due to both the presence of pyrrolidine ring, and the lack of sphingoid base chain, allowing the molecule to adopt an optimal disposition leading to a higher binding energy. Finally, the acyl chain-lacking analogue **88** showed unreproducible results, which might be attributed to a complete lack of interaction with CD1d.

Regarding the fluorinated derivatives (**1-3**, **50-52** and **85** in Figure 7.3), compounds **50**, **51** and **52**, bearing short fluoroalkyl moieties at acyl chain (C₆F₁₃, C₃F₇ and CF₃, respectively) showed the lowest IC₅₀ values. Therefore, they possess higher binding affinities towards CD1d protein than the rest of analogues, including KRN7000. Among them, analogue **52** provided the strongest binding affinity (IC₅₀ = 0.81 μM) followed by **51** (IC₅₀ = 4.7 μM) and **50** (IC₅₀ = 24.7 μM). Interestingly, the IC₅₀ values increased along with the number of CF₂ moieties present in the acyl chain. In fact, the rest of analogues, bearing higher fluorination degree at

acyl chain (**1**), sphingoid base (**2** and **85**) or at both lipid chains (**3**) presented much lower binding affinities than KRN7000.

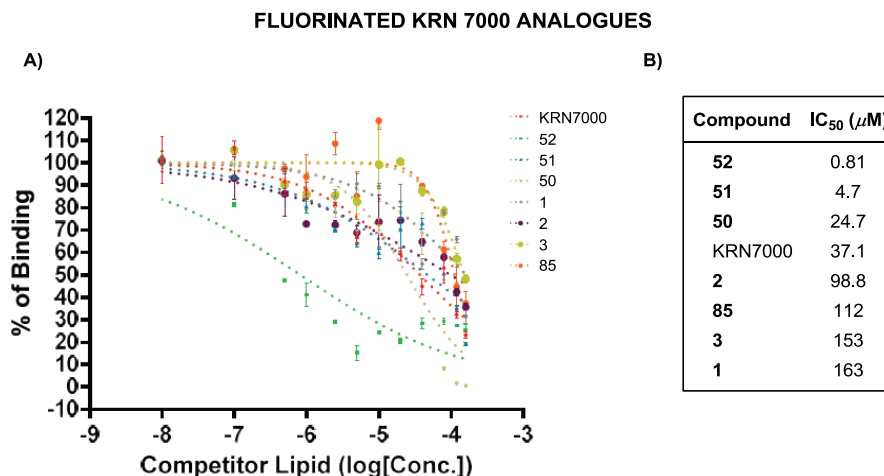


Figure 7.3. Results of the competition ELISA assay for fluorinated analogues. A) Representation of % binding front log[conc.] for the different glycolipids. B) Half maximal inhibitory concentration (IC₅₀) values for each glycolipid.

Taken together, it should be emphasized that the introduction of a limited number of fluorine atoms at acyl chain of KRN7000, cause dramatic to modest increase in the ligand binding affinity towards CD1d protein, as evidenced by compounds **52**, **51** and **50**. However, our results also show a clear tendency in which the substrate binding to CD1d progressively decrease as the number of fluorinated carbons on the acyl chain increase (Figure 7.4).

This fact suggests a dual effect of fluorine in the process of ligand interaction with CD1d. On the one hand, we hypothesize that fluorine atoms might undergo beneficial non-covalent interactions with amino acid residues of CD1d cavities, leading to higher binding energies. Nevertheless, fluoroalkyl chains are known to suffer from enhanced conformational rigidity as well as larger cross section (27-30 Å for fluoroalkyl chains vs. 18-21 Å for alkyl chains) than their hydrocarbon

Preliminar biological evaluation of the synthesized KRN7000 analogues

counterparts do.³ Therefore, this loss of chain flexibility might difficult the correct accommodation of the lipidic tails into CD1d protein cavities.

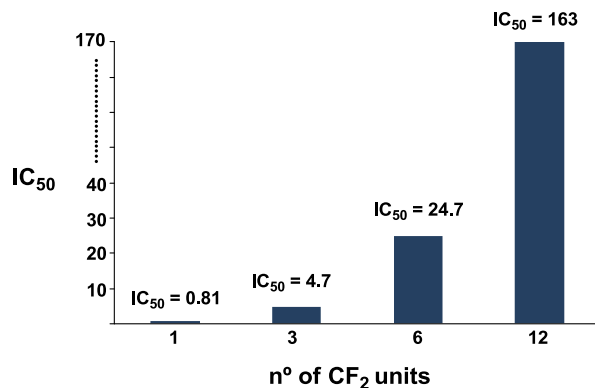


Figure 7.4. Correlation between number of fluorinated carbons and the glycolipid IC₅₀ value for CD1d affinity.

Furthermore, the rigid nature of fluoroalkyl chains might also explain the higher detrimental impact of fluoroalkylation on acyl chain than on sphingoid base (**1** vs. **2**). While the first is accommodated in the A' pocket of CD1d, which is known to have a curved structure, the second one is positioned in the F' cavity adopting a straighter conformation.⁴ Therefore, the rigid fluoroalkyl chain might not fit correctly the curved shape of A' tunnel while accommodation of fluoro-sphingoid base chain in F' groove might be less complicated, although still being unfavourable.

7.2.2. Computer simulation of TCR-glycolipid-CD1d interaction

In the context of a collaboration with Dr. Francisco Corzana (Department of Chemistry, University of La Rioja), Molecular Dynamic

³ Krafft, M. P.; Riess, J. G. *Chem Rev* **2009**, *109*, 1714–92.

⁴ Koch, M.; Stronge, V. S.; Shepherd, D.; Gadola, S. D.; Mathew, B.; Ritter, G.; Fersht, A. R.; Besra, G. S.; Schmidt, R. R.; Jones, E. Y.; Cerundolo, V. *Nat. Immunol.* **2005**, *6*, 819–826.

(MD) simulations of interaction process between our designed analogues and mouse CD1d protein were performed. The simulations were carried out using the crystal structure of mouse CD1d- α -galactosylceramide with mouse V α 14-V β 8.2 iNKT TCR (PDB ID: 3HE6). Proton bonding interactions between -OH and -NH moieties of each ligand and aminoacid residues of CD1d were evaluated through calculation of % of population of each hydrogen bond during 200 ns in the performed MD simulations. Interactions with TCR are not discussed.

Hydrogen bond populations in conformationally rigid KRN7000 series are shown in Figure 7.5, A. Interestingly, marked differences between them and KRN7000 were observed, indicating the role of the pyrrolidine ring in their interaction with CD1d.

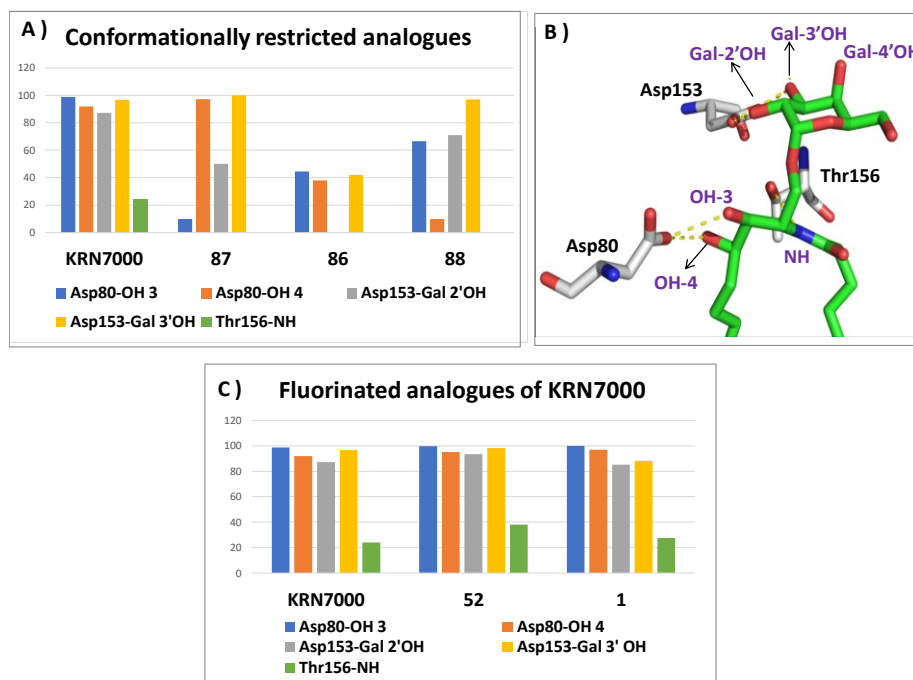


Figure 7.5. Population (%) of the hydrogen bonds calculated by 200 ns MD simulations with A) Conformationally rigid analogues and C) Fluorinated analogues. B) Crystal structure of mouse CD1d- α -GalCer.

| *Preliminar biological evaluation of the synthesized KRN7000 analogues*

Comparison of molecular simulations with KRN7000 and analogue **87**, the conformationally rigid analogue exhibiting the strongest protein binding affinity, provided interesting results. Sugar fragment of **87** displays reduced hydrogen bonding interaction of Gal-2'OH moiety with Asp153 residue compared to that of KRN7000, while interaction of Gal-3'OH with the same residue is similar for both glycolipids. In contrast, major differences were noticed in the interactions occurring with pyrrolidine ring heteroatoms in **87**. First, complete disappearance of NH interaction with amino acid Thr156 is observed. This result was expected due to the lack of NH group in the *N*-acylated pyrrolidine moiety of **87**. Despite the 4-OH interaction with Asp80 is high in both analogues, the 3-OH hydrogen bond is drastically reduced in pyrrolidine-containing **87**. This result suggests that pyrrolidine 4-OH moiety plays a more relevant role than 3-OH for the correct ligand-CD1d binding in **87**. Superposition of KRN7000 and **87** structures (Figure 7.6, A) showed a marked different positioning of 3-OH and 4-OH moieties in **87**, due to the presence of the pyrrolidine ring. In contrast, both glycolipids maintain similar spatial disposition of the galactose heads. The distinct disposition of both hydroxyl groups of pyrrolidine ring might be the reason for the loss of 3-OH interaction with Asp80.

Although these results provide useful information evidencing the different interaction modes for KRN7000 and **87** with CD1d, they do not explain the higher CD1d binding affinity of **87** (IC_{50} values for **87** (5.17 μ M) in relation to KRN7000 (11.21 μ M)). In this sense, it seems that hydrogen bonds occurring between the glycolipid and CD1d protein are not the unique responsible for their final binding affinity.

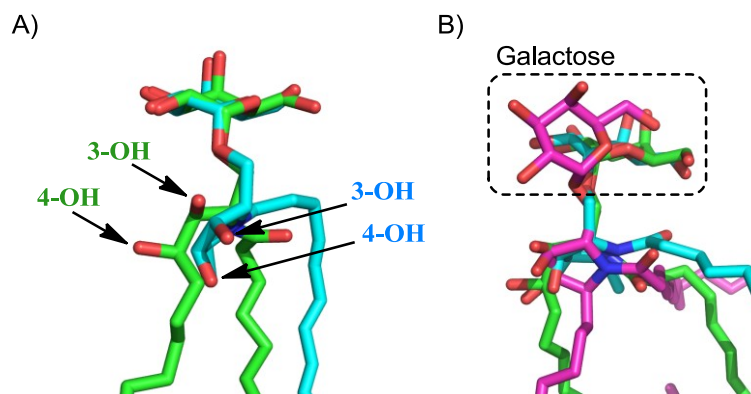


Figure 7.6. A) Superposition of KRN7000 (green) and **87** (light blue) structures in MD simulations with mouse CD1d protein; B) Superposition of KRN7000 (green), **87** (light blue) and **86** (purple) in MD simulations with mouse CD1d protein.

MD simulations results on analogue **86** (Figure 7.5, A), presenting higher IC_{50} value than **87** ($14.87 \mu\text{M}$ vs $5.17 \mu\text{M}$), showed a general decrease in hydrogen bond interactions of both Gal-2'OH (no interaction observed) and Gal-3'OH hydroxyl groups in carbohydrate fragment with Asp153 residue. Interactions of 4-OH group in pyrrolidine moiety with Asp80 are also reduced in comparison to **87**. In contrast, binding of pyrrolidine 3-OH moiety with Asp80 is increased, although still presenting a modest 40% population level. Superposition of structures of **86**, KRN7000 and **87** showed a clear different positioning of the sugar head of **86**, in relation to the other glycolipids, which might explain the reduction of interaction levels performed by the galactose moiety in **86** (Figure 7.6, B). We suggest that galactose head might be repositionated in order to favor correct accommodation of both lipid chains in the hydrophobic pockets. We also hypothesize that the general loss of hydrogen bonding interactions in **86**, compared to **87**, outweighs the gain in hydrophobic interactions of the extra lipid chain of **86**. Therefore, the final binding energy is decreased.

Preliminar biological evaluation of the synthesized KRN7000 analogues

Finally, results on analogue **88** (Figure 7.5, A) showed, in contrast to **87**, considerable enhanced H-bonding interactions of Asp80 with pyrrolidine 3-OH than with 4-OH, while sugar-CD1d interactions remain similar. This result suggests a different positioning of pyrrolidine ring because of both the presence of the sphingoid base tail and the absence of the acyl chain. Superposition of both **87** and **88** structures will be shortly performed. Since compounds **88** and **87** present similar overall interaction levels, we assume that the loss of binding affinity of **88** compared to **87** is mainly due to the lack of acyl chain, which seems to have a higher role in binding to CD1d than the sphingoid base chain.

Computational simulations with low fluorinated analogue **52** and highly fluorinated **1** were also performed, providing valuable insights into the effect of fluorination of glycolipid acyl chain on their recognition by CD1d (Figure 7.5, B).

In contrast to pyrrolidine-containing analogues, both fluorinated derivatives display similar hydrogen bond networks than KRN7000. Only a slight increase in the interaction of NH moiety with Thr156 is observed. These results indicate that their remarkable different binding affinities (IC₅₀ values for KRN7000 (37.1 μ M), **52** (0.81 μ M) and **1** (163 μ M)) could not be explained in base of drastic differences in proton bonding network of the glycolipid polar head. Therefore, the explanation for such difference in affinity might reside in the interactions of the alkyl vs fluoroalkyl chains with hydrophobic residues in A' and F' channels of CD1d protein and not to a different positioning of the polar part of the lipid. In this sense, possible evidences for beneficial specific fluorine interaction with CD1d residues, explaining the higher binding affinity observed, are now underway.

On the other hand, our results showed a clear influence of the degree of fluorination of acyl chain on its spatial disposition inside the CD1d A' channel (Figure 7.7). While acyl tails of both KRN7000 and **52** present similar spatial arrangement, fitting the curved nature of A' pocket, the highly fluorinated chain of **1** adopts a straighter conformation. This should be, as commented before, because of the high rigidity of perfluoroalkyl structures, which prevent chain bending. Therefore, the different chain orientation in **1** might prevent a correct accommodation of the lipid chain in the A' pocket, leading to a lower binding affinity. Further MD simulations with the rest of fluorinated analogues might explain the previously observed tendency in which glycolipid binding affinity decreased as the degree of fluorination of its acyl chain increased (Figure 7.4).

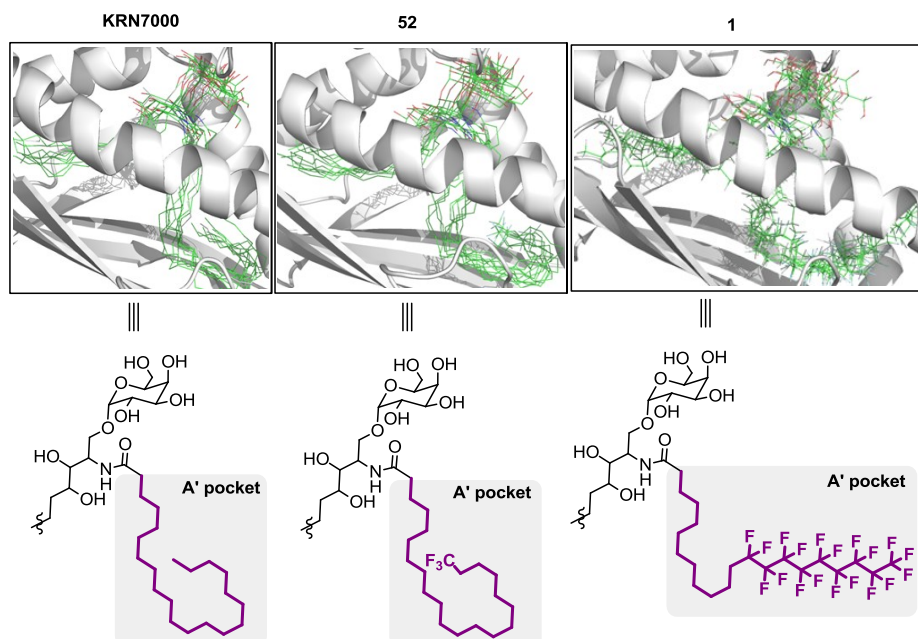


Figure 7.7. Superposition of various frames obtained by 200 ns MD simulations of KRN7000, **52** and **1** with their respective schematic representation below.

7.2.3. *In vitro* assays with human iNKT cells

In the context of a collaboration with prof. Gennaro De Libero (Department of Biomedicine, University of Basel), the ability of the designed ligands to stimulate the cytokine release from human iNKT cells was studied. In case the galactosylceramides have iNKT TCR preference, two different human iNKT cell clones, expressing two different TCRs were used for this experiment. Thus, levels of IFN- γ in supernatants from human iNKT cell clones, cultured with human CD1d-containing APC cells and the glycolipids were measured. The results of the experiment are shown in Figure 7.8.

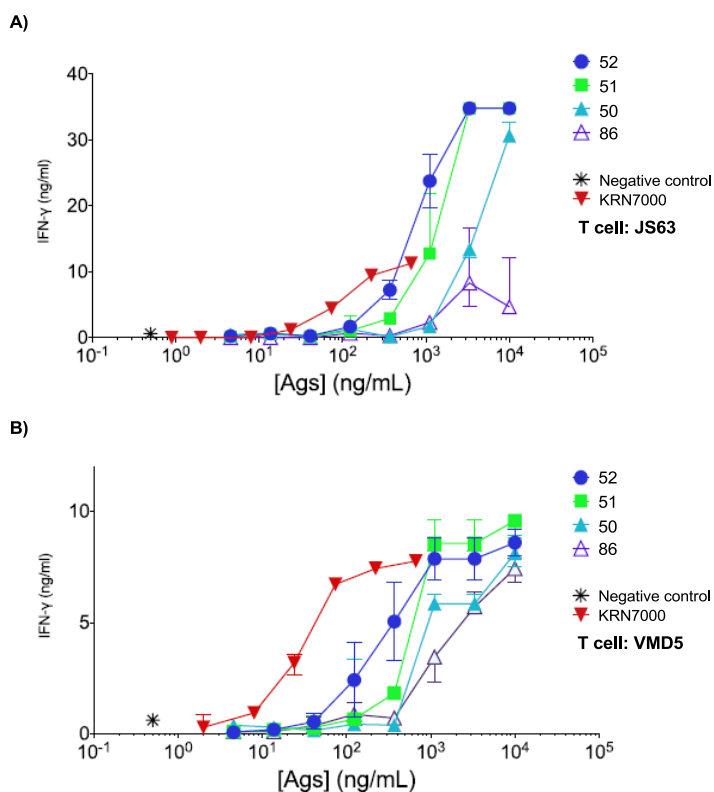


Figure 7.8. IFN- γ secretion by human splenocytes *in vitro*.

Derivatives **52**, **51** and **50**, bearing low fluorination degree at their acyl chains, proved highly active with both clones. They showed a lower potency than α -GalCer, but a much higher efficacy with JS63 clone. Indeed they induced much more IFN- γ release than KRN7000 itself at higher concentrations with this iNKT cell line. Instead, they induced similar maximum levels of IFN- γ secretion than KRN7000 with the clone VMD5. The rest of fluorine-containing analogues, bearing highly fluorinated lipid chains (**1**, **2**, **3** and **85**) presented complete lack of iNKT cell stimulation (data not shown).

These results follow a similar trend as those observed in the previous CD1d binding affinity test. Therefore, it seems that introduction of short fluoroalkyl moieties such as CF₃ (**52**), C₃F₇ (**51**) and to a lower extent C₆F₁₃ (**50**) at acyl chain of a glycolipid results in higher CD1d binding affinity, that might contribute to an enhanced ability to stimulate some iNKT cell lines. The fact that they are less potent than KRN7000, could be due to solubility, cell internalisation or partition in the membrane different than α -GalCer.

Regarding the conformationally restricted derivatives (**86-88**), only the strictly cyclic counterpart of KRN7000, **86**, showed stimulatory activity. However, it induced decreased amount of cytokines, with both iNKT cell clones, compared to KRN7000. Analogues lacking of sphingoid base chain (**87**) or acyl chain (**88**) proved inactive (data not shown). These results are in line with the ones reported by Mori and co-workers⁵ evidencing that the conformational restriction of KRN7000 does not provide enhanced iNKT cell activation.

⁵ Fuhshuku, K.-I.; Hongo, N.; Tashiro, T.; Masuda, Y.; Nakagawa, R.; Seino, K.-I.; Taniguchi, M.; Mori, K. *Bioorg. Med. Chem.* **2008**, *16*, 950-964.

Preliminar biological evaluation of the synthesized KRN7000 analogues

However, comparison between stimulatory activity of conformationally restricted analogues and their previously evaluated CD1d binding affinities showed some contrasting results. Particularly, while compound **87** showed a marked higher binding affinity towards CD1d than KRN7000 and the rest of pyrrolidine-containing analogues, it proved unable to stimulate iNKT cells. These results indicate that strong affinities towards CD1d protein does not ensure a potent biological response.

At this point, it should be noted that while the previous binding affinity test was performed on mouse CD1d, the present experiment uses human CD1d. Although human and mouse CD1d structures are quite similar, there are a few structural differences between them that might affect their biological behaviour. Therefore, although activity in humans could be predicted, to a certain extent, through mouse studies, any correlation between the ligand affinity to mouse CD1d and the final stimulatory activity on human iNKT cells must be confirmed by completing the first study with human CD1d protein.

7.3. CONCLUSIONS

In conclusion, our preliminary results highlight the effects of fluoroalkylation of lipid tails (specially acyl chain) of KRN7000 analogues in both their affinity for mouse CD1d protein and their ability to stimulate iNKT cells. We found that limited fluorination of acyl chain enhances ligand binding to CD1d. Moreover, the maximum levels of cytokine release are also increased. In particular, we have identified two KRN7000 analogues: **52** and **51**, bearing trifluoromethyl and perfluoropropyl groups at the end of acyl chains, showing promising

preliminary results. Further experiments are now underway in order to explore their biological properties in greater detail.

Conversely, massive fluorination of the molecule results in drastic loss of CD1d affinity and complete lack of stimulatory activity. Molecular dynamic studies showed a different positioning of highly fluorinated acyl chain in **1**. The lack of flexibility of perfluoroalkyl chain might prevent its correct fitting into the curved A' CD1d pocket which might ultimately contribute in the reduced biological activity of the glycolipid.

On the other hand, as it was also demonstrated before,⁵ our preliminary studies indicate that the conformational restriction of ceramide moiety by construction of a pyrrolidine ring does not provide enhanced stimulatory levels. Interestingly, we found that analogue **87**, lacking of sphingoid base chain, possessed particularly high binding affinity towards CD1d protein. However, it did not induce any observable levels of cytokines. Molecular dynamic results indicated changes in spatial disposition of 3-OH and 4-OH hydroxyl moieties because of the presence of pyrrolidine ring, which modifies its hydrogen bond network with CD1d.

Although the presented preliminary results have provided important insights into the biological impact of fluoroalkylation and conformational restriction of KRN7000 ceramide fragment, deeper studies on the biological behaviour of the designed analogues as well as the synthesis of new fluorinated analogues will be performed in *due course*.

CHAPTER 8

GENERAL CONCLUSIONS

The main objectives proposed in the different chapters of this PhD thesis have been reached.

Chapter 3

- The synthesis of KRN7000 analogues bearing highly fluorinated fragments at acyl chain and/or sphingoid base moiety have been accomplished.
- Perfluoroalkylation of acyl chain was achieved with high yield (86%) via AIBN mediated radical methodology.
- Differently, introduction of fluoroalkyl scaffold into the sphingoid base moiety was initially tackled via Wittig olefination or CM coupling strategies. The first proved unsuccessful under our reaction conditions. On the other hand, CM reaction resulted in good yields, after extensive optimization of the reaction conditions.
- Although Wittig olefination with long polyfluoroalkylphosphonium salts failed, the reaction provided good yields (67%) for the reaction with shorter fluoroalkyl salts.

Chapter 4

- A set of KRN7000 analogues bearing low fluorinated acyl chains have been successfully prepared.
- Preparation of the long carboxylic acids bearing short fluoroalkyl fragments at end of chain was accomplished via AIBN-mediated radical mechanism or Li_2CuCl_4 catalyzed coupling of ω -bromo carboxylic acids with long ω -perfluoropropyl and trifluoromethyl alkyl bromides.

Chapter 5

- A new and divergent route to KRN7000 analogues bearing pyrrolidine rings as conformational restriction units have been established. The key reaction of the synthesis is a one pot azidation-1,3-dipolar cycloaddition of hydroxyalkenes.
- Intramolecular azide-alkene cycloaddition (IAOC) proved to be sensitive to the nature of alkenes providing different reaction products. While substituted alkenes afforded the corresponding cyclic imines in high yields, reaction of terminal alkenes resulted in mixtures of imines and aziridines.
- With this methodology, different conformationally rigid KRN7000 analogues differing in both acyl chain and sphingoid base were synthesized.

Chapter 6

- Replacement of thioglycosides by sulfoxides have effectively permitted glycosylation of challenging steroidal acceptors at -80°C leading to a higher stereocontrol of the reaction. High β stereoselectivities ($\beta/\alpha > 21:1$) have been achieved with this methodologies.
- Formation of sulfoxides have been performed via *m*-CBPA oxidation of the corresponding sulphides. Although glycosyl sulfoxides were not isolated, their formation was demonstrated by low-temperature NMR studies of the glycosylation process and MS analysis.
- This methodology was successfully applied for the synthesis of two β -configured cardiac glycosides.

Chapter 7

- Preliminary biological evaluation of the synthesized KRN7000 analogues have been performed, in addition to MD simulations of mCD1d-ligand recognition process.
- Our results indicate that introduction of short fluoroalkyl moieties, such as CF_3 and C_3F_7 at the end of acyl chain enhances ligand binding to CD1d protein. Moreover, the maximum levels of cytokine release are also increased. In particular, we have identified two KRN7000 analogues: **52** and **51**, bearing trifluoromethyl and perfluoropropyl groups at the end of acyl chains, showing promising preliminary results.
- On the contrary, analogues bearing high degree of fluorination at any of the two lipid chains showed low CD1d binding affinity as well as complete lack of stimulatory activity. Molecular dynamic studies showed a different positioning of highly fluorinated acyl chain in **1**. The lack of flexibility of perfluoroalkyl chain might prevent its correct fitting into the curved A' CD1d pocket which might ultimately contribute in the reduced biological activity of the glycolipid.
- Regarding the conformationally restricted analogues, our results indicate that the conformational restriction of ceramide moiety by construction of a pyrrolidine ring does not provide enhanced stimulatory levels. Although analogue **87** lacking of sphingoid base chain exhibited strong CD1d binding affinity, it was unable to stimulate iNKT cells. Molecular dynamic results indicated changes in spatial disposition of 3-OH and 4-OH hydroxyl moieties because of the presence of pyrrolidine ring, which modifies its hydrogen bond network with CD1d.
- Despite the useful information provided by these preliminary biological results, further investigations into the biological impact of

| *General conclusions*

fluoroalkylation and conformational restriction of KRN7000 ceramide fragment will be performed in *due course*.

CHAPTER 9

EXPERIMENTAL SECTION

9.1. GENERAL CONSIDERATIONS

All reagents were purchased from Sigma Aldrich, Alfa Aesar and Carbosynth chemical companies. Fluorinated reagents were acquired from Fluorochem and Apollo Scientific. Dichloromethane (DCM) and perfluorotoluene were distilled from CaH₂, tetrahydrofuran (THF) was distilled from sodium/benzophenone.¹ Proton (¹H NMR) and carbon (¹³C NMR) nuclear magnetic resonance spectra were recorded on a Varian Mercury spectrometer or a Bruker Avance Ultrashield (400 MHz for ¹H) and (100.6 MHz for ¹³C). Fluorine (¹⁹F NMR) and phosphorus (³¹P NMR) nuclear magnetic resonance spectra were recorded on a Varian Mercury spectrometer (376 MHz for ¹⁹F) and (162 MHz for ³¹P). Spectra were fully assigned using COSY, HSQC, HMBC, and NOESY. All chemical shifts are quoted on the δ scale in ppm using the residual solvent (¹H NMR: CDCl₃ = 7.26, CD₃OD = 3.31 and ¹³C NMR: CDCl₃ = 77.16, CD₃OD = 49.0), tetramethylsilane (TMS) or H₃PO₄ (³¹P NMR) as internal standard. Coupling constants (*J*) are reported in Hz with the following splitting abbreviations: s = singlet, d = doublet, t = triplet, q = quartet, quin = quintet, app = apparent and br = broad. Infrared (IR) spectra were recorded on a Jasco FT/IR-600 Plus ATR Specac Golden Gate spectrophotometer. Optical rotations were measured on a Perkin-Elmer 241 polarimeter with a path length of 1.0 dm and are reported with implied units of 10⁻¹ deg cm² g⁻¹. Concentrations (*c*) are given in g/100 mL. High-resolution mass spectra (HRMS) were recorded on an Agilent 1100 Series LC/MSD mass spectrometer with electrospray ionization (ESI). Exact *m/z* values are reported in Daltons. Thin layer chromatography (TLC) was carried out using commercial aluminium backed sheets coated with 60F₂₅₄ silica gel. Visualization of the silica

¹ Perrin D.D.; Armarego, W. L. F. *Purification of Laboratory Chemicals*, 3rd. ed., Pergamon Press, Oxford, 1989.

| *Experimental section*

plates was achieved using a UV lamp ($\lambda_{\max} = 254 \text{ nm}$), 6% H_2SO_4 in EtOH, and/or p-anisaldehyde stain. Flash column chromatography was carried out using silica gel 60 A CC (230–400 mesh). Mobile phases are reported in relative composition (e.g. 1:1 EtOAc/hexane v/v). All reactions using anhydrous conditions were performed using flame-dried apparatus under an atmosphere of argon. Anhydrous magnesium sulphate (MgSO_4) was used as drying agent after reaction work-up, as indicated.

9.2. GENERAL PROCEDURES

General procedure for Wittig reaction.

A mixture of the corresponding carbohydrate (1 equiv.) and phosphonium salt (2 equiv.) in dry THF was cooled to 0 °C under argon atmosphere. Then, a 1.0 M solution of LHMDs in THF (2 equiv.) was added and the mixture was allowed to stir for 6h at 0 °C. Water was then added to quench the reaction and the mixture was extracted with EtOAc. The organic phase was dried over anhydrous MgSO_4 , filtered, and concentrated. The residue was purified by column chromatography (silica gel).

General procedure for Mitsunobu azidation.

Corresponding alcohol (1 equiv.) and triphenylphosphine (3 equiv.) were dissolved in dry THF and the solution was cooled to 0 °C. Then, diisopropyl azodicarboxylate (3 equiv.) and diphenylphosphoryl azide (3.2 equiv.) were sequentially added dropwise. After complete addition, the reaction mixture was allowed to warm to r.t. and stirred for 1h. The solution was then diluted with EtOAc and washed with water. The organic phase was dried over anhydrous MgSO_4 , filtered and

concentrated *in vacuo*. The crude was used for the next step without further purification.

General procedure for acylation.

A solution of the amino-containing compound (1 equiv.) in dry DCM was sequentially treated with EDC·HCl (1.8 equiv.), the corresponding acid (1.3 equiv.), HOBt (1.8 equiv.) and NEt₃ (1 equiv.). The reaction was stirred overnight at rt. Then, the mixture was diluted with EtOAc and washed with water. The organic phase was dried over anhydrous MgSO₄, filtered, and concentrated *in vacuo*. The crude was purified by column chromatography (silica gel).

General procedure for cross-metathesis reaction.

A mixture of corresponding olefin (1 equiv.) and fluorinated olefin (2 equiv.) were dissolved in dry perfluorotoluene. Then, catalyst (0.1 equiv.) and benzoic acid (0.1 equiv.) were added and the reaction was stirred for the indicated time at 40 °C. Subsequent additions of all reagents every time indicated were required depending on the substrate. The crude was concentrated *in vacuo* and purified by column chromatography (silica gel).

General procedure for isopropylidene ketal hydrolysis.

A 4M aqueous solution of HCl (1.25 mL/mmol) was added to a solution of the corresponding isopropylidene-containing compound (1 equiv.) in the indicated solvent. The mixture was stirred at rt. for the time indicated. Then, saturated aqueous solution of NaHCO₃ was added to quench the reaction. The mixture was extracted with DCM and the organic layers were combined, dried over anhydrous MgSO₄ and

| *Experimental section*

concentrated *in vacuo*. The crude was purified by column chromatography (silica gel).

General procedure for hydrogenolysis reaction.

Benzyl-containing compound (1 equiv.) was dissolved in the solvent indicated and Pd/C (2000 mg/mmol) was then added. The vessel was equipped with a hydrogen balloon and the mixture was stirred at r.t. for 48h. The mixture was then filtered through Celite, concentrated *in vacuo* and purified by column chromatography (silica gel).

General procedure for preparation of fluorinated phosphonium salts.

A mixture of the appropriate polyfluoroalkyl iodide (1 mmol) and PPh₃ (3 mmol) were dissolved in toluene and the solution was refluxed for 24h. Then, the solution was cooled and the white precipitated was filtered, washed with diethyl ether and dried *in vacuo* to give the corresponding pure product.

General procedure for Swern oxidation.

To a solution of oxalyl chloride (1.5 mmol) in CH₂Cl₂ at -78 °C, DMSO (2.2 mmol) was added dropwise and stirred for 30 minutes at the same temperature. A solution of the appropriate alcohol (1 mmol) in CH₂Cl₂ was slowly added and stirred at the same temperature for 20 minutes. Next, Et₃N (4 mmol) was added at -78 °C and the solution was warmed to room temperature and stirred for additional 30 minutes. The reaction was quenched by the addition of a saturated solution of NH₄Cl, extracted with CH₂Cl₂ dried over MgSO₄ and concentrated *in vacuo*. The crude was purified by column chromatography using hexane as elutant.

General procedure for Cu-catalyzed coupling of Grignard reagents with alkyl bromides.

A mixture of corresponding bromide (2 mmol), Mg ribbons (2.5 mmol) and a iodine crystal was dissolved in THF. The solution was refluxed during 3h and then was allowed to reach rt. In a separate flask, fluoroalkyl-containing compound (1 mmol) was dissolved in THF and cooled to -10 °C. Then, Li_2CuCl_4 (0.1 mmol) was added and the solution was further cooled to -20 °C and stirred vigorously while initial Grignard reagent solution was added slowly via cannula. The reaction mixture was stirred for 1.5h at -20 °C and further 2h at r.t. A sulphuric acid aqueous solution (10 %) was then added to quench the reaction. The mixture was extracted with Et_2O and the organic layers were dried over MgSO_4 , filtered and concentrated *in vacuo*. The crude was purified by column chromatography (silica gel).

General procedure for one pot Mitsunobu azidation-1,3-dipolar cycloaddition.

Corresponding alcohol (1 mmol) and triphenylphosphine (3 mmol) were dissolved in dry THF and the solution was cooled to 0 °C. Then, diisopropyl azodicarboxylate (3 mmol) and diphenylphosphoryl azide (3.2 mmol) were sequentially added dropwise. After complete addition, the reaction mixture was allowed to warm to r.t. and stirred for 1h. The solution was then diluted with EtOAc and washed with water. The organic phase was dried over anhydrous MgSO_4 , filtered and concentrated *in vacuo*. The crude azide was dissolved in THF/ H_2O (5:1), unless otherwise indicated, and heated, during 12h, at different temperatures depending on the substrate. The reaction mixture was extracted with DCM, and the organic phase was dried over anhydrous MgSO_4 , filtered, and concentrated *in vacuo*. The crude was purified by column chromatography (silica gel).

General procedure for imine reduction to amine.

Sodium borohydride (2 equiv) was added to a solution of the corresponding imine (1 equiv) in MeOH at 0°C and the temperature was allowed to reach rt. After stirring at rt for 4.5h, the mixture was concentrated *in vacuo* and purified by column chromatography (silica gel).

General method A for glycosylation of thiophenyl glycosides.

A mixture of thioglycoside (1 mmol), glycosyl acceptor (2 mmol) and 4Å MS in CH₂Cl₂ was stirred at -80 °C for 30 minutes. NIS (3 mmol) and TfOH (0.2 mmol) were subsequently and allowed to react at the indicated time and temperature. The reaction mixture was then diluted with EtOAc and washed with saturated aqueous Na₂S₂O₃. The organic layer was dried with Na₂SO₄, filtered and the solvent evaporated. The residue was then purified by column chromatography (silica gel).

General method B for oxydation/glycosylation of thiophenyl glycosides.

A mixture of thioglycoside (1 mmol) and 4Å MS in CH₂Cl₂ (30 ml) was cooled to -80 °C and stirred for 30 minutes. Then *m*CPBA (1.05 mmol) was added and the reaction mixture was stirred at -80°C and the temperature was gradually warmed to -50 °C until TLC showed completion of the reaction. NaHCO₃ (5 mmol) was added and the reaction mixture was stirred for 15 minutes at -80 °C. The supernatant was transferred under argon to a Schlenck flask containing acceptor (2 mmol), DTBMP (3 mmol) and 4Å MS at -80 °C and the mixture stirred at this temperature for 30 minutes. Tf₂O (2 mmol) was added and the reaction mixture at -80 °C for 30 minutes. The reaction mixture was diluted with EtOAc, washed with saturated aqueous NaHCO₃, dried with

anhydrous Na_2SO_4 , filtered and the solvent evaporated. The residue was then purified by column chromatography (silica gel).

Competitive ELISA with 18:1 PE lipid as indicator.

Affinities between glycolipid analogues and mouse CD1d molecules were measured by a competitive ELISA, using 18:1 BiotinylPE (Avanti Polar Lipids, USA), as an indicator. For this purpose Nunc MaxiSorp flat-bottom 96 well plates (Thermo Fisher Scientific, Denmark) were coated with 100 μL of Goat anti-mouse IgG Fc gamma antibody (ThermoFisher Scientific, Denmark) (10 $\mu\text{g}/\text{mL}$ in 0.1 M NaHCO_3 , pH 9.6) for overnight at 4 °C, and the plates were washed with PBST (PBS containing 0.05% Tween-20) three times and blocked with blocking buffer (1% Bovine Serum Albumin) for 1 h. The plates were washed three times with PBST and 100 μL of lipid- CD1 dimer (BD Biosciences, UK) mixture was added to the plates immediately after washing. The mixture solution was prepared by mixing CD1dimer (5 $\mu\text{g}/\text{mL}$) and lipids in the presence of Biotinyl PE (2 $\mu\text{g}/\text{mL}$) in PBS. In view of the slow kinetics of Biotinyl PE binding to CD1d, we incubated the mixture for overnight at 37 °C. After that, the plates were washed three times with PBST and CD1-Biotinyl PE complex was detected with HRP-labeled Avidin (GE Healthcare, UK). Inhibition curves were constructed using GraphPad Prism software (version 4.0; GraphPad).

Molecular dynamics (MD) simulations protocol.

The crystal structure of mouse CD1d-alpha-galactosylceramide with mouse Valpha14-Vbeta8.2 NKT TCR (PDB ID: 3HE6) was used in the MD simulations. Each complex was then immersed in a water box with a 10 Å buffer of TIP3P water molecules.² The simulations were

² Kiyohara, K.; Gubbins, K.; Panagiotopoulos, A. *Mol. Phys.* **1998**, *94*, 803-808.

| *Experimental section*

carried out with AMBER 16 package³ implemented with ff14SB,⁴ GAFF⁵ and GLYCAM06⁶ force fields. The parameters and charges for the unnatural amino acids were generated with the antechamber module of AMBER, using GAFF force field and AM1-BCC method for charges.⁷ A two-stage geometry optimization approach was performed. The first stage minimizes only the positions of solvent molecules and the second stage is an unrestrained minimization of all the atoms in the simulation cell. The systems were then gently heated by incrementing the temperature from 0 to 300 K under a constant pressure of 1 atm and periodic boundary conditions. Harmonic restraints of 30 kcal·mol⁻¹ were applied to the solute, and the Andersen temperature-coupling scheme was used to control and equalize the temperature. The time step was kept at 1 fs during the heating stages, allowing potential inhomogeneities to self-adjust. Long-range electrostatic effects were modelled using the particle-mesh-Ewald method.⁸ An 8 Å cut-off was applied to Lennard-Jones interactions. Each system was equilibrated for 2 ns with a 2 fs time step at a constant volume and temperature of 300 K. Production trajectories were then run for additional 200 ns under the same simulation conditions.

³ Case, D.A.; Betz, R.M.; Cerutti, D.S.; Cheatham, T.E.; Darden, T.A.; Duke, R.E.; Giese, T.J.; Gohlke, H.; Goetz, A.W.; Homeyer, N.; Izadi, S.; Janowski, P.; Kaus, J.; Kovalenko, A.; Lee, T.S.; LeGrand, S.; Li, P.; Lin, C.; Luchko, T.; Luo, R.; Madej, B.; Mermelstein, D.; Merz, K.M.; Monard, G.; Nguyen, H.; Nguyen, H.T.; Omelyan, I.; Onufriev, A.; Roe, D.R.; Roitberg, A.; Sagui, C.; Simmerling, C.L.; Botello-Smith, W.M.; Swails, J.; Walker, R.C.; Wang, J.; Wolf, R.M.; Wu, X.; Xiao, L.; Kollman, P.A. (2016), AMBER 2016, University of California, San Francisco.

⁴ Maier, J. A.; Martinez, C.; Kasavajhala, K.; Wickstrom, L.; Hauser, K. E.; Simmerling, C. *J. Chem. Theory Comput.* **2015**, *11*, 3696-3713.

⁵ Wang, J.; Wolf, R. M.; Caldwell, J. W.; Kollman, P. A.; Case, D. A.; *J. Comput. Chem.* **2004**, *25*, 1157-1174.

⁶ Kirschner, K. N.; Yongye, A. B.; Tschampel, S. M.; González-Outeiriño, J.; Daniels, C. R.; Foley, B. L.; Woods, R. J. *J. Comput. Chem.* **2008**, *29*, 622-655.

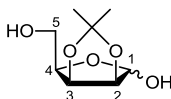
⁷ Jakalian, A.; Jack, D. B.; Bayly, C. I.; *J. Comput. Chem.* **2002**, *23*, 1623-1641.

⁸ Darden, T.; York, D.; Pedersen, L.; *J. Chem. Phys.* **1993**, *98*, 10089-10092.

9.3. COMPOUND CHARACTERIZATION

Data of compounds. Note: although the name of products follows the IUPAC criteria, for clarity and comparative purpose, the numbering of protons and carbons in the NMR data is consistent with that corresponding to the KRN7000 and specified in the drawings of the corresponding structures.

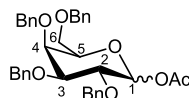
2,3-O-isopropylidene-D-lyxofuranose (**14**)⁹



H₂SO₄ (75 μ L, 1.33 mmol) was added to a solution of D-lyxose (2.5 g, 16.7 mmol) in dry acetone (25 mL). The mixture was stirred overnight at rt. The reaction was quenched adding portions of Na₂CO₃ and shaking vigorously until neutral pH was reached. The suspension was filtered and concentrated *in vacuo*. The reaction crude was purified by short column chromatography (2:1 EtOAc/Hexane) to afford **14** as an unseparable mixture of isomers as a colorless syrup (3.4 g, 75 %); *R_f* = 0.48 (EtOAc); data shown for α anomer: ¹H NMR (400 MHz, CDCl₃) δ in ppm: 5.41 (s, 1 H, H-1), 4.78 (dd, $J_{3,2} = 5.9$ Hz, $J_{3,4} = 3.7$ Hz, 1H, H-3), 4.60 (d, $J_{2,3} = 5.9$ Hz, 1H, H-2), 4.27 (dd, $J_{4,3} = 9.2$ Hz, $J_{4,5} = 5.4$ Hz, 1H, H-4), 3.89 (d, $J_{5,6} = 5.6$ Hz, 2H, H-5), 1.44 (s, 3 H, CH₃), 1.29 (s, 3 H, CH₃); ¹³C NMR (100.6 MHz, CDCl₃) δ in ppm: 112.7 (C-ketal), 100.9 (C-1), 85.6 (C-2), 80.3 (C-3), 79.9 (C-4), 61.2 (C-5), 25.9 (CH₃), 24.5 (CH₃).

⁹ Tsai, Y.-F.; Shih, C.-H.; Su, Y.-T.; Yao, C.-H.; Lian, J.-F.; Liao, C.-C.; Hsia, C.-W.; Shui, H.-A.; Rani, R. *Org. Biomol. Chem.* **2012**, *10*, 931-934.

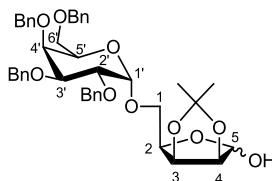
2,3,4,6-tetra-O-benzyl-D-galactopyranosyl acetate (**16**)¹⁰



A solution of 2,3,4,6-tetra-O-benzyl-D-galactopyranose **15** (6 g, 11.1 mmol) in DCM (106 mL) was sequentially treated with triethylamine (5.7 mL, 41.1 mmol) and acetic anhydride (1.31 mL, 13.8 mmol) and stirred for 2h at rt. The reaction was quenched by addition of H₂O. The organic phase was extracted with DCM, dried over anhydrous MgSO₄, filtered, and concentrated *in vacuo*. The reaction crude was purified by column chromatography (1:5 EtOAc/Hexane) to afford **16** as inseparable 3:97 α/β anomeric mixture as a colorless syrup (6.4 g, quant.) *Rf* = 0.26 (EtOAc/Hexane 1:4); data shown for β anomer: ¹H NMR (400 MHz, CDCl₃) δ in ppm: 7.28-7.17 (m, 20H, H-Ar), 5.50 (d, $J_{1,2}$ = 8.1 Hz, 1H, H-1), 4.87 (d, J_{gem} = 11.5 Hz, 1H, CH₂Ph), 4.77 (d, J_{gem} = 11.2 Hz, 1H, CH₂Ph), 4.71 (m, 3H, 3 \times CH₂Ph), 4.55 (d, J_{gem} = 11.5 Hz, 1H, CH₂Ph), 4.36 (d, J_{gem} = 11.7 Hz, 1H, CH₂Ph), 4.31 (d, J_{gem} = 11.7 Hz, 1H, CH₂Ph), 3.91-3.86 (m, 2H, H-2, H-4), 3.63-3.60 (m, 1H, H-5), 3.55-3.48 (m, 3H, H-3, H-6a, H-6b), 1.95 (s, 3H, CH₃); ¹³C NMR (100.6 MHz, CDCl₃) δ in ppm: 169.5 (CO), 138.6 (C-Ar), 138.5 (C-Ar), 138.3 (C-Ar), 137.9 (C-Ar), 128.6-127.5 (CH-Ar), 94.4 (C-1), 82.5 (C-3), 78.3 (C-2), 75.4 (CH₂Ph), 74.8 (CH₂Ph), 74.2 (C-5), 73.6 (CH₂Ph), 73.1 (C-4), 73.0 (CH₂Ph), 68.0 (C-6), 21.2 (CH₃).

¹⁰ Kulkarni, S. S.; Gervay-Hague, J. *Org. Lett.* **2006**, *8*, 5765-5768.

2,3-O-isopropylidene-5-O-(2,3,4,6-tetra-O-benzyl- α -D-galactopyranosyl)-D-lyxofuranose (**12**)¹¹



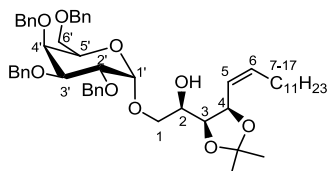
A solution of galactopyranoside **16** (3 g, 5.2 mmol) and MgO (423 mg, 10.4 mmol) in CH_2Cl_2 was cooled to 0°C under Ar atmosphere. TMSI (0.89 mL, 6.5 mmol) was then added and the solution was stirred for 30 min. The reaction crude was concentrated *in vacuo* and redissolved in toluene (15 mL). In a separate flask, a mixture of lyxofuranose **14** (1.1 g, 5.7 mmol), TBAI (5.8 g, 15.6 mmol), DIPEA (0.9 mL, 5.2 mmol) and 4Å MS in toluene (15 mL) was stirred for 10 min at 65°C . The solution of the galactose derivative was added to the reaction vessel via cannula and the mixture was stirred for 1 h at 65°C . The reaction was quenched by addition of EtOAc, and the mixture was cooled to 0°C . The solution was filtered through Celite and the filtrate was washed with aq. $\text{Na}_2\text{S}_2\text{O}_3$ and brine. The organic phase was dried over anhydrous MgSO_4 , filtered, and concentrated *in vacuo*. The crude was purified by column chromatography (1:2 EtOAc/Hexane) to afford **12** (2.2 g, 60%) as a colorless syrup. $R_f = 0.27$ (EtOAc/Hexane 1:2); $^1\text{H NMR}$ (400 MHz, CDCl_3) δ in ppm: 7.31-7.15 (m, 20H, H-Ar), 5.26 (s, 1H, H-1), 4.85 (d, $J_{\text{gem}} = 11.4$ Hz, 1H, CH_2Ph), 4.80 (d, $J_{1',2'} = 3.3$ Hz, 1H, H-1'), 4.74 (d, $J_{\text{gem}} = 11.6$ Hz, 1H, CH_2Ph), 4.72 (d, $J_{\text{gem}} = 11.9$ Hz, 1H, CH_2Ph), 4.66-4.62 (m, 2H, H-2, CH_2Ph), 4.60 (d, $J_{\text{gem}} = 11.9$ Hz, 1H, CH_2Ph), 4.46 (d, $J_{\text{gem}} = 11.6$ Hz, 1H, CH_2Ph), 4.45 (d, $J_{3,4} = 5.6$ Hz, 1H, H-3), 4.38 (d, $J_{\text{gem}} = 11.8$ Hz, 1H, CH_2Ph), 4.35-4.33 (m, 1H, H-4), 4.30 (d, $J_{\text{gem}} = 11.8$ Hz, 1H,

¹¹ Yen, Y. F.; Kulkarni, S. S.; Chang, C. W.; Luo, S. Y. *Carbohydr. Res.* **2013**, *368*, 35-39.

Experimental section

CH₂Ph), 3.97-3.89 (m, 4H, H-2', H-3', H-4', H-5'), 3.78 (dd, $J_{gem} = 11.0$ Hz, $J_{5a,4} = 7.2$ Hz, 1H, H-5a), 3.70 (dd, $J_{gem} = 11.0$ Hz, $J_{5b,4} = 4.29$ Hz, 1H, H-5b), 3.44 (d, $J_{6,5} = 6.42$ Hz, 2H, H-6'), 3.27 (bs, 1H, OH), 1.31 (s, 3H, CH₃), 1.18 (s, 3H, CH₃); ¹³C NMR (100.6 MHz, CDCl₃) δ in ppm: 138.9 (C-Ar), 138.7 (C-Ar), 138.6 (C-Ar), 137.9 (C-Ar), 128.4-127.4 (CH-Ar), 112.5 (C-ketal), 101.0 (C-1), 97.9 (C-1'), 85.4 (C-2), 80.0 (C-3), 79.0 (C-4), 78.6 (C-3'), 76.4 (C-2'), 75.0 (CH₂Ph), 74.7 (CH₂Ph), 73.4 (CH₂Ph), 73.2 (CH₂Ph), 73.0 (C-4'), 69.2 (C-5'), 68.9 (C-6'), 66.4 (C-5), 26.1 (CH₃), 24.9 (CH₃).

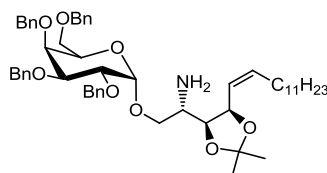
(2R,3S,4R,5Z)-3,4-O-isopropylidene-1-O-(2,3,4,6-tetra-O-benzyl- α -D-galactopyranosyl)-heptadec-5-en-1,2,3,4-tetraol (9)



The title compound was prepared following the general procedure for Wittig olefination, starting from disaccharide **12** (550 mg, 0.77 mmol), a 1M solution of LHMDS in THF (1.5 mL, 1.5 mmol) and (C₁₂H₂₅)PPh₃Br (770 mg, 1.5 mmol) in THF (5.5 mL). After standard workup the crude was purified by column chromatography (1:3 EtOAc/Hexane) to afford **9** (550 mg, 82%) as an unseparable mixture of *E/Z* isomers as a colorless syrup. $R_f = 0.43$ (EtOAc/Hexane 1:2); $[\alpha]_D^{25} -11.0$ (c 0.9, CHCl₃); IR (neat): 3486, 2923, 2853, 1454, 1095, 733 cm⁻¹; Data shown for the major isomer (*Z*): ¹H NMR (400 MHz, CDCl₃) δ in ppm: 7.30-7.15 (m, 20H, H-Ar), 5.57 (m, 2H, H-5, H-6), 4.88-4.82 (m, 2H, CH₂Ph, H-4), 4.75-4.69 (m, 3H, 2xCH₂Ph, H-1'), 4.65 (d, $J_{gem} = 11.7$ Hz, 1H, CH₂Ph), 4.57 (d, $J_{gem} = 11.9$ Hz, 1H, CH₂Ph), 4.48 (d, $J_{gem} = 11.5$ Hz, 1H, CH₂Ph),

4.39 (d, $J_{gem} = 12.0$ Hz, 1H, CH₂Ph), 4.31 (d, $J_{gem} = 12.0$ Hz, 1H, CH₂Ph), 4.05 (d, $J_{3,4} = 6.9$ Hz, H-3), 3.96 (m, 1H, H-2', H-5'), 3.87 (m, 1H, H-3', H-4'), 3.69 (m, 1H, H-2), 3.57 (dd, $J_{gem} = 10.6$ Hz, $J_{1a,2} = 7.0$ Hz, H-1a), 3.46-3.38 (m, 3H, H-6a', H-6b', H-1b), 2.6 (d, $J_{OH,2} = 6.6$ Hz, 1H, OH), 2.02-1.93 (m, 2H, H-7a, H-7b), 1.41 (s, 3H, CH₃), 1.27 (s, 3H, CH₃), 1.16 (m, 18H, CH₂), 0.79 (t, $J_{17,16} = 6.7$ Hz, 3H, CH₃); ¹³C NMR (100.6 MHz, CDCl₃) δ in ppm: 138.7 (C-Ar), 138.6 (C-Ar), 138.6 (C-Ar), 138.0 (C-Ar), 135.4 (C-6), 128.4-127.5 (CH-Ar), 125.2 (C-5), 108.5 (C-ketal), 98.1 (C-1'), 79.1 (C-3'), 77.5 (C-3), 76.4 (C-2'), 74.9 (C-4'), 74.8 (CH₂Ph), 73.5 (CH₂Ph), 73.5 (CH₂Ph), 73.1 (CH₂Ph), 73.0 (C-4), 70.1 (C-1), 69.5 (C-5'), 69.0 (C-6'), 68.7 (C-2), 32.0 (CH₂), 29.7-29.3 (CH₂), 27.8 (C-7), 27.2 (CH₃-ketal), 25.1 (CH₃-ketal), 22.8 (CH₂), 14.2 (CH₃); HRMS (TOF ES+) for [M+Na]⁺ C₅₄H₇₂NaO₉ (m/z): calculated: 887.5069, found: 887.5050.

(2S,3S,4R,5Z)-2-amino-3,4-O-isopropylidene-1-O-(2,3,4,6-tetra-O-benzyl-α-D-galactopyranosyl)-heptadec-5-en-1,3,4-triol (7)

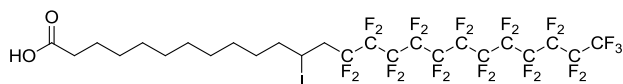


The corresponding azide compound **19** was prepared following the general procedure for Mitsunobu azidation starting from alcohol **9** (150 mg, 0.17 mmol), triphenylphosphine (133 mg, 0.51 mmol), diisopropylazodicarboxylate (100 μL, 0.51 mmol) and diphenyl phosphoryl azide (117 μL, 0.54 mmol) in THF (1.9 mL). Upon completion of the reaction, the reaction mixture was diluted in AcOEt and washed with water. The organic layer was dried over anhydrous MgSO₄, filtered

| *Experimental section*

and concentrated *in vacuo*. The resulting crude azide was then dissolved in THF/H₂O (5:1) (2.6 mL) followed by addition of triphenylphosphine (89 mg, 0.34) and pyridine (0.54 mL). The mixture was then heated at 60°C and stirred for 12h. The solvent was concentrated *in vacuo* and the crude was purified with column chromatography (EtOAc/Hexane/NEt₃ 1:3:0.05) to afford amine **7** (119 mg, 81%) as a colorless oil; *R*_f = 0.42 (EtOAc/Hexane/NEt₃ 1:3:0.05); $[\alpha]_{\text{D}}^{25} +11.4$ (c 0.7, CHCl₃); **IR** (neat): 3383, 2921, 2852, 1454, 1095, 1053, 734 cm⁻¹; **¹H NMR** (400 MHz, CDCl₃) δ in ppm: 7.33-7.17 (m, 20H, HAr), 5.61 (dt, $J_{6,5} = 10.9$ Hz, $J_{6,7} = 7.2$ Hz, 1H, H-6), 5.44 (m, 1H, H-5), 4.87 (d, $J_{\text{gem}} = 11.4$ Hz, 1H, CH₂Ph), 4.86 (d, $J_{1',2'} = 3.7$ Hz, 1H, H-1'), 4.85 (m, 1H, H-4), 4.76 (d, $J_{\text{gem}} = 11.6$ Hz, 1H, CH₂Ph), 4.73 (d, $J_{\text{gem}} = 11.6$ Hz, 1H, CH₂Ph), 4.65 (d, $J_{\text{gem}} = 11.6$ Hz, 1H, CH₂Ph), 4.61 (d, $J_{\text{gem}} = 11.6$ Hz, 1H, CH₂Ph), 4.51 (d, $J_{\text{gem}} = 11.4$ Hz, 1H, CH₂Ph), 4.40 (d, $J_{\text{gem}} = 11.8$ Hz, 1H, CH₂Ph), 4.33 (d, $J_{\text{gem}} = 11.8$ Hz, 1H, CH₂Ph), 3.98 (dd, $J_{2',3'} = 10.0$ Hz, $J_{2',1'} = 3.7$ Hz, 1H, H-2'), 3.92-3.83 (m, 5H, H-3', H-4', H-5', H-1a, H-3), 3.48 (m, 2H, H-6'a, H-6'b), 3.33 (dd, $J_{\text{gem}} = 10.0$ Hz, $J_{1b-2} = 7.7$ Hz, H-1b), 3.02 (m, 1H, H-2), 2.14-1.93 (m, 2H, H-7a, H-7b), 1.36 (s, 3H, CH₃), 1.30 (m, 2H, CH₂), 1.24 (s, 3H, CH₃), 1.19 (m, 16H, CH₂), 0.79 (t, $J_{17,16} = 6.8$ Hz, 3H, CH₃); **¹³C NMR** (100.6 MHz, CDCl₃) δ in ppm: 138.9 (C-Ar), 138.8 (C-Ar), 138.7 (C-Ar), 138.1 (C-Ar), 135.6 (C-6), 128.5-127.4 (CH, Ar), 125.4 (C-5), 108.7 (C-ketal), 99.1 (C-1'), 79.5 (C-3'), 79.3 (C-3), 76.8 (C-2'), 74.9 (C-4'), 74.9 (CH₂Ph), 73.6 (CH₂Ph), 73.4 (CH₂Ph), 73.1 (CH₂Ph), 73.1 (C-4), 71.5 (C-1), 69.5 (C-5'), 69.0 (C-6'), 51.0 (C-2), 32.0 (CH₂), 29.8-29.5 (CH₂), 28.1 (CH₃-ketal), 27.8 (C-7), 25.7 (CH₃-ketal), 22.8 (CH₂), 14.3 (CH₃); **HRMS** (TOF ES+) for [M+H] C₅₄H₇₄NO₈ (m/z): calculated for C₅₄H₇₄NO₈ : 864.5414; found: 864.5461.

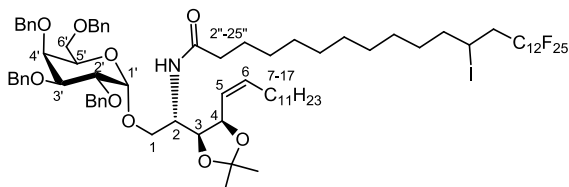
12-iodo-13-perfluorododecyltridecanoic acid (**22**)



A mixture of perfluorododecyl iodide **21** (589 mg, 0.79 mmol) and 13-tridecenoic acid **20** (250 mg, 1.18 mmol) were dissolved in toluene in a three-necked round bottomed flask equipped with a reflux condenser. The mixture was heated to 80 °C and then, AIBN (2 mg, 0.012 mmol) dissolved in 0.5 mL of toluene was injected in three portions over a period in 1.5 h. The reaction mixture was stirred for 24h. After solvent evaporation under reduced pressure, the solid was purified by recrystallization from *n*-hexane to afford 12-iodo-13-perfluorododecyltridecanoic acid **22** (650 mg, 86%) as a white waxy solid; $R_f = 0.48$ (EtOAc/Hexane/AcOH, 1:4:0.25); **IR** (neat): 2921, 2851, 1701, 1208, 1151, 648 cm^{-1} ; **$^1\text{H NMR}$** (400 MHz, CDCl_3) δ in ppm: 4.32 (m, 1H, H-12), 2.98-2.72 (m, 2H, H-13), 2.13 (t, $J_{2,3} = 7.5$ Hz, 2H, H-2), 1.82-1.76 (m, 2H, H-11), 1.66-1.55 (m, 4H, CH_2), 1.28 (m, 12H, CH_2); **$^{13}\text{C NMR}$** (100.6 MHz, CDCl_3) δ in ppm: 178.3 (C=O), 45.1 (app.t, $J_{\text{C,F}} = 20.1$ Hz, C-13), 41.8 (C-11), 33.8 (C-2), 29.7-28.6 (CH_2), 24.8 (C-3), 21.2 (C-12); **$^{19}\text{F NMR}$** (376 MHz, CDCl_3) δ in ppm: -80.7 (t, $J_{12,11} = 9.8$ Hz, 3F, CF_3), -111.8 (d, $J_{\text{gem}} = 274.3$ Hz, 1F, CF_2CH_2), -114.7 (d, $J_{\text{gem}} = 274.3$ Hz, 1F, CF_2CH_2), -121.8 (m, 13F, CF_2), -122.7 (m, 2F, CF_2), -123.7 (m, 2F, CF_2), -126.1 (m, 2F, CF_2); **HRMS** (TOF ES+) for $[\text{M}+\text{Na}] \text{C}_{25}\text{H}_{24}\text{INaO}_2$: calculated: 981.0319; found: 981.0325.

Experimental section

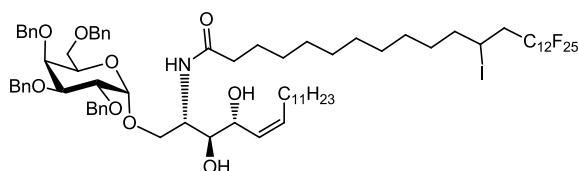
(2S,3S,4R,5Z)-2-(12-iodo-13-perfluorododecyl-tridecanoyl)-amino-3,4-O-isopropylidene-1-O-(2,3,4,6-tetra-O-benzyl- α -D-galactopyranosyl)-heptadec-5-en-1,3,4-triol (23)



The title compound was prepared following the general procedure for acylation, starting from amine **7** (700 mg, 0.81 mmol), EDC·HCl (280 mg, 1.45 mmol), 13-perfluorododecyl-10-iodo-1-tridecanoic acid **22** (1.05 g, 1.1 mmol), HOBT (197 mg, 1.45 mmol) and NEt₃ (0.11 mL, 0.81 mmol). The crude was purified by column chromatography (EtOAc/Hexane, 1:5, then, EtOAc/Hexane, 1:4) to provide the desired amide **23** as a white gel (564 mg, 60% yield); R_f = 0.39 (EtOAc/Hexane, 1:3). $[\alpha]_D^{25}$ 11.7 (*c* 1.2, CHCl₃); IR (neat): 3316, 2923, 2852, 1644, 1454, 1208, 1152, 1055, 751 cm⁻¹; ¹H NMR (400 MHz, CDCl₃) δ in ppm: 7.32-7.18 (m, 20H, HAr), 5.97 (d, $J_{NH,2}$ = 9.0 Hz, 1H, NH), 5.50 (m, 1H, H-6), 5.34 (m, 1H, H-5), 4.86 (d, J_{gem} = 11.7 Hz, 1H, CH₂Ph), 4.85 (m, 1H, H-1'), 4.79 (m, 1H, H-4), 4.74 (d, J_{gem} = 11.6 Hz, 1H, CH₂Ph), 4.73 (d, J_{gem} = 11.5 Hz, 1H, CH₂Ph), 4.67 (d, J_{gem} = 11.6 Hz, 1H, CH₂Ph), 4.61 (d, J_{gem} = 11.5 Hz, 1H, CH₂Ph), 4.49 (d, J_{gem} = 11.7 Hz, 1H, CH₂Ph), 4.42 (d, J_{gem} = 12.0 Hz, 1H, CH₂Ph), 4.32 (d, J_{gem} = 12.0 Hz, 1H, CH₂Ph), 4.23 (m, 1H, H-12''), 4.15 (dd, $J_{3,2}$ = 9.0 Hz, $J_{3,4}$ = 6.0 Hz, 1H, H-3), 4.02 (m, 1H, H-2), 3.97 (dd, $J_{2',3'}$ = 9.9 Hz, $J_{2',1'}$ = 3.7 Hz, 1H, H-2'), 3.93 (dd, J_{gem} = 11.4 Hz, $J_{1a,2}$ = 3.6 Hz, 1H, H-1a), 3.91-3.86 (m, 2H, H-4', H-5'), 3.83 (dd, $J_{3',2'}$ = 9.9 Hz, $J_{3',4'}$ = 2.8 Hz, 1H, H-3'), 3.58 (dd, J_{gem} = 11.4 Hz, $J_{1b,2}$ = 2.6 Hz, 1H, H-1b), 3.44 (dd, J_{gem} = 9.3 Hz, $J_{6a',5}$ = 6.5 Hz, 1H, H-6a'), 3.33 (dd, J_{gem} = 9.3 Hz, $J_{6b',5}$ = 6.2 Hz, 1H, H-6b'), 2.91-2.65 (m, 2H, H-13''), 2.05-1.89 (m, 3H, H-7a, H-11''), 1.86-1.63 (m, 3H, H-7b, H-11''), 1.50 (s, 3H, CH₃), 1.48 (m, 2H,

CH₂), 1.29 (s, 3H, CH₃), 1.30-1.10 (m, 32H, CH₂), 0.81 (t, $J_{17,16} = 6.9$ Hz, 3H, CH₃); ¹³C NMR (100.6 MHz, CDCl₃) δ in ppm: 172.5 (C=O), 138.9 (C-Ar), 138.6 (C-Ar), 138.5 (C-Ar), 137.7 (C-Ar), 135.1 (C-6), 128.6-127.6 (CH, Ar), 124.4 (C-5), 108.5 (C-ketal), 99.4 (C-1'), 78.9 (C-3'), 77.2 (C-2'), 76.0 (C-3), 74.7 (CH₂Ph), 74.6 (C-4'), 73.5 (CH₂Ph), 73.4 (CH₂Ph), 73.1 (CH₂Ph), 72.9 (C-4), 69.7 (C-1), 69.7 (C-5'), 69.1 (C-6'), 49.1 (C-2), 41.6 (t, $J_{C-F} = 20.2$ Hz, C-13"), 40.3 (C-11"), 36.7 (C-2"), 31.9 (CH₂), 29.7-29.4 (CH₂), 28.7 (CH₂), 28.1 (CH₃), 27.8 (C-7), 25.8 (CH₂), 25.6 (CH₃), 22.7 (CH₂), 20.9 (C-12"), 14.1 (CH₃); ¹⁹F NMR (376 MHz, CDCl₃) δ in ppm: -80.8 (t, $J_{25,24} = 9.8$ Hz, 3F, CF₃), -111.8 (d, $J_{gem} = 271.1$ Hz, 1F, CF₂CH₂), -114.7 (d, $J_{gem} = 271.1$ Hz, 1F, CF₂CH₂), -121.8 (m, 13F, CF₂), -122.8 (m, 2F, CF₂), -123.7 (m, 2F, CF₂), -126.2 (m, 2F, CF₂); HRMS (TOF ES+) for [M+H] C₇₉H₉₆F₂₅INO₉ calculated: 1804.5731; found: 1804.5719.

(2S,3S,4R,5Z)-2-(12-iodo-13-perfluorododecyl-tridecanoyl)-amino-3,4-dihydroxy-1-O-(2,3,4,6-tetra-O-benzyl-α-D-galactopyranosyl)-heptadec-5-en-1,3,4-triol (24)

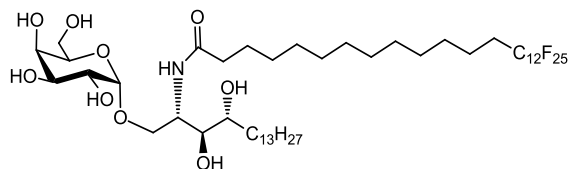


The title compound was prepared following the general procedure for isopropylidene ketal hydrolysis, starting from amide **23** (300 mg, 0.17 mmol) and using 4M HCl (0.21 mL) in a mixture of CH₂Cl₂/MeOH (5:1). The reaction was allowed to stir for 24 h and was stopped by adding a saturated aqueous solution of Na₂CO₃. The crude was purified by column chromatography (EtOAc/Hexane, 1:3) to provide the desired amide **23** as a white waxy solid (210 mg, 73% yield). $R_f = 0.19$ (EtOAc/Hexane,

| *Experimental section*

1:2). $[\alpha]_D^{25} +0.69$ (c 1.3, CHCl_3); **IR** (neat): 3324, 2923, 2852, 1642, 1454, 1205, 1150, 1043, 751 cm^{-1} ; **$^1\text{H NMR}$** (400 MHz, CDCl_3) δ in ppm: 7.32-7.18 (m, 20H, HAr), 6.28 (d, $J_{\text{NH},2} = 8.3$ Hz, 1H, NH), 5.52 (dt, $J_{6,5} = 11.0$ Hz, $J_{6,7} = 7.3$ Hz, 1H, H-6), 5.34 (m, 1H, H-5), 4.86 (d, $J_{\text{gem}} = 11.5$ Hz, 1H, CH_2Ph), 4.86 (m, 1H, H-1'), 4.80 (d, $J_{\text{gem}} = 11.8$ Hz, 1H, CH_2Ph), 4.70 (d, $J_{\text{gem}} = 11.7$ Hz, 1H, CH_2Ph), 4.67 (d, $J_{\text{gem}} = 11.8$ Hz, 1H, CH_2Ph), 4.63 (d, $J_{\text{gem}} = 11.7$ Hz, 1H, CH_2Ph), 4.49 (d, $J_{\text{gem}} = 11.5$ Hz, 1H, CH_2Ph), 4.39 (d, $J_{\text{gem}} = 11.7$ Hz, 1H, CH_2Ph), 4.37 (m, 1H, H-4), 4.30 (d, $J_{\text{gem}} = 11.7$ Hz, 1H, CH_2Ph), 4.23 (m, 1H, H-12"), 4.10 (m, 1H, H-2), 3.99 (dd, $J_{2',3'} = 10.0$ Hz, $J_{2',1'} = 3.8$ Hz, 1H, H-2'), 3.89 (m, 1H, H-4'), 3.89-3.78 (m, 4H, H-3', H-5', H-6a', H-1a), 3.60 (d, $J_{\text{OH},4} = 7.1$ Hz, 1H, OH), 3.52-3.39 (m, 3H, H-6'b, H-1b, H-3), 2.85-2.65 (m, 1H, H-13"), 2.58 (d, $J_{\text{OH},3} = 4.3$ Hz, 1H, OH), 2.05-1.89 (m, 4H, H-7, H2"), 1.79-1.65 (m, 2H, H-11"), 1.48 (m, 2H, CH_2), 1.30-1.10 (m, 32H, CH_2), 0.80 (t, $J_{17,16} = 6.9$ Hz, 3H, CH_3); **$^{13}\text{C NMR}$** (100.6 MHz, CDCl_3) δ in ppm: 173.1 (C-1"), 138.4 (C-Ar), 138.4 (C-Ar), 137.8 (C-Ar), 137.5 (C-Ar), 135.0 (C-6), 128.5-127.5 (CH, Ar), 127.9 (C-5), 99.3 (C-1'), 79.2 (C-3'), 76.0 (C-2'), 75.6 (C-3), 74.7 (CH_2Ph), 74.5 (C-4'), 74.1 (CH_2Ph), 73.6 (CH_2Ph), 72.7 (CH_2Ph), 70.0 (C-1), 70.0 (C-5'), 69.0 (C-6'), 69.0 (C-4), 49.9 (C-2), 41.6 (t, $J_{\text{C-F}} = 19.7$ Hz, C-13"), 40.3 (C-11"), 36.7 (C-2"), 31.9 (CH_2), 29.7-29.4 (CH_2), 28.5 (CH_2), 28.1 (C-7), 25.7 (CH_2), 22.8 (CH_2), 21.0 (C-12"), 14.1 (CH_3); **$^{19}\text{F NMR}$** (376 MHz, CDCl_3) δ in ppm: -80.7 (t, $J_{25,24} = 9.5$ Hz, 3F, CF_3), -111.8 (d, $J_{\text{gem}} = 270.9$ Hz, 1F, CF_2CH_2), -114.7 (d, $J_{\text{gem}} = 270.9$ Hz, 1F, CF_2CH_2), -121.7 (m, 13F, CF_2), -122.7 (m, 2F, CF_2), -123.6 (m, 2F, CF_2), -126.1 (m, 2F, CF_2); **HRMS** (TOF ES+) for $[\text{M}+\text{Na}] \text{C}_{76}\text{H}_{91}\text{F}_{25}\text{I}\text{NNaO}_9$ calculated: 1786,5237; Found: 1786,5227.

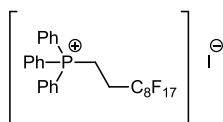
(2S,3S,4R)-2-(13-perfluorododecyl-tridecanoyl)-3,4-dihydroxy-1-O-(α -D-galactopyranosyl)-heptadeca-1,3,4-triol (1)



The title compound was prepared following the general procedure for hydrogenolysis reaction starting from protected glycolipid **24** (40 mg, 0.023 mmol) and using Pd/C (18 mg), H₂ (1 atm) in MeOH/CHCl₃ (3:1) (2.3 mL). The resulting crude was purified using column chromatography (CH₂Cl₂/MeOH, 9:1) to afford **1** (23 mg, 79%) as a white waxy solid; *R_f* = 0.19 (CHCl₃/MeOH, 9:1). [α]_D²⁵ +16.7 (c 0.6, MeOH/CHCl₃ (1:1)); **IR** (neat): 3400, 2916, 2850, 1637, 1206, 1153, 1051, 753 cm⁻¹; **¹H NMR** (400 MHz, CDCl₃ / MeOD (1:1)) δ in ppm: 4.82 (d, *J*_{1',2'} = 3.8 Hz, 1H, H-1'), 4.11 (q, *J*_{2,1a} = *J*_{2,3} = 4.6 Hz, 1H, H-2), 3.85 (d, *J*_{4',3'} = 3.2 Hz, 1H, H-4'), 3.80 (dd, *J*_{1a,1b} = 10.7 Hz, *J*_{1a,2} = 4.6 Hz, 1H, H-1a), 3.73-3.58 (m, 6H, H-2', H-3', H-5', H-6', H-1b), 3.46 (m, 2H, H-3, H-4), 2.12 (t, *J*_{2'',3''} = 7.6 Hz, 2H, H-2''), 1.98 (m, 2H, H-13''), 1.53 (m, 4H, CH₂), 1.25 (m, 40H, CH₂), 0.79 (t, *J*_{17,16} = 6.9 Hz, CH₃); **¹³C NMR** (100.6 MHz, CDCl₃ / MeOD (1:1)) δ in ppm: 174.4 (CO), 99.6 (C-1'), 74.6 (C-3), 71.9 (C-4), 70.7 (C-3'), 70.2 (C-5'), 69.6 (C-4'), 68.8 (C-2'), 67.2 (C-1), 61.7 (C-6'), 50.3 (C-2), 36.4 (C-2''), 32.5 (CH₂), 31.8 (CH₂), 30.7 (C-13''), 29.6-29.0 (CH₂), 25.8 (CH₂), 22.6 (CH₂), 20.0 (C-12''), 13.8 (CH₃); **¹⁹F NMR** (376 MHz, CDCl₃) δ in ppm: -81.5 (t, *J*_{12,11} = 9.1 Hz, 3F, CF₃), -114.9 (m, 2F, CF₂CH₂), -122.3 (m, 13F, CF₂), -123.2 (m, 2F, CF₂), -124.0 (m, 2F, CF₂), -126.7 (m, 2F, CF₂); **HRMS** (TOF ES+) for [M+Na] C₄₈H₇₀F₂₅NNaO₉ (m/z): calculated: 1302.4549, found: 1302.4549.

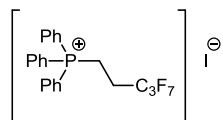
| *Experimental section*

1H, 1H, 2H, 2H-perfluorodecanyltriphenylphosphonium iodide (27)



The title compound was prepared following the general procedure for preparation of fluorinated phosphonium salts, starting from 1H, 1H, 2H, 2H-perfluorodecyl iodide **25** (2 g, 3.4 mmol) and triphenylphosphine (2.7 g, 10.5 mmol) in toluene (2.7 mL). The solution was cooled and the white precipitated was filtered, washed with diethyl ether and dried *in vacuo* to afford **27** as a white solid (2.7 g, 94 % yield); **¹H NMR** (400 MHz, CDCl₃) δ in ppm: 7.86-7.66 (m, 15H, H-Ar.), 4.12 (m, 2H, H-2), 2.53 (m, 2H, H-3); **¹³C NMR** (100.6 MHz, CDCl₃): δ in ppm: **¹³C NMR** (100.6 MHz, CDCl₃): δ in ppm: 135.6 (C-Ar), 133.6 (d, *J*_{C,P} = 10.3 Hz, CH-Ar), 130.7 (d, *J*_{C,P} = 12.9 Hz, CH-Ar), 116.3 (d, *J*_{C,P} = 87.3 Hz, CH-Ar), 24.3 (m, C-3), 15.9 (m, C-2); **¹⁹F NMR** (376 MHz, CDCl₃) δ in ppm: -80.8 (t, *J*_{F,H} = 9.8 Hz, 3F, CF₃), -112.9 (m, 2F, CF₂), -121.6 (m, 2F, CF₂), -122.0 (m, 4F, CF₂), -122.7 (m, 4F, CF₂), -126.2 (m, 2F, CF₂); **³¹P NMR** (162 MHz, CDCl₃) δ in ppm: 25.1 (s)

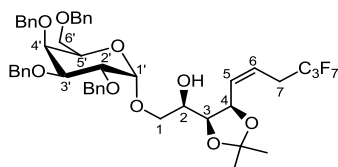
3,3,4,4,5,5-heptafluoropentyltriphenylphosphonium iodide (28)



The title compound was prepared following the general procedure for preparation of fluorinated phosphonium salts starting from 1,1,1,2,2,3,3,3-heptafluoro-5-iodopentane (5 g, 15.4 mmol) and triphenylphosphine (12.1 g, 46.3 mmol) in toluene (12 mL). The solution

was cooled and the white precipitated was filtered, washed with diethyl ether and dried *in vacuo* to afford **66** as a white solid (6.9 g, 77 % yield); $^1\text{H NMR}$ (400 MHz, CDCl_3) δ in ppm: 7.93-7.74 (m, 15H, H-Ar.), 4.20 (m, 2H, H-2), 2.58 (m, 2H, H-3); $^{13}\text{C NMR}$ (100.6 MHz, CDCl_3): δ in ppm: 135.8 (d, $J_{\text{C,P}} = 3.0$ Hz, C-Ar), 133.8 (d, $J_{\text{C,P}} = 10.3$ Hz, CH-Ar), 130.9 (d, $J_{\text{C,P}} = 12.8$ Hz, CH-Ar), 116.6 (d, $J_{\text{C,P}} = 87.4$ Hz, CH-Ar), 24.3 (t, $J_{\text{C,F}} = 22.8$ Hz, C-3), 16.1 (d, $J_{\text{C,P}} = 56.4$ Hz, C-2); $^{19}\text{F NMR}$ (376 MHz, CDCl_3) δ in ppm: -80.3 (t, $J_{\text{F,H}} = 9.7$ Hz, 3F, CF_3), -113.8 (m, 2F, CF_2), -127.0 (m, 2F, CF_2); $^{31}\text{P NMR}$ (162 MHz, CDCl_3) δ in ppm: 25.7 (s)

(2R,3S,4R,5Z)-3,4-O-isopropylidene-1-O-(2,3,4,6-tetra-O-benzyl- α -D-galactopyranosyl)-7-perfluoropropyl-hepta-5-en-1,2,3,4-tetraol (30)

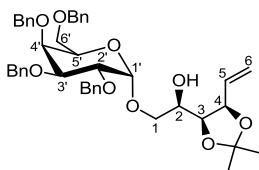


The title compound was prepared following the general procedure for Wittig olefination, starting from disaccharide **12** (34 mg, 0.048 mmol), a 1M solution of LHMDS in THF (95 μL , 0.095 mmol) and **28** (56 mg, 0.095 mmol) in THF (0.35 mL). After standard workup the crude was purified by column chromatography (1:3 EtOAc/Hexane) to afford **30** (26 mg, 67%) as an unseparable mixture of *E/Z* isomers as a colorless syrup. $R_f = 0.31$ (EtOAc/Hexane 1:3); Data shown for the major isomer (*Z*): $^1\text{H NMR}$ (400 MHz, CDCl_3) δ in ppm: 7.30-7.19 (m, 20H, H-Ar), 6.02 (dd, $J_{5,6} = 11.0$ Hz, $J_{5,4} = 9.3$ Hz, 1H, H-5), 5.63 (dt, $J_{6,5} = 11.0$ Hz, $J_{6,7} = 7.5$ Hz, 1H, H-6), 4.85 (d, $J_{\text{gem}} = 11.5$ Hz, 1H, CH_2Ph), 4.79-4.72 (m, 4H, H-1', 2x CH_2Ph , H-4), 4.65 (d, $J_{\text{gem}} = 11.7$ Hz, 1H, CH_2Ph), 4.59 (d, $J_{\text{gem}} = 11.9$ Hz, 1H, CH_2Ph), 4.48 (d, $J_{\text{gem}} = 11.5$ Hz, 1H, CH_2Ph), 4.40 (d, $J_{\text{gem}} = 11.9$

Experimental section

Hz, 1H, CH₂Ph), 4.31 (d, $J_{\text{gem}} = 11.9$ Hz, 1H, CH₂Ph), 4.10 (dd, $J_{3,4} = 7.0$ Hz, $J_{3,2} = 2.5$ Hz, 1H, H-3), 3.98-3.92 (m, 2H, H-2', H-4'), 3.87-3.83 (m, 2H, H-3', H-5'), 3.66 (m, 1H, H-2), 3.61 (dd, $J_{\text{gem}} = 10.3$ Hz, $J_{6a',5'} = 7.2$ Hz, 1H, H-6a'), 3.47-3.36 (m, 3H, H-1a, H-1b, H-6b'), 2.77 (m, 2H, H-7), 2.64 (m, 1H, OH), 1.42 (s, 3H, CH₃), 1.28 (s, 3H, CH₃); **¹³C NMR** (100.6 MHz, CDCl₃) δ in ppm: 138.8 (C-Ar), 138.7 (C-Ar), 138.6 (C-Ar), 138.0 (C-Ar), 132.9 (C-5), 128.5-127.5 (CH-Ar), 120.6 (C-6), 109.2 (C-ketal), 98.3 (C-1'), 79.2 (C-3'), 77.6 (C-4), 76.5 (C-2'), 75.0 (C-3), 74.9 (CH₂Ph), 73.7 (CH₂Ph), 73.6 (CH₂Ph), 73.2 (CH₂Ph), 73.0 (C-4'), 70.4 (C-6'), 69.8 (C-5'), 69.2 (C-1), 68.5 (C-2), 29.7 (t, $J_{\text{C,F}} = 22.0$ Hz, C-7), 27.0 (CH₃), 25.0 (CH₃); **¹⁹F NMR** (376 MHz, CDCl₃) δ in ppm: -80.5 (t, $J_{10,9} = 9.6$ Hz, 3F, CF₃), -113.3 (brd, $J_{\text{gem}} = 268.1$ Hz, 1F, CF₂CH₂), -114.2 (brd, $J_{\text{gem}} = 268.1$ Hz, 1F, CF₂CH₂) -127.2 (brs, 2F, CF₂).

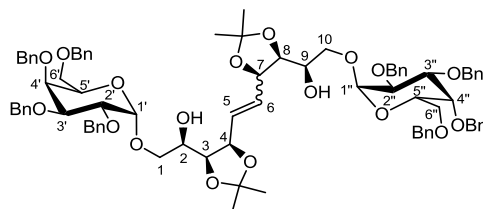
(2R,3S,4R)-3,4-O-isopropylidene-1-O-(2,3,4,6-tetra-O-benzyl- α -D-galactopyranosyl)-hex-5-en-1,2,3,4-tetraol (11)



The title compound was prepared following the general procedure for Wittig olefination, starting from disaccharide **12** (108 mg, 0.152 mmol), a 1M solution of LHMDS in THF (684 μ L, 0.684 mmol) and MePPh₃Br (244 mg, 0.684 mmol) in THF (1.0 mL). After standard workup the crude was purified by column chromatography (1:3 EtOAc/Hexane) to afford **11** (86 mg, 80%) as a colorless syrup. $R_f = 0.21$ (EtOAc/Hexane 1:3); $[\alpha]_{\text{D}}^{25} -53.3$ (c 3.3, CHCl₃); **IR** (neat): 3468, 2921, 2854, 1455, 1098 cm⁻¹; **¹H NMR** (400 MHz, CDCl₃) δ in ppm: 7.32-7.17 (m, 20H, H-Ar), 5.95

(ddd, $J_{5,6a} = 17.2$ Hz, $J_{5,6b} = 10.1$ Hz, $J_{5,4} = 8.2$ Hz, 1H, H-5), 5.24 (d, $J_{6a,5} = 17.2$ Hz, 1H, H-6a), 5.18 (d, $J_{6b,5} = 10.1$ Hz, 1H, H-6b), 4.86 (d, $J_{gem} = 11.6$ Hz, 1H, CH₂Ph), 4.75 (d, $J_{gem} = 11.6$ Hz, 1H, CH₂Ph), 4.74 (m, 2H, CH₂Ph, H-1'), 4.66 (d, $J_{gem} = 11.8$ Hz, 1H, CH₂Ph), 4.59 (d, $J_{gem} = 11.9$ Hz, 1H, CH₂Ph), 4.49 (m, 2H, CH₂Ph, H-4), 4.39 (d, $J_{gem} = 11.8$ Hz, 1H, CH₂Ph), 4.31 (d, $J_{gem} = 11.8$ Hz, 1H, CH₂Ph), 4.12 (dd, $J_{3,4} = 6.9$ Hz, $J_{3,2} = 3.9$ Hz, 1H, H-3), 3.96 (dd, $J_{2',3'} = 9.9$ Hz, $J_{2',1'} = 3.6$ Hz, 1H, H-2'), 3.93-3.83 (m, 3H, H-5', H-3', H-4'), 3.70 (br. s, 1H, H-2), 3.60 (dd, $J_{gem} = 10.6$ Hz, $J_{1a,2} = 6.4$ Hz, 1H, H-1a), 3.46 (dd, $J_{gem} = 10.6$ Hz, $J_{1b,2} = 5.2$ Hz, 1H, H-1b), 3.42-3.39 (m, 2H, H-6a', H-6b'), 2.79 (d, $J_{OH,2} = 6.7$ Hz, 1H, OH), 1.43 (s, 3H, CH₃), 1.28 (s, 3H, CH₃); **¹³C NMR** (100.6 MHz, CDCl₃) δ in ppm: 138.6, 138.5, 138.4, 137.8 (C Ar), 134.1 (C-5), 128.4-127.4 (CH Ar), 119.6 (C-6), 108.8 (C-ketal), 98.2 (C-1'), 79.1 (C-3'), 78.9 (C-4), 77.5 (C-3), 77.4 (CH₂Ph), 76.3 (C-2'), 74.7 (CH₂Ph), 73.5 (CH₂Ph), 73.4 (CH₂Ph), 72.9 (C-4'), 69.9 (C-1), 69.6 (C-5'), 68.9 (C-2), 68.4 (C-6'), 27.1 (CH₃), 25.0 (CH₃); **HRMS** (TOF ES+) for [M+Na] C₄₃H₅₀NaO₉ (m/z): calculated: 733.3342, found: 733.3336.

(2R,3S,4R)-2,9-dihydroxy-3,4,7,8-diisopropylidene-1,10-di-O-(2,3,4,6-tetra-O-benzyl- α -D-galactopyranosyl)-dec-5-ene (34)

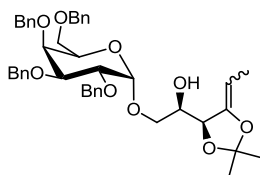


Hoveyda-Grubbs second generation catalyst (2 mg, 0.01 mmol) was added, to a mixture of olefin **11** (200 mg, 0.28 mmol) and perfluorobutylethene (94 μ L, 0.56 mmol) in DCM (6.5 mL). The resulting

Experimental section

solution was stirred for 48h at 40 °C. The crude mixture was concentrated *in vacuo* and purified via column chromatography on silica gel (AcOEt/Hexane 1:2) affording **34** (108 mg, 54%) as a colorless syrup; *Rf* = 0.15 (AcOEt/Hexane 1:2); ¹H NMR (400 MHz, CDCl₃) δ in ppm: 7.29-7.18 (m, 40H, H-Ar), 5.92 (m, 2H, H-5, H-6), 4.84 (d, *J*_{gem} = 11.4 Hz, 2H, 2xCH₂Ph), 4.79 (d, 2H, *J*_{1',2'} = *J*_{1'',2''} = 3.6 Hz, H1', H1''), 4.72 (d, *J*_{gem} = 11.8 Hz, 2H, 4xCH₂Ph), 4.62 (d, *J*_{gem} = 11.8 Hz, 2H, 2xCH₂Ph), 4.59 (d, *J*_{gem} = 11.9 Hz, 2H, 2xCH₂Ph), 4.54 (m, 2H, H-4, H-7), 4.47 (d, *J*_{gem} = 11.4 Hz, 2H, 2xCH₂Ph), 4.40 (d, *J*_{gem} = 11.8 Hz, 2H, 2xCH₂Ph), 4.31 (d, *J*_{gem} = 11.8 Hz, 2H, 2xCH₂Ph), 4.13 (dd, *J*_{3,4} = *J*_{8,7} = 6.9 Hz, *J*_{3,2} = *J*_{8,9} = 2.7 Hz, 2H, H-3, H-8), 3.97-3.83 (m, 8H, H-2', H-5', H-3', H-4', H-2'', H-5'', H-3'', H-4''), 3.68 (m, 2H, H-2, H-9), 3.61 (dd, *J*_{gem} = 10.3 Hz, *J*_{1a,2} = *J*_{10a,9} = 6.2 Hz, 2H, H-1a, H-10a), 3.45-3.38 (m, 6H, H-1b, H-10b, H-6', H6''), 2.68 (d, 2H, 2xOH), 1.40 (s, 6H, 2xCH₃), 1.24 (s, 6H, 2xCH₃); HRMS (TOF ES+) for [M+Na] C₈₄H₉₅NaO₁₈ (m/z): calculated: 1415.6483, found: 1415.6441.

(2R,3S,4R)-3,4-O-isopropylidene-1-O-(2,3,4,6-tetra-O-benzyl-α-D-galactopyranosyl)-hexa-5-en-1,2,3,4-tetraol (35)

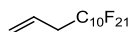


Hoveyda-Grubbs second generation catalyst (5 mg, 0.01 mmol) was added, to a mixture of olefin **11** (150 mg, 0.21 mmol) and perfluorobutylethene (355 μL, 2.1 mmol) in perfluorotoluene (5 mL). The resulting solution was stirred for 20min at 40 °C under MW irradiation (200W). Then, perfluorobutylethene (355 μL, 2.1 mmol) and Hoveyda-

Grubbs second generation catalyst (5 mg, 0.01 mmol) were again added to the mixture. The crude mixture was concentrated *in vacuo* and purified via column chromatography on silica gel (AcOEt/Hexane 1:3) affording **35** (117 mg, 78%) as an inseparable 85:15 *Z/E* mixture as a colorless syrup; *Rf* = 0.19 (AcOEt/Hexane 1:3); **IR** (neat): 3490, 2921, 2861, 1454, 1101 cm^{-1} ; Data shown for *Z* isomer: **$^1\text{H NMR}$** (400 MHz, CDCl_3) δ in ppm: 7.32-7.17 (m, 20H, HAr), 4.86 (d, $J_{\text{gem}} = 11.5$ Hz, 1H, CH_2Ph), 4.75 (m, 3H, $2\times\text{CH}_2\text{Ph}$, H-1'), 4.66 (d, $J_{\text{gem}} = 11.9$ Hz, 1H, CH_2Ph), 4.61 (d, $J_{\text{gem}} = 11.9$ Hz, 1H, CH_2Ph), 4.55 (m, 1H, H-3), 4.49 (d, $J_{\text{gem}} = 11.5$ Hz, 1H, CH_2Ph), 4.40 (d, $J_{\text{gem}} = 11.9$ Hz, 1H, CH_2Ph), 4.31 (d, $J_{\text{gem}} = 11.9$ Hz, 1H, CH_2Ph), 4.25 (qd, $J_{4,5} = 6.8$ Hz, $J_{4,3} = 1.7$ Hz, 1H, H-5), 4.00 (m, 2H, H-2', H-5'), 3.87 (m, 2H, H-3', H-4'), 3.77 (m, 1H, H-2), 3.68 (dd, $J_{\text{gem}} = 10.9$ Hz, $J_{1a,2} = 6.9$ Hz, 1H, H-1a), 3.62 (dd, $J_{\text{gem}} = 10.9$ Hz, $J_{1b,2} = 5.1$ Hz, 1H, H-1b), 3.44 (dd, $J_{\text{gem}} = 9.3$ Hz, $J_{6a,5} = 6.2$ Hz, 1H, H-6a'), 3.39 (dd, $J_{\text{gem}} = 9.3$ Hz, $J_{6b,5} = 6.6$ Hz, 1H, H-6b'), 2.65 (d, $J_{\text{OH},2} = 6.3$ Hz, 1H, OH), 1.55 (dd, $J_{6,5} = 6.8$ Hz, $J_{6,3} = 1.8$ Hz, 3H, H-6), 1.43 (s, 3H, CH_3), 1.28 (s, 3H, CH_3); **$^{13}\text{C NMR}$** (CDCl_3 , 100.6 MHz) δ in ppm: 149.5 (C-4), 138.8 (C-Ar), 138.7 (C-Ar), 138.6 (C-Ar), 138.0 (C-Ar), 128.5-127.6 (CH, Ar), 110.5 (C-ketal), 98.6 (CH-1'), 90.9 (CH-5), 79.2 (CH-3'), 77.2 (CH-3), 76.5 (CH-2'), 75.0 (CH-4'), 74.9 (CH_2Ph), 73.7 (CH_2Ph), 73.6 (CH_2Ph), 73.2 (CH_2Ph), 70.8 (CH-2), 70.2 (CH_2 -1), 69.8 (CH-5'), 69.2 (CH_2 -6'), 26.5 (CH_3), 25.7 (CH_3), 10.5 (CH_3); **HRMS** (TOF ES+) for $[\text{M}+\text{Na}] \text{C}_{43}\text{H}_{50}\text{NaO}_9$ (*m/z*): calculated: 733.3342, found: 733.3341.

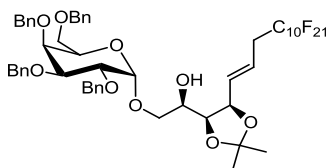
Experimental section

3-perfluorodecylprop-1-ene (**37**)¹²



A mixture of 1-iodo-perfluorodecane **36** (100 mg, 0.174 mmol), allyltributyltin (0.11 mL, 0.348 mmol) and AIBN (6 mg, 0.0348 mmol) was dissolved in anhydrous hexane (1.5 mL). The system was degassed (3 x freeze-pump-thaw) and it was allowed to stir at 80 °C during 2h. The crude was concentrated *in vacuo* and was dissolved in DCM. The solution was extracted with perfluorohexane and the fluoruous phase was concentrated *in vacuo* affording pure 3-perfluorodecylprop-1-ene **37** (92 mg, 95%) as colorless oil. *Rf* = 0.8 (C₆F₁₄ / ethyl ether, 2:1); ¹H NMR (400 MHz, CDCl₃) δ in ppm: 5.75-5.64 (m, 1 H, H-2), 5.01-4.94 (m, 2 H, H-1a, H-1b), 2.10-1.91 (m, 4 H, H-3a, H-3b, H-5a, H-5b), 1.68-1.60 (m, 2 H, H-4a, H-4b); ¹³C NMR (100.6 MHz, CDCl₃): δ in ppm: 125.2 (s, C-2), 122.6 (s, C-1), 36.0 (t, *J*_{C,F} = 22.7 Hz, C-3); ¹⁹F NMR (376 MHz, CDCl₃): δ in ppm = -80.9 (t, *J*₁₃₋₁₂ = 10.0 Hz, 3 F, CF₃), -114.4 (pseudoquint, 2 F, CF₂CH₂), -121.2 (m, 2 F, CF₂), -122.0 (m, 4 F, CF₂), -122.8 (m, 2 F, CF₂), -123.6 (m, 2 F, CF₂), -126.2 (m, 2 F, CF₂).

(2*R*,3*S*,4*R*,5*E*)-3,4-*O*-isopropylidene-1-*O*-(2,3,4,6-tetra-*O*-benzyl- α -D-galactopyranosyl)-7-perfluorodecyl-hepta-5-en-1,2,3,4-tetraol (**10**)



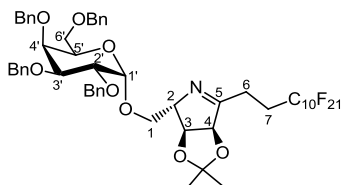
¹² Ryu, I.; Kreimerman, S.; Niguma, T.; Minakata, S.; Komatsu, M.; Luo, Z.; Curran, D. P. *Tetrahedron Lett.* **2001**, *42*, 947-950.

The title compound was prepared following the general procedure for CM reaction, starting from alkene **11** (179 mg, 0.25 mmol), 3-perfluorodecylprop-1-ene **37** (170 μ L, 0.5 mmol), HG-II catalyst (16 mg, 0.025 mmol) and benzoic acid (3 mg, 0.025 mmol) in perfluorotoluene (6 mL). After 24h, fluoroolefin **37** (170 μ L, 0.5 mmol), HG-II catalyst (16 mg, 0.025 mmol) and benzoic acid (3 mg, 0.025 mmol) were once again added. The crude was concentrated *in vacuo* and purified by column chromatography (EtOAc/Hexane 3:1) to afford **10** (236 mg, 76%) as an unseparable mixture of *E/Z* isomers as a colorless syrup. *Rf* = 0.38 (EtOAc/Hexane 1:3); $[\alpha]_D^{25}$ 11.5 (c 1.0, CHCl₃); IR (neat): 3745, 3468, 2921, 2361, 1454, 1205, 1150, 1098 cm⁻¹; Data shown for the major isomer (*E*): ¹H NMR (400 MHz, CDCl₃) δ in ppm: 7.31-7.18 (m, 20H, H-Ar), 5.93 (dd, $J_{5,6}$ = 15.5 Hz, $J_{5,4}$ = 8.1 Hz, 1H, H-5), 5.69-5.62 (m, 1H, H-6), 4.86 (d, J_{gem} = 11.4 Hz, 1H, CH₂Ph), 4.77-4.72 (m, 1H, H-1'), 4.76 (d, J_{gem} = 11.7 Hz, 1H, CH₂Ph), 4.74 (d, J_{gem} = 11.9 Hz, 1H, CH₂Ph), 4.67 (d, J_{gem} = 11.9 Hz, 1H, CH₂Ph), 4.60 (d, J_{gem} = 11.7 Hz, 1H, CH₂Ph), 4.54 (apt, J = 7.6 Hz, 1H, H-4), 4.49 (d, J_{gem} = 11.4 Hz, 1H, CH₂Ph), 4.40 (d, J_{gem} = 11.9 Hz, 1H, CH₂Ph), 4.32 (d, J_{gem} = 11.9 Hz, 1H, CH₂Ph), 4.20 (dd, $J_{3,4}$ = 7.0 Hz, $J_{3,2}$ = 3.1 Hz, 1H, H-3), 3.98 (dd, $J_{2,3'}$ = 10.0 Hz, $J_{2,1'}$ = 3.6 Hz, 1H, H-2'), 3.92 (t, $J_{4',5'}$ = $J_{4',3'}$ = 6.5 Hz, 1H, H-4'), 3.89-3.83 (m, 2H, H-3', H-5'), 3.67 (br s, 1H, H-2), 3.62 (dd, J_{gem} = 10.3 Hz, $J_{6a',5'}$ = 6.4 Hz, 1H, H-6a'), 3.46 – 3.37 (m, 3H, H-1a, H-1b, H-6b'), 2.77 (br t, $J_{7,F}$ = 17.5 Hz, 2H, H-7), 1.42 (s, 3H, CH₃), 1.27 (s, 3H, CH₃); ¹³C NMR (100.6 MHz, CDCl₃) δ in ppm: 138.7 (C-Ar), 138.6 (C-Ar), 138.5 (C-Ar), 137.9 (C-Ar), 134.6 (C-5), 128.5 – 127.5 (CH-Ar), 122.3 (C-6), 109.0 (C-ketal), 98.4 (C-1'), 79.1 (C-3'), 78.1 (C-4), 76.5 (C-2'), 76.2 (C-3), 74.8 (CH₂Ph), 74.8 (CH₂Ph), 73.6 (CH₂Ph), 73.6 (CH₂Ph), 73.1 (C-4'), 70.0 (C-6'), 69.7 (C-5'), 69.1 (C-1), 68.4 (C-2), 34.5 (C-7), 27.1 (CH₃), 24.9 (CH₃); ¹⁹F NMR (376 MHz, CDCl₃) δ in ppm: -80.7 (t, $J_{17,16}$ = 10.7 Hz, 3F, CF₃), -

Experimental section

113.2 (m, 2 F, CF₂CH₂), -121.7 (m, 10 F, CF₂), -122.7 (m, 2 F, CF₂), -123.1 (m, 2 F, CF₂), -126.1 (m, 2 F, CF₂); **HRMS** (TOF ES+) for [M+Na] C₅₄H₅₁F₂₁NaO₉ (m/z): calculated: 1265.3095, found: 1265.3086.

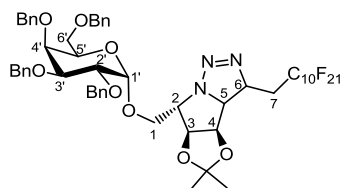
(3R,4S,5S)-5-(1-O-(2,3,4,6-tetra-O-benzyl- α -D-galactopyranosyl)-methanol)-2-(2-perfluorodecylethyl)-3,4-O-isopropylidene- Δ^1 pyrroline (39**)**



The title compound was prepared following the general procedure for one pot Mitsunobu azidation-1,3-dipolar cycloaddition, starting from alcohol **10** (80 mg, 0.06 mmol), triphenylphosphine (51 mg, 0.19 mmol), diisopropyl azodicarboxylate (37 μ L, 0.19 mmol) and diphenylphosphoryl azide (44 μ L, 0.21 mmol) in THF (0.7 mL). After 12 h stirring at room temperature, the reaction mixture was quenched and the crude was dissolved in THF/H₂O (0.9 mL) and heated at 45°C for 12h. The reaction mixture was quenched and the crude was purified by column chromatography (1:3 EtOAc/Hexane) to afford **39** (62 mg, 78%) as a colorless oil. *R_f* = 0.18 (1:3 EtOAc/Hexane); [α]_D²⁵ +24.6 (c 1.8, CHCl₃); **IR** (neat): 2920, 2867, 1651, 1455, 1210, 1151, 1097, 1055, 734 cm⁻¹; **¹H NMR** (400 MHz, CDCl₃) δ in ppm: 7.31 – 7.16 (m, 20H, H-Ar), 4.84 (d, *J*_{gem} = 11.4 Hz, 1H, CH₂Ph), 4.77 (d, *J*_{gem} = 11.7 Hz, 1H, CH₂Ph), 4.73 (m, 2H, H-1', H-3), 4.66 (d, *J*_{gem} = 12.5 Hz, 1H, CH₂Ph), 4.63 (d, *J*_{gem} = 12.5 Hz, 1H, CH₂Ph), 4.55 (d, *J*_{gem} = 11.7 Hz, 1H, CH₂Ph), 4.47 (d, *J*_{gem} = 11.4 Hz, 1H, CH₂Ph), 4.45 (d, *J*_{4,3} = 5.3 Hz, 1H, H-4), 4.38 (d, *J*_{gem} = 11.8

Hz, 1H, CH₂Ph), 4.30 (d, $J_{\text{gem}} = 11.8$ Hz, 1H, CH₂Ph), 4.19 (brs, 1H, H-2), 3.92 (dd, $J_{2,3'} = 10.0$ Hz, $J_{2,1'} = 3.6$ Hz, 1H, H-2'), 3.82 (m, 1H, H-4'), 3.77 (dd, $J_{1a,1b} = 10.0$ Hz, $J_{1a,2} = 2.8$ Hz, H-1a), 3.60 (brt, $J_{5',6'} = 6.6$ Hz, 1H, H-5'), 3.51 (dd, $J_{3',2'} = 10.0$ Hz, $J_{3',4'} = 2.8$ Hz, H-3'), 3.44 (dd, $J_{1b,1a} = 10.0$ Hz, $J_{1b,2} = 2.9$ Hz, 1H, H-1b), 3.39 (d, $J_{6',5'} = 6.6$ Hz, 2H, H-6'), 2.61 (m, 1H, H-6a), 2.40 (m, 2H, H-7), 2.15 (m, 1H, H-6b), 1.25 (s, 3H, CH₃), 1.19 (s, 3H, CH₃); **¹³C NMR** (100.6 MHz, CDCl₃) δ in ppm: 175.6 (C=N), 138.7 (C-Ar), 138.6 (C-Ar), 138.4 (C-Ar), 137.9 (C-Ar), 128.5-127.5 (CH-Ar), 111.7 (C-ketal), 97.9 (C-1'), 87.0 (C-3), 81.9 (C-4), 77.7 (C-3'), 76.6 (C-2'), 75.4 (C-2), 74.9 (CH₂Ph), 74.4 (C-4'), 73.5 (CH₂Ph), 73.4 (CH₂Ph), 71.2 (CH₂Ph), 69.6 (C-5'), 68.7 (C-6'), 67.5 (C-1), 27.3 (C-7), 27.0 (CH₃), 25.6 (CH₃), 21.5 (C-6); **¹⁹F NMR** (376 MHz, CDCl₃) δ in ppm: -80.7 (t, $J_{F,F} = 10.6$ Hz, 3F, CF₃), -113.2 (m, 2F, CF₂), -121.7 (m, 10F, CF₂), -122.8 (m, 2F, CF₂), -123.2 (m, 2F, CF₂), -126.1 (m, 2F, CF₂); **HRMS** (TOF ES+) for [M+H]⁺ C₅₄H₅₁F₂₁NO₈ (m/z): calculated: 1240.3274, found: 1240.3270.

(4*R*,5*R*,6*S*)-6-(1-*O*-(2,3,4,6-tetra-*O*-benzyl- α -D-galactopyranosyl)-methanol)-3-(2-perfluorodecylethyl)-4,5-*O*-isopropylidene-3a,4,5,6-tetrahydro-3H-pyrrolo[1,2-*c*][1,2,3]triazole (40)

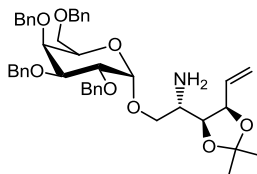


The title compound was prepared following the general procedure for one pot Mitsunobu azidation-1,3-dipolar cycloaddition, starting from alcohol **8** (80 mg, 0.06 mmol), triphenylphosphine (51 mg, 0.19 mmol), diisopropyl azodicarboxylate (37 μ L, 0.19 mmol) and diphenylphosphoryl azide (44 μ L, 0.21 mmol) in THF (0.7 mL). After 1h stirring at room

| *Experimental section*

temperature, the reaction mixture was quenched and the crude was dissolved in THF (0.9 mL) and heated at 45°C for 12h. The reaction mixture was quenched and the crude was purified by column chromatography (1:1 EtOAc/Hexane) to afford **40** (79 mg, 78%) as a colorless oil. $R_f = 0.19$ (1:3 EtOAc/Hexane); $^1\text{H NMR}$ (400 MHz, CDCl_3) δ in ppm: 7.30 – 7.15 (m, 20H, H-Ar), 5.10 (m, 1H, H-6), 4.86 (d, $J_{\text{gem}} = 11.4$ Hz, 1H, CH_2Ph), 4.79 (d, $J_{\text{gem}} = 11.8$ Hz, 1H, CH_2Ph), 4.76 (d, $J_{1',2'} = 3.7$ Hz, 1H, H-1'), 4.64 (s, 2H, $2\times\text{CH}_2\text{Ph}$), 4.58 (brt, $J_{2,1a} = J_{2,1b} = 2.5$ Hz, 1H, H-2), 4.56 (d, $J_{3,4} = 5.6$ Hz, 1H, H-3), 4.53 (d, $J_{\text{gem}} = 11.8$ Hz, 1H, CH_2Ph), 4.49 (d, $J_{\text{gem}} = 11.4$ Hz, 1H, CH_2Ph), 4.41 (t, $J_{4,3} = J_{4,5} = 5.6$ Hz, 1H, H-4), 4.38 (d, $J_{\text{gem}} = 11.7$ Hz, 1H, CH_2Ph), 4.29 (d, $J_{\text{gem}} = 11.7$ Hz, 1H, CH_2Ph), 3.97 (dd, $J_{2',3'} = 10.1$ Hz, $J_{2',1'} = 3.7$ Hz, 1H, H-2'), 3.93 (dd, $J_{\text{gem}} = 10.1$ Hz, $J_{1a,2} = 2.5$ Hz, 1H, H-1a), 3.90 (m, 1H, H-4'), 3.72 (t, $J_{5',6'} = 6.6$ Hz, 1H, H-5'), 3.64 (dd, $J_{3',2'} = 10.1$ Hz, $J_{3',4'} = 2.8$ Hz, 1H, H-3'), 3.47-3.39 (m, 4H, H-1b, H-6', H-5), 2.57-2.43 (m, 1H, H-7a), 2.08-1.93 (m, 1H, H-7b), 1.18 (s, 3H, CH_3), 1.02 (s, 3H, CH_3); $^{13}\text{C NMR}$ (100.6 MHz, CDCl_3) δ in ppm: 138.6 (C-Ar), 138.5 (C-Ar), 138.4 (C-Ar), 137.8 (C-Ar), 128.6-127.4 (CH-Ar), 111.8 (C-ketal), 99.0 (C-1'), 83.8 (C-3), 81.5 (C-4), 79.1 (C-3'), 76.4 (C-2'), 75.0 (CH_2Ph), 74.4 (C-4'), 73.8 (CH_2Ph), 73.6 (CH_2Ph), 72.9 (C-6), 72.6 (CH_2Ph), 70.0 (C-5'), 69.9 (C-1), 68.8 (C-6'), 66.4 (C-5), 65.7 (C-2), 32.0 (t, $J_{\text{C,F}} = 20.9$ Hz, C-7), 26.0 (CH_3), 23.9 (CH_3); $^{19}\text{F NMR}$ (376 MHz, CDCl_3) δ in ppm: -80.8 (t, $J_{\text{F,F}} = 9.9$ Hz, 3F, CF_3), -114.5 (m, 2F, CF_2), -121.7 (m, 10F, CF_2), -122.7 (m, 2F, CF_2), -123.5 (m, 2F, CF_2), -126.2 (m, 2F, CF_2); **HRMS** (TOF ES+) for $[\text{M}+\text{Na}]^+$ $\text{C}_{54}\text{H}_{50}\text{F}_{21}\text{N}_3\text{NaO}_8$ (m/z): calculated: 1290,3155, found: 1290,3158.

(2S,3S,4R)-2-amino-3,4-O-isopropylidene-1-O-(2,3,4,6-tetra-O-benzyl- α -D-galactopyranosyl)-hex-5-en-1,3,4-triol (42)

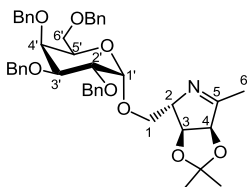


The corresponding azide **41** was prepared following the general procedure for Mitsunobu azidation starting from alcohol **11** (465 mg, 0.66 mmol), triphenylphosphine (515 mg, 1.96 mmol), diisopropylazodicarboxylate (0.39 mL, 1.96 mmol) and diphenyl phosphoryl azide (0.46 mL, 2.13 mmol) in THF (7.5 mL). Upon completion of the reaction, the reaction mixture was diluted in AcOEt and washed with water. The organic layer was dried over anhydrous MgSO_4 , filtered and concentrated *in vacuo*. The resulting crude azide was then dissolved in THF/MeOH/ H_2O (3:1:1, 12.5 mL) followed by addition of Zn (427 mg, 6.5 mmol) and NH_4Cl (348 mg, 6.5 mmol). The mixture was allowed to stir for 3h at r.t. The crude was then filtered over celite, concentrated *in vacuo* and purified by column chromatography (EtOAc/Hexane/ NEt_3 1:3:0.05) to afford amine **42** (308 mg, 66%) as a colorless oil; $R_f = 0.18$ (EtOAc/Hexane/ NEt_3 1:3:0.05); $[\alpha]_D^{25} +52.0$ (c 1.1, CHCl_3). IR (neat): 3310, 3121, 2920, 2851, 1523, 1455, 1213, 1096, 1043 cm^{-1} ; $^1\text{H NMR}$ (400 MHz, CDCl_3) δ in ppm: 7.32 – 7.17 (m, 20H, H-Ar), 5.88 (ddd, $J_{5,6a} = 17.2$ Hz, $J_{5,6b} = 10.2$ Hz, $J_{5,4} = 8.2$ Hz, 1H, H-5), 5.28 (bd, $J_{6a,5} = 17.2$ Hz, 1H, H-6a), 5.20 (bd, $J_{6b,5} = 10.2$ Hz, 1H, H-6b), 4.88 – 4.85 (m, 2H, H-1', CH_2Ph), 4.75 (d, $J_{\text{gem}} = 11.6$ Hz, 1H, CH_2Ph), 4.73 (d, $J_{\text{gem}} = 11.7$ Hz, 1H, CH_2Ph), 4.67 (d, $J_{\text{gem}} = 11.6$ Hz, 1H, CH_2Ph), 4.61 (d, $J_{\text{gem}} = 11.7$ Hz, 1H, CH_2Ph), 4.51– 4.46 (m, 2H, H-4, CH_2Ph), 4.40 (d, $J_{\text{gem}} = 11.7$ Hz, 1H, CH_2Ph), 4.33 (d, $J_{\text{gem}} = 11.9$ Hz, 1H, CH_2Ph), 3.98 (dd, $J_{2,3'} = 10.0$ Hz, $J_{2,1'} = 3.6$ Hz, 1H, H-2'), 3.94 – 3.84 (m, 5H, H-

Experimental section

3', H-4', H-5', H-1a, H-3), 3.48 – 3.45 (m, 2H, H-6'a, H-6'b), 3.34 (dd, J_{gem} = 9.8 Hz, $J_{1b,2}$ = 7.2 Hz, 1H, H-1b), 3.01 – 2.96 (m, 1H, H-2), 1.37 (s, 3H, CH₃), 1.24 (s, 3H, CH₃); **¹³C NMR** (100.6 MHz, CDCl₃) δ in ppm: 138.7 (C-Ar), 138.6 (C-Ar), 138.6 (C-Ar), 137.9 (C-Ar), 134.5 (C-5), 128.4 – 127.4 (CH-Ar), 118.9 (C-6), 108.8 (C-ketal), 99.0 (C-1'), 79.3 (C-3'), 79.2 (C-4), 79.1 (C-3), 77.2 (C-2') 74.8 (C-4'), 73.5 (CH₂Ph), 73.3 (CH₂Ph), 73.3 (CH₂Ph), 72.9 (CH₂Ph), 71.5 (C-1), 69.4 (C-5'), 68.9 (C-6'), 50.6 (C-2), 28.0 (CH₃), 25.5 (CH₃); **HRMS** (TOF ES+) for [M+H] C₄₃H₅₂NO₈: 710.3694; found: 710.3710.

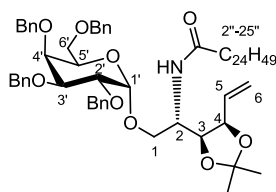
(3R,4S,5S)-5-(1-O-(2,3,4,6-tetra-O-benzyl- α -D-galactopyranosyl)-methanol)-2-methyl-3,4-O-isopropylidene- Δ^1 pyrroline (44)



The title compound was prepared following the general procedure for one pot Mitsunobu azidation-1,3-dipolar cycloaddition, starting from alcohol **11** (104 mg, 0.15 mmol), triphenylphosphine (115 mg, 0.44 mmol), diisopropyl azodicarboxylate (87 μ L, 0.44 mmol) and diphenylphosphoryl azide (0.1 mL, 0.47 mmol) in THF (1.6 mL). After 1 h stirring at room temperature, the reaction mixture was quenched and the crude was dissolved in THF/H₂O (2.2 mL) and heated at 45°C for 12h. The reaction mixture was quenched and the crude was purified by column chromatography (1:1 EtOAc/Hexane) to afford **103** (27 mg, 26%) as a colorless oil. R_f = 0.30 (1:1 EtOAc/Hexane); $[\alpha]_D^{25}$ +24.7 (c 1.3, CHCl₃); **IR** (neat): 2922, 2869, 1650, 1454, 1098, 1057, 736 cm⁻¹; **¹H**

NMR (400 MHz, CDCl_3) δ in ppm: 7.31 – 7.19 (m, 20H, H-Ar), 4.86 (d, $J_{\text{gem}} = 11.4$ Hz, 1H, CH_2Ph), 4.76 - 4.72 (m, 3H, H-1', H-3, CH_2Ph), 4.65 (s, 2H, $2\times\text{CH}_2\text{Ph}$), 4.56 (d, $J_{\text{gem}} = 11.7$ Hz, 1H, CH_2Ph), 4.50 (d, $J_{\text{gem}} = 11.4$ Hz, 1H, CH_2Ph), 4.42 (d, $J_{4,3} = 5.3$ Hz, 1H, H-4), 4.38 (d, $J_{\text{gem}} = 11.7$ Hz, 1H, CH_2Ph), 4.30 (d, $J_{\text{gem}} = 11.7$ Hz, 1H, CH_2Ph), 4.17 (brs, 1H, H-2), 3.92 (dd, $J_{2',3'} = 10.0$ Hz, $J_{2',1'} = 3.6$ Hz, 1H, H-2'), 3.85 (m, 1H, H-4'), 3.78 (dd, $J_{1a,1b} = 9.8$ Hz, $J_{1a,2} = 2.9$ Hz, H-1a), 3.68 (brt, $J_{5',6'} = 6.7$ Hz, 1H, H-5'), 3.56 (dd, $J_{3',2'} = 10.0$ Hz, $J_{3',4'} = 2.8$ Hz, H-3'), 3.46-3.37 (m, 3H, H-1b, $2\times\text{H-6'}$), 1.84 (s, 3H, H-6), 1.26 (s, 3H, CH_3), 1.19 (s, 3H, CH_3); **^{13}C NMR** (100.6 MHz, CDCl_3) δ in ppm: 175.4 (C=N), 138.8 (C-Ar), 138.7 (C-Ar), 138.6 (C-Ar), 138.0 (C-Ar), 128.5-127.6 (CH-Ar), 111.6 (C-ketal), 97.9 (C-1'), 87.6 (C-3), 81.2 (C-4), 78.0 (C-3'), 76.7 (C-2'), 75.4 (C-2), 74.9 (CH_2Ph), 74.7 (C-4'), 73.6 (CH_2Ph), 73.4 (CH_2Ph), 72.3 (CH_2Ph), 69.4 (C-5'), 68.7 (C-6'), 67.9 (C-1), 27.2 (CH_3), 25.9 (CH_3), 16.9 (C-6); **HRMS** (TOF ES+) for $[\text{M}+\text{H}]^+$ $\text{C}_{43}\text{H}_{50}\text{NO}_8$ (m/z): calculated: 708.3531, found: 708.3529.

(2S,3S,4R)-2-pentacosanoylamino-3,4-O-isopropylidene-1-O-(2,3,4,6-tetra-O-benzyl- α -D-galactopyranosyl)-hex-5-en-1,3,4-triol (43)

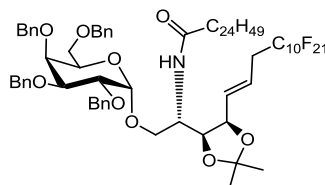


The title compound was prepared following the general procedure for acylation, starting from **42** (578 mg, 0.81 mmol), EDC·HCl (278 mg, 1.46 mmol), pentacosanoic acid **45** (405 mg, 1.05 mmol), HOBT (196 mg, 1.46 mmol) and NEt_3 (0.11 mL, 0.81 mmol). The crude was purified by column chromatography (EtOAc /Hexane, 1:5, then, EtOAc /Hexane, 1:3)

| *Experimental section*

to provide the desired amide **43** as a white waxy solid (573 mg, 66% yield). $R_f = 0.21$ (EtOAc/Hexane, 1:3). $[\alpha]_D^{25} +34.1$ (c 0.7, CHCl_3); **IR** (neat): 3350, 3112, 2918, 2849, 1644, 1540, 1455, 1213, 1044 cm^{-1} ; **^1H NMR** (400 MHz, CDCl_3) δ in ppm: 7.34-7.16 (m, 20H, H-Ar), 6.22 (d, $J_{\text{NH},2} = 9.3$ Hz, 1H, NH), 5.65 (ddd, $J_{5,6a} = 17.0$ Hz, $J_{5,6b} = 10.3$ Hz, $J_{5,4} = 7.3$ Hz, 1H, H-5), 5.09 (ddd, $J_{6a,5} = 17.0$ Hz, $J_{6a,4} = 1.7$ Hz, $J_{\text{gem}} = 1.2$ Hz, 1H, H-6a), 5.04 (ddd, $J_{6b,5} = 10.3$ Hz, $J_{\text{gem}} = 1.2$ Hz, $J_{6b,4} = 0.9$ Hz, 1H, H-6b), 4.87 (d, $J_{\text{gem}} = 11.6$ Hz, 1H, CH_2Ph), 4.80 (d, $J_{1',2'} = 3.6$ Hz, 1H, H-1'), 4.75 (d, $J_{\text{gem}} = 11.7$ Hz, 1H, CH_2Ph), 4.73 (d, $J_{\text{gem}} = 11.5$ Hz, 1H, CH_2Ph), 4.67 (d, $J_{\text{gem}} = 11.7$ Hz, 1H, CH_2Ph), 4.59 (d, $J_{\text{gem}} = 11.5$ Hz, 1H, CH_2Ph), 4.51 (d, $J_{\text{gem}} = 11.6$ Hz, 1H, CH_2Ph), 4.41 (d, $J_{\text{gem}} = 11.8$ Hz, 1H, CH_2Ph), 4.30 (m, 2H, CH_2Ph , H-4), 4.18 (dd, $J_{3,2} = 9.7$ Hz, $J_{3,4} = 6.0$ Hz, 1H, H-3), 4.02 (dd, $J_{1a,1b} = 11.6$ Hz, $J_{1a,2} = 3.0$ Hz, 1H, H-1a), 3.99-3.89 (m, 3H, H-2, H-2', H-5'), 3.84 (m, 2H, H-4', H-3'), 3.54 (dd, $J_{1b,1a} = 11.6$ Hz, $J_{1b,2} = 2.4$ Hz, 1H, H-1b), 3.47 (dd, $J_{6a',6b'} = 9.4$ Hz, $J_{6a',5'} = 7.2$ Hz, 1H, H-6a'), 3.26 (dd, $J_{6b',6a'} = 9.4$ Hz, $J_{6b',5'} = 5.3$ Hz, 1H, H-6b'), 1.98-1.85 (m, 2H, H-2''), 1.45 (m, 2H, CH_2), 1.37 (s, 3H, CH_3), 1.23 (s, 3H, CH_3), 1.18 (m, 44H, CH_2), 0.81 (t, $J_{24'',23''} = 6.9$ Hz, 3H, CH_3); **^{13}C NMR** (100.6 MHz, CDCl_3) δ in ppm: 172.5 (C-1''), 138.8 (C-Ar), 138.4 (C-Ar), 138.4 (C-Ar), 137.6 (C-Ar), 133.3 (C-5), 128.6-127.6 (CH-Ar), 118.4 (C-6), 108.8 (C-ketal), 100.0 (C-1'), 79.0 (C-3'), 79.0 (C-4), 76.9 (C-2'), 76.1 (C-3), 74.8 (C-4'), 74.7 (CH_2Ph), 73.8 (CH_2Ph), 73.6 (CH_2Ph), 73.2 (CH_2Ph), 70.8 (C-1), 70.0 (C-5'), 69.8 (C-6'), 49.1 (C-2), 36.9 (C-2''), 32.1 (CH_2), 29.9 (CH_2), 29.9 (CH_2), 29.8 (CH_2), 29.8 (CH_2), 29.6 (CH_2), 29.6 (CH_2), 29.5 (CH_2), 28.0 (CH_3), 25.8 (CH_3), 25.6 (CH_2), 22.8 (CH_2), 14.3 (CH_3); **HRMS** (TOF ES+) for $[\text{M}+\text{H}]^+$ $\text{C}_{68}\text{H}_{100}\text{NO}_9$ calculated: 1074.7398; found: 1074.7389

**(2*S*,3*S*,4*R*,5*E*)-2-pentacosanoylamino-3,4-*O*-isopropylidene-1-*O*-
(2,3,4,6-tetra-*O*-benzyl- α -D-galactopyranosyl)-7-perfluorodecyl-
hepta-5-en-1,3,4-triol (**5**)**

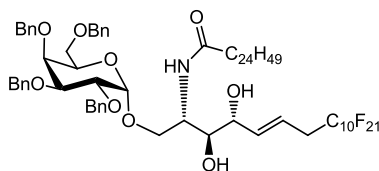


The title compound was prepared following the general procedure for cross-metathesis reaction, starting from **43** (400 mg, 0.37 mmol), perfluorodecylpropene **37** (414 mg, 0.74 mmol), HG-II catalyst (23 mg, 0.037 mmol) and benzoic acid (5 mg, 0.037 mmol) in perfluorotoluene (9 mL). Three subsequent additions of fluoroolefin **37** (414 mg, 0.74 mmol), HG-II catalyst (23 mg, 0.037 mmol) and benzoic acid (5 mg, 0.037 mmol) were performed every 48h during 6 days of reaction. The resulting crude was purified using column chromatography (EtOAc/Hexane, 1:4) to afford the desired fluorinated olefin **5** as an inseparable mixture of isomers as a colourless syrup (481 mg; 81% yield). $R_f = 0.31$ (EtOAc/Hexane, 1:3). $[\alpha]_D^{25} +68.3$ (c 1.0, CHCl₃); IR (neat): 3358, 2919, 2851, 1644, 1543, 1455, 1225, 1042, 805 cm⁻¹; Data shown for major isomer (*E*) ¹H NMR (400 MHz, CDCl₃) δ in ppm: 7.35-7.17 (m, 20H, H-Ar), 6.17 (d, $J_{NH,2} = 9.7$ Hz, 1H, NH), 5.46 (m, 2H, H-5, H-6), 4.87 (d, $J_{gem} = 11.6$ Hz, 1H, CH₂Ph), 4.78-4.74 (m, 3H, H-1', 2 x CH₂Ph), 4.67 (d, $J_{gem} = 11.7$ Hz, 1H, CH₂Ph), 4.57 (d, $J_{gem} = 11.6$ Hz, 1H, CH₂Ph), 4.52 (d, $J_{gem} = 11.6$ Hz, 1H, CH₂Ph), 4.38 (d, $J_{gem} = 11.5$ Hz, 1H, CH₂Ph), 4.29 (d, $J_{gem} = 11.5$ Hz, 1H, CH₂Ph), 4.22 (apt, $J_{4,3} = J_{4,5} = 5.9$ Hz, 1H, H-4), 4.11 (dd, $J_{3,2} = 10.1$ Hz, $J_{3,4} = 5.9$ Hz, 1H, H-3), 4.08 (dd, $J_{1a,1b} = 11.8$ Hz, $J_{1a,2} = 2.4$ Hz, 1H, H-1a), 3.98 (dd, $J_{2',3'} = 10.0$ Hz, $J_{2',1'} = 3.7$ Hz, 1H, H-2'), 3.93 (m, 2H, H-5', H-2), 3.85 (m, 2H, H-4', H-3'), 3.51 (m, 2H, H-1b, H-6a'), 3.27 (dd, $J_{6b',6a'} = 9.5$ Hz, $J_{6b',5} = 4.9$ Hz, 1H, H-6b'), 2.77-2.60 (m, 2H, H-

Experimental section

7a, H-7b), 1.98-1.82 (m, 2H, H-2''), 1.45 (m, 2H, CH₂), 1.37 (s, 3H, CH₃), 1.23 (s, 3H, CH₃), 1.18 (m, 44H, CH₂), 0.81 (t, $J_{25'',24''} = 6.9$ Hz, 3H, CH₃); ¹³C NMR (100.6 MHz, CDCl₃) δ in ppm: 172.4 (C-1''), 138.8 (C-Ar), 138.5 (C-Ar), 138.5 (C-Ar), 137.6 (C-Ar), 133.1 (C-5), 128.7-127.7 (CH-Ar), 120.8 (m, C-6), 109.0 (C-ketal), 100.6 (C-1'), 79.1 (C-3'), 77.8 (C-4), 76.9 (C-2'), 75.9 (C-3), 74.9 (C-4'), 74.9 (CH₂Ph), 73.9 (CH₂Ph), 73.8 (CH₂Ph), 73.3 (CH₂Ph), 71.3 (C-1), 70.3 (C-5'), 70.2 (C-6'), 48.9 (C-2), 36.9 (C-2''), 34.5 (C-7), 32.1 (CH₂), 29.9 (CH₂), 29.8 (CH₂), 29.7 (CH₂), 29.6 (CH₂), 28.1 (CH₃), 25.9 (CH₂), 25.7 (CH₃), 22.9 (CH₂), 14.3 (CH₃); ¹⁹F NMR (376 MHz, CDCl₃) δ in ppm: -80.8 (t, $J_{17,16} = 9.9$ Hz, 3F, CF₃), -113.2 (m, 2 F, CF₂CH₂), -121.8 (m, 10 F, CF₂), -122.7 (m, 2 F, CF₂), -123.1 (m, 2 F, CF₂), -126.2 (m, 2 F, CF₂); HRMS (TOF ES+) for [M+H] C₇₉H₁₀₁F₂₁NO₉ calculated: 1606.7141; found: 1606.7102

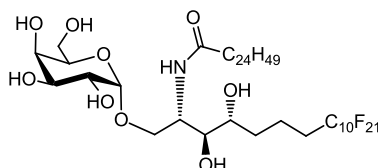
(2S,3S,4R,5E)-2-pentacosanoylamino-3,4-dihydroxy-1-O-(2,3,4,6-tetra-O-benzyl- α -D-galactopyranosyl)-7-perfluorodecyl-hepta-5-en-1,3,4-triol (46)



The title compound was prepared following the general procedure for isopropylidene ketal hydrolysis, starting from **5** (30 mg, 0.019 mmol) and using 4M HCl (24 μ L) in CH₂Cl₂/MeOH (5:1) (0.24 mL). The resulting crude was purified using column chromatography (EtOAc/Hexane, 1:4 to 1:2) to afford **46** as a white waxy solid (21 mg; 70% yield); $R_f = 0.19$ (EtOAc/Hexane, 1:2) $[\alpha]_D^{25} +25.3$ (c 1.8, CHCl₃); IR (neat): 3321, 2918, 2850, 1639, 1208, 1151, 805 cm⁻¹; ¹H NMR (400 MHz, CDCl₃) δ in ppm:

7.33 – 7.17 (m, 20H, H-Ar), 6.25 (d, $J_{NH,2} = 9.0$ Hz, 1H, NH), 5.72 (dd, $J_{5,6} = 15.4$ Hz, $J_{5,4} = 5.0$ Hz, 1H, H-5), 5.64 (m, 1H, H-6), 4.86-4.81 (m, 2H, 2 x CH₂Ph), 4.78 (d, $J_{1',2'} = 3.6$ Hz, 1H, H-1'), 4.70 (bs, 2H, 2 x CH₂Ph), 4.61 (d, $J_{gem} = 11.8$ Hz, 1H, CH₂Ph), 4.49 (d, $J_{gem} = 11.5$ Hz, 1H, CH₂Ph), 4.40 (d, $J_{gem} = 11.6$ Hz, 1H, CH₂Ph), 4.31 (d, $J_{gem} = 11.6$ Hz, 1H, CH₂Ph), 4.11– 3.97 (m, 3H, H-2, H-4, H-2'), 3.89 (m, 1H, H-4'), 3.84 – 3.74 (m, 4H, H-3', H-1a, H-1b, H-5'), 3.60 (d, $J_{OH,3} = 7.6$ Hz, OH), 3.52 – 3.38 (m, 3H, H-3, H-6a', H-6b'), 2.75 (td, $J_{7,6} = 18.4$ Hz, $J_{7,8} = 6.8$ Hz, 2H, H-7a, H-7b), 2.55 (d, $J_{OH,4} = 5.5$ Hz, 1H, OH), 2.02 (m, 2H, H-2''), 1.55 (m, 2H, CH₂), 1.40 - 1.18 (m, 42H, CH₂), 0.81 (t, $J_{25'',24''} = 6.7$ Hz, 3H, CH₃); **¹³C NMR** (100.6 MHz, CDCl₃) δ in ppm: 173.3 (CO), 138.5 (C-Ar), 138.4 (C-Ar), 137.9 (C-Ar), 137.6 (C-Ar), 137.1 (C-5), 128.7 – 127.6 (CH-Ar), 119.3 (C-6), 99.6 (C-1'), 79.3 (C-3'), 76.3 (C-2'), 75.5 (C-3), 74.9 (CH₂Ph), 74.6 (CH₂Ph, C-4'), 73.8 (CH₂Ph), 72.9 (C-4), 72.8 (CH₂Ph), 70.3 (C-5'), 70.0 (C-1), 69.2 (C-6'), 49.9 (C-2), 36.8 (C-2''), 34.7 (C-7), 32.1 (CH₂), 29.9 – 29.5 (CH₂), 25.9 (CH₂), 22.9 (CH₂), 14.3 (CH₃); **¹⁹F NMR** (376 MHz, CDCl₃) δ in ppm: -80.8 (t, $J_{F,F} = 9.7$ Hz, 3F, CF₃), -113.3 (m, 2F, CF₂CH₂), -121.8 (m, 11F, CF₂), -122.3 (m, 2F, CF₂), -123.2 (m, 2F, CF₂), -126.2 (m, 2F, CF₂); **HRMS** (TOF ES+) for [M+Na] C₇₆H₉₆F₂₁NNaO₉ calculated: 1588.6642; Found: 1588.6633.

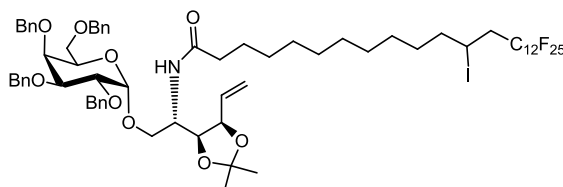
(2S,3S,4R)-2-pentacosanoylamino-3,4-dihydroxy-1-O-(α -D-galactopyranosyl)-7-perfluorodecyl-hepta-1,3,4-triol (2)



| *Experimental section*

The title compound was prepared following the general procedure for hydrogenolysis reaction starting from **46** (20 mg, 0.013 mmol), Pd/C (10 mg), H₂ (5 bar) in EtOAc/MeOH (1:1) (1.3 mL). The resulting crude was purified using column chromatography (CH₂Cl₂/MeOH, 9:1) to afford **2** (15 mg, 75%) as a white waxy solid. $R_f = 0.15$ (CHCl₃ / MeOH, 9:1). $[\alpha]_D^{25} +9.1$ (c 0.3, CHCl₃); **IR** (neat): 3334, 2916, 2850, 1639, 1206, 1151, 1051, 754 cm⁻¹; **¹H NMR** (400 MHz, CDCl₃ / MeOD (1:1)) δ in ppm: 4.82 (d, $J_{1',2'} = 3.8$ Hz, 1H, H-1'), 4.11 (q, $J_{2,1} = J_{2,3} = 4.6$ Hz, 1H, H-2), 3.85 (d, $J_{4',3'} = 3.2$ Hz, 1H, H-4'), 3.80 (dd, $J_{1a,1b} = 10.7$ Hz, $J_{1a,2} = 4.6$ Hz, 1H, H-1a), 3.73-3.58 (m, 6H, H-2', H-3', H-5', H-6', H-1b), 3.46 (m, 2H, H-3, H-4), 2.12 (t, $J_{2'',3''} = 7.6$ Hz, 2H, H-2''), 2.05 (m, 2H, H-7), 1.53 (m, 4H, CH₂), 1.18 (m, 44H, CH₂), 0.79 (t, $J_{25'',24''} = 6.8$ Hz, 3H, CH₃); **¹³C NMR** (100.6 MHz, CDCl₃ / MeOD (1:1)) δ in ppm: 175.4 (CO), 100.4 (C-1'), 74.9 (C-3), 71.9 (C-4), 71.7 (C-3'), 70.9 (C-5'), 70.4 (C-4'), 69.6 (C-2'), 67.7 (C-1), 62.3 (C-6'), 51.1 (C-2), 37.0 (C-2''), 32.6 (CH₂), 32.0 (CH₂), 31.4 (C-7), 30.2-29.8 (CH₂), 27.8 (CH₂), 26.5 (CH₂), 26.4 (CH₂), 23.2 (CH₂), 17.4 (C-6), 14.4 (CH₃); **¹⁹F NMR** (376 MHz, CDCl₃) δ in ppm: -81.5 (t, $J_{F,F} = 9.9$ Hz, 3F, CF₃), -113.5 (m, 2H, CF₂), -122.2 (m, 10F, CF₂), -123.2 (m, 2F, CF₂), -123.5 (m, 2F, CF₂), -126.7 (m, 2F, CF₂); **HRMS** (TOF ES+) for [M+Na] C₄₈H₇₄F₂₁NNaO₉ (m/z): calculated: 1230.4920, found: 1230.4910.

(2S,3S,4R)-2-(12-iodo-13-perfluorododecyl-tridecanoyl)-amino-3,4-O-isopropylidene-1-O-(2,3,4,6-tetra-O-benzyl- α -D-galactopyranosyl)-hex-5-en-1,3,4-triol (47)

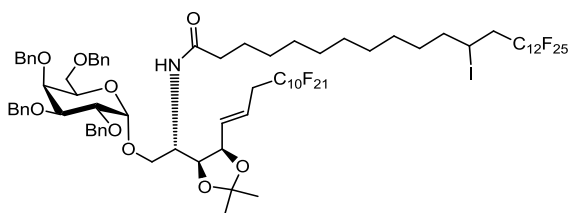


The title compound was prepared following the general procedure for acylation, starting from **42** (340 mg, 0.48 mmol), EDC·HCl (166 mg, 0.86 mmol), 14-perfluorododecyl-1-tridecanoic acid (598 mg, 0.62 mmol), HOBt (117 mg, 0.86 mmol) and NEt₃ (67 μ L, 0.48 mmol). The resulting crude was purified using column chromatography (EtOAc/Hexane, 1:3) to afford compound **47** as a white waxy solid (569 mg; 72% yield); R_f = 0.3 (EtOAc/Hexane, 1:3); $[\alpha]_D^{25}$ +6.5 (c 0.6, CHCl₃); IR (neat): 3324, 2926, 2854, 1650, 1207, 1150, 1056, 749 cm⁻¹; ¹H NMR (400 MHz, CDCl₃) δ in ppm: 7.34-7.17 (m, 20H, H-Ar), 6.19 (d, $J_{NH,2}$ = 9.2 Hz, 1H, NH), 5.66 (ddd, $J_{5,6a}$ = 17.3 Hz, $J_{5,6b}$ = 10.3 Hz, $J_{5,4}$ = 7.3 Hz, 1H, H-5), 5.10 (bd, $J_{6a,5}$ = 17.3 Hz, 1H, H-6a), 5.04 (bd, $J_{5b,6}$ = 10.3 Hz, 1H, H-6b), 4.87 (d, J_{gem} = 11.5 Hz, 1H, CH₂Ph), 4.81 (d, $J_{1',2'}$ = 3.7 Hz, 1H, H-1'), 4.76 (d, J_{gem} = 11.7 Hz, 1H, CH₂Ph), 4.73 (d, J_{gem} = 11.6 Hz, 1H, CH₂Ph), 4.67 (d, J_{gem} = 11.7 Hz, 1H, CH₂Ph), 4.58 (d, J_{gem} = 11.5 Hz, 1H, CH₂Ph), 4.52 (d, J_{gem} = 11.6 Hz, 1H, CH₂Ph), 4.38 (d, J_{gem} = 11.8 Hz, 1H, CH₂Ph), 4.33-4.23 (m, 3H, CH₂Ph, H-12'', H-4), 4.18 (dd, $J_{3,2}$ = 9.6 Hz, $J_{3,4}$ = 6.1 Hz, 1H, H-3), 4.03 (dd, J_{gem} = 11.7 Hz, $J_{1a,2}$ = 3.0 Hz, 1H, H-1a), 3.98-3.87 (m, 3H, H-2, H-2', H-5'), 3.84 (m, 2H, H-3', H-4'), 3.55 (dd, J_{gem} = 11.7 Hz, $J_{1b,2}$ = 2.5 Hz, 1H, H-1b), 3.48 (dd, J_{gem} = 9.4 Hz, $J_{6a',5}$ = 7.2 Hz, 1H, H-6a'), 3.27 (dd, J_{gem} = 9.4 Hz, $J_{6b',5}$ = 5.3 Hz, 1H, H-6b'), 2.86-2.66 (m, 2H, H-13''), 1.98-1.89 (m, 2H, H-2''), 1.75-1.68 (m, 2H, H-11''), 1.45 (m, 2H, CH₂), 1.38 (s, 3H, CH₃), 1.27 (s, 3H, CH₃), 1.23-1.17 (m, 14H, CH₂); ¹³C NMR

Experimental section

(100.6 MHz, CDCl₃) δ in ppm: 172.4 (C-1''), 138.9 (C-Ar), 138.6 (C-Ar), 138.5 (C-Ar), 137.7 (C-Ar), 133.4 (C-5), 128.7-127.7 (CH-Ar), 118.4 (C-6), 108.9 (C-ketal), 100.1 (C-1'), 79.2 (C-3'), 79.0 (C-4), 76.9 (C-2'), 76.2 (C-3), 74.8 (C-4'), 74.8 (CH₂Ph), 73.8 (CH₂Ph), 73.7 (CH₂Ph), 73.3 (CH₂Ph), 71.0 (C-1), 70.2 (C-5'), 69.9 (C-6'), 49.2 (C-2), 41.9 (t, $J_{F,C}$ = 21.0 Hz, C-13''), 40.5 (C-11''), 36.9 (C-2''), 29.8-29.6 (CH₂), 28.7 (CH₂), 28.1 (CH₃), 25.9 (CH₃), 25.7 (CH₂), 21.2 (C-12''); **¹⁹F NMR** (376 MHz, CDCl₃) δ in ppm: -80.8 (t, $J_{F,F}$ = 9.7 Hz, 3F, CF₃), -111.9 (d, J_{gem} = 270.0 Hz, 1F, CF₂CH₂), -114.7 (d, J_{gem} = 270.0 Hz, 1F, CF₂CH₂), -121.8 (m, 12F, CF₂), -122.8 (m, 2F, CF₂), -123.6 (m, 2F, CF₂), -126.2 (m, 2F, CF₂); **HRMS** (TOF ES+) for [M+Na] C₆₈H₇₃F₂₅INO₉Na calculated: 1672.3829; Found: 1672.3829.

(2S,3S,4R,5E)-2-(12-iodo-13-perfluorododecyl-tridecanoyl)-amino-3,4-O-isopropylidene-1-O-(2,3,4,6-tetra-O-benzyl- α -D-galactopyranosyl)-7-perfluorodecyl-hepta-5-en-1,3,4-triol (48)

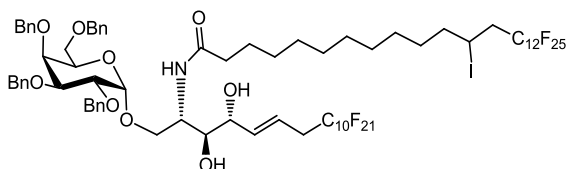


The title compound was prepared following the general procedure for cross-metathesis reaction, starting from **47** (425mg, 0.25 mmol), perfluorodecyl propene **37** (280 mg, 0.5 mmol), Hoveyda-Grubbs 2nd Generation (15 mg, 0.025 mmol) and benzoic acid (3 mg, 0.025 mmol) in perfluorotoluene (6.3 mL). The reaction was allowed to stir for 6 days, adding new portions of perfluorodecyl propene **37**, HG-II and benzoic acid every 48h. The resulting crude was purified using column chromatography (EtOAc/Hexane, 1:4) to afford the desired fluorinated

olefin **48** as an inseparable mixtures of isomers as a white waxy solid (400 mg; 71% yield); $R_f = 0.38$ (EtOAc/Hexane, 1:3); $[\alpha]_D^{25} +9.7$ (c 1.4, CHCl₃); **IR** (neat): 3326, 2926, 2849, 1645, 1208, 1146, 1045, 801 cm⁻¹; Data shown for major isomer (*E*) **¹H NMR** (400 MHz, CDCl₃) δ in ppm: 7.34-7.17 (m, 20H, H-Ar), 6.26 (d, $J_{NH,2} = 9.8$ Hz, 1H, NH), 5.47 (m, 2H, H-5, H-6), 4.88 (d, $J_{gem} = 11.7$ Hz, 1H, CH₂Ph), 4.78-4.73 (m, 3H, H-1', 2 x CH₂Ph), 4.67 (d, $J_{gem} = 11.7$ Hz, 1H, CH₂Ph), 4.58 (d, $J_{gem} = 11.5$ Hz, 1H, CH₂Ph), 4.53 (d, $J_{gem} = 11.6$ Hz, 1H, CH₂Ph), 4.39 (d, $J_{gem} = 11.5$ Hz, 1H, CH₂Ph), 4.29 (d, $J_{gem} = 11.5$ Hz, 1H, CH₂Ph), 4.25 (m, 2H, H-4, H-12"), 4.10 (dd, $J_{3,2} = 10.1$ Hz, $J_{3,4} = 5.9$ Hz, 1H, H-3), 4.06 (dd, $J_{gem} = 12.0$ Hz, $J_{1a,2} = 2.0$ Hz, 1H, H-1a), 3.98 (m, 1H, H-2'), 3.94-3.84 (m, 4H, H-2, H-5', H-3', H-4'), 3.53-3.46 (m, 2H, H-1b, H-6a'), 3.26 (dd, $J_{gem} = 9.4$ Hz, $J_{6b',5} = 5.0$ Hz, 1H, H-6b'), 2.90-2.55 (m, 4H, H-13", H-7), 1.96-1.85 (m, 2H, H-2"), 1.75-1.68 (m, 2H, H-11"), 1.45 (m, 2H, CH₂), 1.37 (s, 3H, CH₃), 1.26 (s, 3H, CH₃), 1.25-1.13 (m, 14H, CH₂); **¹³C NMR** (100.6 MHz, CDCl₃) δ in ppm: 172.4 (C-1"), 138.7 (C-Ar), 138.4 (C-Ar), 138.4 (C-Ar), 137.6 (C-Ar), 132.9 (C-5), 128.7-127.7 (CH-Ar), 120.7 (m, C-6), 109.0 (C-ketal), 100.2 (C-1'), 79.0 (C-3'), 77.7 (C-4), 77.4 (C-2'), 75.8 (C-3), 74.8 (C-4'), 74.7 (CH₂Ph), 73.9 (CH₂Ph), 73.8 (CH₂Ph), 73.2 (CH₂Ph), 71.2 (C-1), 70.2 (C-5'), 70.1 (C-6'), 48.8 (C-2), 41.7 (t, $J_{C,F} = 21.4$ Hz, C-13"), 40.4 (C-11"), 36.8 (C-2"), 34.5 (t, $J_{F,C} = 21.5$ Hz, C-7), 30.4 (CH₂), 29.7-29.5 (CH₂), 28.6 (CH₂), 28.0 (CH₃), 25.8 (CH₃), 25.6 (CH₂), 21.1 (C-12"); **¹⁹F NMR** (376 MHz, CDCl₃) δ in ppm: -80.8 (m, 6F, CF₃), -111.9 (d, $J_{gem} = 270.4$ Hz, 1F, CF₂CH₂), -113.2 (m, 2F, CF₂CH₂) -114.8 (d, $J_{gem} = 270.4$ Hz, 1F, CF₂CH₂), -121.8 (m, 24F, CF₂), -122.8 - -123.2 (m, 6F, CF₂), -123.7 (m, 2F, CF₂), -126.2 (m, 4F, CF₂); **HRMS** (TOF ES+) for [M+Na] C₇₉H₇₄F₄₆INNaO₉ calculated: 2204.3571; Found: 2204.3563.

Experimental section

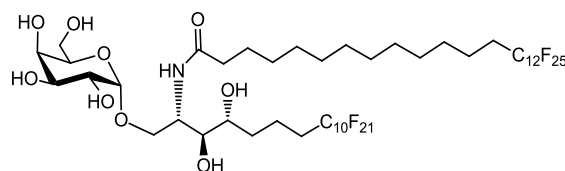
(2S,3S,4R,5E)-2-(12-iodo-13-perfluorododecyl-tridecanoyl)-3,4-dihydroxy-1-O-(2,3,4,6-tetra-O-benzyl- α -D-galactopyranosyl)-7-perfluorodecyl-hepta-5-en-1,3,4-triol (49)



The title compound was prepared following the general procedure for isopropylidene ketal hydrolysis, starting from **48** (31 mg, 0.014 mmol) and using 4M HCl (18 μ L) in DCM/(CF₃)₂CHOH (5:1) (0.18 mL). The resulting crude was purified using column chromatography (EtOAc/Hexane, 1:3) to afford **49** as a white waxy solid (23 mg; 76% yield); R_f = 0.25 (EtOAc/Hexane, 1:2). $[\alpha]_D^{25}$ +11.9 (c 1.0, CHCl₃); **IR** (neat): 3326, 2925, 2854, 1653, 1205, 1150, 754 cm⁻¹; **¹H NMR** (400 MHz, CDCl₃) δ in ppm: 7.32 - 7.18 (m, 20H, H-Ar), 6.26 (d, $J_{NH,2}$ = 8.6 Hz, 1H, NH), 5.71 (dd, $J_{5,6}$ = 15.6 Hz, $J_{5,4}$ = 5.0 Hz, 1H, H-5), 5.61 (m, 1H, H-6), 4.87-4.81 (m, 2H, 2 x CH₂Ph), 4.78 (d, $J_{1',2'}$ = 3.7 Hz, 1H, H-1'), 4.69 (bs, 2H, 2 x CH₂Ph), 4.61 (d, J_{gem} = 11.6 Hz, 1H, CH₂Ph), 4.50 (d, J_{gem} = 11.5 Hz, 1H, CH₂Ph), 4.40 (d, J_{gem} = 11.6 Hz, 1H, CH₂Ph), 4.30 (d, J_{gem} = 11.6 Hz, 1H, CH₂Ph), 4.28 - 4.22 (m, 1H, H-12''), 4.06 (m, 1H, H-2), 4.02 - 3.97 (m, 2H, H-4, H-2'), 3.89 (m, 1H, H-4'), 3.84 - 3.74 (m, 4H, H-3', H-1a, H-1b, H-5'), 3.60 (d, $J_{OH,3}$ = 7.7 Hz, OH), 3.52 - 3.40 (m, 3H, H-3, H-6a', H-6b'), 2.92 - 2.60 (m, 5H, H-7, OH, H-13''), 2.03 (td, $J_{2'',3''}$ = 7.2 Hz, $J_{2'',NH}$ = 2.5 Hz, 2H, H-2''), 1.70 (m, 2H, CH₂), 1.50 (m, 2H, CH₂), 1.35 - 1.10 (m, 14H, CH₂); **¹³C NMR** (100.6 MHz, CDCl₃) δ in ppm: 173.3 (CO), 138.5 (C-Ar), 138.4 (C-Ar), 137.9 (C-Ar), 137.6 (C-Ar), 137.1 (C-5), 128.7 - 127.6 (CH-Ar), 118.8 (C-6), 99.6 (C-1'), 79.3 (C-3'), 76.2 (C-2'), 75.4 (C-3), 74.9 (CH₂Ph), 74.5 (CH₂Ph, C-4'), 73.8 (CH₂Ph), 72.9 (C-4), 72.8 (CH₂Ph), 70.2 (C-5'), 70.0 (C-1), 69.2 (C-6'), 49.9 (C-2), 41.8 (t, J_{C-F}

= 21.0 Hz, C-13"), 40.4 (CH₂), 36.8 (C-2"), 34.6 (t, J_{C-F} = 21.9 Hz, C-7), 29.9 – 29.4 (CH₂), 25.7 (CH₂), 21.1 (C-12"); **¹⁹F NMR** (376 MHz, CDCl₃) δ in ppm: -80.7 (m, 6F, CF₃), -111.8 (d, J_{gem} = 277.4 Hz, 1F, CF₂CH₂), -113.1 (m, 2F, CF₂CH₂) -114.6 (d, J_{gem} = 277.4 Hz, 1F, CF₂CH₂), -121.7 (m, 23F, CF₂), -122.6 (m, 4F, CF₂), -123.0 (m, 2F, CF₂), -123.6 (m, 2F, CF₂), -126.1 (m, 2F, CF₂); **HRMS** (TOF ES+) for [M+Na] C₇₆H₇₀F₄₆INNaO₉ calculated: 2164.3253; Found: 2164.3236.

(2S,3S,4R)-2-(13-perfluorododecyl-tridecanoyl)-3,4-dihydroxy-1-O-(α -D-galactopyranosyl)-7-perfluorodecyl-hepta-1,3,4-triol (3)

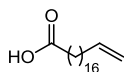


The title compound was prepared following the general procedure for hydrogenolysis reaction starting from **49** (20 mg, 0.009 mmol), Pd/C (7 mg), H₂ (1 atm) in (CF₃)₂CHOH / C₆F₁₄ (1:1) (0.93 mL). The resulting crude was purified using column chromatography (CH₂Cl₂/MeOH, 9:1) to afford **3** (9 mg, 73%) as a white waxy solid. R_f = 0.23 (CHCl₃ / MeOH, 9:1). $[\alpha]_D^{25}$ +13.3 (c 0.4, MeOH/CF₃C₆F₆ (1:1)); **IR** (neat): 3376, 2916, 2851, 1640, 1206, 1153, 1051, 756 cm⁻¹; **¹H NMR** (400 MHz, MeOD / CF₃C₆F₆ (1:1)) δ in ppm: 4.94 (d, $J_{1',2'}$ = 3.3 Hz, 1H, H-1'), 4.23 (q, $J_{2,1}$ = $J_{2,3}$ = 5.9 Hz, 1H, H-2), 3.90 (m, 2H, H-1a, H-4'), 3.83 (m, 2H, H-5', H-3'), 3.78-3.55 (m, 6H, H-2', H-1b, H-6', H-3, H-4), 2.30 (t, $J_{2'',3''}$ = 7.5 Hz, 2H, H-2''), 2.25-1.90 (m, 4H, H-13'', H-7), 1.68 (m, 4H, CH₂), 1.35 (m, 20H, CH₂); **¹³C NMR** (100.6 MHz, MeOD/CF₃C₆F₆ (1:1)) δ in ppm: 176.2 (CO), 101.4 (C-1'), 75.5 (C-3), 72.8 (C-4), 72.7 (C-3'), 71.8 (C-5'), 71.3 (C-4'), 70.5 (C-2'), 68.4 (C-1), 63.0 (C-6'), 52.1 (C-2), 37.5 (C-2''), 32.5 (CH₂),

| *Experimental section*

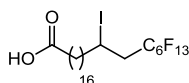
33.2 (CH₂), 32.4 (CH₂), 32.2-31.7 (m, C-13", C-7), 31.0-30.4 (CH₂), 27.3 (CH₂), 23.9 (CH₂), 21.3 (C-12"), 18.1 (C-6).; **HRMS** (TOF ES+) for [M+Na] C₄₈H₄₉F₄₆NNaO₉ calculated: 1680,2570; Found: 1680,2547.

18-nonadecenoic acid (**72**)



The title compound was prepared following the general procedure for Li₂CuCl₄ catalyzed coupling of Grignard reagents with alkyl bromides starting from 8-bromo-1-octene (2.88 g, 15.1 mmol), Mg ribbons (385 mg, 15.8 mmol) in THF (13 mL). In a separate flask, 11-bromo-undecanoic acid **61** (2.0 g, 7.5 mmol) was reacted with ethylmagnesium bromide 1M in THF (8.3 mL, 8.3 mmol) and Li₂CuCl₄ 0.1M in THF (1.5 mL, 0.15 mmol) in THF (8 mL). The crude was concentrated *in vacuo* and purified by column chromatography (EtOAc/Hexane/AcOH, 1:3:0.05) to afford **72** as a white solid (2.3 g, quantitative yield); R_f = 0.44 (EtOAc/Hexane/AcOH, 1:3:0.05); **¹H NMR** (400 MHz, CDCl₃) δ in ppm: 5.81 (ddt, J_{trans} = 16.9 Hz, J_{cis} = 10.2 Hz, J_{2,3} = 6.7 Hz, 1H, H-18), 4.95 (m, 2H, H-19), 2.35 (t, J_{2,3} = 7.5 Hz, 2H, H-2), 2.03 (m, 2H, H-17), 1.60 (m, 2H, CH₂), 1.39-1.25 (m, 28 H, CH₂); **¹³C NMR** (100.6 MHz, CDCl₃) δ in ppm: 179.9 (CO), 139.3 (C-18), 114.1 (C-19), 34.0 (C-2), 33.8 (C-17), 29.7-28.9 (CH₂), 24.7 (CH₂).

18-iodo-19-perfluorohexyl-nonadecanoic acid (**74**)



A mixture of perfluorohexyl iodide (500 mg, 1.12 mmol) and 18-nonadecenoic acid **72** (500 mg, 1.7 mmol) were dissolved in toluene in a three-necked round bottomed flask equipped with a reflux condenser. The mixture was heated to 80 °C and then, AIBN (92 mg, 0.065 mmol) dissolved in 0.5 mL of toluene was injected in three portions over a period in 1.5 h. The reaction mixture was stirred for 24h. After solvent evaporation under reduced pressure, the solid was purified by recrystallization from *n*-hexane to afford 18-iodo-19-perfluorohexyl-heptadecanoic acid **74** (723 mg, 87%) as a white waxy solid; $R_f = 0.45$ (EtOAc/Hexane/AcOH, 1:4:0.25); IR (neat): 2926, 2855, 1708, 1213, 1144, 751 cm^{-1} ; $^1\text{H NMR}$ (400 MHz, CDCl_3) δ in ppm: 4.32 (m, 1H, H-18), 2.98-2.69 (m, 2H, H-19), 2.23 (t, $J_{2,3} = 7.5$ Hz, 2H, H-2), 1.83-1.74 (m, 2H, H-17), 1.62 (m, 2H, CH_2), 1.46-1.20 (m, 26H, CH_2); $^{13}\text{C NMR}$ (100.6 MHz, CDCl_3) δ in ppm: 180.6 (CO), 121.5 (C-F), 41.7 (t, $J_{\text{C,F}} = 21.0$ Hz, C-19), 40.4 (C-17), 39.5 (CH_2), 34.2 (C-2), 29.8-28.6 (CH_2), 24.8 (C-3), 23.5 (CH_2), 21.0 (C-18); $^{19}\text{F NMR}$ (376 MHz, CDCl_3) δ in ppm: -80.9 (t, $J_{25,24} = 9.9$ Hz, 3F, CF_3), -111.9 (d, $J_{\text{gem}} = 269.6$ Hz, 1F, CF_2CH_2), -114.7 (d, $J_{\text{gem}} = 269.6$ Hz, 1F, CF_2CH_2), -121.9 (m, 2F, CF_2), -123.0 (m, 2F, CF_2), -123.8 (m, 2F, CF_2), -126.3 (m, 2F, CF_2); HRMS (TOF ES+) for $[\text{M}+\text{Na}] \text{C}_{25}\text{H}_{36}\text{F}_{13}\text{I}\text{NaO}_2$: calculated: 765.1445; found: 765.1424.

9-bromo-nonanal (**64**)¹³



The title compound was prepared following the general procedure for Swern oxidation starting from oxalyl chloride (1.5 mL, 17.5 mmol) in CH₂Cl₂ (9.2 mL), DMSO (1.8 mL, 25.7 mmol) in CH₂Cl₂ (10.2 mL), 9-bromo-1-nonanol (2.6 g, 11.7 mmol) in CH₂Cl₂ (52.0 mL) and NEt₃ (6.5 mL, 46.8 mmol). The crude was concentrated *in vacuo* and purified by column chromatography (EtOAc/Hexane/ 1:3) to afford **64** as a colorless oil (2.26 g, 88 % yield); R_f = 0.56 (EtOAc/Hexane 1:3)

11-bromo-undecanal (**65**)¹⁴

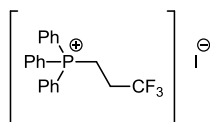


The title compound was prepared following the general procedure for Swern oxidation starting from oxalyl chloride (1.5 mL, 17.9 mmol) in CH₂Cl₂ (9.3 mL), DMSO (1.9 mL, 26.2 mmol) in CH₂Cl₂ (10.5 mL), 11-bromo-1-undecanol (3 g, 11.9 mmol) in CH₂Cl₂ (52.4 mL) and NEt₃ (6.6 mL, 47.6 mmol). The crude was concentrated *in vacuo* and purified by column chromatography (EtOAc/Hexane/ 1:3) to afford **65** as a colorless oil (2.66 g, 92 % yield); R_f = 0.56 (EtOAc/Hexane 1:3)

¹³ Yuasa, Y.; Tsuruta, H. *Flavour Fragr. J.* **2004**, *19*, 199–204.

¹⁴ Houghton, S. R.; Furst, L.; Boddy, C. N. *J. Org. Chem.* **2009**, *74*, 1454–1463.

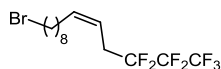
3,3,3-trifluoropropyltriphenylphosphonium iodide (**66**)¹⁵



The title compound was prepared following the general procedure for preparation of fluorinated phosphonium salts starting from 1,1,1-trifluoro-4-iodopropane (5 g, 22.3 mmol) and triphenylphosphine (17.5 g, 66.9 mmol) in toluene (18 mL). The solution was cooled and the white precipitated was filtered, washed with diethyl ether and dried *in vacuo* to afford **66** as a white solid (6.5 g, 60 % yield).

¹H NMR (400 MHz, CDCl₃) δ in ppm: 7.67-7.54 (m, 15H, H-Ar.), 3.70 (m, 2H, H-2), 2.38 (m, 2H, H-3); **¹³C NMR** (100.6 MHz, CDCl₃): δ in ppm: 135.2 (C-Ar), 133.1 (m, CH-Ar), 130.4 (d, $J_{C,P}$ = 12.9 Hz, CH-Ar), 124.8 (dq, $J_{C,F}$ = 277.6 Hz, $J_{C,P}$ = 17.3 Hz, CF₃), 115.8 (d, $J_{C,P}$ = 87.4 Hz, CH-Ar), 27.0 (q, $J_{C,F}$ = 31.6 Hz, C-3), 17.0 (d, $J_{C,P}$ = 56.7 Hz, C-2); **¹⁹F NMR** (376 MHz, CDCl₃) δ in ppm: -65.9 (t, $J_{F,H}$ = 9.9 Hz, 3F, CF₃); **³¹P NMR** (162 MHz, CDCl₃) δ in ppm: 24.2 (s).

(9Z)-1-bromo-12,12,13,13,14,14,14-heptafluoro-tetradec-8-ene (**75**)



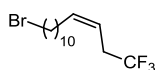
The title compound was prepared following the general procedure for Wittig reaction starting from 3,3,4,4,5,5,5-heptafluoropentyl triphenylphosphonium iodide **28** (4.4 g, 7.5 mmol) and KHMDS 1.0M solution (7.2 mL, 7.2 mmol) in THF (13 mL) and 9-bromo-nonanal **64** (1.3

¹⁵ Liu, Z.; Kumar, K. *Synthesis* **2010**, 1905-1908

| *Experimental section*

g, 5.8 mmol) in THF (13 mL). The crude was concentrated *in vacuo* and purified by column chromatography (Hexane) to afford a 1:1 mixture of **75** and the corresponding iodide **76**. The crude was then dissolved in THF (74 mL), TBAB (7.4 g, 23 mmol) was added and the mixture was allowed to stir overnight at rt. The crude was filtered through a silica pad affording pure **75** as a colorless oil (1.77g, 77% yield); $R_f = 0.38$ (Hexane); **IR** (neat): 2929, 2857, 1217, 1170, 1111, 740 cm^{-1} ; **$^1\text{H NMR}$** (400 MHz, CDCl_3) δ in ppm: 5.75 (dt, $J_{9,10} = 10.7$ Hz, $J_{9,8} = 7.5$ Hz, $J_{9,11} = 1.6$ Hz, 1H, H-9), 5.41 (m, 1H, H-10), 3.41 (t, $J_{2,3} = 6.9$ Hz, 2H, H-1), 2.84 (td, $J_{H,F} = 18.3$ Hz, $J_{11'',10''} = 6.7$ Hz, 2H, H-11), 2.05 (q, $J_{8,9} = J_{8,7} = 7.2$ Hz, 2H, H-8), 1.85 (m, 2H, H-2), 1.45-1.26 (m, 10H, CH_2); **$^{13}\text{C NMR}$** (100.6 MHz, CDCl_3) δ in ppm: 137.3 (C-9), 115.5 (t, $J_{C,F} = 4.3$ Hz, C-10), 34.0 (C-2), 33.0 (C-3), 29.4 (CH_2), 29.3 (t, $J_{C,F} = 22.7$ Hz, C-11), 29.2 (CH_2), 29.2 (CH_2), 28.8 (CH_2), 28.3 (CH_2), 27.5 (CH_2); **$^{19}\text{F NMR}$** (376 MHz, CDCl_3) δ in ppm: -80.6 (t, $J_{14,13} = 9.8$ Hz, 3F, CF_3), -114.2 (m, 2F, CF_2CH_2), -127.5 (m, 2F, CF_2).

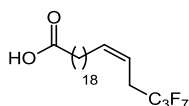
(11Z)-1-bromo-14,14,14-trifluoro-tetradec-10-ene (77)



The title compound was prepared following the general procedure for Wittig reaction starting from (5,5,5-trifluoropentyl) triphenylphosphonium iodide **66** (5.1 g, 10.5 mmol), KHMDS 1.0M solution (10.0 mL, 10.0 mmol) in THF (18.5 mL) and 11-bromo-undecanal **65** (2 g, 8.1 mmol) in THF (18.5 mL). The crude was concentrated *in vacuo* and purified by column chromatography (Hexane) to afford a 87:13 mixture of **77** with the corresponding iodide **78**. The mixture was then dissolved in THF (85 mL), TBAB (10.4 g, 32.4 mmol)

was added and was allowed to stir overnight at rt. The crude was filtered through a silica pad affording pure **77** as a colorless oil (2.3g, 87% yield); Only *Z* isomer was observed; $R_f = 0.38$ (Hexane); **IR** (neat): 2925, 2854, 1250, 1132, 1089, 722 cm^{-1} ; **$^1\text{H NMR}$** (400 MHz, CDCl_3) δ in ppm: 5.71 (m, 1H, H-11), 5.37 (dt, $J_{12,11} = 10.7$ Hz, $J_{12,13} = 7.3$ Hz, $J_{12,10} = 1.7$ Hz, 1H, H-12), 3.40 (t, $J_{2,3} = 6.9$ Hz, 2H, H-1), 2.84 (m, 2H, H-13), 2.03 (q, $J_{10,11} = J_{10,9} = 6.9$ Hz, 2H, H-10), 1.85 (m, 2H, H-2), 1.45-1.27 (m, 14H, CH_2); **$^{13}\text{C NMR}$** (100.6 MHz, CDCl_3) δ in ppm: 136.8 (C-11), 126.4 (q, $J_{\text{C,F}} = 276.5$ Hz, CF_3), 116.8 (q, $J_{\text{C,F}} = 3.4$ Hz, C-12), 34.1 (C-2), 33.0 (C-3), 32.3 (q, $J_{\text{C,F}} = 29.5$ Hz, C-13), 29.6 (CH_2), 29.6 (CH_2), 29.5 (CH_2), 29.3 (CH_2), 29.3 (CH_2), 28.9 (CH_2), 28.3 (CH_2), 27.5 (CH_2); **$^{19}\text{F NMR}$** (376 MHz, CDCl_3) δ in ppm: - 66.3 (t, $J_{\text{F,H}} = 10.9$ Hz, 3F, CF_3).

(20Z)-23,23,24,24,25,25,25-heptafluoropentacos-20-enoic acid (59).

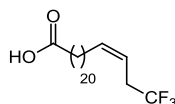


The title compound was prepared following the general procedure for Li_2CuCl_4 catalyzed coupling of Grignard reagents with alkyl bromides starting from **75** (754 mg, 1.9 mmol) and using Mg ribbons (48 mg, 2.0 mmol) in THF (1.7 mL). In a separate flask, 11-bromoundecanoic acid **61** (250 mg, 0.9 mmol) was reacted with ethylmagnesium bromide 1M in THF (1.0 mL, 1.0 mmol) and Li_2CuCl_4 0.1M in THF (0.2 mL, 0.02 mmol) in THF (1 mL). The crude was concentrated *in vacuo* and purified by column chromatography (EtOAc/Hexane/AcOH, 1:3:0.05) to afford **59** as a white waxy solid (450 mg, 95 % yield); $R_f = 0.44$ (EtOAc/Hexane/AcOH, 1:3:0.05); **IR** (neat): 3021, 2917, 2849, 1705, 1214, 1113, 753 cm^{-1} ; **$^1\text{H NMR}$** (400 MHz, CDCl_3) δ in ppm: 5.75 (m, 1H,

| *Experimental section*

H-20), 5.41 (m, 1H, H-21), 2.84 (td, $J_{H,F} = 18.4$ Hz, $J_{22,21} = 7.0$ Hz, 2H, H-22), 2.34 (t, $J_{2,3} = 7.5$ Hz, 2H, H-2), 2.04 (q, $J_{19,20} = J_{19,18} = 6.8$ Hz, 2H, H-19), 1.63 (m, 2H, H-3), 1.42-1.20 (m, 30H, CH₂); **¹³C NMR** (100.6 MHz, CDCl₃) δ in ppm: 180.6 (CO), 137.4 (C-20), 115.4 (t, $J_{C,F} = 4.2$ Hz, C-21), 34.3 (C-2), 29.9-29.2 (CH₂), 29.3 (t, $J_{C,F} = 22.2$ Hz, C-22), 27.6 (C-19), 24.9 (C-3); **¹⁹F NMR** (376 MHz, CDCl₃) δ in ppm: -80.6 (t, $J_{25,24} = 9.7$ Hz, 3F, CF₃), -114.2 (m, 2F, CF₂CH₂), -127.5 (m, 2F, CF₂).

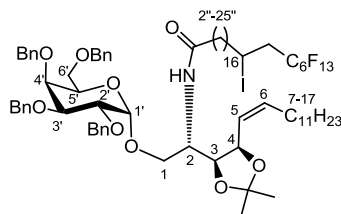
(22Z)-25,25,25-trifluoro-pentacos-22-enoic acid (60).



The title compound was prepared following the general procedure for Li₂CuCl₄ catalyzed coupling of Grignard reagents with alkyl bromides starting from **77** (742 mg, 2.3 mmol) and using Mg ribbons (57 mg, 2.4 mmol) in THF (2 mL). In a separate flask, 11-bromoundecanoic acid **61** (300 mg, 1.1 mmol) was reacted with ethylmagnesium bromide 1M in THF (1.2 mL, 1.2 mmol) and Li₂CuCl₄ 0.1M in THF (0.2 mL, 0.02 mmol) in THF (1.2 mL). The crude was concentrated *in vacuo* and purified by column chromatography (EtOAc/Hexane/AcOH, 1:3:0.05) to afford **60** as a white waxy solid (552 mg, 96 % yield); $R_f = 0.44$ (EtOAc/Hexane/AcOH, 1:3:0.05); **IR** (neat): 3031, 2917, 2848, 1701, 1250, 1159, 843 cm⁻¹; **¹H NMR** (400 MHz, CDCl₃) δ in ppm: 5.71 (m, 1H, H-22), 5.37 (m, 1H, H-23), 2.84 (td, $J_{H,F} = 18.4$ Hz, $J_{24,23} = 7.0$ Hz, 2H, H-24), 2.35 (t, $J_{2,3} = 7.5$ Hz, 1H, H-2), 2.04 (q, $J_{21,22} = J_{21,20} = 6.8$ Hz, 2H, H-21), 1.63 (m, 2H, H-3), 1.38-1.20 (m, 34H, CH₂); **¹³C NMR** (100.6 MHz, CDCl₃) δ in ppm: 180.1 (CO), 136.9 (C-22), 126.4 (t, $J_{C,F} = 276.5$ Hz, CF₃), 116.8 (q, $J_{C,F} = 3.4$ Hz, C-23), 34.2 (C-2), 32.3 (q, $J_{C,F} = 29.5$ Hz, C-

24), 29.9-29.2 (CH₂), 27.5 (C-19), 24.8 (C-3); ¹⁹F NMR (376 MHz, CDCl₃) δ in ppm: -66.3 (t, *J*_{F,H} = 10.9 Hz, 3F, CF₃); HRMS (TOF ES+) for [M+Na]⁺ C₂₅H₄₅F₃NaO₂ (m/z): calculated: 457.3264; found: 457.3232.

(2S,3S,4R,5Z)-2-(18-iodo-19-perfluorohexyltridecanoyl)-amino-3,4-O-isopropylidene-1-O-(2,3,4,6-tetra-O-benzyl-α-D-galactopyranosyl)-heptadec-5-en-1,3,4-triol (79)

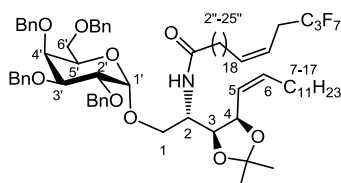


The title compound was prepared following the general procedure for *N*-acylation, starting from amine **7** (350 mg, 0.41 mmol), EDC·HCl (141 mg, 0.74 mmol), 19-perfluorohexyl-18-iodo-1-tridecanoic acid **74** (393 mg, 0.53 mmol), HOBt (99 mg, 0.74 mmol) and NEt₃ (57 μL, 0.41 mmol). The crude was purified by column chromatography (EtOAc / Hexane, 1:4) to provide the desired amide **79** as a white gel (519 mg, 80% yield); *R*_f = 0.34 (EtOAc/Hexane, 1:3). [α]_D²⁵ +8.7 (c 1.0, CHCl₃); IR (neat): 3311, 2923, 2853, 1652, 1455, 1237, 1206, 1145, 1056, 734 cm⁻¹; ¹H NMR (400 MHz, CDCl₃) δ in ppm: 7.33-7.16 (m, 20H, HAr), 5.96 (d, *J*_{NH,2} = 9.0 Hz, 1H, NH), 5.50 (m, 1H, H-6), 5.34 (m, 1H, H-5), 4.86 (d, *J*_{gem} = 11.7 Hz, 1H, CH₂Ph), 4.85 (d, *J*_{1,2'} = 3.7 Hz, 1H, H-1'), 4.79 (m, 1H, H-4), 4.74 (d, *J*_{gem} = 11.6 Hz, 1H, CH₂Ph), 4.73 (d, *J*_{gem} = 11.5 Hz, 1H, CH₂Ph), 4.67 (d, *J*_{gem} = 11.6 Hz, 1H, CH₂Ph), 4.61 (d, *J*_{gem} = 11.5 Hz, 1H, CH₂Ph), 4.49 (d, *J*_{gem} = 11.7 Hz, 1H, CH₂Ph), 4.42 (d, *J*_{gem} = 12.0 Hz, 1H, CH₂Ph), 4.32 (d, *J*_{gem} = 12.0 Hz, 1H, CH₂Ph), 4.25 (m, 1H, H-12''), 4.17 (dd, *J*_{3,2} = 9.0 Hz, *J*_{3,4} = 6.0 Hz, 1H, H-3), 4.02 (m, 1H, H-2),

Experimental section

3.97 (dd, $J_{2',3'} = 9.9$ Hz, $J_{2',1'} = 3.7$ Hz, 1H, H-2'), 3.93 (dd, $J_{gem} = 11.4$ Hz, $J_{1a,2} = 3.6$ Hz, 1H, H-1a), 3.91-3.86 (m, 2H, H-4', H-5'), 3.83 (dd, $J_{3',2'} = 9.9$ Hz, $J_{3',4'} = 2.8$ Hz, 1H, H-3'), 3.58 (dd, $J_{gem} = 11.4$ Hz, $J_{1b,2} = 2.7$ Hz, 1H, H-1b), 3.44 (dd, $J_{gem} = 9.3$ Hz, $J_{6a',5} = 6.5$ Hz, 1H, H-6a'), 3.33 (dd, $J_{gem} = 9.3$ Hz, $J_{6b',5} = 6.1$ Hz, 1H, H-6b'), 2.92-2.62 (m, 2H, H-19''), 2.01-1.88 (m, 3H, H-7a, H2''), 1.86-1.64 (m, 3H, H-7b, H-17''), 1.48 (m, 2H, CH₂), 1.38 (s, 3H, CH₃), 1.28 (s, 3H, CH₃), 1.30-1.10 (m, 44H, CH₂), 0.81 (t, $J_{17,16} = 6.9$ Hz, 3H, CH₃); ¹³C NMR (100.6 MHz, CDCl₃) δ in ppm: 172.4 (C=O), 138.9 (C-Ar), 138.6 (C-Ar), 138.5 (C-Ar), 137.7 (C-Ar), 135.1 (C-6), 128.6-127.6 (CH, Ar), 124.4 (C-5), 108.5 (C-ketal), 99.5 (C-1'), 79.1 (C-3'), 77.2 (C-2'), 76.0 (C-3), 74.8 (CH₂Ph), 74.8 (C-4'), 73.5 (CH₂Ph), 73.4 (CH₂Ph), 73.1 (CH₂Ph), 72.9 (C-4), 69.7 (C-1), 69.7 (C-5''), 69.2 (C-6''), 49.3 (C-2), 42.0 (t, $J_{C-F} = 20.2$ Hz, C-19''), 40.5 (C-11''), 36.7 (C-2''), 31.9 (CH₂), 29.7-29.4 (CH₂), 28.7 (CH₂), 28.1 (CH₃), 27.8 (C-7), 25.8 (CH₂), 25.6 (CH₃), 22.7 (CH₂), 21.0 (C-18''), 14.3 (CH₃); ¹⁹F NMR (376 MHz, CDCl₃) δ in ppm: -80.8 (t, $J_{25'',24''} = 9.9$ Hz, 3F, CF₃), -111.8 (d, $J_{gem} = 260.0$ Hz, 1F, CF₂CH₂), -114.7 (d, $J_{gem} = 260.0$ Hz, 1F, CF₂CH₂), -121.8 (m, 2F, CF₂), -122.9 (m, 2F, CF₂), -123.7 (m, 2F, CF₂), -126.2 (m, 2F, CF₂); HRMS (TOF ES+) for [M+Na]⁺ C₇₉H₁₀₇F₁₃INNaO₉ (m/z): calculated: 1610,6675; found: 1610,6668.

(2S,3S,4R,5Z)-2-((20Z)-23,23,24,24,25,25,25-heptafluoropentacos-20-enoyl)-amino-3,4-O-isopropylidene-1-O-(2,3,4,6-tetra-O-benzyl- α -D-galactopyranosyl)-heptadec-5-en-1,3,4-triol (80)

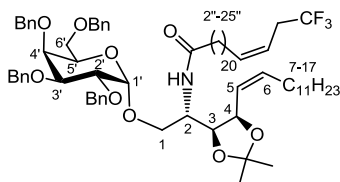


The title compound was prepared following the general procedure for *N*-acylation, starting from amine **7** (192 mg, 0.22 mmol), EDC·HCl (77 mg, 0.40 mmol), 22-heptafluoropropyltetracosanoic acid **59** (146 mg, 0.29 mmol), HOBT (54 mg, 0.40 mmol) and NEt₃ (31 μL, 0.22 mmol). The crude was purified by column chromatography (EtOAc / Hexane, 1:4) to provide the desired amide **80** as a white gel (268 mg, 89% yield); R_f = 0.33 (EtOAc/Hexane, 1:3). [α]_D²⁵ +13.7 (c 1.5, CHCl₃); IR (neat): 3316, 2922, 2853, 1652, 1456, 1100, 1057, 736 cm⁻¹; ¹H NMR (400 MHz, CDCl₃) δ in ppm: 7.33-7.16 (m, 20H, HAr), 6.07 (d, J_{NH,2} = 9.1 Hz, 1H, NH), 5.68 (dt, J_{20'',21''} = 10.5 Hz, J_{20'',19''} = 7.3 Hz, J_{20'',22''} = 1.5 Hz, 1H, H-20''), 5.49 (m, 1H, H-6), 5.39-5.27 (m, 2H, H-5, H-21''), 4.86 (m, 1H, H-1'), 4.84 (d, J_{gem} = 11.6 Hz, 1H, CH₂Ph) 4.77 (dd, J_{4,5} = 9.4 Hz, J_{4,3} = 5.9 Hz, 1H, H-4), 4.73 (m, 2H, 2 x CH₂Ph), 4.66 (d, J_{gem} = 11.7 Hz, 1H, CH₂Ph), 4.60 (d, J_{gem} = 11.5 Hz, 1H, CH₂Ph), 4.49 (d, J_{gem} = 11.6 Hz, 1H, CH₂Ph), 4.42 (d, J_{gem} = 12.0 Hz, 1H, CH₂Ph), 4.30 (d, J_{gem} = 12.0 Hz, 1H, CH₂Ph), 4.16 (dd, J_{3,2} = 9.1 Hz, J_{3,4} = 6.0 Hz, 1H, H-3), 4.02 (m, 1H, H-2), 3.97 (dd, J_{2',3'} = 10.0 Hz, J_{2',1'} = 3.7 Hz, 1H, H-2'), 3.92 (dd, J_{gem} = 11.4 Hz, J_{1a,2} = 3.5 Hz, 1H, H-1a), 3.89-3.86 (m, 2H, H-4', H-5'), 3.83 (dd, J_{3',2'} = 10.0 Hz, J_{3',4'} = 2.8 Hz, 1H, H-3'), 3.58 (dd, J_{gem} = 11.4 Hz, J_{1b,2} = 2.5 Hz, 1H, H-1b), 3.43 (dd, J_{gem} = 9.2 Hz, J_{6a',5'} = 6.6 Hz, 1H, H-6a'), 3.33 (dd, J_{gem} = 9.2 Hz, J_{6b',5'} = 6.3 Hz, 1H, H-6b'), 2.76 (td, J_{H,F} = 18.6 Hz, J_{22'',21''} = 7.3 Hz, 2H, H-22''), 1.99-1.77 (m, 6H, H-7, H2'', H-19''), 1.46 (m, 2H, H-3''), 1.37 (s, 3H, CH₃), 1.28 (s, 3H, CH₃), 1.33-1.12 (m, 48H, CH₂), 0.80 (t, J_{17,16} = 6.9 Hz, 3H, CH₃); ¹³C NMR (100.6 MHz, CDCl₃) δ in ppm: 172.4 (C=O), 138.8 (C-Ar), 138.5 (C-Ar), 138.5 (C-Ar), 137.7 (C-Ar), 137.4 (C-20''), 135.1 (C-6), 128.6-127.6 (CH, Ar), 124.4 (C-5), 115.4 (t, J_{C,F} = 4.2 Hz, C-21''), 108.4 (C-ketal), 99.5 (C-1'), 79.0 (C-3'), 76.9 (C-2'), 76.1 (C-3), 74.8 (CH₂Ph), 74.7 (C-4'), 73.6 (CH₂Ph), 73.5 (CH₂Ph), 73.2 (CH₂Ph), 73.0 (C-4), 69.9 (C-1), 69.8 (C-5'), 69.2 (C-6'), 49.2 (C-2), 36.9

Experimental section

(C-2"), 32.0 (CH₂), 29.9-29.0 (CH₂, C-22"), 28.1 (CH₃), 27.8 (C-7), 27.5 (C-21"), 25.8 (CH₂), 25.6 (CH₃), 22.8 (CH₂), 14.3 (CH₃); ¹⁹F NMR (376 MHz, CDCl₃) δ in ppm: -80.6 (t, *J*_{25",24"} = 9.7 Hz, 3F, CF₃), -114.2 (m, 2F, CF₂CH₂), -127.5 (m, 2F, CF₂); **HRMS** (TOF ES+) for [M+H]⁺ C₇₉H₁₁₃F₇NO₉ (m/z): calculated: 1352,8298; found: 1352.8251.

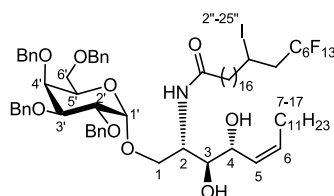
(2S,3S,4R,5Z)-2-((22Z)-25,25,25-trifluoropentacos-22-enoyl)-amino-3,4-O-isopropylidene-1-O-(2,3,4,6-tetra-O-benzyl- α -D-galactopyranosyl)-heptadec-5-en-1,3,4-triol (81)



The title compound was prepared following the general procedure for *N*-acylation, starting from amine **7** (120 mg, 0.14 mmol), EDC·HCl (48 mg, 0.25 mmol), 24-trifluoromethyltetracosanoic acid **60** (79 mg, 0.18 mmol), HOBT (49 mg, 0.25 mmol) and NEt₃ (20 μL, 0.14 mmol). The crude was purified by column chromatography (EtOAc / Hexane, 1:4) to provide the desired amide **81** as a white gel (162 mg, 90% yield); *R*_f = 0.31 (EtOAc/Hexane, 1:3). [α]_D²⁵ +13.9 (c 1.6, CHCl₃); **IR** (neat): 3337, 2922, 2852, 1652, 1456, 1251, 1132, 1094, 1055, 733 cm⁻¹; **¹H NMR** (400 MHz, CDCl₃) δ in ppm: 7.33-7.16 (m, 20H, HAR), 6.08 (d, *J*_{NH,2} = 9.1 Hz, 1H, NH), 5.64 (m, 1H, H-22"), 5.49 (dt, *J*_{6,5} = 10.2 Hz, *J*_{6,7} = 7.3 Hz, 1H, H-6), 5.37-5.27 (m, 2H, H-5, H-23"), 4.86 (d, *J*_{gem} = 11.6 Hz, 1H, CH₂Ph), 4.85 (m, 1H, H-1'), 4.77 (dd, *J*_{4,5} = 9.6 Hz, *J*_{4,3} = 6.0 Hz, 1H, H-4), 4.73 (m, 2H, 2 x CH₂Ph), 4.67 (d, *J*_{gem} = 11.7 Hz, 1H, CH₂Ph), 4.60 (d, *J*_{gem} = 11.4 Hz, 1H, CH₂Ph), 4.50 (d, *J*_{gem} = 11.6 Hz, 1H, CH₂Ph), 4.43 (d,

$J_{gem} = 12.0$ Hz, 1H, CH₂Ph), 4.30 (d, $J_{gem} = 12.0$ Hz, 1H, CH₂Ph), 4.16 (dd, $J_{3,2} = 9.1$ Hz, $J_{3,4} = 6.0$ Hz, 1H, H-3), 4.02 (m, 1H, H-2), 3.97 (dd, $J_{2',3'} = 10.0$ Hz, $J_{2',1'} = 3.7$ Hz, 1H, H-2'), 3.92 (dd, $J_{gem} = 11.3$ Hz, $J_{1a,2} = 3.4$ Hz, 1H, H-1a), 3.89-3.86 (m, 2H, H-4', H-5'), 3.83 (dd, $J_{3',2'} = 10.0$ Hz, $J_{3',4'} = 2.7$ Hz, 1H, H-3'), 3.58 (dd, $J_{gem} = 11.3$ Hz, $J_{1b,2} = 2.3$ Hz, 1H, H-1b), 3.43 (dd, $J_{gem} = 9.2$ Hz, $J_{6a',5} = 6.7$ Hz, 1H, H-6a'), 3.33 (dd, $J_{gem} = 9.2$ Hz, $J_{6b',5} = 6.3$ Hz, 1H, H-6b'), 2.81-2.71 (m, 2H, H-24''), 2.02-1.76 (m, 6H, H-7, H2'', H-21''), 1.45 (m, 2H, H-3''), 1.38 (s, 3H, CH₃), 1.29 (s, 3H, CH₃), 1.33-1.12 (m, 52H, CH₂), 0.81 (t, $J_{17,16} = 6.9$ Hz, 3H, CH₃); **¹³C NMR** (100.6 MHz, CDCl₃) δ in ppm: 172.5 (C=O), 138.8 (C-Ar), 138.5 (C-Ar), 138.5 (C-Ar), 137.7 (C-Ar), 136.9 (C-22''), 135.1 (C-6), 128.6-127.6 (CH, Ar), 126.4 (q, $J_{C,F} = 276.4$ Hz, CF₃), 124.3 (C-5), 116.8 (q, $J_{C,F} = 3.4$ Hz, C-23''), 108.5 (C-ketal), 99.5 (C-1'), 79.0 (C-3'), 76.9 (C-2'), 76.1 (C-3), 74.8 (CH₂Ph), 74.7 (C-4'), 73.6 (CH₂Ph), 73.5 (CH₂Ph), 73.2 (CH₂Ph), 73.0 (C-4), 69.9 (C-1), 69.8 (C-5'), 69.2 (C-6'), 49.2 (C-2), 36.9 (C-2''), 32.3 (q, $J_{C,F} = 29.5$ Hz, C-24''), 32.1 (CH₂), 29.9-29.3 (CH₂), 28.1 (CH₃), 27.8 (C-7), 27.5 (C-21''), 25.8 (CH₂), 25.6 (CH₃), 22.8 (CH₂), 14.3 (CH₃); **¹⁹F NMR** (376 MHz, CDCl₃) δ in ppm: -66.2 (t, $J_{F,H} = 10.9$ Hz, 3F, CF₃); **HRMS** (TOF ES+) for [M+H]⁺ C₇₉H₁₁₇F₃NO₉ (m/z): calculated: 1280,8675; found: 1280.8657

(2S,3S,4R,5Z)-2-(18-iodo-19-perfluorohexyl-tridecanoyl)-amino-3,4-dihydroxy-1-O-(2,3,4,6-tetra-O-benzyl- α -D-galactopyranosyl)-heptadec-5-en-1,3,4-triol (82)

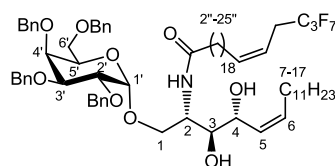


| *Experimental section*

The title compound was prepared following the general procedure for isopropylidene ketal hydrolysis, starting from amide **79** (259 mg, 0.16 mmol) and using 4M HCl (0.2 mL) in a mixture of CH₂Cl₂/MeOH (5:1) (2 mL). The reaction was allowed to stir for 24 h and was stopped by adding a saturated aqueous solution of Na₂CO₃. The crude was purified by column chromatography (EtOAc/Hexane, 1:3) to provide the desired amide **82** as a white waxy solid (173 mg, 70 % yield). $R_f = 0.17$ (EtOAc/Hexane, 1:2). $[\alpha]_D^{25} +14.7$ (c 1.6, CHCl₃); IR (neat): 3325, 2919, 2850, 1643, 1455, 1236, 1206, 1143, 1041, 729 cm⁻¹; **¹H NMR** (400 MHz, CDCl₃) δ in ppm: 7.33-7.16 (m, 20H, HAR), 6.30 (d, $J_{NH,2} = 8.3$ Hz, 1H, NH), 5.51 (dt, $J_{6,5} = 10.8$ Hz, $J_{6,7} = 7.4$ Hz, 1H, H-6), 5.34 (m, 1H, H-5), 4.84 (d, $J_{gem} = 11.5$ Hz, 1H, CH₂Ph), 4.81 (d, $J_{1',2'} = 3.8$ Hz, 1H, H-1'), 4.78 (d, $J_{gem} = 11.8$ Hz, 1H, CH₂Ph), 4.71 (d, $J_{gem} = 11.7$ Hz, 1H, CH₂Ph), 4.66 (d, $J_{gem} = 11.7$ Hz, 1H, CH₂Ph), 4.63 (d, $J_{gem} = 11.8$ Hz, 1H, CH₂Ph), 4.48 (d, $J_{gem} = 11.5$ Hz, 1H, CH₂Ph), 4.40 (d, $J_{gem} = 11.6$ Hz, 1H, CH₂Ph), 4.37 (m, 1H, H-4), 4.30 (d, $J_{gem} = 11.6$ Hz, 1H, CH₂Ph), 4.25 (m, 1H, H-18"), 4.08 (m, 1H, H-2), 3.97 (dd, $J_{2',3'} = 10.0$ Hz, $J_{2',1'} = 3.8$ Hz, 1H, H-2'), 3.88-3.78 (m, 5H, H-3', H-4', H-5', H-6a', H-1a), 3.49 (m, 1H, H-3), 3.47-3.39 (m, 2H, H-6b', H-1b), 2.92-2.63 (m, 2H, H-19"), 2.03-1.87 (m, 4H, H-2", H-7), 1.80-1.64 (m, 2H, H-17"), 1.48 (m, 2H, H-3"), 1.36-1.13 (m, 42H, CH₂), 0.81 (t, $J_{17,16} = 6.9$ Hz, 3H, CH₃); **¹³C NMR** (100.6 MHz, CDCl₃) δ in ppm: 173.2 (C=O), 138.5 (C-Ar), 138.5 (C-Ar), 137.9 (C-Ar), 137.6 (C-Ar), 135.0 (C-6), 128.6-127.6 (CH-Ar, C-5), 99.4 (C-1'), 79.3 (C-3'), 76.1 (C-2'), 75.7 (C-3), 74.8 (CH₂Ph), 74.6 (C-4'), 74.2 (CH₂Ph), 73.7 (CH₂Ph), 72.9 (CH₂Ph), 70.1 (C-1), 69.8 (C-5'), 69.2 (C-6'), 69.2 (C-4), 50.0 (C-2), 41.7 (t, $J_{C-F} = 19.7$ Hz, C-19"), 40.4 (C-17"), 36.8 (C-2"), 32.0 (CH₂), 29.8-29.4 (CH₂), 28.6 (CH₂), 28.2 (C-7), 25.8 (CH₂), 22.8 (CH₂), 21.0 (C-18"), 14.2 (CH₃); **¹⁹F NMR** (376 MHz, CDCl₃) δ in ppm: -80.8 (t, $J_{25'',24''} = 9.9$ Hz, 3F, CF₃), -111.8 (d, $J_{gem} = 262.0$ Hz, 1F, CF₂CH₂), -114.6

(d, $J_{\text{gem}} = 262.0$ Hz, 1F, CF_2CH_2), -121.9 (m, 2F, CF_2), -122.9 (m, 2F, CF_2), -123.7 (m, 2F, CF_2), -126.2 (m, 2F, CF_2); **HRMS** (TOF ES+) for $[\text{M}+\text{Na}]^+$ $\text{C}_{76}\text{H}_{103}\text{F}_{13}\text{INNaO}_9$ (m/z): calculated: 1570,6362; found: 1570,6347.

(2S,3S,4R,5Z)-2-((20Z)-23,23,24,24,25,25-heptafluoropentacos-20-enoyl)-amino-3,4-dihydroxy-1-O-(2,3,4,6-tetra-O-benzyl- α -D-galactopyranosyl)-heptadec-5-en-1,3,4-triol (83)

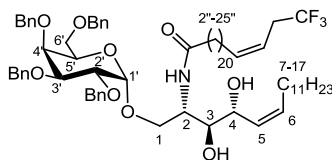


The title compound was prepared following the general procedure for isopropylidene ketal hydrolysis, starting from amide **80** (90 mg, 0.066 mmol) and using 4M HCl (85 μL) in a mixture of $\text{CH}_2\text{Cl}_2/\text{MeOH}$ (5:1) (0.9 mL). The reaction was allowed to stir for 24 h and was stopped by adding a saturated aqueous solution of Na_2CO_3 . The crude was purified by column chromatography (EtOAc/Hexane, 1:2) to provide the desired amide **83** as a white waxy solid (68 mg, 78 % yield). $R_f = 0.18$ (EtOAc/Hexane, 1:2); $[\alpha]_{\text{D}}^{25} +14.1$ (c 1.5, CHCl_3); **IR** (neat): 3320, 2920, 2851, 1639, 1455, 1223, 1109, 1042, 731 cm^{-1} ; **^1H NMR** (400 MHz, CDCl_3) δ in ppm: 7.31-7.18 (m, 20H, HAr), 6.29 (d, $J_{\text{NH}} = 8.3$ Hz, 1H, NH), 5.68 (dtt, $J_{20'',21''} = 10.6$ Hz, $J_{20'',19''} = 7.4$ Hz, $J_{20'',22''} = 1.5$ Hz, 1H, H-20''), 5.53 (dt, $J_{6,5} = 10.8$ Hz, $J_{6,7} = 7.4$ Hz, 1H, H-6), 5.36-5.30 (m, 2H, H-5, H-21''), 4.84 (d, $J_{\text{gem}} = 11.5$ Hz, 1H, CH_2Ph), 4.82 (d, $J_{1',2'} = 3.7$ Hz, 1H, H-1'), 4.80 (d, $J_{\text{gem}} = 11.7$ Hz, 1H, CH_2Ph), 4.71 (d, $J_{\text{gem}} = 11.7$ Hz, 1H, CH_2Ph), 4.67 (d, $J_{\text{gem}} = 11.7$ Hz, 1H, CH_2Ph), 4.63 (d, $J_{\text{gem}} = 11.7$ Hz, 1H, CH_2Ph), 4.49 (d, $J_{\text{gem}} = 11.5$ Hz, 1H, CH_2Ph), 4.40 (d, $J_{\text{gem}} = 11.6$ Hz, 1H, CH_2Ph), 4.38 (m, 1H, H-4), 4.31 (d, $J_{\text{gem}} = 11.6$ Hz, 1H, CH_2Ph), 4.08 (m,

| *Experimental section*

1H, H-2), 3.98 (dd, $J_{2',3'} = 10.0$ Hz, $J_{2',1'} = 3.7$ Hz, 1H, H-2'), 3.88 (m, 1H, H-4'), 3.85 (m, 1H, H-5'), 3.83-3.78 (m, 3H, H-1a, H-1b, H-3'), 3.64 (d, $J_{OH,3} = 6.1$ Hz, OH), 3.49 (m, 1H, H-3), 3.46-3.39 (m, 2H, H-6'), 2.77 (td, $J_{C,F} = 18.5$ Hz, $J_{22'',21''} = 7.2$ Hz, 2H, H-22''), 2.57 (m, 1H, OH), 2.03-1.87 (m, 6H, H-2'', H-19'', H-7), 1.49 (m, 2H, H-3''), 1.36-1.12 (m, 48H, CH₂), 0.81 (t, $J_{17,16} = 6.8$ Hz, 3H, CH₃); **¹³C NMR** (100.6 MHz, CDCl₃) δ in ppm: 173.3 (C=O), 138.5 (C-Ar), 138.5 (C-Ar), 137.9 (C-Ar), 137.7 (C-Ar), 137.4 (C-20''), 135.1 (C-6), 128.6-127.6 (CH-Ar, C-5), 115.4 (t, $J_{C,F} = 4.3$ Hz, C-21''), 99.4 (C-1'), 79.4 (C-3'), 76.1 (C-2'), 75.8 (C-3), 74.9 (CH₂Ph), 74.6 (C-4'), 74.3 (CH₂Ph), 73.8 (CH₂Ph), 72.9 (CH₂Ph), 70.1 (C-1), 70.0 (C-5'), 69.3 (C-6'), 69.2 (C-4), 50.0 (C-2), 36.8 (C-2''), 32.1 (CH₂), 29.9-29.0 (CH₂, C-22''), 28.2 (C-7), 27.5 (C-21''), 25.8 (CH₂), 22.8 (CH₂), 14.3 (CH₃); **¹⁹F NMR** (376 MHz, CDCl₃) δ in ppm: -80.6 (t, $J_{25'',24''} = 9.7$ Hz, 3F, CF₃), -114.2 (m, 2F, CF₂CH₂), -127.5 (m, 2F, CF₂); **HRMS** (TOF ES+) for [M+H]⁺ C₇₆H₁₀₉F₇NO₉ (m/z): calculated: 1312,7985; found: 1312.7963.

(2S,3S,4R,5Z)-2-((22Z)-25,25,25-trifluoropentacos-22-enoyl)-amino-3,4-dihydroxy-1-O-(2,3,4,6-tetra-O-benzyl- α -D-galactopyranosyl)-heptadec-5-en-1,3,4-triol (84)

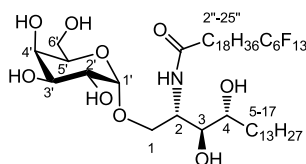


The title compound was prepared following the general procedure for isopropylidene ketal hydrolysis, starting from amide **81** (150 mg, 0.12 mmol) and using 4M HCl (0.15 mL) in a mixture of CH₂Cl₂/MeOH (5:1) (1.5 mL). The reaction was allowed to stir for 24 h and was stopped by adding a saturated aqueous solution of Na₂CO₃. The crude was purified

by column chromatography (EtOAc/Hexane, 1:2) to provide the desired amide **84** as a white waxy solid (116 mg, 78 % yield). $R_f = 0.18$ (EtOAc/Hexane, 1:2); $[\alpha]_D^{25} +18.7$ (c 1.0, CHCl_3); **IR** (neat): 3323, 2920, 2850, 1638, 1456, 1253, 1134, 1042, 729 cm^{-1} ; **$^1\text{H NMR}$** (400 MHz, CDCl_3) δ in ppm: 7.30-7.19 (m, 20H, HAr), 6.30 (d, $J_{\text{NH},2} = 8.3$ Hz, 1H, NH), 5.65 (m, 1H, H-22"), 5.53 (dt, $J_{6,5} = 11.4$ Hz, $J_{6,7} = 7.4$ Hz, 1H, H-6), 5.36-5.27 (m, 2H, H-5, H-23"), 4.84 (d, $J_{\text{gem}} = 11.4$ Hz, 1H, CH_2Ph), 4.85 (d, $J_{1',2'} = 3.8$ Hz, 1H, H-1'), 4.80 (d, $J_{\text{gem}} = 11.5$ Hz, 1H, CH_2Ph), 4.71 (d, $J_{\text{gem}} = 11.7$ Hz, 1H, CH_2Ph), 4.67 (d, $J_{\text{gem}} = 11.7$ Hz, 1H, CH_2Ph), 4.63 (d, $J_{\text{gem}} = 11.4$ Hz, 1H, CH_2Ph), 4.50 (d, $J_{\text{gem}} = 11.5$ Hz, 1H, CH_2Ph), 4.40 (d, $J_{\text{gem}} = 11.6$ Hz, 1H, CH_2Ph), 4.38 (m, 1H, H-4), 4.31 (d, $J_{\text{gem}} = 11.6$ Hz, 1H, CH_2Ph), 4.08 (m, 1H, H-2), 3.98 (dd, $J_{2',3'} = 10.0$ Hz, $J_{2',1'} = 3.8$ Hz, 1H, H-2'), 3.88 (m, 1H, H-4'), 3.85 (m, 1H, H-5'), 3.83-3.78 (m, 3H, H-1a, H-1b, H-3'), 3.64 (d, $J_{\text{OH},3} = 7.1$ Hz, OH), 3.49 (m, 1H, H-3), 3.46-3.38 (m, 2H, H-6'), 2.77 (m, 2H, H-24"), 2.57 (m, 1H, OH), 2.03-1.87 (m, 6H, H-2", H-21", H-7), 1.48 (m, 2H, H-3"), 1.36-1.12 (m, 52H, CH_2), 0.81 (t, $J_{17,16} = 6.9$ Hz, 3H, CH_3); **$^{13}\text{C NMR}$** (100.6 MHz, CDCl_3) δ in ppm: 173.2 (C=O), 138.5 (C-Ar), 138.5 (C-Ar), 137.9 (C-Ar), 137.7 (C-Ar), 136.9 (C-22"), 135.1 (C-6), 128.7-127.6 (CH-Ar, C-5), 126.4 (d, $J_{\text{C},\text{F}} = 276.6$ Hz, CF_3), 116.8 (q, $J_{\text{C},\text{F}} = 3.5$ Hz, C-23"), 99.4 (C-1'), 79.4 (C-3'), 76.1 (C-2'), 75.8 (C-3), 74.9 (CH_2Ph), 74.6 (C-4'), 74.3 (CH_2Ph), 73.8 (CH_2Ph), 72.9 (CH_2Ph), 70.1 (C-1), 70.0 (C-5'), 69.3 (C-6'), 69.2 (C-4), 50.0 (C-2), 36.8 (C-2"), 32.3 (q, $J_{\text{C},\text{F}} = 29.6$ Hz, C-24"), 32.1 (CH_2), 29.9-29.3 (CH_2), 28.2 (C-7), 27.5 (C-21"), 25.8 (CH_2), 22.8 (CH_2), 14.3 (CH_3); **$^{19}\text{F NMR}$** (376 MHz, CDCl_3) δ in ppm: -66.3 (t, $J_{\text{F},\text{H}} = 10.9$ Hz, 3F, CF_3); **HRMS** (TOF ES+) for $[\text{M}+\text{Na}]^+$ $\text{C}_{76}\text{H}_{112}\text{F}_3\text{NNaO}_9$ (m/z): calculated:1262.8181; found: 1262.8149.

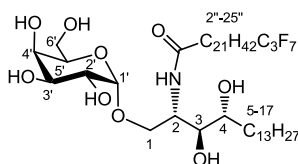
Experimental section

(2S,3S,4R)-2-(19-perfluorohexylnonadecanoyl)-3,4-dihydroxy-1-O-(α -D-galactopyranosyl)-heptadeca-1,3,4-triol (50**)**



The title compound was prepared following the general procedure for hydrogenolysis reaction starting from protected glycolipid **82** (56 mg, 0.036 mmol), Pd/C (72 mg), H₂ (1 atm) in MeOH/ CHCl₃ (3:1) (2.9 mL). The crude purified by column chromatography (CH₂Cl₂/MeOH, 9:1) to provide the desired unprotected compound **50** as a white waxy solid (30 mg, 80 % yield); R_f = 0.24 (CH₂Cl₂/MeOH, 9:1); [α]_D²⁵ +14.0 (c 0.7, MeOH / CHCl₃ (1:1)); IR (neat): 3366, 2917, 2850, 1652, 1456, 1239, 1214, 1144, 1030, 756 cm⁻¹; ¹H NMR (400 MHz, CDCl₃ / MeOD (1:1)) δ in ppm: 4.80 (d, $J_{1,2'}$ = 3.7 Hz, 1H, H-1'), 4.11 (q, $J_{2,1}$ = $J_{2,3}$ = 4.6 Hz, 1H, H-2), 3.85 (m, 1H, H-4'), 3.79 (dd, J_{gem} = 10.7 Hz, $J_{1\alpha,2}$ = 4.6 Hz, 1H, H-1a), 3.75-3.59 (m, 6H, H-2', H-3', H-5', H-6', H-1b), 3.51-3.43 (m, 2H, H-3, H-4), 2.12 (t, $J_{2'',3''}$ = 7.6 Hz, 2H, H-2''), 2.00 (m, 2H, H-19''), 1.53 (m, 6H, H-18'', H-3'', H-5), 1.32-1.16 (m, 46H, CH₂), 0.80 (t, $J_{17,16}$ = 6.8 Hz, CH₃); ¹³C NMR (100.6 MHz, CDCl₃ / MeOD (1:1)) δ in ppm: 175.2 (CO), 100.4 (C-1'), 75.0 (C-3), 72.4 (C-4), 71.6 (C-3'), 70.9 (C-5'), 70.4 (C-4'), 69.6 (C-2'), 67.8 (C-1), 62.3 (C-6'), 51.1 (C-2), 37.0 (C-2''), 32.8 (CH₂), 32.5 (CH₂), 31.4 (m, C-19''), 30.3-29.6 (CH₂), 26.5 (CH₂), 26.5 (CH₂), 23.2 (CH₂), 20.7 (m, C-18''), 14.3 (CH₃); ¹⁹F NMR (376 MHz, CDCl₃) δ in ppm: -80.8 (t, $J_{25'',24''}$ = 9.9 Hz, 3F, CF₃), -111.8 (d, J_{gem} = 261.3 Hz, 1F, CF₂CH₂), -114.6 (d, J_{gem} = 261.3 Hz, 1F, CF₂CH₂), -121.9 (m, 2F, CF₂), -122.9 (m, 2F, CF₂), -123.7 (m, 2F, CF₂), -126.2 (m, 2F, CF₂); HRMS (TOF ES+) for [M+H]⁺ C₄₈H₈₃F₁₃NO₉ (m/z): calculated: 1064,5855; found: 1064.5849.

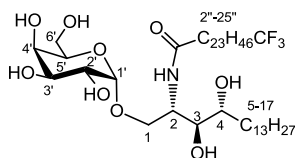
(2S,3S,4R)-2-(23,23,24,24,25,25,25-heptafluoropentacosanoyl)-3,4-dihydroxy-1-O-(α -D-galactopyranosyl)-heptadeca-1,3,4-triol (51)



The title compound was prepared following the general procedure for hydrogenolysis reaction starting from protected glycolipid **83** (31 mg, 0.023 mmol), Pd/C (46 mg), H₂ (1 atm) in MeOH/ CHCl₃ (3:1) (1.9 mL). The crude purified by column chromatography (CH₂Cl₂/MeOH, 9:1) to provide the desired unprotected compound **51** as a white waxy solid (18 mg, 85 % yield); R_f = 0.25 (CH₂Cl₂/MeOH, 9:1); [α]_D²⁵ +17.5 (c 0.6, MeOH / CHCl₃ (1:1)); IR (neat): 3367, 2917, 2849, 1647, 1465, 1255, 1224, 1072, 1029, 798 cm⁻¹; ¹H NMR (400 MHz, CDCl₃ / MeOD (1:1)) δ in ppm: 4.87 (d, J_{1',2'} = 3.7 Hz, 1H, H-1'), 4.26 (brs, 1H, NH), 4.17 (m, 1H, H-2), 3.89 (m, 1H, H-4'), 3.85 (dd, J_{gem} = 10.8 Hz, J_{1a,2} = 4.6 Hz, 1H, H-1a), 3.80-3.64 (m, 6H, H-2', H-3', H-5', H-6', H-1b), 3.56-3.49 (m, 2H, H-3, H-4), 2.18 (t, J_{2'',3''} = 7.6 Hz, 2H, H-2''), 2.13-1.96 (m, 2H, H-22''), 1.65-1.49 (m, 6H, H-21'', H-3'', H-5), 1.41-1.19 (m, 66H, CH₂), 0.85 (t, J_{17,16} = 6.9 Hz, CH₃); ¹³C NMR (100.6 MHz, CDCl₃ / MeOD (1:1)) δ in ppm: 175.1 (CO), 100.2 (C-1'), 75.0 (C-3), 72.4 (C-4), 71.4 (C-3'), 70.8 (C-5'), 70.2 (C-4'), 69.4 (C-2'), 67.7 (C-1), 62.2 (C-6'), 51.0 (C-2), 36.9 (C-2''), 32.8 (CH₂), 32.4 (CH₂), 31.0 (t, J_{C,F} = 22.3 Hz, C-22''), 30.2-29.5 (CH₂), 26.4 (CH₂), 26.3 (CH₂), 23.1 (CH₂), 20.5 (m, C-21''), 14.3 (CH₃); ¹⁹F NMR (376 MHz, CDCl₃) δ in ppm: -80.9 (t, J_{25'',24''} = 9.8 Hz, 3F, CF₃), -114.2 (m, 2F, CF₂CH₂), -127.5 (m, 2F, CF₂); HRMS (TOF ES+) for [M+H]⁺ C₄₈H₈₉F₇NO₉ (m/z): calculated: 956.6420; found: 956.6425.

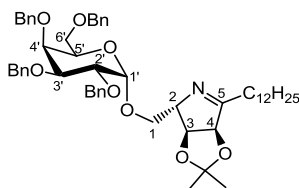
Experimental section

(2S,3S,4R)-2-(25,25,25-trifluoropentacosanoyl)-3,4-dihydroxy-1-O-(α -D-galactopyranosyl)-heptadeca-1,3,4-triol (52**)**



The title compound was prepared following the general procedure for hydrogenolysis reaction starting from protected glycolipid **84** (42 mg, 0.034 mmol), Pd/C (68 mg), H₂ (1 atm) in MeOH/ CHCl₃ (3:1) (2.5 mL). The crude purified by column chromatography (CH₂Cl₂/MeOH, 9:1) to provide the desired unprotected compound **52** as a white waxy solid (25 mg, 84 % yield); R_f = 0.22 (CH₂Cl₂/MeOH, 9:1); [α]_D²⁵ +40.5 (c 0.6, MeOH / CHCl₃ (1:1)); IR (neat): 3324, 2917, 2849, 1647, 1467, 1255, 1214, 1144, 1025 cm⁻¹; ¹H NMR (400 MHz, CDCl₃ / MeOD (1:1)) δ in ppm: 4.87 (d, $J_{1,2'} = 3.7$ Hz, 1H, H-1'), 4.11 (q, $J_{2,1} = J_{2,3} = 4.9$ Hz, 1H, H-2), 3.89 (m, 1H, H-4'), 3.85 (dd, $J_{gem} = 10.7$ Hz, $J_{1a,2} = 4.9$ Hz, 1H, H-1a), 3.80-3.65 (m, 6H, H-2', H-3', H-5', H-6', H-1b), 3.56-3.49 (m, 2H, H-3, H-4), 2.18 (t, $J_{2'',3''} = 7.6$ Hz, 2H, H-2''), 2.11-1.99 (m, 2H, H-24''), 1.66-1.48 (m, 8H, H-23'', H-3'', H-5, CH₂), 1.40-1.19 (m, 58H, CH₂), 0.80 (t, $J_{17,16} = 6.8$ Hz, CH₃); ¹³C NMR (100.6 MHz, CDCl₃ / MeOD (1:1)) δ in ppm: 175.2 (CO), 100.4 (C-1'), 75.0 (C-3), 72.5 (C-4), 71.6 (C-3'), 70.9 (C-5'), 70.4 (C-4'), 69.8 (C-2'), 67.8 (C-1), 62.3 (C-6'), 51.1 (C-2), 37.0 (C-2''), 34.2 (q, $J_{C,F} = 28.2$ Hz, C-24''), 32.8 (CH₂), 32.5 (CH₂), 30.4-29.3 (CH₂), 26.5 (CH₂), 26.5 (CH₂), 23.2 (CH₂), 22.2 (q, $J_{C,F} = 2.7$ Hz, C-23''), 14.4 (CH₃); ¹⁹F NMR (376 MHz, CDCl₃ / MeOD (1:1)) δ in ppm: -66.8 (t, $J_{F,H} = 11.0$ Hz, 3F, CF₃); HRMS (TOF ES+) for [M+H]⁺ C₄₈H₉₃F₃NO₉ (m/z): calculated: 884.6797; found: 884.6765

(3*R*,4*S*,5*S*)-5-(1-*O*-(2,3,4,6-tetra-*O*-benzyl- α -D-galactopyranosyl)-methanol)-2-dodecyl-3,4-*O*-isopropylidene- Δ^1 pyrroline (92**)**

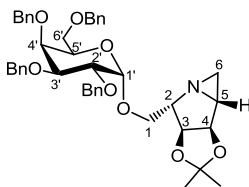


The title compound was prepared following the general procedure for one pot Mitsunobu azidation-1,3-dipolar cycloaddition, starting from alcohol **9** (575 mg, 0.66 mmol), triphenylphosphine (519 mg, 1.98 mmol), diisopropyl azodicarboxylate (0.39 mL, 1.98 mmol) and diphenylphosphoryl azide (0.46 mL, 2.12 mmol) in THF (7 mL). After 1 h stirring at room temperature, the reaction mixture was quenched and the crude was dissolved in THF/H₂O (10 mL) and heated at 60°C for 12h. After work-up, the crude was purified by column chromatography (1:2 EtOAc/Hexane) to afford **92** (368 mg, 71%) as a colorless oil. *R_f* = 0.28 (1:2 EtOAc/Hexane); $[\alpha]_D^{25} +27.1$ (c 1.0, CHCl₃); IR (neat): 2924, 2854, 1643, 1454, 1209, 1057, 735 cm⁻¹; ¹H NMR (400 MHz, CDCl₃) δ in ppm: 7.30 – 7.17 (m, 20H, H-Ar), 4.85 (d, *J*_{gem} = 11.6 Hz, 1H, CH₂Ph), 4.83 (m, 1H, H-1'), 4.76 (m, 1H, H-3), 4.74 (d, *J*_{gem} = 11.8 Hz, 1H, CH₂Ph), 4.66 (d, *J*_{gem} = 12.1 Hz, 1H, CH₂Ph), 4.62 (d, *J*_{gem} = 12.1 Hz, 1H, CH₂Ph), 4.55 (d, *J*_{gem} = 11.8 Hz, 1H, CH₂Ph), 4.47 (d, *J*_{gem} = 11.6 Hz, 1H, CH₂Ph), 4.44 (d, *J*_{4,3} = 5.3 Hz, 1H, H-4), 4.38 (d, *J*_{gem} = 11.8 Hz, 1H, CH₂Ph), 4.30 (d, *J*_{gem} = 11.8 Hz, 1H, CH₂Ph), 4.19 (brs, 1H, H-2), 3.92 (dd, *J*_{2',3'} = 10.0 Hz, *J*_{2',1'} = 3.6 Hz, 1H, H-2'), 3.85 (m, 1H, H-4'), 3.81 (dd, *J*_{1a,1b} = 9.9 Hz, *J*_{1a,2} = 2.8 Hz, H-1a), 3.70 (brt, *J*_{5',6'} = 6.7 Hz, 1H, H-5'), 3.59 (dd, *J*_{3',2'} = 10.0 Hz, *J*_{3',4'} = 2.8 Hz, H-3'), 3.46-3.37 (m, 3H, H-1b, 2xH-6'), 2.28 (ddd, *J*_{6a,6b} = 15.6 Hz, *J*_{6a,7a} = 9.8 Hz, *J*_{6a,7b} = 6.1 Hz, 1H, H-6a), 2.10 (ddd, *J*_{6b,6a} = 15.6 Hz, *J*_{6b,7a} = 9.7 Hz, *J*_{6b,7b} = 5.7 Hz, 1H, H-6b), 1.53 - 1.40 (m, 2H,

Experimental section

2xH-7) 1.26 (s, 3H, CH₃), 1.24-1.13 (m, 21H, CH₃, CH₂), 0.80 (t, $J_{17,16}$ = 6.9 Hz, 3H, CH₃); ¹³C NMR (100.6 MHz, CDCl₃) δ in ppm: 178.6 (C=N), 138.8 (C-Ar), 138.7 (C-Ar), 138.6 (C-Ar), 138.0 (C-Ar), 128.5-127.4 (CH-Ar), 111.4 (C-ketal), 97.9 (C-1'), 86.8 (C-3), 81.0 (C-4), 78.5 (C-3'), 76.8 (C-2'), 75.2 (C-2), 75.0 (CH₂Ph), 74.8 (C-4'), 73.5 (CH₂Ph), 73.3 (CH₂Ph), 72.6 (CH₂Ph), 69.3 (C-5'), 68.6 (C-6'), 68.0 (C-1), 32.1 (CH₂), 30.9 (C-6), 29.8-29.5 (CH₂), 27.1 (CH₃), 26.3 (C-7), 25.9 (CH₃), 22.8 (CH₂), 14.3 (CH₃); HRMS (TOF ES+) for [M+H] C₅₄H₇₂NO₈ (m/z): calculated: 862.5252, found: 862.5244.

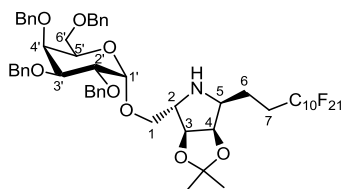
(2S,3S,4R,5R)-2-(1-O-(2,3,4,6-tetra-O-benzyl- α -D-galactopyranosyl)-methanol)-3,4-O-isopropylidene-1-azabicyclo[3.1.0]hexane (95)



The title compound was prepared following the general procedure for one pot Mitsunobu azidation-1,3-dipolar cycloaddition, starting from alcohol **11** (104 mg, 0.15 mmol), triphenylphosphine (115 mg, 0.44 mmol), diisopropyl azodicarboxylate (87 μ L, 0.44 mmol) and diphenylphosphoryl azide (0.1 mL, 0.47 mmol) in THF (1.6 mL). After 12 h stirring at room temperature, the reaction mixture was quenched and the crude was dissolved in THF/H₂O (2.2 mL) and heated at 45°C for 12h. The reaction mixture was quenched and the crude was purified by column chromatography (1:3:0.2 EtOAc/Hexane/NEt₃) to afford **95** (53 mg, 50%) as a colorless oil. R_f = 0.42 (1:1 EtOAc/Hexane); $[\alpha]_D^{25}$ +29.5 (c 1.1, CHCl₃); IR (neat): 2921, 2869, 1496, 1455, 1209, 1097, 1053,

738 cm^{-1} ; $^1\text{H NMR}$ (400 MHz, CDCl_3) δ in ppm: 7.33 - 7.18 (m, 20H, H-Ar), 4.88 (d, $J_{\text{gem}} = 11.4$ Hz, 1H, CH_2Ph), 4.85 (dd, $J_{4,5} = 7.0$ Hz, $J_{4,3} = 4.6$ Hz, 1H, H-4), 4.80 (d, $J_{1',2'} = 3.5$ Hz, 1H, H-1'), 4.76 (d, $J_{\text{gem}} = 11.8$ Hz, 1H, CH_2Ph), 4.72 (d, $J_{\text{gem}} = 12.2$ Hz, 1H, CH_2Ph), 4.68 (d, $J_{\text{gem}} = 12.2$ Hz, 1H, CH_2Ph), 4.60 (m 1H, H-3), 4.55 (d, $J_{\text{gem}} = 11.8$ Hz, 1H, CH_2Ph), 4.51 (d, $J_{\text{gem}} = 11.4$ Hz, 1H, CH_2Ph), 4.38 (d, $J_{\text{gem}} = 11.8$ Hz, 1H, CH_2Ph), 4.32 (d, $J_{\text{gem}} = 11.8$ Hz, 1H, CH_2Ph), 3.98 (dd, $J_{2',3'} = 10.0$ Hz, $J_{2',1'} = 3.5$ Hz, 1H, H-2'), 3.94 (br.t, $J_{5',6'} = 6.8$ Hz, 1H, H-5'), 3.89 (m, 1H, H-4'), 3.82 (dd, $J_{3',2'} = 10.0$ Hz, $J_{3',4'} = 2.8$ Hz, 1H, H-3'), 3.75 (dd, $J_{\text{gem}} = 9.6$ Hz, $J_{1a,2} = 3.8$ Hz, 1H, H-1a), 3.44 (d, $J_{6',5'} = 6.8$ Hz, 1H, 2xH-6'), 3.34 (dd, $J_{\text{gem}} = 9.6$ Hz, $J_{1b,2} = 3.4$ Hz, 1H, H-1b), 3.29 (brt, $J_{2,1a} = J_{2,1b} = 3.5$ Hz, 1H, H-2), 2.35 (m, 1H, H-5), 1.91 (d, $J_{6a,5} = 3.3$ Hz, 1H, H-6a), 1.72 (d, $J_{6b,5} = 5.5$ Hz, 1H, H-6b), 1.41 (s, 3H, CH_3), 1.07 (s, 3H, CH_3); $^{13}\text{C NMR}$ (100.6 MHz, CDCl_3) δ in ppm: 138.9 (C-Ar), 138.8 (C-Ar), 138.6 (C-Ar), 138.0 (C-Ar), 128.5-127.5 (CH-Ar), 112.9 (C-ketal), 98.0 (C-1'), 86.2 (C-3), 81.1 (C-4), 78.2 (C-3'), 76.8 (C-2'), 74.9 (C-4'), 74.9 (CH_2Ph), 73.6 (CH_2Ph), 73.3 (CH_2Ph), 72.6 (CH_2Ph), 70.8 (C-1), 69.5 (C-5'), 68.9 (C-6'), 67.1 (C-2), 44.8 (C-5), 30.8 (C-6), 26.6 (CH_3), 24.1 (CH_3); **HRMS** (TOF ES+) for $[\text{M}+\text{H}] \text{C}_{43}\text{H}_{50}\text{NO}_8$ (m/z): calculated: 708,3531, found: 708.3531.

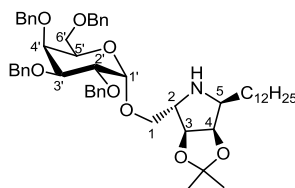
(2S,3S,4R,5S)-2-(1-O-(2,3,4,6-tetra-O-benzyl- α -D-galactopyranosyl)-methanol)-5-(2-perfluorodecylethyl)-3,4-O-isopropylidene pyrrolidine (89)



| *Experimental section*

The title compound was prepared following the general procedure for imine reduction to amine, starting from imine **39** (140 mg, 0.12 mmol) and NaBH₄ (9 mg, 0.24 mmol) in MeOH (1.5 mL). The crude mixture was purified with column chromatography (1:2 EtOAc/Hexane to 1:3:0.05 EtOAc/Hexane/NEt₃) to afford **89** (77 mg, 55%) as a colorless oil; *R_f* = 0.21 (1:2 EtOAc/Hexane); $[\alpha]_{\text{D}}^{25} +7.5$ (c 1.0, CHCl₃); **IR** (neat): 2921, 2868, 1455, 1210, 1151, 1097, 1053, 751 cm⁻¹; **¹H NMR** (400 MHz, CDCl₃) δ in ppm: 7.33-7.17 (m, 20H, HAr), 4.87 (d, $J_{\text{gem}} = 11.5$ Hz, 1H, CH₂Ph), 4.78-4.70 (m, 3H, 2xCH₂Ph, H-1'), 4.67 (d, $J_{\text{gem}} = 11.5$ Hz, 1H, CH₂Ph), 4.57 (d, $J_{\text{gem}} = 11.7$ Hz, 1H, CH₂Ph), 4.54 (d, $J_{3,4} = 5.8$ Hz, 1H, H-3), 4.51 (d, $J_{\text{gem}} = 11.7$ Hz, 1H, CH₂Ph), 4.38 (d, $J_{\text{gem}} = 11.7$ Hz, 1H, CH₂Ph), 4.32 (d, $J_{\text{gem}} = 11.7$ Hz, 1H, CH₂Ph), 4.30 (m, 1H, H-4), 3.96 (dd, $J_{2',3'} = 10.1$ Hz, $J_{2',1'} = 3.7$ Hz, 1H, H-2'), 3.88 (m, 1H, H-4'), 3.82 (brt, $J_{5',4'} = J_{5',6'} = 6.4$ Hz, 1H, H-5'), 3.75 (dd, $J_{3',2'} = 10.1$ Hz, $J_{3',4'} = 2.8$ Hz, 1H, H-3'), 3.55 (dd, $J_{\text{gem}} = 10.1$ Hz, $J_{1a,2} = 5.2$ Hz, 1H, H-1a), 3.43 (m, 2H, H-6'a, H-6'b), 3.35 (dd, $J_{\text{gem}} = 10.1$ Hz, $J_{1b,2} = 5.3$ Hz, 1H, H-1b), 3.26 (brt, $J_{2,1a} = J_{2,1b} = 5.3$ Hz, 1H, H-2), 2.86 (td, $J_{5,6} = 7.0$ Hz, $J_{5,4} = 4.5$ Hz, 1H, H-5), 2.05 (m, 2H, H-7a, H-7b), 1.70 (m, 2H, H-6a, H-6b), 1.44 (s, 3H, CH₃), 1.23 (s, 3H, CH₃); **¹³C NMR** (100.6 MHz, CDCl₃) δ in ppm: 138.7 (C-Ar), 138.6 (C-Ar), 138.4 (C-Ar), 138.0 (C-Ar), 128.5-127.5 (CH-Ar), 111.1 (C-ketal), 98.4 (C-1'), 84.5 (C-3), 82.3 (C-4), 78.7 (C-3'), 76.6 (C-2'), 74.9 (C-4'), 74.8 (CH₂Ph), 73.7 (CH₂Ph), 73.4 (CH₂Ph), 72.8 (CH₂Ph), 69.9 (C-5'), 69.6 (C-1), 69.2 (C-6'), 63.4 (C-2), 61.4 (C-5), 28.7 (t, $J_{\text{C,F}} = 21.8$ Hz, C-7), 26.2 (CH₃), 24.2 (CH₃), 20.7 (C-6); **¹⁹F NMR** (376 MHz, CDCl₃) δ in ppm: -80.7 (t, $J_{\text{F,F}} = 9.8$ Hz, 3F, CF₃), -113.9 (d, $J_{\text{gem}} = 275.2$ Hz, 1F, CF₂CH₂), -114.9 (d, $J_{\text{gem}} = 275.2$ Hz, 1F, CF₂CH₂), -121.8 (m, 10F, CF₂), -122.7 (m, 2F, CF₂), -123.3 (m, 2F, CF₂), -126.1 (m, 2F, CF₂); **HRMS** (TOF ES+) for [M+H]⁺ C₅₄H₅₃F₂₁NO₈ (m/z): calculated: 1242,3430, found: 1242,3425.

(2S,3S,4R,5S)-2-(1-O-(2,3,4,6-tetra-O-benzyl- α -D-galactopyranosyl)-methanol)-5-dodecyl-3,4-O-isopropylidene pyrrolidine (90**)**

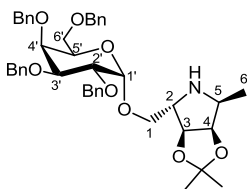


The title compound was prepared following the general procedure for imine reduction to amine, starting from imine **92** (240 mg, 0.28 mmol) and NaBH_4 (21 mg, 0.56 mmol) in MeOH (3.4 mL). The crude mixture was purified with column chromatography (1:1 EtOAc/Hexane to 1:3:0.05 EtOAc/Hexane/ NEt_3) to afford **90** (202 mg, 84%) as a colorless oil; $R_f = 0.23$ (1:1 EtOAc/Hexane); $[\alpha]_D^{25} +34.2$ (c 1.1, CHCl_3); IR (neat): 2923, 2852, 1454, 1207, 1096, 1053, 733 cm^{-1} ; $^1\text{H NMR}$ (400 MHz, CDCl_3) δ in ppm: 7.32-7.17 (m, 20H, HAr), 4.87 (d, $J_{\text{gem}} = 11.5$ Hz, 1H, CH_2Ph), 4.80 (d, $J_{1',2'} = 3.6$ Hz, 1H, H-1'), 4.74 (d, $J_{\text{gem}} = 11.9$ Hz, 1H, CH_2Ph), 4.72 (d, $J_{\text{gem}} = 11.8$ Hz, 1H, CH_2Ph), 4.65 (d, $J_{\text{gem}} = 11.5$ Hz, 1H, CH_2Ph), 4.58 (d, $J_{\text{gem}} = 11.8$ Hz, 1H, CH_2Ph), 4.52 (d, $J_{3,4} = 5.5$ Hz, 1H, H-3), 4.50 (d, $J_{\text{gem}} = 11.9$ Hz, 1H, CH_2Ph), 4.38 (d, $J_{\text{gem}} = 11.8$ Hz, 1H, CH_2Ph), 4.32 (d, $J_{\text{gem}} = 11.8$ Hz, 1H, CH_2Ph), 4.24 (dd, $J_{4,3} = 5.5$ Hz, $J_{4,5} = 4.2$ Hz, 1H, H-4), 3.96 (dd, $J_{2',3'} = 10.0$ Hz, $J_{2',1'} = 3.6$ Hz, 1H, H-2'), 3.88-3.83 (m, 2H, H-4', H-5'), 3.80 (dd, $J_{3',2'} = 10.0$ Hz, $J_{3',4'} = 2.8$ Hz, 1H, H-3'), 3.55 (dd, $J_{\text{gem}} = 10.1$ Hz, $J_{1a,2} = 6.0$ Hz, 1H, H-1a), 3.43 (m, 2H, 2xH-6'), 3.35 (dd, $J_{\text{gem}} = 10.1$ Hz, $J_{1b,2} = 5.7$ Hz, 1H, H-1b), 3.26 (brt, $J_{2,1a} = J_{2,1b} = 5.8$ Hz, 1H, H-2), 2.86 (td, $J_{5,6} = 6.8$ Hz, $J_{5,4} = 4.2$ Hz, 1H, H-5), 1.40 (m, 2H, H-6a, H-6b), 1.37 (s, 3H, CH_3), 1.28-1.12 (m, 23H, CH_2 , CH_3), 0.80 (t, $J_{18,17} = 6.9$ Hz, 3H, CH_3); $^{13}\text{C NMR}$ (100.6 MHz, CDCl_3) δ in ppm: 138.8 (C-Ar), 138.8 (C-Ar), 138.7 (C-Ar), 138.0 (C-Ar), 128.4-127.6 (CH-Ar), 111.1 (C-ketal), 98.1 (C-1'), 84.3 (C-3), 82.6 (C-4), 78.9 (C-3'), 76.6 (C-2'), 75.0 (C-

Experimental section

4'), 74.9 (CH₂Ph), 73.6 (CH₂Ph), 73.2 (CH₂Ph), 73.1 (CH₂Ph), 69.7 (C-5'), 69.2 (C-1), 69.1 (C-6'), 63.4 (C-2), 62.4 (C-5), 32.1 (CH₂), 30.1-29.4 (CH₂), 27.5 (CH₂), 26.3 (CH₃), 24.2 (CH₃), 22.8 (CH₂), 14.3 (CH₃); **HRMS** (TOF ES+) for [M+H]⁺ C₅₄H₇₄NO₈ (m/z): calculated: 864,5409, found: 864.5421.

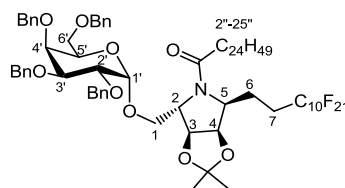
(2S,3S,4R,5S)-2-(1-O-(2,3,4,6-tetra-O-benzyl- α -D-galactopyranosyl)-methanol)-5-methyl-3,4-O-isopropylidene pyrrolidine (91)



The title compound was prepared following the general procedure for imine reduction to amine, starting from imine **44** (98 mg, 0.14 mmol) and NaBH₄ (10 mg, 0.28 mmol) in MeOH (1.7 mL). The crude mixture was purified with column chromatography (1:1 EtOAc/Hexane to 1:3:0.05 EtOAc/Hexane/NEt₃) to afford **91** (82 mg, 84%) as a colorless oil; *R_f* = 0.13 (1:1 EtOAc/Hexane); **IR** (neat): 2928, 1454, 1372, 1096, 1043, 736 cm⁻¹; [α]_D²⁵ +37.2 (c 1.1, CHCl₃); **¹H NMR** (400 MHz, CDCl₃) δ in ppm: 7.32-7.17 (m, 20H, HAr), 4.87 (d, *J*_{gem} = 11.5 Hz, 1H, CH₂Ph), 4.79 (d, *J*_{1',2'} = 3.6 Hz, 1H, H-1'), 4.74 (d, *J*_{gem} = 11.9 Hz, 1H, CH₂Ph), 4.72 (d, *J*_{gem} = 11.8 Hz, 1H, CH₂Ph), 4.66 (d, *J*_{gem} = 11.9 Hz, 1H, CH₂Ph), 4.58 (d, *J*_{gem} = 11.8 Hz, 1H, CH₂Ph), 4.53 (d, *J*_{3,4} = 5.5 Hz, 1H, H-3), 4.51 (d, *J*_{gem} = 11.5 Hz, 1H, CH₂Ph), 4.38 (d, *J*_{gem} = 11.7 Hz, 1H, CH₂Ph), 4.32 (d, *J*_{gem} = 11.7 Hz, 1H, CH₂Ph), 4.28 (dd, *J*_{4,3} = 5.5 Hz, *J*_{4,5} = 4.2 Hz, 1H, H-4), 3.95 (dd, *J*_{2',3'} = 10.1 Hz, *J*_{2',1'} = 3.6 Hz, 1H, H-2'), 3.87 (dd, *J*_{4',3'} = 2.8 Hz, *J*_{4',5'} = 1.0 Hz, 1H, H-4'), 3.84 (brt, *J*_{5',6'} = 5.6 Hz, 1H, H-5'), 3.78 (dd, *J*_{3',2'} = 10.1

Hz, $J_{3',4'} = 2.8$ Hz, 1H, H-3'), 3.55 (dd, $J_{gem} = 10.1$ Hz, $J_{1a,2} = 5.7$ Hz, 1H, H-1a), 3.42 (m, 2H, 2xH-6'), 3.34 (dd, $J_{gem} = 10.1$ Hz, $J_{1b,2} = 5.7$ Hz, 1H, H-1b), 3.26 (brt, $J_{2,1a} = J_{2,1b} = 5.7$ Hz, 1H, H-2), 2.86 (qd, $J_{5,6} = 6.5$ Hz, $J_{5,4} = 4.2$ Hz, 1H, H-5), 1.38 (s, 3H, CH₃), 1.17 (s, 3H, CH₃), 1.04 (d, $J_{6,5} = 6.5$ Hz, 3H, H-6); ¹³C NMR (100.6 MHz, CDCl₃) δ in ppm: 138.8 (C-Ar), 138.8 (C-Ar), 138.7 (C-Ar), 138.0 (C-Ar), 128.5-127.7 (CH-Ar), 110.8 (C-ketal), 98.3 (C-1'), 84.9 (C-3), 83.6 (C-4), 78.6 (C-3'), 76.7 (C-2'), 75.0 (C-4'), 74.9 (CH₂Ph), 73.6 (CH₂Ph), 73.3 (CH₂Ph), 72.9 (CH₂Ph), 69.7 (C-5'), 69.7 (C-1), 69.2 (C-6'), 63.6 (C-2), 57.4 (C-5), 26.3 (CH₃), 24.2 (CH₃), 14.1 (CH₃); HRMS (TOF ES+) for [M+H]⁺ C₄₃H₅₂NO₈ (m/z): calculated: 710.3687, found: 710.3701.

(2S,3S,4R,5S)-2-(1-O-(2,3,4,6-tetra-O-benzyl-α-D-galactopyranosyl)-methanol)-5-(2-perfluorodecylethyl)-3,4-O-isopropylidene-1-pentacosanoylpyrrolidine (99)

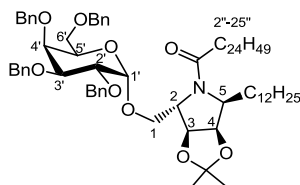


The title compound was prepared following the general procedure for pyrrolidine acylation, starting from pyrrolidine **89** (200 mg, 0.16 mmol), EDC·HCl (55 mg, 0.29 mmol), pentacosanoic acid (80 mg, 0.21 mmol), HOBT (39 mg, 0.29 mmol) and NEt₃ (22 μL, 0.16 mmol) in DCM (2 mL). The crude was purified by column chromatography (1:4 EtOAc/Hexane) to afford **99** (152 mg, 59%) as a colorless oil; *R*_f = 0.31 (1:3 EtOAc/Hexane); [α]_D²⁵ +34.6 (c 1.5, CHCl₃); IR (neat): 2922, 2852, 1652, 1455, 1210, 1152, 1100, 1056, 735 cm⁻¹; ¹H NMR (400 MHz, CDCl₃) δ in

| *Experimental section*

ppm: 7.33-7.17 (m, 20H, HAr), 4.85 (d, $J_{gem} = 11.5$ Hz, 1H, CH₂Ph), 4.80 (d, $J_{gem} = 11.8$ Hz, 1H, CH₂Ph), 4.74 (d, $J_{1';2'} = 3.7$ Hz, 1H, H-1'), 4.67 (brs, 2H, 2xCH₂Ph), 4.57-4.48 (m, 4H, 2xCH₂Ph, H-3, H-4), 4.40 (d, $J_{gem} = 12.1$ Hz, 1H, CH₂Ph), 4.30 (d, $J_{gem} = 12.1$ Hz, 1H, CH₂Ph), 4.09 (brs, 1H, H-2), 3.95 (dd, $J_{2';3'} = 10.0$ Hz, $J_{2';1'} = 3.7$ Hz, 1H, H-2'), 3.83 (m, 1H, H-4'), 3.75 (dd, $J_{gem} = 10.0$ Hz, $J_{1a,2} = 2.9$ Hz, 1H, H-1a), 3.65 (m, 2H, H-5, H-3'), 3.57 (br.t, $J_{5';6a'} = J_{5';6b'} = 7.0$ Hz, 1H, H-5'), 3.40 (dd, $J_{gem} = 9.7$ Hz, $J_{6a',5} = 7.0$ Hz, 1H, H-6a'), 3.24 (m, 2H, H-1b, H-6b'), 2.43 (m, 1H, H-6a), 2.20-1.87 (m, 4H, H-7a, H-7b, H-2a'', H-2b''), 1.74 (m, 1H, H-6b), 1.50 (m, 2H, H-3''), 1.39 (s, 3H, CH₃), 1.26-1.11 (m, 45H, CH₂, CH₃), 0.80 (t, $J_{25';24''} = 6.9$ Hz, 3H, CH₃); **¹³C NMR** (100.6 MHz, CDCl₃) δ in ppm: 174.7 (C-1''), 138.8 (C-Ar), 138.4 (C-Ar), 138.4 (C-Ar), 138.1 (C-Ar), 128.5-127.4 (CH-Ar), 111.3 (C-ketal), 98.0 (C-1'), 82.7 (C-3), 79.3 (C-4), 78.5 (C-3'), 76.5 (C-2'), 74.8 (CH₂Ph), 74.5 (C-4'), 73.7 (CH₂Ph), 73.6 (CH₂Ph), 72.4 (CH₂Ph), 70.2 (C-5'), 69.8 (C-1), 69.7 (C-6'), 62.6 (C-2), 62.1 (C-5), 35.9 (C-2''), 32.1 (CH₂), 29.9-29.5 (CH₂), 27.7 (t, $J_{C,F} = 22.0$ Hz, C-7), 26.0 (CH₃-ketal), 25.6 (C-3''), 24.6 (CH₃-ketal), 22.8 (CH₂), 19.8 (C-6), 14.3 (CH₃); **¹⁹F NMR** (376 MHz, CDCl₃) δ in ppm: -80.8 (t, $J_{F,F} = 9.9$ Hz, 3F, CF₃), -113.2 (m, 2 F, CF₂CH₂), -121.8 (m, 10 F, CF₂), -122.7 (m, 2 F, CF₂), -123.1 (m, 2 F, CF₂), -126.2 (m, 2 F, CF₂); **HRMS** (TOF ES+) for [M+H]⁺ C₇₉H₁₀₁F₂₁NO₉ (m/z): calculated: 1606,7136, found: 1606,7132.

(2S,3S,4R,5S)-2-(1-O-(2,3,4,6-tetra-O-benzyl- α -D-galactopyranosyl)-methanol)-5-dodecyl-3,4-O-isopropylidene-1-pentacosanoylpyrrolidine (100**)**

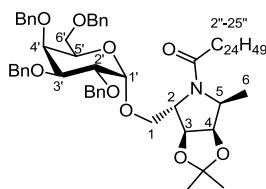


The title compound was prepared following the general procedure for pyrrolidine acylation, starting from pyrrolidine **90** (322 mg, 0.37 mmol), EDC·HCl (127 mg, 0.67 mmol), pentacosanoic acid (185 mg, 0.49 mmol), HOBT (90 mg, 0.67 mmol) and NEt₃ (51 μ L, 0.37 mmol) in DCM (4.6 mL). The crude was purified by column chromatography (1:3 EtOAc/Hexane) to afford **100** (358 mg, 79%) as a colorless oil; *R_f* = 0.25 (1:3 EtOAc/Hexane); $[\alpha]_D^{25}$ +29.9 (*c* 1.9, CHCl₃); IR (neat): 2918, 2849, 1643, 1455, 1214, 1056, 752 cm⁻¹; ¹H NMR (400 MHz, CDCl₃) δ in ppm: 7.31-7.18 (m, 20H, HAr), 4.84 (d, *J*_{gem} = 11.6 Hz, 1H, CH₂Ph), 4.76 (d, *J*_{gem} = 12.0 Hz, 1H, CH₂Ph), 4.73 (d, *J*_{1',2'} = 3.6 Hz, 1H, H-1'), 4.70-4.66 (m, 2H, 2xCH₂Ph), 4.62 (brt, *J*_{4,3} = *J*_{4,5} = 6.0 Hz, 1H, H-4), 4.55-4.52 (m, 2H, H-3, CH₂Ph), 4.48 (d, *J*_{gem} = 11.6 Hz, 1H, CH₂Ph), 4.40 (d, *J*_{gem} = 12.0 Hz, 1H, CH₂Ph), 4.30 (d, *J*_{gem} = 12.0 Hz, 1H, CH₂Ph), 4.07 (brs, 1H, H-2), 3.95 (dd, *J*_{2',3'} = 9.9 Hz, *J*_{2',1'} = 3.6 Hz, 1H, H-2'), 3.83 (brs, 1H, H-4'), 3.74-3.63 (m, 4H, H-1a, H-3', H-5', H-5), 3.39 (dd, *J*_{gem} = 9.2 Hz, *J*_{6a',5} = 7.2 Hz, 1H, H-6a'), 3.26 (m, 2H, H-1b, H-6b'), 2.34 (m, 1H, H-6a), 2.21-2.03 (m, 2H, H-2a'', H-2b''), 1.58-1.35 (m, 8H, H-3'', H-6b, CH₃, CH₂), 1.33-1.10 (m, 80H, CH₂, CH₃), 0.81 (t, *J*_{25'',24''} = *J*_{13'',12''} = 6.8 Hz, 6H, 2xCH₃); ¹³C NMR (100.6 MHz, CDCl₃) δ in ppm: 174.5 (C-1''), 138.8 (C-Ar), 138.6 (C-Ar), 138.4 (C-Ar), 138.1 (C-Ar), 128.5-127.6 (CH-Ar), 110.9 (C-ketal), 97.9 (C-1'), 82.2 (C-3), 79.9 (C-4), 79.0 (C-3'), 76.7 (C-2'), 74.8

Experimental section

(CH₂Ph), 74.8 (C-4'), 73.5 (CH₂Ph), 73.5 (CH₂Ph), 73.2 (CH₂Ph), 70.1 (C-5'), 69.5 (C-1), 69.5 (C-6'), 63.9 (C-5), 63.1 (C-2), 36.0 (C-2''), 32.1 (CH₂), 30.1-29.5 (CH₂), 28.1 (C-6), 26.6 (C-3''), 26.1 (CH₂), 26.0 (CH₃-ketal), 25.0 (CH₃-ketal), 22.9 (CH₂), 14.3 (CH₃); **HRMS** (TOF ES+) for [M+H]⁺ C₇₉H₁₂₂NO₈ (m/z): calculated: 1228,9114, found: 1228.9099.

(2S,3S,4R,5S)-2-(1-O-(2,3,4,6-tetra-O-benzyl- α -D-galactopyranosyl)-methanol)-5-methyl-3,4-O-isopropylidene-1-pentacosanoylpyrrolidine (101)

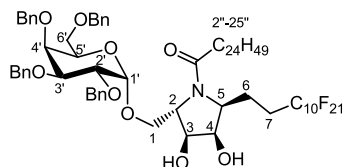


The title compound was prepared following the general procedure for pyrrolidine acylation, starting from pyrrolidine **91** (110 mg, 0.16 mmol), EDC·HCl (55 mg, 0.29 mmol), pentacosanoic acid (77 mg, 0.20 mmol), HOBT (39 mg, 0.29 mmol) and NEt₃ (22 μ L, 0.16 mmol) in DCM (2 mL). The crude was purified by column chromatography (1:3 EtOAc/Hexane) to afford **101** (121 mg, 71%) as a colorless oil; *Rf* = 0.18 (1:3 EtOAc/Hexane); **IR** (neat): 2922, 2852, 1645, 1454, 1210, 1056, 697 cm⁻¹. [α]_D²⁵ +48.0 (c 1.1, CHCl₃); Data for major rotamer: **¹H NMR** (400 MHz, CDCl₃) δ in ppm: 7.31-7.18 (m, 20H, HAr), 4.83 (d, *J*_{gem} = 11.6 Hz, 1H, CH₂Ph), 4.78 (d, *J*_{gem} = 11.7 Hz, 1H, CH₂Ph), 4.73 (d, *J*_{1',2'} = 3.6 Hz, 1H, H-1'), 4.66 (s, 2H, 2 x CH₂Ph), 4.56 (d, *J*_{gem} = 11.7 Hz, 1H, CH₂Ph), 4.54-4.48 (m, 3H, CH₂Ph, H-3, H-4), 4.39 (d, *J*_{gem} = 12.0 Hz, 1H, CH₂Ph), 4.29 (d, *J*_{gem} = 12.0 Hz, 1H, CH₂Ph), 4.08 (m, 1H, H-2), 3.95 (dd, *J*_{2',3'} = 10.0 Hz, *J*_{2',1'} = 3.6 Hz, 1H, H-2'), 3.79 (m, 1H, H-4'), 3.73, 3.71 (m, 2H, H-1a,

H-5), 3.68 (dd, $J_{3',2'} = 10.0$ Hz, $J_{3',4'} = 2.6$ Hz, 1H, H-3'), 3.62-3.55 (m, 1H, H-5'), 3.37 (dd, $J_{gem} = 9.6$ Hz, $J_{6a',5'} = 7.1$ Hz, 1H, H-6a'), 3.28-3.22 (m, 2H, H-1b, H-6b'), 2.19-1.97 (m, 2H, H-2''), 1.52 (m, 2H, H-3''), 1.40 (s, 3H, CH₃), 1.26 (d, $J_{6,5} = 6.5$ Hz, 3H, H-6), 1.23-1.11 (m, 42H, CH₃, CH₂), 0.81 (t, $J_{25'',24''} = 6.9$ Hz, 3H, CH₃); **¹³C NMR** (100.6 MHz, CDCl₃) δ in ppm: 174.0 (C-1''), 138.8 (C-Ar), 138.4 (C-Ar), 138.3 (C-Ar), 138.1 (C-Ar), 128.6-127.5 (CH-Ar), 110.8 (C-ketal), 97.9 (C-1'), 82.5 (C-3), 80.4 (C-4), 78.2 (C-3'), 76.6 (C-2'), 74.8 (CH₂Ph), 74.6 (C-4'), 73.5 (CH₂Ph), 73.5 (CH₂Ph), 72.7 (CH₂Ph), 70.1 (C-5'), 69.6 (C-1), 69.6 (C-6'), 62.6 (C-5), 59.0 (C-2), 35.7 (C-2''), 32.1 (CH₂), 29.9-29.5 (CH₂), 26.0 (C-3''), 25.9 (CH₃-ketal), 25.0 (CH₃-ketal), 22.8 (CH₂), 15.6 (C-6), 14.3 (CH₃). Data for minor rotamer: **¹H NMR** (400 MHz, CDCl₃) δ in ppm: 7.31-7.18 (m, 20H, HAr), 4.87 (d, $J_{gem} = 11.3$ Hz, 1H, CH₂Ph), 4.77-4.73 (m, 2H, CH₂Ph, H-1'), 4.66 (s, 2H, 2 x CH₂Ph), 4.63 (app. t, $J_{4,5} = J_{4,3} = 6.9$ Hz, 1H, H-4), 4.57-4.48 (m, 3H, 2 x CH₂Ph, H-3), 4.39 (d, $J_{gem} = 12.0$ Hz, 1H, CH₂Ph), 4.35 (brs, 1H, H-2), 4.29 (d, $J_{gem} = 12.0$ Hz, 1H, CH₂Ph), 4.19 (dd, $J_{gem} = 9.7$ Hz, $J_{1a,2} = 2.0$ Hz, 1H, H-1a), 3.95 (m, 1H, H-2'), 3.88 (m, 1H, H-4'), 3.75-3.55 (m, 3H, H-3', H-5', H-5), 3.49 (t, $J_{gem} = J_{6a',5'} = 8.4$ Hz, 1H, H-6a'), 3.38 (m, 1H, H-6b'), 3.22 (m, 1H, H-1b), 2.19-1.97 (m, 2H, H-2''), 1.32 (m, 1H, H-3''), 1.23-1.11 (m, 47H, 2 x CH₃, H-6, CH₂), 0.81 (t, $J_{25'',24''} = 6.9$ Hz, 3H, CH₃); **¹³C NMR** (100.6 MHz, CDCl₃) δ in ppm: 173.3 (C-1''), 138.7 (C-Ar), 138.5 (C-Ar), 138.3 (C-Ar), 138.0 (C-Ar), 128.6-127.5 (CH-Ar), 111.4 (C-ketal), 98.1 (C-1'), 82.1 (C-3), 80.2 (C-4), 78.2 (C-3'), 76.7 (C-2'), 75.0 (CH₂Ph), 74.5 (C-4'), 73.5 (CH₂Ph), 73.4 (CH₂Ph), 72.0 (CH₂Ph), 69.4 (C-5'), 68.3 (C-6'), 67.0 (C-1), 61.0 (C-5), 57.7 (C-2), 35.4 (C-2''), 32.1 (CH₂), 29.9-29.5 (CH₂), 25.7 (C-3''), 25.5 (CH₃-ketal), 25.1 (CH₃-ketal), 22.8 (CH₂), 18.7 (C-6), 14.3 (CH₃); **HRMS** (TOF ES+) for [M+Na]⁺ C₆₈H₉₉NNaO₉ (m/z): calculated: 1096.7212, found: 1096.7182.

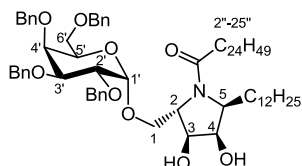
Experimental section

(2S,3S,4R,5S)-2-(1-O-(2,3,4,6-tetra-O-benzyl- α -D-galactopyranosyl)-methanol)-5-(2-perfluorodecylethyl)-1-pentacosanoylpyrrolidin-3,4-diol (102)



The title compound was prepared following the general procedure for isopropylidene ketal hydrolysis, starting from amide **99** (73 mg, 0.045 mmol) and using 4M HCl (57 μ L) in a mixture of CH₂Cl₂/(CF₃)₂CHOH (5:1) (0.6 mL). The reaction was allowed to stir for 5h and was stopped by adding a saturated aqueous solution of Na₂CO₃. The crude was purified by column chromatography (EtOAc/Hexane, 1:2) to provide the desired amide **102** as a colorless oil (53 mg, 76% yield). R_f = 0.18 (EtOAc/Hexane, 1:2). $[\alpha]_D^{25}$ +23.2 (*c* 1.8, CHCl₃); IR (neat): 3382, 2923, 2853, 1615, 1455, 1213, 1152, 1057, 752 cm⁻¹. HRMS (TOF ES+) for [M+H]⁺ C₇₆H₉₇F₂₁NO₉ (m/z): calculated: 1566,6823, found: 1566,6804.

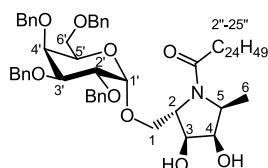
(2S,3S,4R,5S)-2-(1-O-(2,3,4,6-tetra-O-benzyl- α -D-galactopyranosyl)-methanol)-5-(dodecyl)-1-pentacosanoylpyrrolidin-3,4-diol (103)



The title compound was prepared following the general procedure for isopropylidene ketal hydrolysis, starting from amide **100** (300 mg, 0.245 mmol) and using 4M HCl (0.3 mL) in a mixture of

$\text{CH}_2\text{Cl}_2/(\text{CF}_3)_2\text{CHOH}$ (5:1) (3 mL). The reaction was allowed to stir for 5h and was stopped by adding a saturated aqueous solution of Na_2CO_3 . The crude was purified by column chromatography (EtOAc/Hexane, 1:2) to provide the desired amide **103** as a colorless oil (210 mg, 73% yield). $R_f = 0.12$ (EtOAc/Hexane, 1:2). $[\alpha]_D^{25} +30.8$ (c 1.1, CHCl_3); **IR** (neat): 3382, 2921, 2851, 1609, 1454, 1100, 1059, 734 cm^{-1} ; **HRMS** (TOF ES+) for $[\text{M}+\text{H}]^+ \text{C}_{76}\text{H}_{118}\text{NO}_9$ (m/z): calculated: 1188.8801, found: 1188.8766.

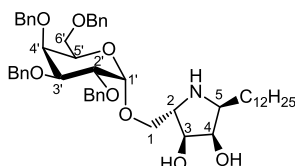
(2S,3S,4R,5S)-2-(1-O-(2,3,4,6-tetra-O-benzyl- α -D-galactopyranosyl)-methanol)-5-(methyl)-1-pentacosanoylpyrrolidin-3,4-diol (104**)**



The title compound was prepared following the general procedure for isopropylidene ketal hydrolysis, starting from amide **101** (91 mg, 0.085 mmol) and using 4M HCl (0.1 mL) in a mixture of $\text{CH}_2\text{Cl}_2/(\text{CF}_3)_2\text{CHOH}$ (5:1) (1 mL). The reaction was allowed to stir for 5h and was stopped by adding a saturated aqueous solution of Na_2CO_3 . The crude was purified by column chromatography (EtOAc/Hexane, 1:2) to provide the desired amide **104** as a colorless oil (70 mg, 80% yield). $R_f = 0.12$ (EtOAc/Hexane, 1:2). $[\alpha]_D^{25} +38.7$ (c 2.0, CHCl_3); **IR** (neat): 3393, 2922, 2852, 1608, 1454, 1100, 1059, 734 cm^{-1} ; **HRMS** (TOF ES+) for $[\text{M}+\text{Na}]^+ \text{C}_{65}\text{H}_{95}\text{NNaO}_9$ (m/z): calculated: 1056.6899, found: 1056.6883.

Experimental section

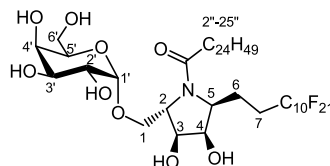
(2S,3S,4R,5S)-2-(1-O-(2,3,4,6-tetra-O-benzyl- α -D-galactopyranosyl)-methanol)-5-(dodecyl)pyrrolidin-3,4-diol (105**)**



The title compound was prepared following the general procedure for isopropylidene ketal hydrolysis, starting from amine **90** (100 mg, 0.116 mmol) and using 4M HCl (0.15 mL) in MeOH (1.5 mL). The reaction was allowed to stir at 50 °C overnight and was stopped by adding a saturated aqueous solution of Na₂CO₃. The crude was purified by column chromatography (EtOAc/Hexane/MeOH/NEt₃, 1:3:0.2:0.2) to provide the desired amine **105** as a colorless oil (75 mg, 79% yield). R_f = 0.23 (EtOAc/Hexane/MeOH/NEt₃, 1:3:0.2:0.2). $[\alpha]_D^{25}$ +36.4 (c 1.0, CHCl₃); IR (neat): 3398, 2921, 2852, 1454, 1095, 1057, 734 cm⁻¹; ¹H NMR (400 MHz, CDCl₃) δ in ppm: 7.32-7.18 (m, 20H, HAr), 4.85 (d, J_{gem} = 11.4 Hz, 1H, CH₂Ph), 4.78 (d, J_{gem} = 11.7 Hz, 1H, CH₂Ph), 4.72-4.65 (m, 3H, 2xCH₂Ph, H-1'), 4.61 (d, J_{gem} = 11.7 Hz, 1H, CH₂Ph), 4.48 (d, J_{gem} = 11.4 Hz, 1H, CH₂Ph), 4.40 (d, J_{gem} = 11.7 Hz, 1H, CH₂Ph), 4.32 (d, J_{gem} = 11.7 Hz, 1H, CH₂Ph), 3.98-3.84 (m, 6H, H-2', H-3', H-4', H-5', H-3, OH), 3.76 (m, 1H, H-4), 3.66 (dd, J_{gem} = 11.0 Hz, $J_{1a,2}$ = 5.6 Hz, 1H, H-1a), 3.47-3.40 (m, 3H, H-1b, H-6'), 3.18 (m, 1H, H-2), 2.87 (td, $J_{5,6}$ = 7.3 Hz, $J_{5,4}$ = 2.4 Hz, 1H, H-5), 2.46 (brs, 1H, OH), 1.53 (m, 1H, H-6a), 1.38 (m, 1H, H-6b), 1.24-1.18 (m, 20H, CH₂), 0.81 (t, $J_{18,17}$ = 6.8 Hz, 3H, CH₃); ¹³C NMR (100.6 MHz, CDCl₃) δ in ppm: 138.6 (C-Ar), 138.6 (C-Ar), 137.9 (C-Ar), 137.8 (C-Ar), 128.6-127.6 (CH-Ar), 98.4 (C-1'), 79.3 (C-3'), 78.6 (C-3), 76.1 (C-2'), 74.9 (C-4'), 74.9 (CH₂Ph), 74.3 (CH₂Ph), 73.6 (CH₂Ph), 73.5 (C-4), 72.9 (CH₂Ph), 71.9 (C-1), 69.8 (C-5'), 69.2 (C-6'), 60.8 (C-5), 59.9 (C-2), 32.1 (CH₂), 30.0-29.5 (CH₂), 27.1 (CH₂), 22.8 (CH₂), 14.3

(CH₃); **HRMS** (TOF ES+) for [M+H]⁺ C₅₁H₇₀NO₈ (m/z): calculated: 824.5096, found: 824.5088.

(2S,3S,4R,5S)-2-(1-O-(α -D-galactopyranosyl)-methanol)-5-(2-perfluorodecylethyl)-1-pentacosanoylpyrrolidin-3,4-diol (85**)**

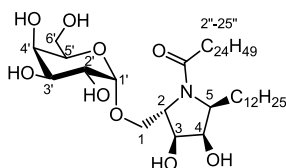


The title compound was prepared following the general procedure for hydrogenolysis, starting from **102** (40 mg, 0.025 mmol), Pd/C (38 mg) and H₂ (1 atm) in 3:1 MeOH/CHCl₃ (2 mL). The crude was purified by column chromatography (9:1 CHCl₃/MeOH) to afford **85** (26 mg, 87%) as a white waxy solid; *R_f* = 0.17 (9:1 CHCl₃/MeOH); [α]_D²⁵ +25.4 (c 1.4, CHCl₃/MeOH (1:1)); **IR** (neat): 3359, 2920, 2852, 1616, 1211, 1150 cm⁻¹; **¹H NMR** (400 MHz, CDCl₃ / MeOD (1:1), 2 rotamers) δ in ppm: 4.81-4.79 (m, 2H, H-1',H-1'), 4.52 (dd, *J*_{4,5} = 8.2 Hz, *J*_{4,3} = 4.7 Hz, 2H, H-4, H-4), 4.30 (brs, 1H, OH), 4.22 (d, *J*_{3,4} = 4.7 Hz, 1H, H-3), 4.17 (d, *J*_{3,4} = 4.7 Hz, 1H, H-3), 4.11 (dd, *J*_{2,1a} = 6.6 Hz, *J*_{2,1b} = 2.6 Hz, 1H, H-2), 4.03 (dd, *J*_{2,1a} = 6.1 Hz, *J*_{2,1b} = 2.2 Hz, 1H, H-2), 3.98 (m, 1H, H-5), 3.89 (m, 3H, H-4', H-4', H-5), 3.78 (m, 2H, H-2', H-2'), 3.74-3.55 (m, 11H, H-1a, H-1a, H-1b, 2xH-6', 2xH-6', H-5', H-5', H-3', H-3'), 3.50 (dd, *J*_{gem} = 10.2 Hz, *J*_{1b,2} = 2.2 Hz, 1H, H-1b), 2.67-2.45 (m, 2H, H-6a, H-7a), 2.42-2.12 (m, 8H, H-2'', H-2'', H-7a, H-7b, H-7b, H-6a), 1.98 (m, 1H, H-6b), 1.77 (m, 1H, H-6b), 1.60 (m, 4H, H-3'', H-3''), 1.34-1.18 (m, 84H, CH₂), 0.85 (t, *J*_{25'',24''} = 6.7 Hz, 6H, CH₃, CH₃); **¹³C NMR** (100.6 MHz, CDCl₃ / MeOD (1:1), 2 rotamers) δ in ppm: 175.4 (C-1''), 175.0 (C-1''), 115-105 (m, CF₂), 99.7 (C-1'), 99.7 (C-1'), 75.6 (C-3), 74.5 (C-3), 72.0 (C-5'), 71.7 (C-5'), 71.5 (C-3'), 70.9 (C-3'), 70.9 (C-4), 70.3 (C-4), 70.2(C-4'), 70.1 (C-2'), 69.5 (C-4'), 69.2 (C-2'),

Experimental section

68.5 (C-1), 66.0 (C-1), 64.5 (C-2), 64.5 (C-2), 62.2 (2xC-6'), 60.1 (C-5), 59.5 (C-5), 35.5 (C-2''), 34.9 (C-2''), 32.5 (CH₂), 30.3-29.9 (CH₂), 29.4-28.9 (m, 2xC-7), 27.7 (CH₂), 26.5 (C-3''), 26.3 (CH₂), 26.2 (C-3''), 23.8 (C-6), 23.2 (CH₂), 20.1 (C-6), 14.3 (CH₃); **¹⁹F NMR** (376 MHz, CDCl₃) δ in ppm: -81.0 (t, $J_{17,16} = 9.9$ Hz, 3F, CF₃), -113.42 (m, 2 F, CF₂CH₂), -122.0 (m, 10 F, CF₂), -123.0 (m, 2 F, CF₂), -123.4 (m, 2 F, CF₂), -126.4 (m, 2 F, CF₂); **HRMS** (TOF ES+) for [M+H]⁺ C₄₈H₇₃F₂₁NO₉ (m/z): calculated: 1206,4945, found: 1206.4928.

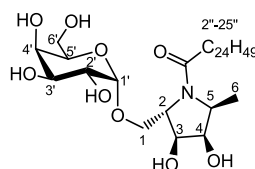
(2S,3S,4R,5S)-2-(1-O-(α-D-galactopyranosyl)-methanol)-5-dodecyl-1-pentacosanoylpyrrolidin-3,4-diol (86)



The title compound was prepared following the general procedure for hydrogenolysis reaction, starting from **103** (38 mg, 0.032 mmol), Pd/C (48 mg) and H₂ (1 atm) in 3:1 MeOH/CHCl₃ (2.5 mL). The crude was purified by column chromatography (9:1 CHCl₃/MeOH) to afford **86** (23 mg, 84%) as a white waxy solid; *R_f* = 0.15 (9:1 CHCl₃/MeOH); [α]_D²⁵ +15.0 (c 1.3, CHCl₃/MeOH); **IR** (neat): 3356, 2918, 2850, 1616, 1467, 1073 cm⁻¹; Data for major rotamer: **¹H NMR** (400 MHz, CDCl₃ / MeOD (1:1)) δ in ppm: 4.81 (d, $J_{1',2'} = 3.7$ Hz, 1H, H-1'), 4.44 (dd, $J_{4,5} = 7.8$ Hz, $J_{4,3} = 4.9$ Hz, 1H, H-4), 4.15 (d, $J_{3,4} = 4.9$ Hz, 1H, H-3), 4.06 (dd, $J_{2,1a} = 6.7$ Hz, $J_{2,1b} = 3.0$ Hz, 1H, H-2), 3.88 (d, $J_{4',3'} = 2.8$ Hz, 1H, H-4'), 3.76 (dd, $J_{2',3'} = 10.0$ Hz, $J_{2',1'} = 3.7$ Hz, 1H, H-2'), 3.75 m (1H, m, H-5), 3.71-3.57 (m, 6H, H-1a, H-1b, 2xH-6', H-5', H-3'), 2.28 (m, 3H, H-6a, H-2''), 1.69-1.52 (m, 2H, H-3''), 1.39-1.19 (m, 61H, H-6b, CH₂), 0.85 (t, $J_{25'',24''} = J_{13'',12''}$

= 6.8 Hz, 6H, 2xCH₃); ¹³C NMR (100.6 MHz, CDCl₃ / MeOD (1:1)) δ in ppm: 175.2 (C-1''), 99.7 (C-1'), 74.5 (C-3), 71.7 (C-5'), 71.4 (C-3'), 70.9 (C-4), 70.3 (C-4'), 69.5 (C-2'), 66.0 (C-1), 64.2 (C-2), 62.2 (C-6'), 61.4 (C-5), 35.6 (C-2''), 33.3 (CH₂), 32.5 (CH₂), 32.5 (C-6), 30.4-30.0 (CH₂), 28.9 (CH₂), 26.2 (C-3''), 23.3 (CH₂), 23.2 (CH₂), 14.4 (2xCH₃); Data for minor rotamer: ¹H NMR (400 MHz, CDCl₃ / MeOD (1:1)) δ in ppm: 4.79 (d, *J*_{1',2'} = 3.7 Hz, 1H, H-1'), 4.44 (m, 1H, H-4), 4.21 (d, *J*_{3,4} = 4.9 Hz, 1H, H-3), 4.00 (dd, *J*_{2,1a} = 6.2 Hz, *J*_{2,1b} = 2.6 Hz, 1H, H-2), 3.92-3.87 (m, 2H, H-4', H-5), 3.79 (dd, *J*_{2',3'} = 10.0 Hz, *J*_{2',1'} = 3.7 Hz, 1H, H-2'), 3.73-3.57 (m, 5H, H-1a, 2xH-6', H-5', H-3'), 3.50 (dd, *J*_{gem} = 10.3 Hz, *J*_{1b,2} = 2.6 Hz, 1H, H-1b), 2.28 (m, 2H, H-2''), 1.85 (m, 1H, H-6a), 1.69-1.52 (m, 3H, H-6b, H-3''), 1.39-1.19 (m, 61H, CH₂), 0.85 (t, *J*_{25'',24''} = *J*_{13'',12''} = 6.8 Hz, 6H, 2xCH₃); ¹³C NMR (100.6 MHz, CDCl₃ / MeOD (1:1)) δ in ppm: 175.1 (C-1''), 99.7 (C-1'), 75.7 (C-3), 72.0 (C-5'), 70.8 (C-4), 70.4 (C-3'), 70.2 (C-4'), 69.2 (C-2') 68.6 (C-1), 64.3 (C-2), 62.2 (C-6'), 60.9 (C-5), 35.0 (C-2''), 29.9 (C-6), 30.4-30.0 (CH₂), 28.5 (CH₂), 26.5 (C-3''), 14.4 (2xCH₃); HRMS (TOF ES+) for [M+H]⁺ C₄₈H₉₄NO₉ (m/z): calculated: 828,6923, found: 828.6924

(2S,3S,4R,5S)-2-(1-O-(α-D-galactopyranosyl)-methanol)-5-(methyl)-1-pentacosanoylpyrrolidin-3,4-diol (87)

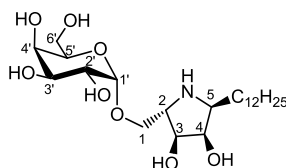


The title compound was prepared following the general procedure for hydrogenolysis reaction, starting from **104** (43 mg, 0.042 mmol), Pd/C (34 mg) and H₂ (1 atm) in 3:1 MeOH/CHCl₃ (3.3 mL). The crude was

| *Experimental section*

purified by column chromatography (9:1 CHCl₃/MeOH) to afford **87** (25 mg, 89%) as a white waxy solid; *R_f* = 0.19 (9:1 CHCl₃/MeOH); [α]_D²⁵ +11.4 (c 0.7, CHCl₃/MeOH); **IR** (neat): 3422, 2916, 2849, 1616, 1467, 1046 cm⁻¹. Data for major rotamer: **¹H NMR** (400 MHz, CDCl₃ / MeOD (1:1)) δ in ppm: 4.82 (d, *J*_{1',2'} = 3.7 Hz, 1H, H-1'), 4.37 (dd, *J*_{4,5} = 8.0 Hz, *J*_{4,3} = 4.8 Hz, 1H, H-4), 4.17 (d, *J*_{3,4} = 4.8 Hz, 1H, H-3), 4.10 (dd, *J*_{2,1a} = 5.9 Hz, *J*_{2,1b} = 4.3 Hz, 1H, H-2), 4.0 (m, 1H, H-5), 3.88 (d, *J*_{4',3'} = 2.8 Hz, 1H, H-4'), 3.76 (dd, *J*_{2',3'} = 10.1 Hz, *J*_{2',1'} = 3.7 Hz, 1H, H-2'), 3.71-3.62 (m, 6H, H-1a, H-1b, 2xH-6', H-5', H-3'), 3.52 (s, 1H, OH), 2.32 (m, 2H, H-2''), 1.60 (m, 2H, H-3''), 1.34 (d, *J*_{6,5} = 6.7 Hz, 2H, H-6), 1.33-1.20 (m, 42H, CH₂), 0.85 (t, *J*_{25'',24''} = 6.7 Hz, 3H, CH₃); **¹³C NMR** (100.6 MHz, CDCl₃ / MeOD (1:1)) δ in ppm: 175.1 (C-1''), 99.7 (C-1'), 74.2 (C-3), 71.6 (C-5'), 71.0 (C-3'), 70.9 (C-4'), 70.3 (C-4), 69.5 (C-2'), 66.2 (C-1), 64.2 (C-2), 62.2 (C-6'), 57.1 (C-5), 35.4 (C-2''), 32.5 (CH₂), 30.2-29.8 (CH₂), 26.3 (C-3''), 23.2 (CH₂), 16.4 (C-6), 14.3 (CH₃); Data for minor rotamer: **¹H NMR** (400 MHz, CDCl₃ / MeOD (1:1)) δ in ppm: 4.80 (d, *J*_{1',2'} = 3.7 Hz, 1H, H-1'), 4.39 (m, 1H, H-4), 4.23 (d, *J*_{3,4} = 4.6 Hz, 1H, H-3), 4.11 (m, 1H, H-5), 4.05 (m, 1H, H-2), 3.90 (d, *J*_{4',3'} = 2.3 Hz, 1H, H-4'), 3.79 (dd, *J*_{2',3'} = 10.0 Hz, *J*_{2',1'} = 3.7 Hz, 1H, H-2'), 3.74-3.56 (m, 5H, H-1a, 2xH-6', H-5', H-3'), 3.53 (m, 1H, H-1b), 3.39 (s, 1H, OH), 2.40-2.15 (m, 2H, H-2''), 1.60 (m, 2H, H-3''), 1.33-1.20 (m, 45H, H-6, CH₂), 0.85 (t, *J*_{25'',24''} = 6.7 Hz, 3H, CH₃); **¹³C NMR** (100.6 MHz, CDCl₃ / MeOD (1:1)) δ in ppm: 175.0 (C-1''), 99.7 (C-1'), 75.6 (C-3), 72.0 (C-5'), 70.8 (C-4'), 70.1 (C-3'), 70.0 (C-4), 69.2 (C-2'), 68.5 (C-1), 64.4 (C-2), 62.1 (C-6'), 56.6 (C-5), 34.8 (C-2''), 32.5 (CH₂), 30.2-29.8 (CH₂), 26.4 (C-3''), 23.2 (CH₂), 14.3 (CH₃), 13.7 (C-6); **HRMS** (TOF ES+) for [M+Na]⁺ C₃₇H₇₁NNaO₉ (m/z): calculated: 696.5021, found: 696.5019.

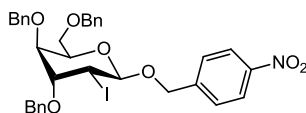
(2S,3S,4R,5S)-2-(1-O-(α -D-galactopyranosyl)-methanol)-5-dodecylpyrrolidin-3,4-diol (88**)**



The title compound was prepared following the general procedure for hydrogenolysis reaction, starting from **105** (40 mg, 0.049 mmol), Pd/C (39 mg) and H₂ (1 atm) in 3:1 MeOH/CHCl₃ (3.9 mL). The crude was purified by column chromatography (9:2 CHCl₃/MeOH) to afford **88** (19 mg, 84%) as a white waxy solid; *R_f* = 0.11 (9:2 CHCl₃/MeOH); $[\alpha]_D^{25} +7.7$ (*c* 0.5, CHCl₃/MeOH); IR (neat): 3338, 2922, 2851, 1128 cm⁻¹; ¹H NMR (400 MHz, CDCl₃ / MeOD (1:1)) δ in ppm: 4.91 (d, *J*_{1',2'} = 3.8 Hz, 1H, H-1'), 4.04 (m, 3H, H-3, H-4, H-1a), 3.89 (d, *J*_{4',3'} = 3.0 Hz, 1H, H-4'), 3.83 (dd, *J*_{2',3'} = 10.1 Hz, *J*_{2',1'} = 3.8 Hz, 1H, H-2'), 3.80 (m, 1H, H-5'), 3.76-3.68 (m, 3H, H-6', H-3'), 3.62 (m, 2H, H-1b, H-2), 3.45 (m, 1H, H-5), 1.85 (m, 1H, H-6a), 1.66 (m, 1H, H-6b), 1.43-1.20 (m, 20H, CH₂), 0.85 (t, *J*_{17,16} = 6.8 Hz, 3H, CH₃); ¹³C NMR (100.6 MHz, CDCl₃ / MeOD (1:1)) δ in ppm: 99.2 (C-1'), 72.6 (C-3), 71.0 (C-5'), 70.2 (C-4), 69.5 (C-3'), 69.3 (C-4'), 68.4 (C-2'), 66.1 (C-1), 61.3 (C-6'), 60.8 (C-5), 60.5 (C-2), 31.4 (CH₂), 29.2-28.9 (CH₂), 26.4 (C-6), 25.6 (CH₂), 22.2 (CH₂), 13.3 (CH₃); HRMS (TOF ES+) for [M+H]⁺ C₂₃H₄₆NO₈ (*m/z*): calculated: 464.3218, found: 464.3226.

| *Experimental section*

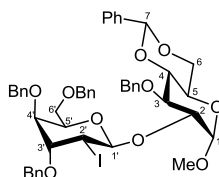
***p*-Nitrobenzyl 3,4,6-tri-*O*-benzyl-2-deoxy-2-iodo- α/β -D-gulo-
pyranoside (**122a**).**



The title compound was prepared following the general method B for oxydation/glycosylation of thiophenyl glycosides using **115** (29.3 mg, 0.045 mmol), 4Å MS (70 mg), *m*-CPBA (10.6 mg, 0.047 mmol) and CH₂Cl₂ (1.3 mL). After addition of NaHCO₃ (18.9 mg, 0.23 mmol) and filtration of the solution, the glycosylation was performed using **121a** (14 mg, 0.09 mmol), DTBMP (27.7mg, 0.135 mmol), Tf₂O (15 μL, 0.09 mmol) and 4Å MS (20 mg) at -80 °C for 30 minutes. After standard work-up, the residue was purified by column chromatography (from hexane to EtOAc:hexane 1:3) to afford the expected product **122a** (25 mg, 80%) as an inseparable 1:40 α/β anomeric mixture as a faint yellow syrup; *R*_f = 0.33 (EtOAc/hexane 1:4); IR (neat) 2929, 2866, 1455, 1260, 1072, 1015, 800, 697; Data for **122a** β : **¹H NMR** (CDCl₃, 400 MHz) δ in ppm: 8.18 (d, *J*_{o-m} = 8.6 Hz, 2H, H-Ar-o), 7.56 (d, *J*_{o-m} = 8.6 Hz, 2H, H-Ar-m), 7.40-7.17 (m, 15H, H-Ar), 4.96 (d, *J*_{gem} = 13.2 Hz, 1H, CH₂PhNO₂), 4.86 (d, *J*_{1,2} = 9.0 Hz, 1H, H-1), 4.67 (d, *J*_{gem} = 13.2 Hz, 1H, CH₂PhNO₂), 4.65 (d, *J*_{gem} = 11.2 Hz, 1H, CH₂Ph), 4.54-4.37 (m, 6H, 5xCH₂Ph, H-2), 4.20 (td, *J*_{5,6} = 6.4 Hz, *J*_{5,4} = 1.4 Hz, 1H, H-5), 3.81 (appt, *J*_{3,4} = *J*_{3,2} = 3.3 Hz, 1H, H-3), 3.61 (dd, *J*_{gem} = 9.6 Hz, *J*_{6a,5} = 6.2 Hz, 1H, H-6a), 3.56 (dd, *J*_{gem} = 9.6 Hz, *J*_{6b,5} = 6.8 Hz, 1H, H-6b), 3.38 (dd, *J*_{4,3} = 3.6 Hz, *J*_{4,5} = 1.4 Hz, 1H, H-4); **¹³C NMR** (CDCl₃, 100.6 MHz) δ in ppm: 147.4 (CNO₂), 145.1 (C-Ar), 138.1 (C-Ar), 137.5 (C-Ar), 137.4 (C-Ar), 128.5-127.7 (CH-Ar), 123.6, 99.8 (C-1), 78.6 (C-3), 74.1 (CH₂Ph), 73.7 (CH₂Ph), 73.6 (C-4), 73.1 (C-5), 73.0 (CH₂Ph), 69.8 (CH₂PhNO₂), 68.9 (C-6), 31.4 (C-2); **HRMS** (TOF

ES⁺) for [M+Na]⁺ C₃₄H₃₄INNaO₇ (m/z): calculated: 718.1272; found 718.1265.

Methyl (3',4',6'-tri-O-benzyl-2'-deoxy-2'-iodo- α/β -D-gulopyranosyl)-(1 \rightarrow 2)-3-O-benzyl-4,6-O-benzylidene- α -D-glucopyranoside (122b**).**

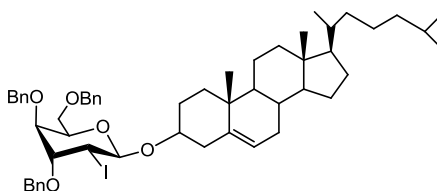


The title compound was prepared following the general method B for oxydation/glycosylation of thiophenyl glycosides using **115** (19.3 mg, 0.03 mmol), 4Å MS (40 mg), *m*-CPBA (7.1 mg, 0.031 mmol) and CH₂Cl₂ (0.9 mL). After addition of NaHCO₃ (12.6 mg, 0.15 mmol) and filtration of the solution, the glycosylation was performed using **121b** (9.3 mg, 0.06 mmol), DTBMP (18.5 mg, 0.09 mmol), Tf₂O (10 μ L, 0.06 mmol) and 4Å MS (13 mg). After stirring for 30 minutes at -80 °C, standard work-up was performed and the residue was purified by column chromatography (from hexane to EtOAc:hexane 1:3) to afford the expected product **122b** (19 mg, 69%) as an 1:24 α/β anomeric mixture as a colorless syrup; *R*_f = 0.31 (EtOAc/hexane 1:3); IR (neat): 2921, 2861, 1454, 1371, 1072, 994, 740, 697; Data for **122b** β : ¹H NMR (CDCl₃, 400 MHz) δ in ppm: 7.50-7.12 (m, 25H, H-Ar), 5.54 (s, 1H, H-7'), 5.08 (d, *J*_{1',2'} = 9.2 Hz, 1H, H-1'), 5.07 (d, *J*_{gem} = 10.6 Hz, 1H, CH₂Ph), 4.86 (d, *J*_{1,2} = 3.7 Hz, 1H, H-1), 4.80 (d, *J*_{gem} = 10.6 Hz, 1H, CH₂Ph), 4.66 (d, *J*_{gem} = 11.5 Hz, 1H, CH₂Ph), 4.50-4.38 (m, 6H, H-2', 5xCH₂Ph), 4.28 (dd, *J*_{gem} = 10.1, *J*_{6a,5} = 4.8 Hz, 1H, H-6a), 4.16 (td, *J*_{5',6'} = 6.4 Hz, *J*_{5',4'} = 1.2 Hz, 1H, H-5'), 4.03 (appt, *J*_{3,4} = *J*_{3,2} = 9.4 Hz, 1H, H-3), 3.85 (apptd, *J*_{5,6b} = *J*_{5,4} = 9.4 Hz, *J*_{5,6a} = 4.8 Hz, 1H, H-

Experimental section

5), 3.80 (appt, $J_{3',2'} = J_{3',4'} = 3.2$ Hz, 1H, H-3'), 3.76-3.69 (m, 2H, H-2, H-6b), 3.59 (appt, $J_{4,5} = J_{4,3} = 9.4$ Hz, 1H, H-4), 3.53 (d, $J_{6',5'} = 6.4$ Hz, 2H, H-6'), 3.39 (s, 3H, OCH₃), 3.36 (dd, $J_{4',3'} = 3.2$ Hz, $J_{4',5'} = 1.4$ Hz, 1H, H-4'); ¹³C NMR (CDCl₃, 100.6 MHz) δ in ppm: 138.8 (C-Ar), 138.1 (C-Ar), 137.7 (C-Ar), 137.6 (C-Ar), 137.6 (C-Ar), 129.0-126.1 (CH-Ar), 101.4 (C-7), 101.4 (C-1'), 100.4 (C-1), 82.8 (C-4), 79.2 (C-3'), 79.1 (C-2), 77.7 (C-3), 75.3 (CH₂Ph), 74.1 (CH₂Ph), 73.9 (C-4'), 73.5 (CH₂Ph), 73.0 (CH₂Ph), 72.8 (C-5'), 69.3 (C-6), 69.0 (C-6'), 62.2 (C-5), 55.4 (OCH₃), 30.7 (C-2'); HRMS (TOF ES⁺) for [M+Na]⁺ C₄₈H₅₁INaO₁₀ (m/z): calculated: 937.2419; found 937.2412.

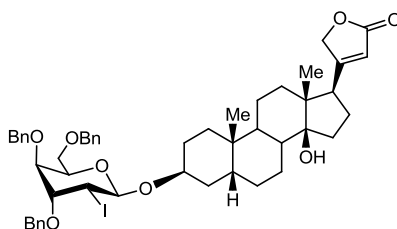
Cholesteryl 3,4,6-Tri-O-benzyl-2-deoxy-2-iodo- α/β -D-gulo-pyranoside (122c).



The title compound was prepared following the general method B for oxydation/glycosylation of thiophenyl glycosides using **115** (10.3 mg, 0.016 mmol), 4Å MS (20 mg), *m*CPBA (3.8 mg, 0.016 mmol) and CH₂Cl₂ (0.48 mL). After addition of NaHCO₃ (6.7 mg, 0.08 mmol) and filtration of the solution, the glycosylation was performed using **121c** (4.9 mg, 0.03 mmol), DTBMP (9.9 mg, 0.048 mmol), Tf₂O (5.3 μL, 0.032 mmol) and 4Å MS (6.9 mg). After stirring for 30 minutes at -80 °C, standard work-up was performed and the residue was purified by column chromatography (from hexane to EtOAc:hexane 1:3) to afford the expected product **122c** (9 mg, 63%) as an 1:21 α/β anomeric mixture as a colorless syrup; *R*_f =

0.62 (EtOAc/hexane 1:3); **IR** (neat) 2929, 2865, 1455, 1260, 1072, 1015, 800, 697; Data for **122c** β : **$^1\text{H NMR}$** (CDCl_3 , 400 MHz) δ in ppm: 7.39-7.13 (m, 15H, H-Ar), 5.35 (bs, 1H, $\text{CH}=\text{cholesteryl}$), 4.82 (d, $J_{1,2} = 9.5$ Hz, 1H, H-1), 4.64 (d, $J_{\text{gem}} = 11.4$ Hz, 1H, CH_2Ph), 4.53-4.32 (m, 6H, H-2, $5\times\text{CH}_2\text{Ph}$), 4.16 (t, $J_{5,6} = 6.3$ Hz 1H, H-5), 3.78 (appt, $J_{3,2} = J_{3,4} = 3.2$ Hz, 1H, H-3), 3.56 (d, $J_{6,5} = 6.3$ Hz, 2H, H6), 3.49 (m, 1H, $\text{HCOR}_{\text{cholesteryl}}$), 3.34 (m, 1H, H-4), 2.39-0.67 (m, 44H, $\text{H}_{\text{cholesteryl}}$); **$^{13}\text{C NMR}$** (CDCl_3 , 100.6 MHz) δ in ppm: 140.9 (C-Ar), 137.8 (C-Ar), 137.6 (C-Ar), 128.6-127.6 (CH-Ar, $=\text{C}_{\text{cholesteryl}}$), 121.9 ($\text{CH}=\text{cholesteryl}$), 98.9 (C-1), 79.6 ($\text{CHOR}_{\text{cholesteryl}}$), 78.8 (C-3), 74.0 (CH_2Ph), 73.7 (C-4), 73.5 (CH_2Ph), 72.9 (CH_2Ph), 72.8 (C-5), 69.1 (C-6), 56.9-12.0 ($24\text{C}_{\text{cholesteryl}}$)¹⁶, 33.5 (C-2); **HRMS** (TOF ES^+) for $[\text{M}+\text{Na}]^+$ $\text{C}_{54}\text{H}_{73}\text{INaO}_5$ (m/z): calculated: 951.4395; found 951.4391.

Digitoxigenyl 3,4,6-Tri-*O*-benzyl-2-deoxy-2-iodo- α/β -D-gulopyranoside (**124**).



The title compound was prepared following the general method B for oxydation/glycosylation of thiophenyl glycosides using **115** (14.1 mg, 0.022 mmol), 4Å MS (25 mg), *m*-CPBA (5.2 mg, 0.022 mmol) and CH_2Cl_2 (0.7 mL). After addition of NaHCO_3 (9.2 mg, 0.11 mmol) and filtration of the solution, the glycosylation was performed using **123** (6.7 mg, 0.04

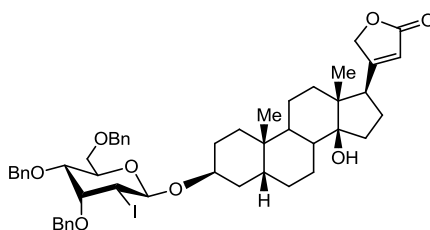
¹⁶ ^{24}C cholesteryl peaks: 56.3, 50.3, 42.5, 39.9, 39.7, 38.7, 37.4, 36.9, 36.3, 35.9, 32.1, 32.0, 29.9, 29.7, 28.4, 28.2, 24.4, 24.0, 23.0, 22.7, 21.2, 19.6, 18.9, 12.0

| *Experimental section*

mmol), DTBMP (13.6 mg, 0.066 mmol), Tf₂O (7.3 μL, 0.044 mmol) and 4Å MS (9 mg). After stirring for 30 minutes at -80 °C, standard work-up was performed and the residue was purified by column chromatography (from hexane to EtOAc:hexane 1:2) to afford the expected product **124** (12 mg, 60%) as an 1:22 α/β anomeric mixture as a colorless syrup; *R*_f = 0.44 (EtOAc/hexane 1:1); **IR** (neat): 3488, 2923, 2854, 1742, 1454, 1067, 1025, 736, 698; Data for **124**β: **¹H NMR** (400 MHz, CDCl₃) δ in ppm: 7.41–7.14 (m, 15H, H-Ar), 5.88 (bs, 1H, H-22_{dig}), 5.00 (dd, *J*_{gem} = 18.2 Hz, 1H, H-21a_{dig}), 4.82 (dd, *J*_{gem} = 18.3, *J*_{21b, 22} = 1.5 Hz, 1H, H-21b_{dig}), 4.77 (d, *J*_{1,2} = 9.2 Hz, 1H, H-1), 4.66 (d, *J*_{gem} = 11.6 Hz, 1H, CH₂Ph), 4.53-4.34 (m, 6H, H-2, 5xCH₂Ph), 4.15 (t, *J*_{5,6} = 6.3 Hz, 1H, H-5), 3.99 (bs, 1H, H-3_{dig}), 3.79 (appt, *J*_{3,2} = *J*_{3,4} = 3.3 Hz, 1H, H-3), 3.59-3.50 (m, 2H, H-6), 3.34 (dd, *J*_{4,3} = 3.3, *J*_{4,5} = 0.8 Hz, 1H, H-4), 2.79 (m, 1H, OH_{dig}), 2.20–1.18 (m, 21H, H_{dig}), 0.94 (s, 3H, CH₃), 0.87 (s, 3H, CH₃); **¹³C NMR** (100.6 MHz, CDCl₃) δ in ppm: 174.7 (C=O_{dig}), 174.7 (C-20_{dig}), 138.3 (C-Ar), 137.7 (C-Ar), 137.6 (C-Ar), 128.6-127.7 (CH-Ar), 117.8 (C-22_{dig}), 98.1 (C-1), 85.8 (C-14_{dig}), 78.9 (C-3), 74.1 (C-3_{dig}), 73.9 (CH₂Ph), 73.8 (C-4), 73.6 (C-21_{dig}), 73.5 (CH₂Ph), 72.9 (CH₂Ph), 72.8 (C-5), 69.1 (C-6), 51.0-14.4 (17C_{dig})¹⁷, 33.4 (C-2); **HRMS** (TOF ES⁺) for [M+Na]⁺ C₅₀H₆₁INaO₈ (m/z): calculated: 939.3303; found: 939.3292.

¹⁷ 17C digitoxigenine peaks: 51.0, 49.7, 42.0, 40.2, 36.1, 36.0, 35.2, 33.3, 30.1, 29.8, 29.3, 27.0, 26.5, 23.7, 21.5, 21.3, 15.9.

Digitoxigenyl 3,4,6-Tri-*O*-benzyl-2-deoxy-2-iodo- α/β -D-*allo*-pyranoside (**125**).

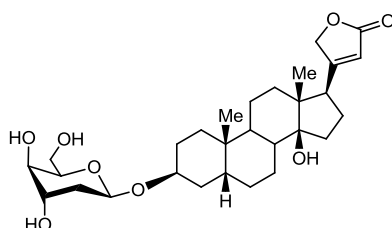


The title compound was prepared following the general method B for oxydation/glycosylation of thiophenyl glycosides using **116** (15.4 mg, 0.024 mmol), 4Å MS (25 mg), *m*-CPBA (5.7 mg, 0.024 mmol) and CH₂Cl₂ (0.8 mL). After addition of NaHCO₃ (10 mg, 0.12 mmol) and filtration of the solution, the glycosylation was performed using **123** (7.3 mg, 0.044 mmol), DTBMP (14.8 mg, 0.072 mmol), Tf₂O (7.9 μL, 0.048 mmol) and 4Å MS (10 mg). After stirring for 30 minutes at -80 °C, standard work-up was performed and residue was purified by column chromatography (from hexane to EtOAc:hexane 1:2) to afford the expected product **125** (14 mg, 64%) as an 1:24 α/β anomeric mixture as a colorless syrup; *R*_f = 0.45 (EtOAc/hexane 1:1); IR (neat): 3490, 2924, 2854, 1742, 1454, 1067, 1026, 737, 698; Data for **125** β : ¹H NMR (400 MHz, CDCl₃) δ in ppm: 7.49–7.23 (m, 15H, H-Ar), 5.87 (bs, 1H, H-22_{dig}), 4.99 (d, *J*_{gem} = 17.9 Hz, 1H, H-21a_{dig}), 4.88 (d, *J*_{gem} = 10.5 Hz, 1H, CH₂Ph), 4.80 (d, *J* = 17.9 Hz, 1H H-21b_{dig}), 4.79 (d, *J*_{1,2} = 8.0 Hz, 1H, H-1), 4.78 (d, *J*_{gem} = 10.5 Hz, 1H, CH₂Ph), 4.67–4.48 (m, 4H, 4xCH₂Ph), 4.17 (bs, 1H, H-3), 4.12 (m, 1H, H-3), 4.05 (dd, *J*_{2,1} = 9.0 Hz, *J*_{2,3} = 2.4 Hz, 1H, H-2), 3.96 (bs, 1H, H-3_{dig}), 3.75–3.67 (m, 2H, H-4, H-6a), 3.64 (dd, *J*_{gem} = 10.9 Hz, *J*_{6b,4} = 4.7 Hz, H-6b), 2.78 (m, 1H, OH_{dig}), 2.23–1.14 (m, 21H, H_{dig}), 0.94 (s, 3H, CH₃), 0.87 (s, 3H, CH₃); ¹³C NMR (100.6 MHz, CDCl₃) δ in ppm: 174.7 (CO_{dig}) 174.7 (C-20_{dig}), 138.5 (2xC-Ar), 137.7 (C-Ar), 128.6–127.7 (CH-Ar), 117.8

| *Experimental section*

(C-22_{dig}), 98.7 (C-1), 85.8 (C-14_{dig}), 78.6 (C-3), 76.7 (C-4), 75.8 (CH₂Ph), 74.5 (C-3_{dig}), 73.6 (C-21_{dig}), 73.5 (CH₂Ph), 73.2 (CH₂Ph), 72.3 (C-5), 69.4 (C-6), 51.1-15.9 (17C_{dig})¹⁸, 33.3 (C-2); **HRMS** (TOF ES⁺) for [M+Na]⁺ C₅₀H₆₁INaO₈ (m/z): calculated: 939.3303; found: 939.3397.

Digitoxigenyl 2-deoxy- α/β -D-gulo-pyranoside (119).

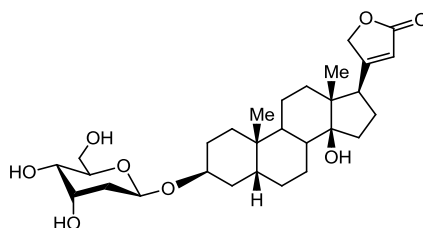


To a solution of **124** (16 mg, 0.017 mmol) in toluene (0.17 mL) were consecutively added Bu₃SnH (27 mL, 0.10 mmol) and Et₃B (10 mL, 0.01 mmol). The reaction mixture was stirred at room temperature for 1 h, then diluted with EtOAc and washed with saturated aqueous NaHCO₃. The combined organic extracts were dried with anhydrous Na₂SO₄ and concentrated under reduced pressure. The crude was filtered through a short path of SiO₂ (from 1:9 to 1:1 EtOAc/hexane and 5% Et₃N) to remove tin contaminants. Fractions containing the crude product were concentrated under reduced pressure, dissolved in 1:1 EtOAc/MeOH (0.7 mL) and 10% Pd/C (19 mg) was added. The mixture was stirred at 0 °C under H₂ atmosphere (1 atm). After 1 h, the reaction mixture was diluted with EtOAc and filtered through a short path of Celite[®]. The residue was purified by column chromatography (from EtOAc to EtOAc/MeOH 95:5 and 5% Et₃N) to afford **119** (7.6 mg, 86% over two steps) as an 1:22 α/β anomeric mixture as a colorless syrup; *R*_f = 0.33 (1:9 MeOH/CH₂Cl₂); **IR**

¹⁸ 17C digitoxigenine peaks: 51.1, 49.7, 42.0, 40.2, 36.2, 36.0, 35.3, 30.2, 29.9, 29.6, 27.0, 26.6, 26.5, 23.8, 21.5, 21.3, 15.9.

(neat): 3392, 2923, 2853, 1754, 1456, 1024; Data for **119** β : $^1\text{H NMR}$ (400 MHz, $\text{CDCl}_3/\text{CD}_3\text{OD}$ 1:1) δ in ppm: 5.84 (bs, 1H, H-22_{dig}), 5.04 (d, $J_{\text{gem}} = 18.6$ Hz, 1H, H-21a_{dig}), 4.90-4.82 (m, 2H, H-1, H-21b_{dig}), 4.07 (bs, 1H, H-3_{dig}), 3.95 (appq, $J_{3,2} = J_{3,4} = 3.2$ Hz, 1H, H-3), 3.84 (t, $J_{5,6} = 5.8$ Hz, 1H, H-5), 3.73 (d, $J_{6,5} = 5.8$ Hz, 2H, H-6), 3.47 (m, 1H, H-4), 2.80 (m, 1H, OH_{dig}), 2.21-1.13 (m, 23H, H-2, H_{dig}), 0.91 (s, 3H, CH₃), 0.85 (s, 3H, CH₃); $^{13}\text{C NMR}$ (100.6 MHz, CD_3OD) δ in ppm: 177.3 (CO_{dig}), 176.6 (C-20_{dig}), 117.4 (C-22_{dig}), 96.8 (C-1), 85.7 (C-14_{dig}), 74.6 (C-21_{dig}), 73.8 (C-5), 73.4 (C-3_{dig}), 69.2 (C-3), 68.6 (C-4), 62.7 (C-6), 51.6-16.2 (17C_{dig})¹⁹, 34.8 (C-2); **HRMS** (TOF ES⁺) for $[\text{M}+\text{Na}]^+$ C₂₉H₄₄NaO₈ (m/z): calculated: 543.2928; found: 543.2918.

Digitoxigenyl 2-deoxy- β -D-*allo*-pyranoside (**120**).



To a solution of **125** (9.8 mg, 0.0107 mmol) in toluene (0.4 mL) were consecutively added Bu_3SnH (17.2 μL , 0.064 mmol) and Et_3B (1 M, 6.4 μL , 0.006 mmol). The reaction mixture was stirred at room temperature for 1 h, then diluted with EtOAc and washed with saturated aqueous NaHCO_3 . The combined organic extracts were dried with anhydrous Na_2SO_4 and concentrated under reduced pressure. The crude was filtered through a short path of SiO_2 (from 1:9 to 1:1 EtOAc /hexane

¹⁹ ^{13}C digitoxigenine peaks: 51.6, 50.4, 41.9, 40.5, 37.0, 36.2, 35.7, 33.0, 30.7, 30.3, 27.4, 27.2, 27.0, 24.0, 21.9, 21.7, 16.2.

| *Experimental section*

and 5% Et₃N) to remove tin contaminants. Fractions containing the crude product were concentrated under reduced pressure, dissolved in 1:1 EtOAc/MeOH (0.7 mL) and 10% Pd/C (16 mg) was added. The mixture was stirred at 0 °C under H₂ atmosphere (1 atm). After 3 h, the reaction mixture was diluted with EtOAc and filtered through a short path of Celite[®]. The residue was purified by column chromatography (from EtOAc to EtOAc/MeOH 95:5 and 5% Et₃N) to afford **120** (5.3 mg, 95% over two steps) as an 1:24 α/β anomeric mixture as a colorless syrup; *R*_f = 0.29 (1:9 MeOH/CH₂Cl₂); **IR** (neat): 3392, 2924, 2854, 1736, 1450, 1025; Data for **120**β: **¹H NMR** (400 MHz, CD₃OD) δ in ppm: 5.87 (bs, 1H, H-22_{dig}), 5.04 (dd, *J*_{gem} = 18.4 Hz, 1H, H-21a_{dig}), 4.98-4.87 (m, 2H, H-1, H-21b_{dig}), 4.10 (bs, 1H, H-3_{dig}), 4.05 (apqq, *J*_{3,2} = *J*_{3,4} = 3.1 Hz, 1H, H-3), 3.82 (d, *J*_{gem} = 10.9 Hz, 1H, H-6a), 3.73-3.63 (m, 2H, H-6b, H-5), 3.45 (dd, *J*_{4,5} = 9.4 Hz, *J*_{4,3} = 3.1 Hz, 1H, H-4), 2.83 (m, 1H, OH_{dig}), 2.24–1.22 (m, 23H, H-2, H_{dig}), 0.95 (s, 3H, CH₃), 0.88 (s, 3H, CH₃); **¹³C NMR** (100.6 MHz, CD₃OD) δ in ppm: 178.5 (CO_{dig}), 177.3 (C-20_{dig}), 117.8 (C-22_{dig}), 96.9 (C-1), 86.5 (C-14_{dig}), 75.5 (C-5), 75.4 (C-21_{dig}), 74.1 (C-3_{dig}), 69.3 (C-3), 69.1 (C-4), 63.6 (C-6), 52.1-22.4 (17C_{dig})²⁰, 34.1 (C-2); **HRMS** (TOF ES⁺) for [M+Na]⁺ C₂₉H₄₄NaO₈ (m/z): calculated: 543.2928; found: 543.2920.

²⁰ 17C digitoxigenine peaks: 52.1, 51.1, 42.7, 41.0, 39.5, 38.0, 36.9, 36.4, 33.4, 31.4, 30.8, 28.1, 27.9, 27.6, 24.3, 22.6, 22.4.

UNIVERSITAT ROVIRA I VIRGILI
SYNTHESIS OF FLUORINATED ANALOGS OF KRN7000
David Collado Fernández

